Kinetic and Mechanistic Study of Oxidative Degradation of Fluoroquinolone Antibacterial Agents in Aqueous Medium

A thesis

Submitted for the award of the

Doctor of Philosophy

Degree in

CHEMISTRY

(Faculty in Science)

to the

University of Kota, Kota

by

Gajala Tazwar

Under the co-supervision of

Dr. Naveen Mittal

Associate Professor

Under the supervision of

Dr. (Mrs.) Vijay Devra

Associate Professor

Department of Chemistry

J.D.B. Govt. Girls College, Kota

UNIVERSITY OF KOTA, KOTA

2018

CERTIFICATE

I feel great pleasure in certifying that the thesis entitled "**Kinetic and Mechanistic Study of Oxidative Degradation of Fluoroquinolone Antibacterial Agents in Aqueous Medium**" by **Gajala Tazwar** under my guidance. She has completed the following requirements as per Ph.D. regulations of the University.

(a) Course work as per the university rules.

(b) Residential requirements of the university (200 days).

(c) Regularly submitted annual progress report.

(d) Presented his work in the departmental committee.

(e) Published/accepted minimum of one research paper in a referred research journal,

I recommend the submission of thesis.

Date:

Dr. (Mrs.) Vijay Devra

Supervisor

ANTI-PLAGIARISM CERTIFICATE

It is certified that Ph.D. thesis entitled "**Kinetic and Mechanistic Study of Oxidative Degradation of Fluoroquinolone Antibacterial Agents in Aqueous Medium**" by **Gajala Tazwar** has been examined by us with the following anti-plagiarism tools. We undertake the follows:

a. Thesis has significant new work/knowledge as compared already published or are under consideration to be published elsewhere. No sentence, equation, diagram, table, paragraph or section has been copied verbatim from previous work unless it is placed under quotation marks and duly referenced.
b. The work presented is original and own work of the author (i.e. there is no plagiarism). No ideas, processes, results or words of others have been presented as author's own work.
c. There is no fabrication of data or results which have been compiled and analysed.
d. There is no falsification by manipulating research materials, equipment or processes, or changing or omitting data or results such that the research is not accurately represented in the research record.
e. The thesis has been checked using SMALL SAE TOOLS – Plagiarism checker website and found within limits as per HEC plagiarism policy and instructions issued from time to time.

(Name & Signature of Research Scholar)	(Name & Signature and seal of Research Supervisor)
Place: Kota	Place: Kota
Date:	Date:

ABSTRACT

Pharmaceuticals, specifically fluoroquinolone antibiotics, have acknowledged increasing global concern, due to their intensive use in the environment and potential harm to ecological system as well as human health. Fluoroquinolones are a group of synthetic antibacterial agents that have been extensively used in human and veterinary medicines. Since, their incomplete metabolism is a large fraction of fluoroquinolone released into water system. The existence and accumulation of antibacterial drugs in environment, may pose threats to the ecological community and human health. Hence, oxidation process is important to reduce possibility of health risk that may be combined with fluoroquinolones residues in water. Degradation of antibiotics, such as oxidative degradation by metal oxides, usually plays huge role in the removal of antibiotics from the environment.

The present study gives a a brief review of chemical kinetics, fluoroquinolone antibacterial agents with their environmental impacts, reactive species of oxidants manganese dioxide, hexacyanoferrate(III) and diperiodatocuprate(III) and also covered kinetic and mechanistic study of oxidative degradation of environmentally significant fluoroquinolones by various oxidants in aqueous acidic/alkaline medium in the introduction part. The experimental section describes the details of numerous reagents, chemicals and their solutions with other specifications employed in kinetic study of various reactions and also deal with the description of apparatus, characterization techniques, and analytical procedures to oxidation study.

In this research work soluble colloidal manganese dioxide was formed by the reduction of potassium permanganate by sodium thiosulphate in neutral aqueous medium at 25ºC. The obtained nano sized colloidal manganese dioxide was found to be dark reddish brown in color and stable for several months. Primarily, the formation of manganese dioxide was confirmed by U.V-Visible spectrophotometer. The effect of different concentration of sodium thiosulphate on formation of

manganese dioxide was also studied. The nano sized colloid manganese dioxide was characterized by transmission electron microscopy (TEM) and Fourier transform infrared (FTIR) spectrophotometer. The formed soluble colloidal manganese dioxide was used as an oxidant in oxidation of ciprofloxacin in perchloric acid medium at 35ºC. The reaction was first order with respect to concentration of manganese dioxide and hydrogen ion but fractional order with ciprofloxacin. The rate of reaction is inhibited by F^- ions in particular have been analyzed on the basis of formation of complexes of intermediate by these ions.

This study includes the kinetics of oxidation of levofloxacin by water-soluble manganese dioxide has been studied in aqueous acidic medium at 25˚C temperature. The stoichiometry for the reaction indicates that the 1 mol of levofloxacin oxidized by 1 mol of manganese dioxide. The reaction is second order that is first order with respect to manganese dioxide and levofloxacin. The rate of reaction increases with the increasing $[H^+]$ ion concentration. The Cu(II) catalyzed oxidation of ciprofloxacin (CIP) by hexacyanoferrate(III) (HCF(III)) has been also investigated spectrophotometrically in an aqueous alkaline medium at 40˚C. The stoichiometry for the reaction indicates that, the oxidation of one mole of CIP requires two moles of HCF(III). The reaction exhibited first order kinetics with respect to [HCF(III)] and less than unit order with respect to [CIP] and $[OH^-]$. All the possible reactive species of the reactants have been discussed and a most probable kinetic model has been envisaged.

$$\frac{[Cu(II)]}{k_{obs}} = \left[\frac{1}{kK_1K_2[CIP]}\right]\frac{1}{[OH^-]} + \frac{1}{kK_2[CIP]} + \frac{1}{k}$$

The present study aimed to uncatalysed and Cu(II) catalyzed oxidative degradation of antibacterial drug ofloxacin by hexacyanoferrate(III) in aqueous alkaline medium at 40˚C temperature. The stoichiometry of the reaction indicates that the oxidation of one mole of ofloxacin requires two moles of hexacyanoferrate(III).

The uncatalysed reaction exhibited first order kinetics with respect to [hexacyanoferrate(III)] and [ofloxacin] and less than unit order with respect to [OH^-]. The catalyzed reaction gives first order kinetics with respect to [hexacyanoferrate(III)] and [OH^-] and less than unit order with respect to [ofloxacin]. The major product of the reaction obtained by the decarboxylation of the quinolones moiety and hence it may retain the antibacterial activity. Uncatalysed reaction simultaneously occurs with the Cu(II) catalyzed reaction and the following rate law confirms to all experimental data observed in the reaction.

$$k'' = k_{un} + \frac{K_1 K_3 k\left[Cu(II)\right]\left[OH^-\right]\left[OFL\right]}{K_2 + K_3\left[OFL\right]}$$

Where k'' = (k_{un} + k_c) is the total observed first order rate constant.

This research also explains a kinetic study of oxidation of moxifloxacin (MF) by diperiodatocuprate(III) (DPC) in aqueous alkaline medium. The stoichiometry of the reaction indicates one mole MF oxidizes by two mole of DPC. The reaction was first order with respect to [DPC] and less than unity order with [MF]. The pseudo-first-order rate constant (k_{obs}) changes differently under different concentration of alkali. The results indicates at higher hydroxyl ion concentration DPC complex exist in CuL whereas at lower hydroxyl ion concentration in form of $Cu(HL)_2$.

In all reactions the products were also identified on the basis of stoichiometric results and confirm by the characterization results of LC-MS and FT-IR analysis. A reaction mechanism accounting for all these experimental results has been suggested. All the possible reactive species of the reactants have been discussed and a most probable kinetic model has been envisaged. The activation parameters with respect to the slow step of the mechanism were computed and thermodynamic quantities were also determined.

Candidate's Declaration

I, hereby, certify that the work, which is being presented in the thesis, entitled "**Kinetic and Mechanistic Study of Oxidative Degradation of Fluoroquinolone Antibacterial Agents in Aqueous Medium**" in partial fulfillment of the requirement for the award of the Degree of Doctor of Philosophy, carried under the supervision of Associate Professor **Dr. (Mrs.) Vijay Devra** and submitted to the (**Department of Chemistry**/University Research Center), University of Kota, Kota represents my ideas in my own words and where others ideas or words have been included. I have adequately cited and referenced the original sources. The work presented in this thesis has not been submitted elsewhere for the award of any other degree or diploma from any Institutions. I also declare that I have adhered to all principles of academic honesty and integrity and have not misrepresented or fabricated or falsified any idea/data/fact/source in my submission. I understand that any violation of the above will cause for disciplinary action by the University and can also evoke penal action from the sources which have thus not been properly cited or from whom proper permission has not been taken when needed.

Date: **Gajala Tazwar**

Research Scholar

This is to certify that the above statement made by **Gajala Tazwar** (Enrolment No. 08/000845 and Registration No. RS/1779/ 16) is correct to the best of my knowledge.

Date: **Dr. (Mrs.) Vijay Devra**

Supervisor

ACKNOWLEDGEMENT

All extol and exalt to **Allah the Almighty** who is the cause of all the comprehension, understanding and astuteness the most Gracious the most Compassionate and Beneficent. All peace to the greatest teacher of humanity and mankind, **Holy prophet Muhammad** (Peace Be Upon Him).

First and foremost, I would like to express my deepest sense of Gratitude to my supervisor, **Dr. (Mrs.) Vijay Devra,** Associate Professor, Department of Chemistry, J. D. B. Govt. Girls College, Kota, who always offered her invaluable continuous advice, encouragement and support. Her wisdom, knowledge and commitment to the highest standards inspired and motivated me throughout the course of this thesis. I truly feel thankful to her for managing time out of her busy routine and for his valuable efforts to discuss problems as well as to clarify the fundamentals.

I acknowledge my very sincere gratitude to my co-supervisor **Dr. Naveen Mittal,** Associate Professor, Department of Chemistry, Govt. College, Kota, who has always supported me since the beginning of this very enriching experience. I would like to expand my thanks to **Dr. (Mrs.) Reeta Gulati,** Principal; **Dr. (Mrs.) Laxmi Bhal,** Head, Department of Chemistry and **all faculty members of J.D.B. Govt. Girls College, Kota** for their inspiring guidance and generous support.

My special words of thanks should also go to **Prof. Ashu Rani** (Professor, University of Kota, Kota), **Dr. Arti Shah** and **Dr. Manju Bala Yadav** for her guidance and support throughout the research work. It is an honor for me to convey my special regards to **Dr. Pankaj Kachhawah,** for his genuine interest, continuous encouragement and optimistic support. I would also like to extend my love and thanks to **Pranav** for his scientific inputs and friendly nature.

I would also like to thank my seniors **Dr. Shanu Mathur, Dr. Dhanraj Meena, Dr. Khushboo Shrivastava, Dr. Renu Hada, Dr. Shikha jain and Dr. Ankita Jain** for their guidance and moral support. I would like to thank my fellow researchers **Mahima Sharma, Ajay Rathore, Rashmi** and my friend **Pragya.** I give my worm thanks to **Niharika Nagar** for a great research companion from the very beginning. Our countless discussions, at some times almost on a day to day basis, brought up so many ideas and merged them together in all way.

Finally, I consider myself fortunate to have such wonderful and encouraging parents, my mother **Mrs. Shamim Begam** and my father **Mr. Bundu Ali** who taught me to believe in myself and follow my dreams. I dedicate this thesis to my lovely parents. I express my heartfelt gratitude to my sisters **Tabassum Tazwar, Tarannum Tazwar, Farheen**, my brother in laws **Abdul Mateen, Abdul Asif** and heartbeat of my family, lovely kids **Noor, Aaira** and **Ahad**. I love them so much, and I would not have made it this far without them. I am also very much grateful to all my family members for their constant inspiration and encouragement.

I gratefully acknowledge **SAIF/CIL, Panjab University, Chandigarh** and **MNIT, Jaipur** for sample analysis and characterization. I would also like to thank **ALDOC Pharmaceutical, Kota** for providing drug samples.

Finally, a note of thanks to each and every person who was directly or indirectly involved in this research work. ‘Thanks a lot to everyone….for making me reach this landmark of my life’.

Gajala Tazwar

Contents **Page No.**

List of Tables

List of Figures

List of Schemes

Abbreviations

AOPs	Advanced oxidation processes
CAB	Chloramine-B
CBT	N-chlorobenzotriazole
CIP	Ciprofloxacin
DPA	Diperiodatoargentate(III)
DPC	Diperiodatocuprate(III)
DPN	Diperiodatonickelate(IV)
EDX	Energy dispersive X-ray
ENR	Enrofloxacin
FMQ	Flumequine
FQs	Fluoroquinolones
FTIR	Fourier-transform infrared spectroscopy
HCF(III)	Hexacyanoferrate(III)
LC-MS	Liquid chromatography mass spectrometry
LEV	Levofloxacin
LMF	Lomefloxacin
MF	Moxifloxacin
MnO_2	Manganese dioxides
MPC	Monoperiodatocuptrate (III)
NAL	Nalidixic acid
NOR	Norfloxacin
OFL	Ofloxacin
PIP	Pipemidic acid
SD	Standard Deviation
TEM	Transmission Electron Microscopy
UV-Vis	Ultraviolet-Visible Spectrophotometer

Chapter – 1

Introduction

1.1. Chemical Kinetics

Chemical Kinetics is a very important tool to better understand and describe a chemical process and its complexity. The movement or change in the concentration of a reactant or a product with time, known as "kinetic" in which the velocity of a reaction refers. Thus it is a consolidate study covering the whole of chemistry not only aspects of physical chemistry. Many aspects of biochemistry and pharmaceutical industries can explain by this topic. It plays an important role in the administration of drugs, in addition to respiration and metabolism mechanisms.

On the basis of the observation within the experimental limits, a suitable mechanism is proposed for every reaction. In the reaction molecular bonds break and atoms rearrange according to the order of a reaction with respect to distinct reactive species, this is known as reaction mechanism.The rate of reaction can explain various practical applications during the kinetic study. Although, kinetic studies exactly implement the fundamental facts of the reaction with analytical aspects. Regrettably, the order of a reaction concerning to the reactants and thermodynamic specifications can't explain all the chemical events in a chemical reaction mainly owing to the evidence that the reactions infrequently follow in a single step. In the conversion of the reactants to the products continuously a series of elementary reactions occur and such types of reactions are either complex or composite in nature.

Chemical kinetics has immense scope in which experimental studies includes effect of the concentration, temperature and hydrostatic pressure are discussed on numerous types of reaction. For interrogate of these effects, various types of chemical reactions and broad range of empirical approach has been used. An extensive number of exercises have been applied for the kinetic and mechanistic study of the reaction in the gas phase. In liquid phase, most of kinetic work has been done on reactions, since it is of huge significance to the organic and inorganic reactions, whereas few studies have been reported in solid phase reactions. The present work highly emphasized on kinetic oxidative studies of

fluoroquinolones by different oxidants. The objective of this study is to analysis the role of different oxidizing species of oxidants in the oxidation of fluoroquinolones drugs and on the basis of experimental results, mechanism and rate law have been derived.

1.2. The Fluoroquinolones Antibacterial Agents

Synthetic broad spectrum antibiotics are classified into various types of antibiotics such as fluoroquinolone antibiotics, β- lactum antibiotics, macrolide antibiotics, sulphonamides, lincosamides and tetracycline antibiotics etc. Among these antibiotics fluoroquinolones (FQs) are broadly used antibacterial agents in various applications such as treatment of infections of bacterial origin, treatment of urinary tract infections, treatment of sexually transmitted diseases, bone and joint infections, typhoid fever and tuberculosis etc. [1]. To enhance the antimicrobial spectrum and pharmacological properties numerous derivatives of FQ family drugs have been synthesized. Fluoroquinolone family has diversities in structures mainly within R1 and R7 substituents in the quinolone ring which have comparatively independent properties **(Figure 1.1)**. FQs are interesting from analytical view point due to the presence of double bond between C2 & C3 and presence of both the reducible groups on C3 and C4.

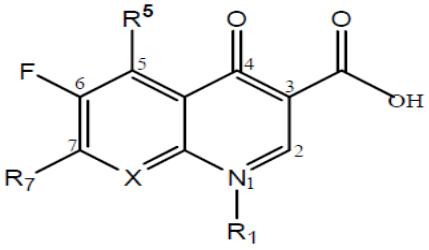

Figure 1.1: General structure of all fluoroquinolones antibacterials.

Fluoroquinolones existof a bicyclic ring arrangement in which there is a substitution at position N-1, with an alkyl group. For antimicrobial activity,carboxylic acid is present at position 3 and similarly a keto group at position 4. On the quinolone carboxylic acid nucleus at position 6 a fluorine atom reinforce adequacy of these compounds and broadens the spectrum of activity across gram-negative pathogens and gram-positive pathogens respectively. The

pharmacokinetics of the compound developed by modifications of the basic structure at positions 2, 5 and 7. These antibacterial agents considered as zwitterions and amphoteric due to the presence of carboxylic acid and one or several basic amines functional groups. In acidic or basic media both functions are uncertain and yield a good solubility for the quinolones.

1.3. Classification of Fluoroquinolones

Fluoroquinolones (FQs) are classified on the basis of their antibacterial activity on gram-positive and gram-negative organisms with the first generation being the narrowest and the subsequent ones having a wider spectrum of activity [2]. They are among the most important classes of synthetic antibacterial agents used in human and veterinary medicines [3]. They are active against many pathogenic bacterial species (both gram-negativeand gram-positive) as gyrase inhibitors, which selectively inhibit bacterial DNA synthesis [4].

Fluoroquinolones can be classified into four generations based on their antibacterial spectrum [5] **(Figure 1.2)**. As a by-product of an antibacterial agent synthesis, quinolones develop unintentionally, with accepted and validate antibacterial activity. The first-generation is now rarely used; various alterations were done to improve their antibacterial activity [6-15]. As a consequence, other quinolones have been arranged and certified that broaden the antibacterial spectrum and the convenience of these drugs.

Second-generation drugs with the addition of fluorine at position 6 of quinolone have improved gram-negative activity and tissue distribution but limited gram-positive activity. These antibiotics are useful for the treatment of a number of bacterial infections.Ciprofloxacin is most commonly used second-generation fluoroquinolone and used in the treatment of many infections.Third-generation FQs have increased activity against gram-positive bacteria and some anaerobic bacteria. Levofloxacin, a chiral fluorinated carboxy quinolone, is the pure (−)-(*S*)-enantiomer of the racemic ofloxacin [16]. It is a third generation fluoroquinolone antibiotic, usually results in death of the bacteria. Fourth-

generation FQs are also unique structurally with a five-member pyrrolidine group at position 7, resulting in improved activity against anaerobic and gram-positive organisms. In this generation gatifloxacin, gemifloxacin and moxifloxacin fluoroquinolone are most ordinarily used drugs. These are worked in the treatment of acute sinusitis, chronic bronchitis, infections of the skin and soft tissues, cystitis, complicated urinary infections and gonorrhea etc. [17] **(Figure 1.3)**.

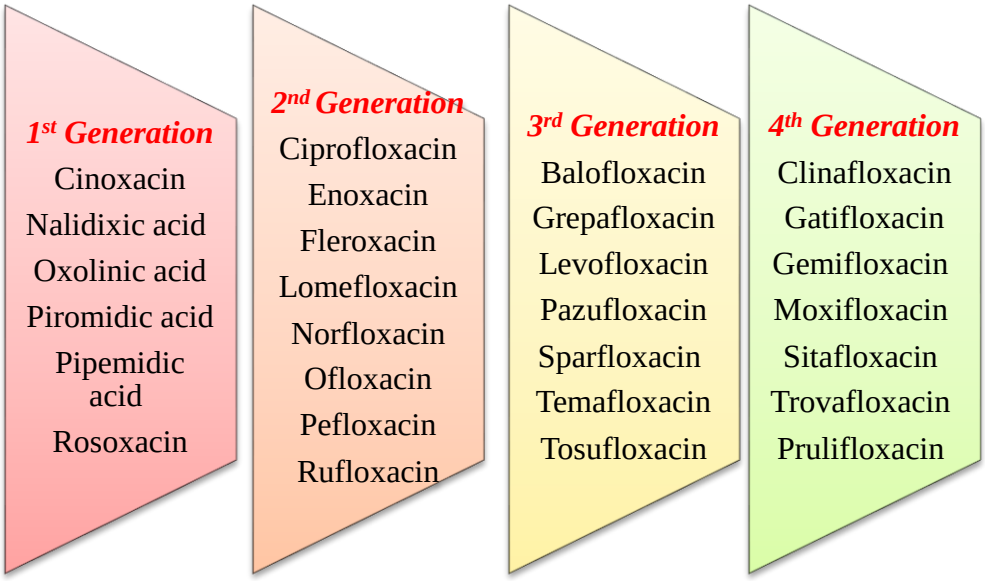

Figure 1.2: Classification of fluoroquinolones.

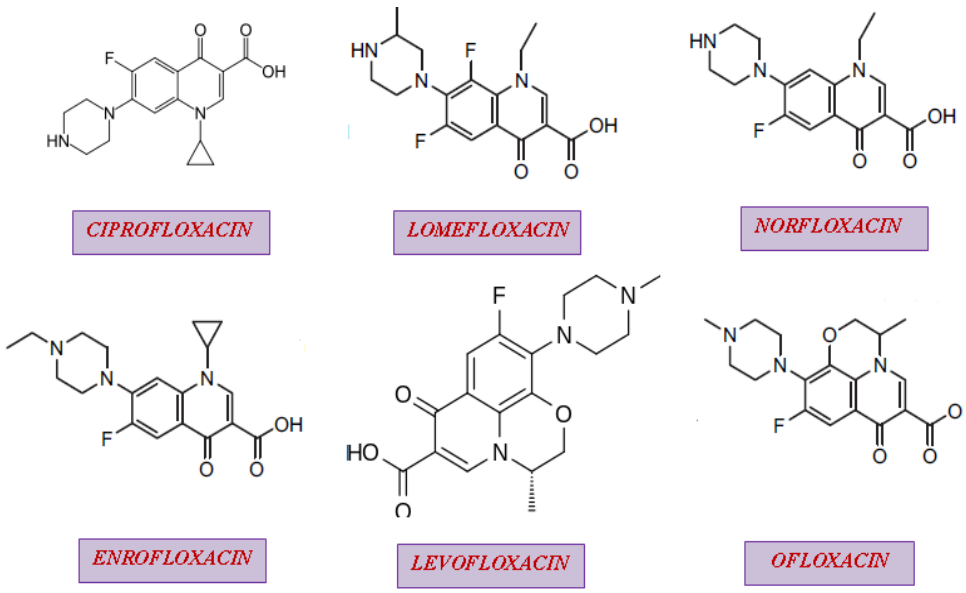

Figure 1.3: Structure of some fluoroquinolones.

1.4. Environmental Impacts of fluoroquinolones

Fluoroquinolones (FQs) are a class of extensively recommended antibiotics and have been usually exposed in the aquatic environment due to their applications. Mostly FQs spilled into waste water through humans and animals due to its partial metabolization [18]. Presence of these antibacterial agents has great concern and big threat for the environment. The possible effects of FQs on the environment are of appropriate interest because of their qualities as bio-active chemicals. Due to complex chemical structure, their behaviour in the environment is not always easy to estimate. Pharmaceutical wastes are received into the environment through hospitals, veterinary clinics, pharmaceutical industry effluents, and household effluents **(Figure 1.4)** [19].

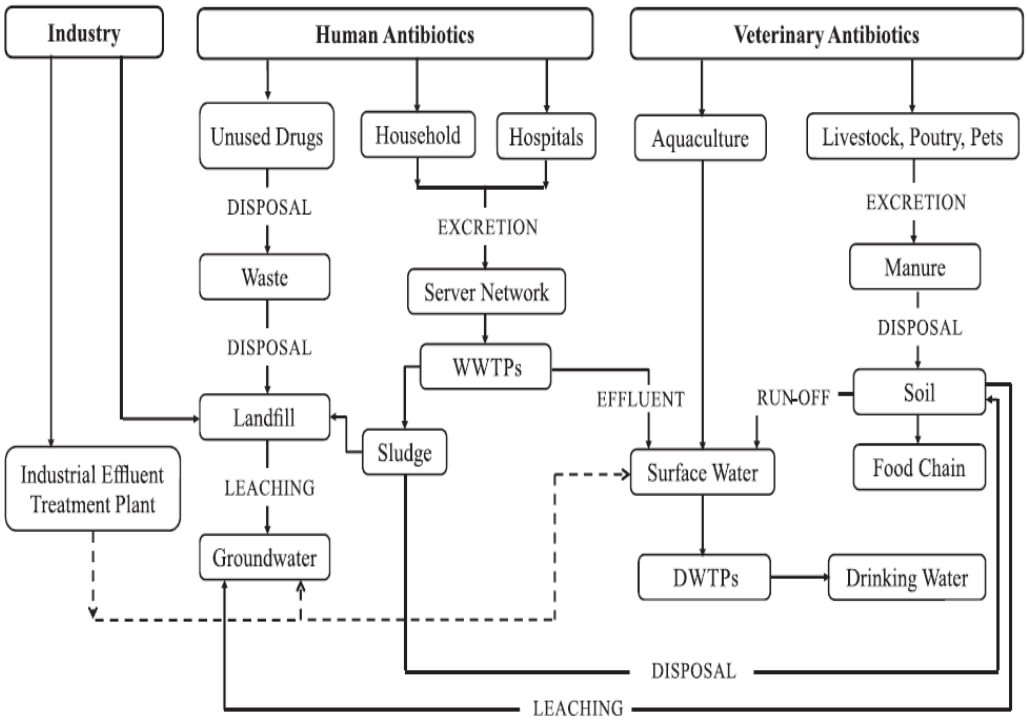

Figure 1.4: Distribution of fluoroquinolones antibacterial agents in the environment [19].

There is major concern that antibiotics emitted into the aquatic environment can reach drinking water, or that they may effect on-target organisms in the environment. These pharmaceuticals have risen as a unique class of

pollutants because of their probable unfriendly effects on human health and the environment [20, 21]. So to dispose of these undesirable pollutants from environment that can probably source various injurious effects to human health, many medication procedures are selected to make convinced the water discharged is antibiotic free. For the treatment of these deadly antibiotics several methods have been employed for example photo fenton, ozonation, chlorination, ion exchange filtration, biodegradation etc [22]. Among these methods oxidative degradation of antibacterials are of great interest due to their conversion into inactive intermediates **(Figure 1.5)**.

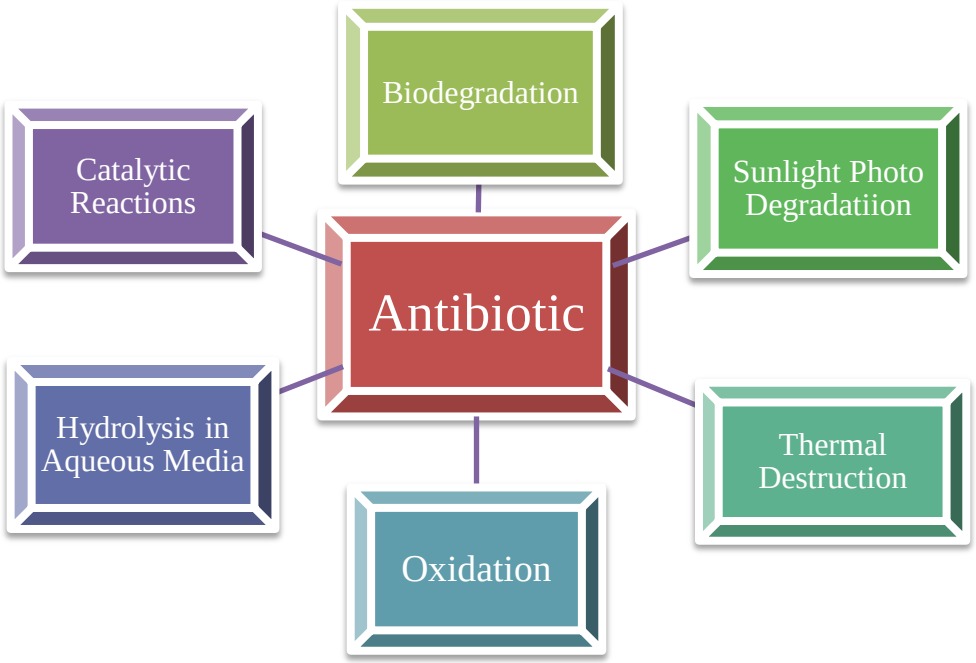

Figure 1.5: Degradation of antibiotics through various techniques.

1.5. Oxidation of Fluoroquinolones

Oxidation process has ability to oxidize organics to inactive intermediates or CO_2, H_2O, and salts and play important role in water treatment. Advanced oxidation processes (AOPs) [23] have been analysed as potential transformation procedures for degradation of fluoroquinolones. Several studies have reported the formation of degradation products through the oxidation of fluoroquinolone antibiotics by AOPs [24-34]. AOPs are alternatives to conventional waste-water remedies. These processes apply free radical mechanisms to directly degrade

fluoroquinolones. Taicheng et al reported kinetics and mechanism of AOPs in the degradation of ciprofloxacin (CIP) with several free radicals, $^{\bullet}OH$, $^{\bullet}N_3$, $SO_4^{\bullet}$ and hydrated electrons [35].

The various oxidation studies by potassium permanganate were reported for oxidation of FQs [36-43]. Among these studies the kinetic and mechanistic investigation of oxidation of emerging contaminant Lomefloxacin (LMF) by alkaline permanganate was carried out spectrophotometrically [44]. The stoichiometry was found to be 1:2, that is, 1 mol of LMF reacted with 2 mol Mn(VII) **(Scheme 1.1)**. The oxidation–degradation mechanism and pathway suggested for LMF, along with the eradication of piperazynilic ring, propose the efficient oxidation by permanganate can be used in thewater treatment at the place polluted by fluoroquinolone antibacterial agents. These results indicate that attractive treatment technologies for the degradation of FQs in aqueous solution are needed because under oxidation–degradation process mostly produced intermediates can be finally mineralized into CO_2, water, and mineral species.

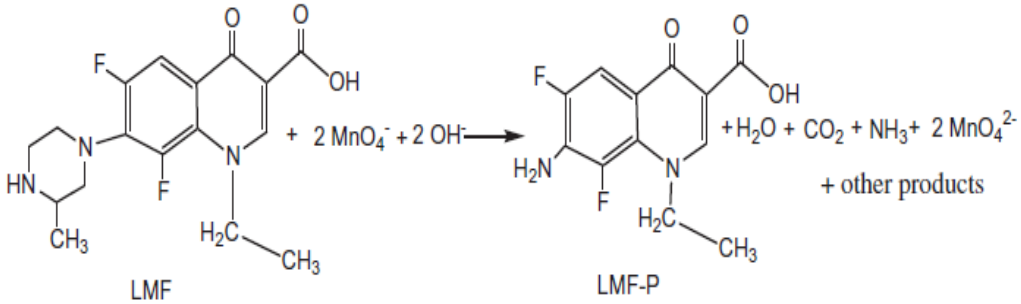

Scheme 1.1: Stoichiometric equation for the oxidation of lomifloxacin by alkaline permanganate [44].

Whereas another study [45] describes the oxidation of another fluoroquinolone drug, ciprofloxacin by $KMnO_4$ shows stoichiometry 5:2, that is, 5 mol of CIP reacted with 2 mol Mn(VII) **(Scheme 1.2)**. This reaction proceeds through ring opening, dealkylation and deamination, which finally yielded 7-amino fluoroquinolone product.

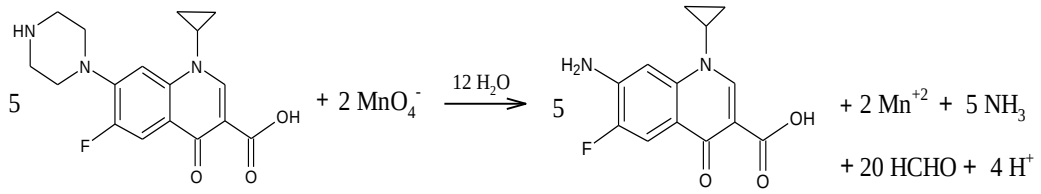

Scheme 1.2: Stoichiometric equation for the oxidation of ciprofloxacin by alkaline permanganate [45].

Oxidation study of ClO_2 with seven FQs {ciprofloxacin (CIP), enrofloxacin (ENR), norfloxacin (NOR), ofloxacin (OFL), lomefloxacin (LMF), pipemidic acid (PIP) and flumequine (FMQ)} and three structurally related amines described that FQs with piperazine groups are more reactive to ClO_2 [46]. FQs follow the order of OFL > ENR >CIP ~ NOR ~ LOM >> PIP in reactivity. Oxidation of dealkylation, hydroxylation and intramolecular ring closure at the piperazine moiety, while quinolones ring remain mostly intact. In contrast, ENR reacted faster than CIP with chlorine dioxide [46]. Similarly, during ozone oxidation ENR reacted at higher rates than CIP at neutral pH [47]. However, ENR and CIP had comparable reaction rates with manganese oxide [48]. De Witte et al. [49,50] analyzed twelve degradation products formed in the case of the oxidation of ciprofloxacin by ozone although eleven species were recognised for levofloxacin.

The oxidation of levofloxacin (LEV) was reported by different oxidants like O_3 and hydroxyl radical, Cl_2, chloramine-T and N- bromo succinimide in acidic/alkaline media [51-56]. A Kinetic study of chlorination of LEV was performed at pH 7.2 [52]. Whereas Najjar et al. [53] reported between the pH values 4.2 and 8.2 **(Scheme 1.3)**. Xiao et al. [57] reports the degradation study of ciprofloxacin (m/z 332) by cryptomelane-type manganese(III/IV) oxides and Nanda et al considered kinetic and mechanistic study on the oxidation of ciprofloxacin by chloramine-B in acidic medium [58].

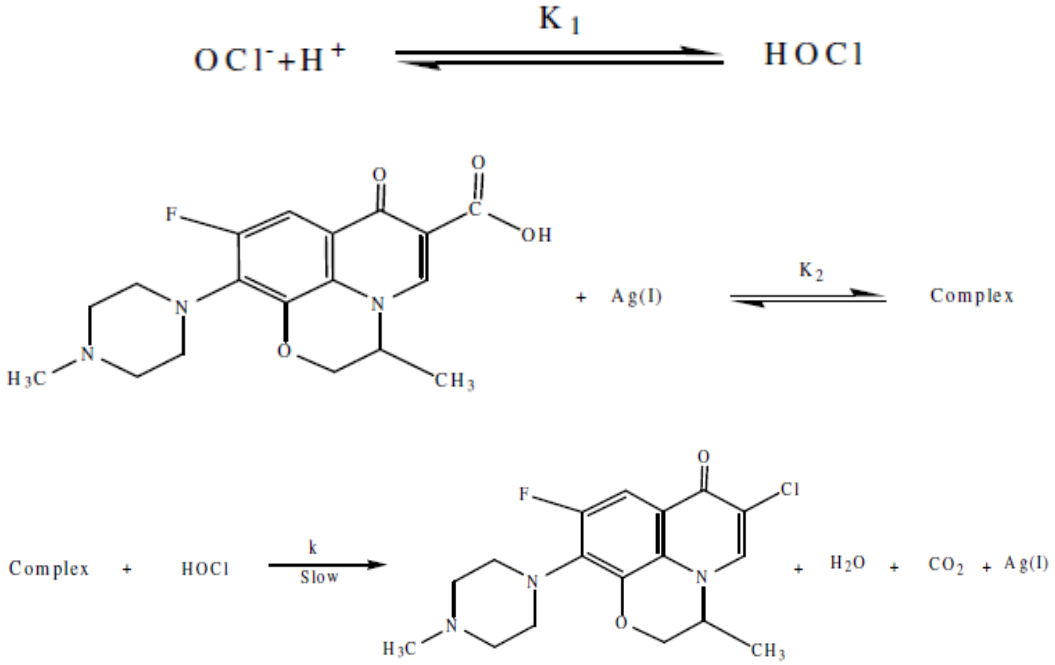

Scheme 1.3: Chlorination of levofloxacin [53].

Their actions of ozone and hydroxyl radicals with enrofloxacin and ciprofloxacin lead to stoichiometric elimination of antibacterial activity, indicating that the oxidation products retained significantly less antibacterial potency [59]. Some structural changes such as dealkylation, amides in piperazine ring, oxygen transfer to the double bond in quinolone structure and formation of alcohols, are analysed in CIP and ENR molecule. In the oxidation reaction of CIP and ENR, by Fe(VI), dealkylation and formation of alcohols in piperazine ring performed by these antibacterial drugs [60]. As well as, hydroxylation of the rings and cleavage of the double bond at the six member heterocyclic ring occurred in kinetics of CIP with Fe(VI) [61].

Zhang et al. [62] studied the adsorption and oxidation of seven fluoroquinolones (CIP, ENR, NOR, OFL, LMF, PIP, FMQ) and structurally related amines with goethite. The piperazinyl ring is favourable to oxidation while the carboxylic group of fluoroquinolone is critical for adsorption. In comparison to the work of Zhang et al. [48] on the interactions of FQs with manganese oxide,exhibited reactivity in the order of CIP ≈ ENR ≈ NOR ≈ OFL> LMF > PIP>> FMQ. FQs have different adsorption sites (piperazine ring versus

carboxylic group, respectively) but the same oxidation site (the piperazine ring) toward manganese and iron oxides. Although different adsorption behaviour is involved with these two oxides, the same radical-based oxidation mechanism is present in both cases. The reaction kinetics ofantibacterial with MnO_2 is also illustrated by Zhang et al. [63] and explained that it is controlled by the rate of electron transfer within the precursor complex.

Various fluoroquinolone antibacterial agents also oxidized by cerium(IV) sulphate in acidic medium such as ofloxacin, levofloxacin, ciprofloxacin, pefloxacin and sparfloxacin [64-67]. Oxidation of norfloxacin with cerium(IV) was studied in 0.3 M hydrochloric acid media [68] through the following reaction **(Scheme 1.4)** with the stoichiometry of the reaction 1:4 (norfloxacin: Ce^{4+}).

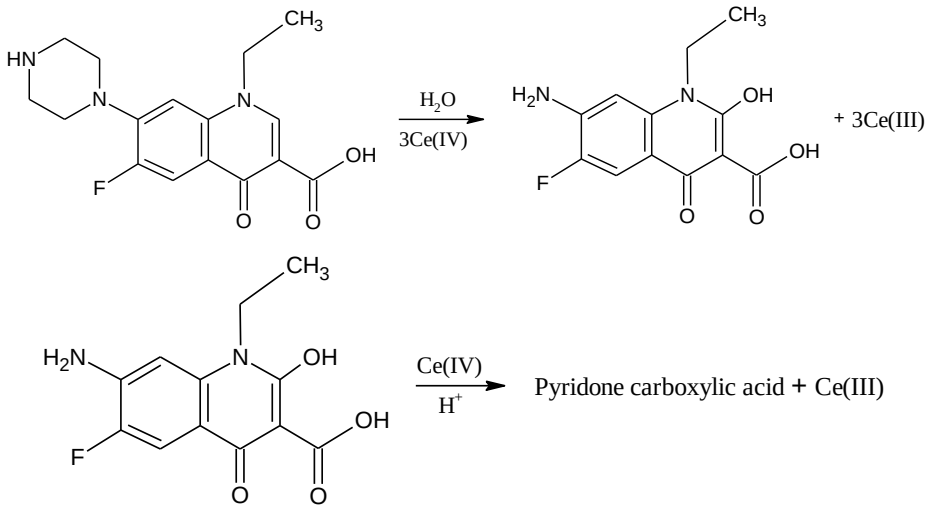

Scheme 1.4: Oxidation of Norfloxacin with Ce(IV) [68].

Nanda et al. considered kinetic and mechanistic studies on the oxidation of norfloxacin by chloramine-B (CAB), N-chlorobenzotriazole (CBT) [69]. These studies illustrated 4:1 DPA:NOR stoichiometry and the reaction follows a first-order dependence on [oxidant], a fractional order on [NOR], and an inverse-fractional order on $[H^+]$. Padavathil et al has been find out the reactivity of norfloxacin toward Diperiodatoargentate(III) (DPA) and appear at a plausible mechanism [70]. The reaction illustrates 1:1 DPA:NORstoichiometry and is first order in DPA but fractional order in both NOR and alkali. The main reaction

products were established as Ag(I) and 1-ethyl-6-fluoro-2-hydroxy-4-oxo-7-piperazin-1-yl-1,4-hydro-quinoline-3-carboxylic acid. Among various species of DPA in alkaline medium, $[Ag(H_2IO_6)(H_3IO_6)]^{2-}$ is treated as active species for thetitle reaction **(Scheme 1.5).**

$$[Ag(H_3IO_6)_2]^- + OH^- \overset{K_1}{\rightleftharpoons} [Ag(H_2IO_6)(H_3IO_6)]^{2-} + H_2O$$

$$[Ag(H_2IO_6)(H_3IO_6)_2]^{2-} + 2H_2O \overset{K_2}{\rightleftharpoons} [Ag(H_2IO_6)(H_2O)_2] + H_3IO_6^{2-}$$

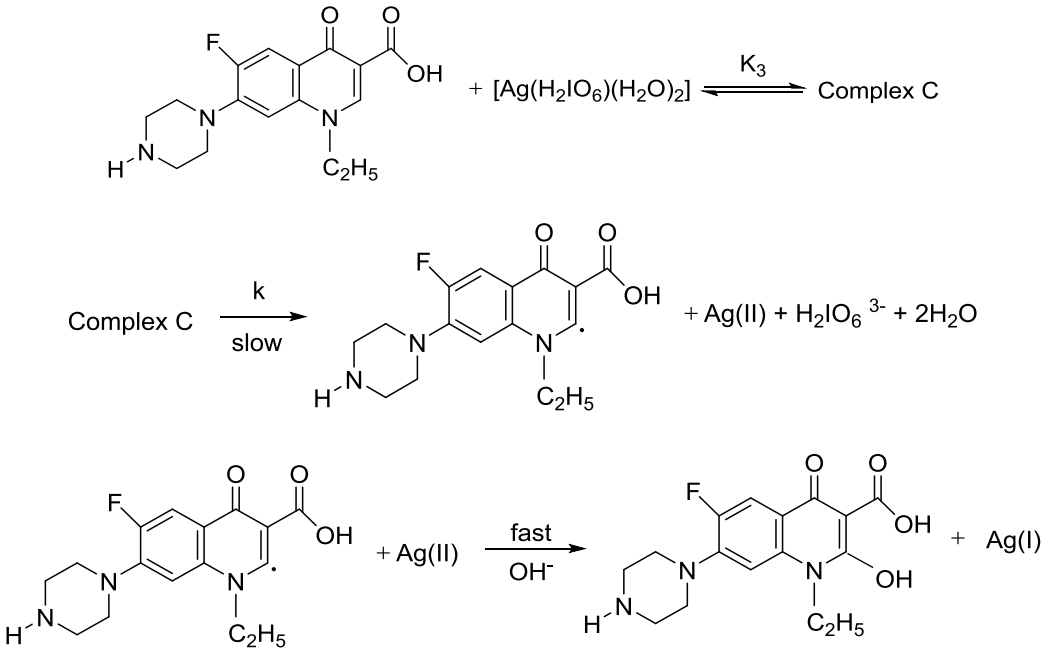

Scheme 1.5: Oxidation of norfloxacin by diperiodatoargentate(III) [70].

Fluoroquinolones are compounds responsive to photodegradation process, which may lead to reduction of their antibacterial activity and to producephoto toxicity as a side effect. Hubicka et al [71] illustrate an elementary, precise UPLC-MS/MS method for the persistence of CIP, OFL, NOR and moxifloxacin (MF) in the presence of photo degradationproducts. The photo degradation process was found mainly to affect 7-amine substituent, while the fluoroquinolone origin remained unchanged. The only exception was MF, which assembled product of decarboxylation and partial reduction of dihydropiridine ring. Therefore oxidation study is more significant due to drug degrade into inactive intermediates and products.

1.6. Oxidants

1.6.1. Manganese dioxide

Manganese shows variable oxidation state from +7 to +2. Among them, the most stable oxidation states are +2, +4and +7. Manganese, frequently present as Mn(IV) oxide/hydroxide colloidal particles shows an essential appearance in inducing chemical conversions of organic compounds in the aquatic ambience. Due to the presence of manganese ions with different oxidation states manganese dioxides (MnO_2) exhibit appreciable activity in oxidation–reduction reactions. It has been most broadlyconsidered due to its valuable oxidizing property [72-75] and logically immense catalytic activity [76-80]. MnO_2 has fascinated comprehensive significance by cause of its low price, high strength, environmental-affinity and generous availability [81-83]. It display variable valence and thus has been universally explored and extensively used in catalysis, oxidation and electrochemical capacitor objectives [84–89].

Nano structure materials acquire enhanced physical and chemical properties so it's become more and more attractive use in recent years. Manganese oxide is one of the most fascinating materials, which has a large diversity of structure with huge surface area and utilized in environment protection ground as anadvanced generation of environmental friendly catalyst. The diverse structures, chemical properties of manganese oxides are appropriated advantage of in potential wide catalytic applications, such as photocatalytic oxidation of organic pollutants and waste water treatment [90]. MnO_2 with various physical and chemical properties, such as crystallinity, amount of combined water, unique surface areas, and electrochemical performance, can be yielded under different synthesis conditions.

It is a kind of attractive inorganic material, and material scientists have made great attempt on the synthesis of MnO_2 [91-93]. Although heterogeneous reaction conditions are relevant for synthetic chemistry, the insolubility of manganese dioxide in water has limited its analytical application. Perez-Benito *et al*. [94] creates quantitatively first time that water-soluble colloidal manganese

dioxide can be prepared from reduction of aqueous $KMnO_4$ by $Na_2S_2O_3$ under neutral condition. It has been also prepared by the reduction of $KMnO_4$ by $Mn(ClO_4)_2$ in aqueous solutions [95], and also by $MnSO_4$ in the presence of sodium polyphosphate [96]. Several forms of stable and perfectly transparent colloidal MnO_2, either in aqueous [97] or organic media [98] have been synthesized and the kinetic study of its oxidizing behaviour in redox reaction was studied by ordinary UV-visible spectrophotometeric approach [99]. Due to the solubility of colloidal manganese dioxide, it has various applications in many reactions as a homogeneous catalyst.

$$2MnO_4^- + 3MnSO_4 + 2H_2O = 5MnO_2 + 4H^+ + 3SO_4^{2-}$$

$$8MnO_4^- + 3S_2O_3^{2-} + 2H^+ = 8MnO_2 + H_2O + 6SO_4^{2-}$$

$$2MnO_4^- + 3HCOOH + 2H^+ = 2MnO_2 + 4H_2O + 3CO_2$$

The reduced manganese ions changes brown transparent solutions with a distinctive absorption spectrum, in the favourable conditions. The formation of reduced entities is observed by measuring the absorbance of the reaction mixture at around 400 nm, and composingneeded corrections for the contribution of the starting materials. The $KMnO_4$ concentration shows gradually decreases till the certain stage of the reaction is reached; then, shows a quick decrease [100]. Initially, the forming manganese species was Mn(V) [101,102]. The later reactions have described that only soluble form of Mn(IV) is exist and it has been preliminary analysed as H_2MnO_3 [103,104]. Colloidal nature of forming manganese compounds presenting as soluble colloidal MnO_2 has been recently established [105–110]. The spectrum of MnO_2 shows a broad band with a wide maximum at 390 nm covering the unified visible region, and the absorbance evenly decreases with increasing wave length [111].

Manganese oxide minerals generallyexist as coatings and fine-grained aggregates with large surface areas; they easily perform a wide variety of oxidation–reduction and cation exchange reactions in soils and sediments [112]. It has been verified that manganese oxide plays an essential role in determining the

fateand transformation of organic/inorganic pollutants via adsorption, hydrolysis, and/or redox reactions. For example, manganese oxides act as catalysts in the formation of humic substance via their reactions with naturally occurring polyphenols [113,114], and act as strong oxidants in the transformation of a wide range of anthropogenic organic/inorganic pollutants.

Manganese dioxide (MnO_2) is one of the most important natural oxidant with an oxidation potential of 1.23 V [115]. It has been shown to be capable of oxidizing a wide range of organic contaminants [116-119]. By adsorption, hydrolysis, and redox reactions in soil and aquatic environments MnO_2 has reactive surfaces for affecting the fate and transformation of organic pollutants [120,121]. It has been extensively studied as an oxidative agent in soils, sediments, and marine environments [122].

The characteristics of the oxidative transformation of the antibiotic levofloxacin (LEV) bymanganese oxide were reported by Yuan Li et al [123]. A tentative transformation route of LEV in the manganese oxide scheme involving oxidation and dealkylation was recommended. The molecular structures of the products and parent LEV basically differed in the variations of the piperazine ring **(Figure 1.6**). This result indicated that the original piperazine ring had the strongest genotoxicity effect, and any conversion (such as oxidation, dealkylation) of the piperazine ring decreases the genotoxicity of the compound. These results illustrate that the piperazine ring skeleton naturally contributed to the antibacterial activity of quinolones antibiotics.

Singh et al. [124] studied the kinetics of the oxidation of norfloxacin by alkaline water soluble colloidal MnO_2 at 25 °C. NOR and Mn(IV) show 1:1 stoichiometry respectively. Oxidation reaction of NOR with MnO_2 illustrated the presence of product with molecular mass and molecular formula m/z 310 and $C_{14}H_{16}FN_3O_4$ respectively. This reaction indicates loss of C_2H_2 at the piperazinyl substituent and addition of oxygen atom via opening of the piperazinyl ring and formed hydroxyl derivatives **(Scheme 1.6)**. The product formation of this study

resembles with the Yuan Li et al [123] reaction mechanism which also describe the ring opening of piperazine moiety and dealkylation process.

$$C_{16}F_{18}N_3O_3 + 2H_2O + MnO_2 \rightarrow C_{14}H_{16}FN_3O_4 + MnO_2^{2+} + 2OH^- + CH_3CHO$$

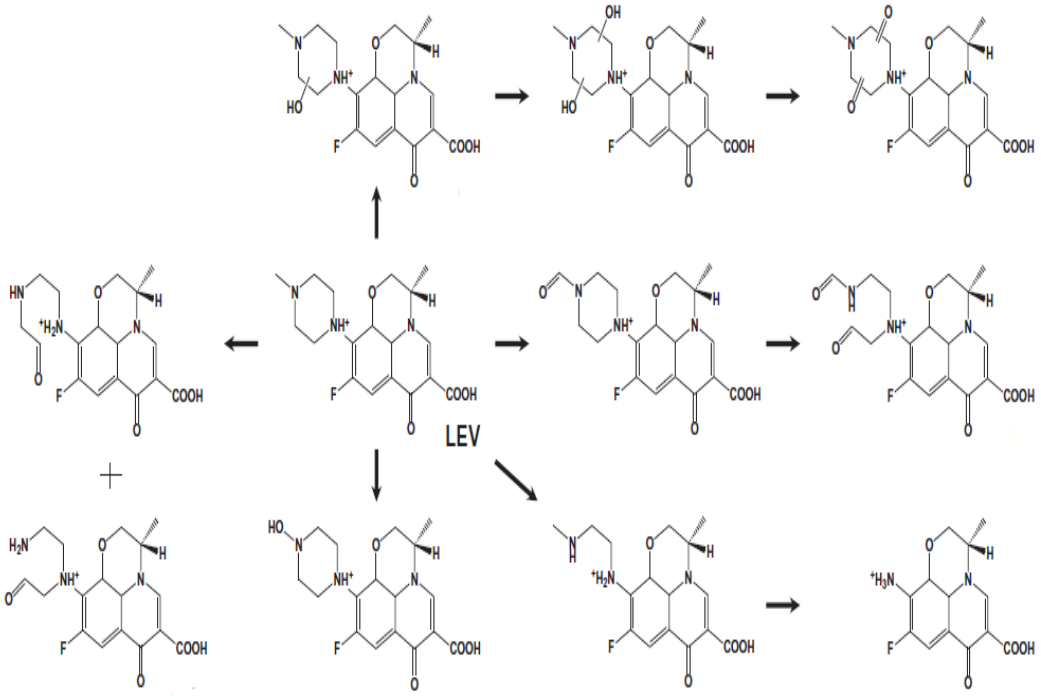

Figure 1.6: Different oxidation products of levofloxacin by manganese dioxide [123].

More recently, MnO_2 has been applied to remove different kinds of organic micro pollutants, including antibacterials and related compounds with phenolic and fluoroquinolonic moieties, aromatic *N*-oxides, tetracyclines, and estrogenic compounds such as the synthetic hormone 17R-ethinyl estradiol [125]. A mechanism involving sorption of the compound to the oxide surface and subsequent electron transfer has been proposed [48]. The removal of micro pollutants such as synthetic hormones, anti-inflammatory drugs, antibacterial agents, bisphenol A, phenols, sulfides , 2-mercaptobenzothiazole (2MBT) and sulfadiazine have been achieved by MnO_2 [126, 127]. MnO_2 nano materials may offer efficient and innovative solutions for organic pollutant degradation [128, 129].

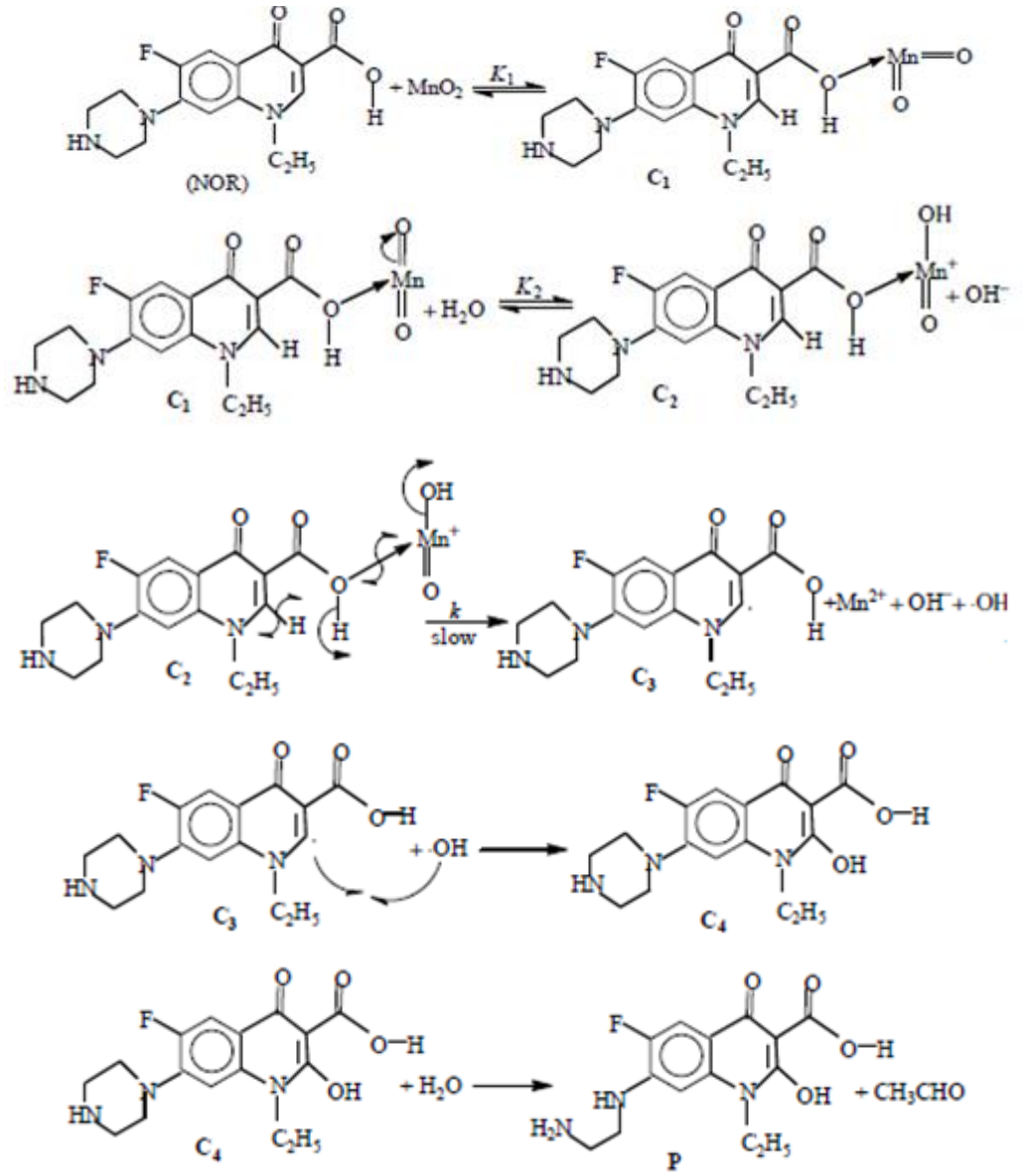

Scheme 1.6: Mechanism for the oxidation of norfloxacin by alkaline Mn(IV) [124].

Organic pollutant degradation (catalysis and oxidation) by active metal oxides strongly depends on pollutant approximation to the surface, thus, MnO_2 with high specific surface area (existing unique layers or tunnels in crystal lattices) is expected to show superior property in the degradation of environmental effluents in different surroundings. The colloidal MnO_2 has been used as the auto catalyst in many reactions of permanganate [130,131]. Among the oxides of

manganese Mn(III) and Mn(IV) oxides play important role as a oxidizing agents for various organic compounds.

In supported or unsupported forms only manganese oxides or with other transition metal, it is highly active and thermally stable catalysts for oxidation of various organic compounds e.g., catalytic oxidation/degradation of volatile organic pollutants, ozone decomposition, nitric oxide reduction, selective oxidations of carbon monoxide, cyclo hexane, ethyl benzene, ethanol and 2-propanol, decomposition of hydrogen peroxide [132] etc.

1.6.2. Hexacyanoferrate(III)

Various oxidation states of iron from +3 to +6 have gained much attention as environmental friendly oxidants. Iron (III) complexes as oxidant has acknowledged great interest due to cost-effective availability, less adversity involved in the evaluation and its capability to react in both acidic and alkaline medium. Due to the loss of degeneracy of the d orbitals, these transition metal and transition metal complexes and ions are often coloured. Hexacyanoferrate(III){HCF(III)} is a transition metal complex, consisting of a central iron ion, surrounded by six negative cyanide ions, or ligands, in an octahedral arrangement. Iron (III) is an environment friendly oxidant and used as coagulant for water and waste water treatment [133,134]. The oxidation capacity completely depends on their redox potential [135]. It is a one electron oxidant with a redox potential of couple $[Fe(CN)_6]^{3-}/Fe(CN)_6]^{4-}$ is +0.36 V in acidic medium and +0.45 V in basic medium.

$$\mathbf{[Fe(CN)_6]^{3-} + e^- \rightarrow [Fe(CN)_6]^{4-}}$$

In most of the oxidations, hexacyanoferrate(III) is mainly used as hydrogen atom abstractor [136, 137] and/or free radical generator [138]. HCF(III) is an efficient one-electron oxidant that has been observed to be inert to substitution [139]. It is highly stable, water soluble and has moderate reduction potential of 0.45 V and reduce into a stable product as hexacyanoferrate(II) [140]. Further, it adds less error to the experimental results; since data can be evaluate

extremely to build the reaction path. Due to its strong oxidizing properties, it has been extensively employed as reagent in analytical investigation of many compounds like hydrazine hydrate, atropine sulphate and arginine, esters, etc. [141-143]. Potassum ferricyanide is used to determine the reducing power potential of a sample (extract, chemical compound, etc.) into ferric [144], this determination helps to measurethe antioxidant property of a sample.

HCF(III) has been widely used to oxidise numerous organic and inorganic compounds in alkaline media [145-149]. Principally, its stability over the unified pH scale and being a moderate oxidant, its reactions with nitrogen containing compounds are not facile so require catalyst for reaction with measurable rate [150]. Therefore, metal/metal oxide has been used widely for catalysing such reactions [151, 152]. Kinetic study of oxidation of the fluoroquinolones such as ciprofloxacin (CIP), norfloxacin (NOR), enrofloxacin (ENR) and nalidixic acid (NAL) was investigated with HCF(III) by measuring the absorbance at 420 nm. In absence of catalyst alkaline hexacyanoferrate(III) exhibit almost no reaction with these quinolones whereas in presence of catalyst react with the remarkable rate. In alkaline medium kinetic study of osmium tetra oxide catalyzed oxidation of these fluoroquinolones (CIP, NOR, and ENR) with HCF(III) show that the rate of reaction is directly proportional to the concentration of OsO_4.

Among these FQs nalidixic acid showed no reaction with HCF(III) even in the presence of the catalyst, suggests that piperazine ring is the active site for oxidation of fluoroquinolones by HCF(III), which agrees with theresults of this investigation using electrochemical oxidation methods.The dependence of other reaction parameters such as concentration of reactants, catalyst, hydroxide ion, potassium hexacyanoferrate(III) and salts, as well asthe temperaturewas investigated [153]. Results indicates that rate of oxidation increased withincreasing the hydroxide ion concentration, and decreased withincreasing the $K_4[Fe(CN)_6]$ concentration and the rate was unaffected by the added salts concentration.

In these FQs the inner nitrogen (N_1) of the piperazine ring is the rate limiting reactive site which explains the reactivity of the FQs. For example, CIP and NOR differ only in the substituent (i.e. cyclopropyl versus ethyl) at the nitrogen atom of the aromatic heterocyclic ring. ENR differs from CIP only in its ethyl substituent at the outer nitrogen (N_6) of the piperazine ring.

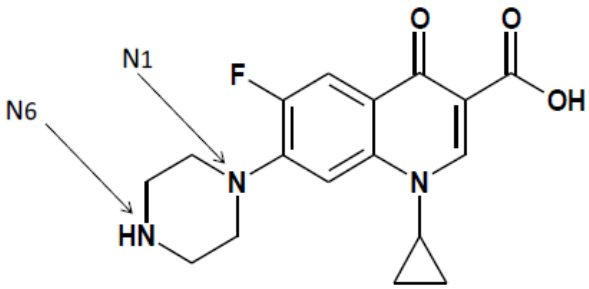

Figure 1.7: The chemical structure expresses the positions of the substituent at the different nitrogen of the piperazine ring [153].

So the rate of oxidation of the studied fluoroquinolones by HCF(III) is followed the order: CIP> NOR> ENR. The rate of oxidation of aliphatic amines was initiated to follow the order; primary < secondary < tertiary due to the increased basicity of nitrogen atom of the amine. Tertiary amines reacted at an average 4-fold faster rate than secondary amines [154]. If the rate-limiting step was associated with the outer nitrogen atom, then CIP (a secondary amine) would react slower than ENR (a tertiary amine). Oxidation of anilines and substituted anilines with hexacyanoferrate (III) was studied by Dasgupta and Mahanti [155] suggests formation of an aminium radical cation and radical intermediate. Due to some synthetic utility ferricyanide oxidation has become known as Decker oxidation [156].

The kinetic study of oxidation of levofloxacin by HCF(III) in aqueous alkaline medium studied by Patgar et al. [157]. The oxidant and reductant modified their oxidation state by diverse number of units, thus this oxidation is a non-complementary reaction with oxidant carry one equivalent change **(Scheme 1.7).**

Alkaline HCF (III) ion simply acts as an electron abstracting reagent in redox reactions. Though, Speakman and Waters [158] have recommended different paths of oxidation of aldehydes, ketones and nitroparaffins. While, Singh and co-workers [159] have recommended the oxidation study of formaldehyde, acetone and ethyl methyl ketone through an electron transfer process via a free radical intermediate formation.

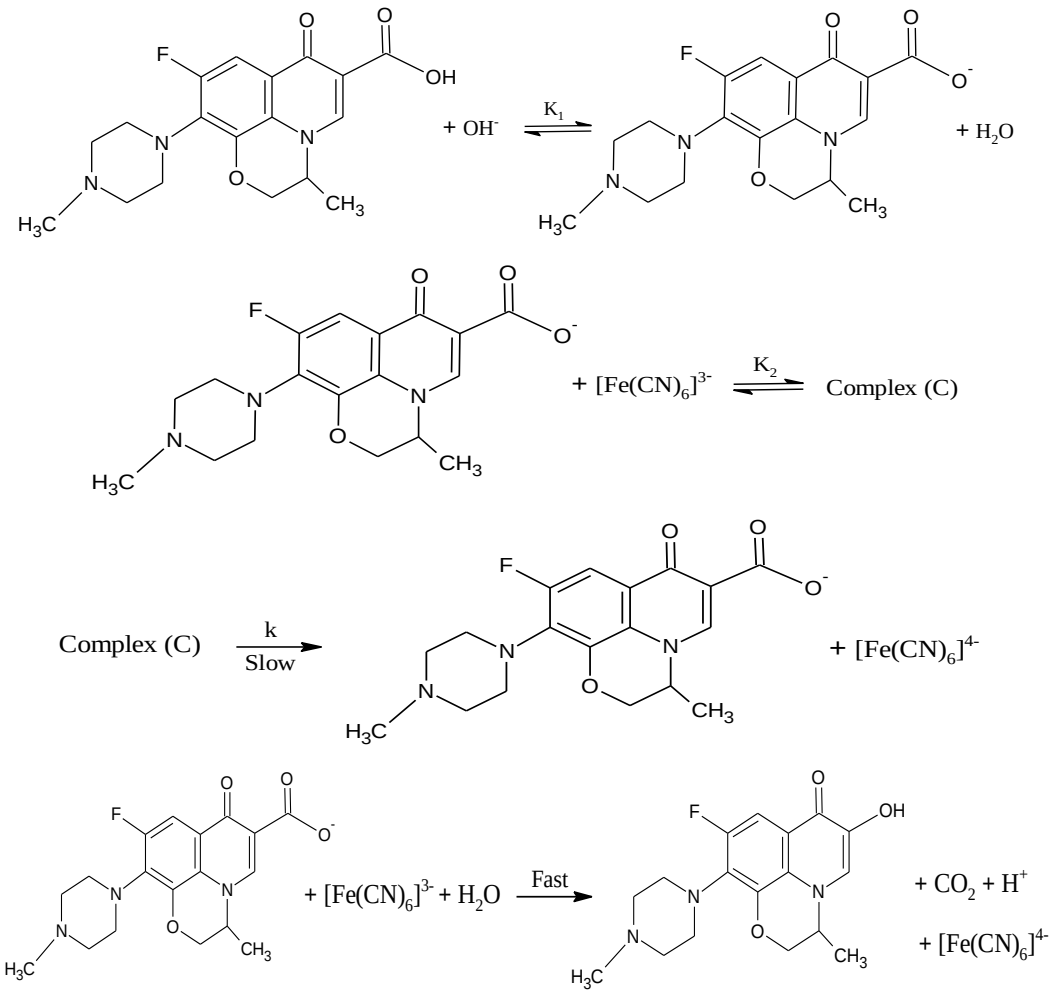

Scheme 1.7: Mechanism shows the oxidation of levofloxacin by hexacyanoferrate(III) [157].

1.6.3. Diperiodatocuprate(III)

Transition metals such as diperiodatocuprate(III) (DPC), diperiodatoargentate(III) (DPA) and diperiodatonickelate(IV) (DPN) which exhibit multiple oxidation states can form stable complex compounds at higher oxidation states with suitable polydentate ligands [160-162]. A flexible one-electron oxidant, DPC [163] is inadequate or scantyin oxidation reactions due to its poor solubility and stability in aqueous medium [164-169]. It also used as an analytical reagent [170].

Diperiodatocuprate(III) was first synthesized by Malatesta [171] more than half a century ago. A considerable amount of research has been reported since on the synthesis, structural determination and analytical applications of this complex [172-174]. However, some of the results are mutually contradictory regarding the extent of protonation of the DPC species in alkaline medium, and the various equilibria existing between them. Copper(III) has more oxidizingproperty than dichromate and permanganate in alkaline media. Due to its abundance it explains various oxidation reaction and important in biological chemistry [175]. It is also an analytical reagents and play essential role in biological electron transfer. Copper complexes areattractive due to their uses as antimicrobial, antiviral, anti-inflammatory, antitumor agents, etc. [176]. Copper(III) periodate complex has multiple equilibria between differentcopper(III) species and it describe species as an active oxidant.

A metal chelate, DPC is a good oxidant[177] in a medium with an appropriate pH value. The synthesis, structural determination and characterization of DPC have been reported [178,179]. In the analysis of certain organic compounds trivalent state periodate complexes of copper have been largely used [180]. The kinetics of self-decomposition ofthese complexes was studied with detail [181]. Diperiodatocuprate(III) (DPC) is used in kinetic studies of the oxidation of various inorganic and organic substrates [182]. As a green and inexpensive oxidant, DPC has been widely used in the oxidative degradation study of antibacterial agents for waste water treatment processes. Considerable

amount of work has been done on the oxidation of various drugs by DPC in aqueous acidic/alkaline medium.

In earlier report on kinetic and mechanistic study of oxidation of fluoroquinolone antibacterial agent, norfloxacin by DPC in aqueous alkaline media has been studied spectrophotometrically at 300 K and at constant ionic strength of 0.20 mol dm^{-3} [183]. The stoichiometry was found to be 1:2 ([NOR]:[DPC]). LC–ESI–MS and other spectral techniques were used for the characterization of oxidation products. Mono periodatocuprate(III) is an effective species of DPC. On the basis of experimental results an applicable scheme was planned (**Scheme 1.8**).

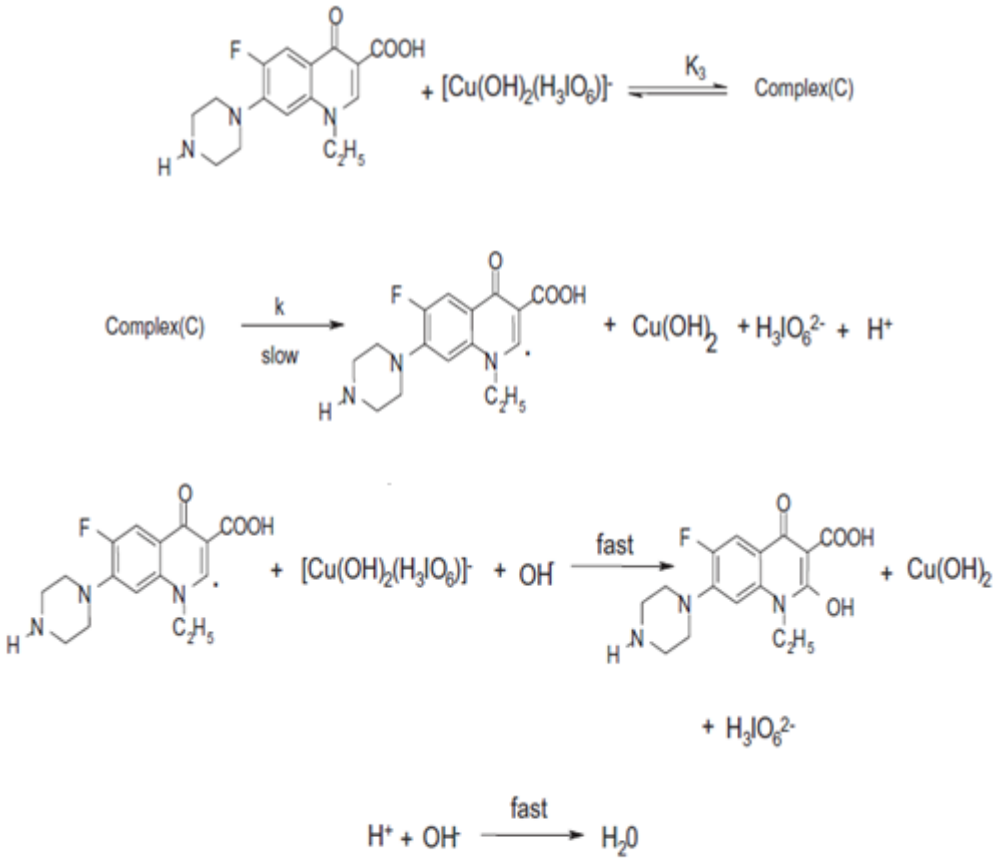

Scheme 1.8: The oxidation of norfloxacin by alkaline diperiodatocuprate(III) [183].

The oxidation of ciprofloxacin by DPC has been explained through different pathways **(Scheme 1.9) [184]**. Among various species of DPC in alkaline medium, mono periodatocuptrate (III) (MPC) is considered as active species for this reaction. Pathway I exhibits N-dealkylation process and through the formation of iminium ion finally hydrolysed to the dealkylated product and further oxidized in aniline. Whereas, pathway II is a hydroxylation process and through theformation of iminium ion finally oxidized in dialdehyde and two monoaldehyde products. The possibility of other products such as N-oxide product and coupling product can be explained by pathway III. Thus the formation of different types of oxidation products can be explained by these three pathways. This study shows high reactivity and fast reaction of ciprofloxacin with DPC.

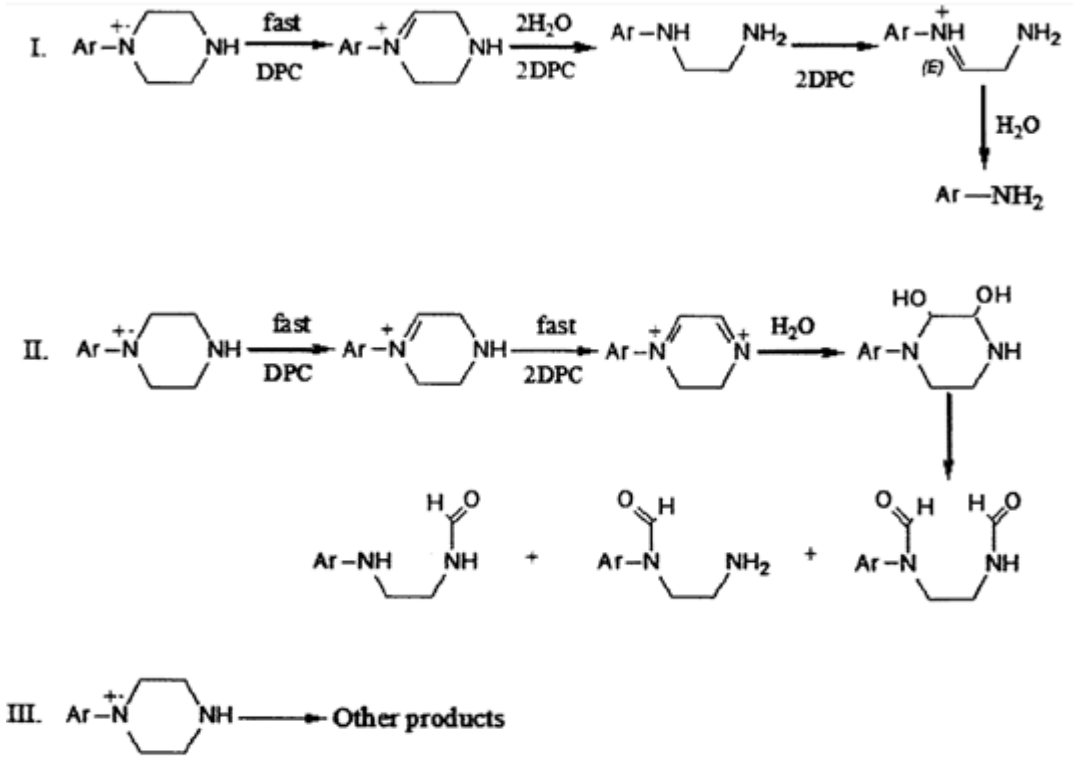

Scheme 1.9: Oxidation of ciprofloxacin by alkaline diperiodatocuprate(III) through different pathways [184].

On the other hand, many other oxidation studies such as acebutalol, ampiciline, atenolone, atropine and chloremphenicole drugs have been reported by DPC in alkaline medium [185-189]. DPC also used in the study of biological electron transfer reactions [190], numeral titration of organic mixtures and the evaluation of chromium, calcium and magnesium from their ores, antimony, arsenicand tin from their alloys [191].

Detailed literature survey revealed oxidative degradation of various fluoroquinolones antibacterial agents by different oxidants in aqueous acidic/alkaline medium **(Table 1.1)**. The survey conclude that activity site of different fluoroquinolone are depend on the nature of oxidant, pH of the reaction medium. Therefore, on the basis of different experimental results rate law were derived.

TABLE: 1.1

Oxidation of fluoroquinolones in aqueous acidic/alkaline medium by different oxidants.

S. No.	Fluoro quinolones	Oxidant	Medium	Products	Rate Law	Ref.
1.	Ciprofloxacin (m/z = 332)	$KMnO_4$	KOH	m/z = 263 (Full dealkylation) Mn(VI)	$\frac{Rate}{[MnO_4^-]} = \frac{k_1K_1[CIP][H^+]}{1+K_1[H^+]}$	36
2.	Norfloxacin (m/z = 319.3)	$KMnO_4$	NaOH	m/z = 335 (Hydroxylation) Mn(VI)	$\frac{Rate}{[MnO_4^-]} = \frac{kK_1K_2[OH^-][NF]}{1+K_1[OH^-]+K_1K_2[OH^-][NF]}$	37
3.	Levofloxacin (m/z = 361.4)	$KMnO_4$	KOH	Hydroxylated LEV, Mn(VI)	$\frac{Rate}{[MnO_4^-]} = \frac{kK_1K_2[H^+][LF]}{1+K_1[H^+]+K_1K_2[H^+][LF]}$	38
4.	Moxifloxacin (m/z = 400.4)	$KMnO_4$	KOH	m/z = 415.41 (Oxo derivative) Mn(VI)	$\frac{Rate}{[MnO_4^-]} = \frac{kK_1K_2[OH^-][MOX]}{1+K_1[OH^-]+K_1K_2[MOX][OH^-]}$	39

5.	Enrofloxacin (m/z = 359.4)	$KMnO_4$	NaOH	m/z = 263 (Dealkylation) Mn(VI)	$\frac{Rate}{[MnO_4^-]} = \frac{k_1 K_1 [ENR][OH^-]}{1 + K_1[OH^-]}$	40
6.	Ofloxacin (m/z = 279)	$KMnO_4$	H_2SO_4	m/z = 279 (Dealkylation) Mn(VI)	$\frac{Rate}{[MnO_4^-]} = \frac{kK_1K_2[H^+][OFL]}{1 + K_1[H^+] + K_1K_2[H^+][OFL]}$	41
7.	Lomefloxacin (m/z = 351)	$KMnO_4$	NaOH	m/z = 268 (Dealkylation) Mn(VI)	$\frac{Rate}{[MnO_4^-]} = \frac{kK_1K_2[OH^-][LMF]}{1 + K_1[OH^-] + K_1K_2[OH^-][LMF]}$	44
8.	Levofloxacin (m/z = 361.4)	CAT	$HClO_4$	Oxo derivative of LEV	$\frac{Rate}{[CAT]_t} = \frac{K_1K_2k[LF]}{[H^+] + K_1\{1 + K_2[LF]\}}$	53
9.	Levofloxacin (m/z = 361.4)	NBS	HCl	m/z = 330 (Hydroxylated LEV, Succinimide)	$\frac{Rate}{[RNBr]_t} = \frac{K_1K_2k[LF][H^+]}{1 + K_1[H^+] + K_1K_2[LF][H^+]}$	55
10.	Norfloxacin (m/z = 319.3)	CAB CBT	$HClO_4$	3-fluoro-4-piperazinyl-6-Nethylaminophenyl glyoxalic acid	$\frac{Rate}{[oxidant]_T} = \frac{K_1K_2k[S]}{[H^+] + K_1\{1 + K_2[S]\}}$	69

11.	Norfloxacin (m/z = 319.3)	DPA	KOH	m/z = 335 (Hydroxylation) Ag(I)	$\frac{Rate}{[DPA]} = \frac{kK_1K_2K_3[NF][OH^-]}{[H_3IO_6^{2-}] + K_1[OH^-][H_3IO_6^{2-}] + K_1K_2[OH^-] + K_1K_2K_3}$	70
12.	Norfloxacin (m/z = 319.3)	MnO_2	Aqueous	m/z = 335 (Hydroxyl derivative)	$\frac{Rate}{[MnO_2]_T} = \frac{kK_1K_2[NOR]}{\{[OH^-] + K_1K_2[NOR]\}}$	124
13.	Levofloxacin (m/z = 361.4)	HCF(III)	KOH	m/z = 333 (Decarboxylation, hydroxylation)	$\frac{Rate}{[Fe(CN)_6]^{3-}} = \frac{kK_1K_2[OH^-][LF]}{1 + K_1K_2[OH^-][LF] + K_1[OH^-] + K_1^2K_2[LF][OH^-]^2}$	157
14.	Norfloxacin (m/z = 319.3)	DPC	NaOH	m/z = 335 (Hydroxyl derivative)	$\frac{Rate}{[DPC]} = \frac{kK_1K_2[NOR][OH^-]}{[H_2IO_6^{3-}] + K_1[OH^-][H_2IO_6^{3-}] + K_1K_2[OH^-] + kK_1K_2[OH^-][NOR]}$	183
15.	Ciprofloxacin (m/z = 332)	DPC	NaOH	m/z = 263 (Full dealkylation) m/z = 306 (Partial dealkylation)	$\frac{Rate}{[DPC]} = \frac{kK_4K_5K_6[CIP][OH^-]}{[H_2IO_6^{3-}] + K_4K_5K_6[OH^-][CIP] + K_4K_5[OH^-] + K_4[H_2IO_6^{3-}][OH^-]}$	184

1.7. Scope of the Work

Antibiotics are essential part of research due to their high detection frequency in the environment and the increasing bacterial resistance formation. Among various antibiotics, fluoroquinolones are of extreme interest, since they are broad spectrum antibacterials with agrowing demand in hospitals, households, and veterinary applications. There is major concern that antibiotics emitted into the aquatic environment can influence drinking water. Contamination with FQs has been widely disclosed all around the world in various aquatic forms including discharge or waste samples, surface water and ground water. For the degradation of FQs in aqueous solution, interesting remedy processes are desired because under oxidation–degradation process most of composed intermediates can be definitely mineralized into CO_2, water, and mineral species.

Thus the present investigation is oxidative in nature, mostly drug transformations under the natural environment are most likely to follow oxidation path. Present study is based upon the kinetic and mechanistic study of oxidation-reduction reactions between useful oxidants with few of the most frequently used fluoroquinolone antibacterial agents. The proposed work will gives a novel application in the field of pharmaceuticals as well as kinetics. Nano sized colloidal manganese dioxide, hexacyanoferrate(III), diperiodatocuprate(III) used as an effective oxidants for oxidative degradation of different fluoroquinolone antibacterial agents in aqueous acidic/alkaline system. So this study will be adequately used in waste-water treatment at the sites polluted by fluoroquinolone antibacterial agents.

1.8. References

[1] D. P. Rocha, G. F. Pinto, R. Ruggiero, C. A. Oliveria, W. Guerra, . P. S. Fontes, T. T. Tavares, I. M. Marzano, E. C. Pereira-Maia, ***Quím. Nova,*** 34 (2011) 111.

[2] J. A. Wiles, B. J. Bradbury, M. J. Pucci, ***Expert Opinion on Therapeutic Patents,*** 20 (2010) 1295.

[3] E. M. Golet, A. C. Alder, A. Hartmann, T. A. Ternes, W. Giger, ***Analytical Chemistry,***73 (2001) 3632.

[4] M. Scheer, ***Veterinary Medical Review***, 2 (1987) 90.

[5] D. E. King, R. Malone, S.H. Lilley, ***Am. Fam. Physician,*** 61 (2000) 2741.

[6] D. Sriram, P. Yogeeswari, J. S. Basha, D. R. Radha, V. Nagaraja, ***Bioorg. Med. Chem.,*** 13 (2003) 5774.

[7] A. Foroumadi, S. Emami, M. Mehni, M. H. Moshafi, A. Shafiee, ***Bioorg. Med. Chem. Lett.***, 15 (2005) 4536.

[8] Y. L. Zhao, Y. L. Chen, J. Y. Sheu, I. L. Chen, T. C. Wang, C.C.Tzeng, ***Bioorg. Med. Chem.,*** 13 (2005) 3921.

[9] G. V. Reddy, S. R. Kanth, D.Maitraie, ***Eur. J. Med. Chem.***,44 (2009) 1570.

[10] S. Jazayeri, M. H. Moshafi, L. Firoozpour, ***Eur. J. Med. Chem.,*** 44 (2009) 1205.

[11] N. German, P. Wei, G. W. Kaatz, R. J.Kerns, ***Eur. J. Med. Chem.,*** 43 (2008) 2453.

[12] A. B. A. El-Gazzar, M. M. Youssef, A. M. S. Youssef, A. A. Abu-Hashem, F. A.Badria, ***Eur. J. Med. Chem.***, 44 (2009) 609.

[13] R. W. Winter, J. X. Kelly, M. J. Smilkstein, R. Dodean, D. Hinrichs, M. K. Riscoe, ***Exp. Parasitol,*** 118 (2008) 487.

[14] F. Vargas, T. Zoltan, C. Rivas et al., ***J. Photochem. Photobiol. B: Biology,*** 92 (2008) 83.

[15] M. J. Wall, J. Chen, S. Meegalla et al., ***Bioorg. Med. Chem. Lett***.,18 (2008) 2097

[16] K. Valliappan, M. S. Sandeep, ***Chromatographia***, 77 (2014) 1203.

[17] H. V. O. Lopes, ***Rev. Panam. Infectol,*** 6 (2004) 18.

[18] R. M. Kulkarni, M. S. Hanagadakar, R. S. Malladi, M. S. Gudaganatti, H. S. Biswal, S. T. Nandibewoor, ***Indian J. Chem. Technol.,*** 21 (2014) 38.

[19] V. Homem, L. Santos, ***J. Environ. Manage.,*** 92 (2011) 2304.

[20] H. Yuan, X. Zhou, Y. L. Zhang, ***Water,*** 41 (2013) 43.

[21] M.S. Gudaganatti, M. S. Hanagadakar, R. M. Kulkarni, R. S. Malladi, R. K. Nagarale, ***Prog. React. Kinet. Mech.***, 37 (2012) 366.

[22] Z. Derakhshan, M. Mokhtari, F. Babaie, R. M. Ahmadi, M. H. Ehrampoosh, M. Faramarzeian, ***Journal of Environmental Health and Sustainable Development***. 1 (2016) 1.

[23] G. Laera, D. Cassano, A. Lopez, A. Pinto, A. Pollice, G. Ricco, G. Mascolo, ***Environ. Sci. Technol***., 46 (2012) 1010.

[24] M. Sayed, M. Ismail, S. Khan, S. Tabassum, H. M. Khan, ***Environ. Technol.,*** 37 (2016) 590.

[25] N. Barhoumi, L. Labiadh, M. A. Oturan, N. Oturan, A. Gadri, S. Ammara, E. Brillas, ***Chemosphere,*** 141 (2015) 250.

[26] I. Epold, M. Trapido, N. Dulova. ***Chem. Eng. J.***, 279 (2015) 452.

[27] K. S. Tay, N. Madehi, ***Sci. Total Environ***., 520 (2015) 23.

[28] C. Liu, V. Nanaboina, G. V. Korshin, W. Jiang, ***Water Res.***, 46 (2012) 5235.

[29] T. An, H. Yang, G. Li, W. Song, W. J. Cooper, X. Nie, ***Appl. Catal., B Environ***., 94 (2010) 288.

[30] Y. Ji, C. Ferronato, A. Salvador, X. Yanga, J-M.Chovelon, ***Sci. Total Environ.,***472 (2014) 800.

[31] I. Epold, N. Dulova, ***J. Environ. Chem. Eng.***, 3 (2015) 1207.

[32] Z-H Diao, X-R Xu, D. Jiang, G. Li, J-J. Liu, L-J. Kong, L-Z.Zuo, ***J. Hazard. Mater.,*** 327 **(**2017) 108.

[33] K. Ikehata, E. M. Gamal, S. A. Snyder, ***Ozone-Sci Eng.,*** 30 (2008) 21.

[34] A. J. Watkinson, E. J. Murby, S. D. Costanzo, ***Water Res.,*** 41 (2007) 4164.

[35] A. Taicheng, H. Yang, G. Li, W. Song , W. J. Cooper c , X. Nie, ***Applied Catalysis B: Environmental,*** 94 (2010) 288.

[36] K. A. Thabaj, S. D. Kulkarni, S. A. Chimatadar, S. T. Nandibewoor, ***Polyhedron,*** 26 (2007) 4877.

[37] P. N. Naik, S. A. Chimatadar, S. T. Nandibewoor, ***Ind. Eng. Chem. Res.,*** 48 (2009) 2548.

[38] A. Jain, G. Tazwar, V. Devra, ***Int. J. Res. Pharm. Sci.,*** 5 (2015) 1.

[39] S. S. Badi, S. M. Tuwar. ***Res. Chem. Intermed.***, 41 (2015) 7827.

[40] A. Jain, V. Devra, ***J. Pharm. Sci. Innov.,*** 6 (2017) 79.

[41] V. Devra, A. Jain, S. Jain, ***World Journal of Pharmaceutical Research***, 4 (2015) 963.

[42] A. A. P. Khan, M. A. S.Bano, A. Husain, K. S. Siddiqi, Transition***. Met. Chem.,*** 35 (2010) 117.

[43] Y. Xu, S. Liu, F. Guo, F.Cui, ***Journal of Chemistry***, (2015) 1, Article ID 521395, http://dx.doi.org/10.1155/2015/521395.

[44] R. M. Kulkarni, M. S. Hanagadakar, R. S. Malladi, H. S. Biswal, ***Desalination and Water Treatment,*** 57 (2016) 10826.

[45] A. Jain, S. Jain, V. Devra, ***International Journal of Pharmaceutical Sciences and Drug Research***,7 (2015) 205.

[46] P. Wang, H. Yi-Liang, C. H. Ching-Hua, ***Water Res.,*** 44 (2010) 5989.

[47] M. C. Dodd, M. O. Buffle, U. VonGunten, ***Environ. Sci. Technol.,***40 (2006)1969.

[48] H. Zhang, C. H. Huang, ***Environ. Sci. Technol.,*** 39 (2005) 4474.

[49] B. D. Witte, J. Dewulf, K. Demeestere, V. V. D. Yvere, P. D. Wispelaere, H. V. Langenhove, ***Environ. Sci. Technol.,*** 42 (2008) 4889.

[50] B. D. Witte, H. V. Langenhove, K. Hemelsoet, K. Demeestere, P. D. Wispelaere, V. V. Speybroeck, J. Dewulf, ***Chemosphere,*** 76 (2009) 683.

[51] R. J. Pavagada, B. Kanakapura, R. Nagaraju, Z. D. Okram, B. V. Kanakapura, ***J. Appl. Spectrosc.,*** 78(2011) 383.

[52] H. Mandil, A. A. Sakur, B. Nasser, ***Asian J. Chem.,*** 24 (2012) 2985.

[53] N. H. E. Najjar, E. Touffet, M. Deborde, R. Journel, N. K.V.Leitner, ***Chemosphere,*** 93 (2013) 604.

[54] N. H. E. Najjar, M. Deborde, R. Journel, N. K.V.Leitner, ***Water Res.*** 47 (2013) 121.

[55] M. S. Gudaganatti, M. S. Hanagadakar, R. M. Kulkarni, R. S. Malladi, R. K. Nagarale, ***Prog. React. Kinet. Mech.,*** 37 (2012) 366.

[56] R. M. Kulkarni, M. S. Hanagadakar, R. S. Malladi, ***Asian J. Research Chem.,*** 6 (2013) 1124.

[57] X. Xiao, S-P.Sun, M. B. McBride, A. T. Lemley, ***Environ. Sci. Pollut. Res.*** 20 (2013) 10.

[58] N. Nanda, S. Dakshayani, Puttaswamy, ***Oxid. Commun.***, 34 (2011) 44.

[59] M. C. Dood, Kohler H P E, U. VonGunten, ***Environ. Sci. Technol.*** 43 (2009) 2498.

[60] B. Yang, R. S. Kookana, M. Williams, G. G. Ying, J. Du, H. Doan, A. Kumar, ***J. Hazard. Mater.,*** 320 (2016) 296.

[61] Z. Zhou, J-Q. Jiang, **Chemosphere,** S119 (2015) 95.

[62] H. Zhang, C-H. Huang, ***Chemosphere,*** 66 (2007) 1502.

[63] H. Zhang, W. R. Chen, C. H. Huang, ***Environ. Sci. Technol.,*** 42 (2008) 5548.

[64] S. A. M. Ebraheem, A. A. Elbashir, ***American Academic & Scholarly Research Journal,*** 4 (2012) 89.

[65] O. A. Adegoke, B.B.Balogun, ***Int. J. Pharm. Sci. Rev. Res***., 4(2010) 1.

[66] K. Basavaiah, P. Nagegowda, B. C. Somashekar, V. Ramakrishna, ***Science Asia,*** 32 (2006) 403.

[67] A. A. P. Khan, A. M. Asiri, N. Azum et al., ***Ind. Eng. Chem. Res.***, 51 (2012) 4819.

[68] A. A. P. Khan, A. Khan, A. M. Asiri, S. A. Khan, ***J. Mol. Liq.***, 218 (2016) 604.

[69] N. Nanda, S. M. Mayanna, N. M. Gowda, ***Int. J. Chem. Kinet.***, 31 (1999) 153.

[70] H. T. Padavathil, S. Mavalangi, S. T. Nandibewoor, ***American International Journal of Research in Science, Technology, Engineering & Mathematics,*** 3 (2013) 63.

[71] U.Hubicka, P. Zmudzki, P. Talik, B. Z. Witek, J. Krzek,Hubicka et al. ***Chemistry Central Journal,*** 7 (2013) 133.

[72] T. C. Sharma, A. Lal, V. Saksena, ***Bull. Chem. Soc. Jpn.,*** 49 (1976) 2881.

[73] B. Basak, M. A. Malati, ***J. Inorg. Nucl. Chem.,*** 39 (1977) 1081.

[74] F. Kienzle, ***Tetrahedron Lett.,*** 24 (1983) 2213.

[75] S. Taniguchi, ***Bull. Chem. Soc. Jpn.,*** 57 (1984) 2683.

[76] S. B. Kanungo, ***J. Catal.,*** 58 (1979) 419.

[77] S. P. Jiang, W.R. Ashton; A.C. C. Tseung, ***J. Catal.,*** 131 (1991) 88.

[78] L. D. Ahuja, D. Rajeswar, K. C. Nagpal, ***J. Colloidal Interface Sci.,*** 119 (1987) 481.

[79] S. B. Kanungo, K. M. Parida, B. R. Sant, ***Electrochim. Acta.,*** 26(1981) 1157.

[80] K. M. A. Salam, ***J. Phys. Chem.,*** 95 (1975) 139.

[81] P. Simon, Y. Gogotsi, ***Nat. Mater.***, 7 (2008) 845.

[82] W. Wei, X. Cui, W. Chen, D.G. Ivey, ***Chem. Soc. Rev.***, 40 (2011) 1697.

[83] Y.G. Sun, L. Wang, Y.Z. Liu, Y. Ren, ***Small,***11 (2015) 300.

[84] W. Wang, S. Guo, K. N. Bozhilov, D. Yan, M. Ozkan, C. S. Ozkan, ***Small***, 9 (2013) 3714.

[85] J. Zhang, D. Shu, T. Zhang, H. Chen, H. Zhao, Y. Wang, Z. Sun, S. Tang, X. Fang, X.Cao, ***J. Alloys Compd.,*** 532 (2012) 1.

[86] D. L. Fang, B. C. Wu, A. Q. Mao, Y. Yan, C. H. Zheng, ***J. Alloys Compd.***, 507 (2010) 526.

[87] J. H. Cheng, G. Shao, H. J. Yu, J. ***J. Xu, J. Alloys Compd.***, 505 (2010) 163.

[88] Y. Hu, J. Wang, X. Jiang, Y. Zheng, Z. Chen, ***Appl. Surf. Sci.,*** 271 (2013) 193.

[89] L. Zhao, R. Wang, ***Appl. Surf. Sci.,*** 236 (2004) 217.

[90] J. Chen, J. C Lin, V.Purohit, M. B.Cutlip, S. L.Suib. ***Catal. Today,*** 33 (1997) 205.

[91] X. Wang, Y. D. Li, ***Chem. Eur. J.***, 9 (2003) 300.

[92] G. L. Wang, B. Tang, L. H. Zhuo, J. C. Ge, M. Xue, ***Eur. J. Inorg. Chem.,*** (2006) 2313.

[93] Y. Xiong, Y. Xie, Z. Li, C. Wu, ***Chem. Eur. J.,*** 9 (2003) 1645.

[94] J. F. Perez-Benito, ***J. Colloid Interface Sci.,*** 284 (2002) 130.

[95] L. C. Pereira, S. Baral, A. Henglein, E. Janata, ***J. Phys. Chem.,*** 89 (1985) 5772.

[96] O. Horvath, K. Strohmayer, ***J. Photochem. Photo. biol. A,***116 (1998) 69.

[97] J. F. Perez-Benito, E. Brillas, R. Populana, ***Inorg. Chem.,*** 28(1989) 390.

[98] J. F. Perez Benito, D. G. Lee, ***Can. J. Chem.,*** 63 (1985) 6628.

[99] P. K. Satapathy, B. N. Mohanty, ***Journal of Chemical and Pharmaceutical Research,*** 7 (2015) 882.

[100] M. A. Islamaand, M. M.Rahman, ***Colloid Journal,*** 75 (2013) 538.

[101] D. G. Lee, J. R. Brownridge, ***J. Am. Chem. Soc.,*** 95(1973) 3033.

[102] K. B. Wiberg, C. J. Deutsch, J. Rocek, ***J. Am.Chem. Soc.,*** 95 (1973) 3034.

[103] D. G. Lee, J. R. Brownridge, ***J. Am. Chem. Soc.,*** 96 (1974) 5517.

[104] L. I. Simandi, M. J. Jaky, ***J. Am. Chem. Soc.,*** 98 (1976) 1995.

[105] F. Mata Perez, J. F. Perez Benito, ***J. Phys. Chem. Leipzig,*** 267 (1986) 120.

[106] F. Mata Perez, J. F. Perez Benito, ***Can. J. Chem.,*** 63 (1985) 1275.

[107] D. G. Lee, J. F. Perez Benito, ***Can. J. Chem.,*** 63 (1985) 1275.

[108] F. Freeman, L.Y. Chang, ***J. Am. Chem. Soc.,*** 108 (1986) 4504.

[109] M. J. Insausti, F. Mata Perez, P. A. Macho, ***Int. J. Chem. Kinet.,*** 24 (1992) 411.

[110] J. F. Perez Benito, C. Arias, ***J. Colloid Interface Sci.,*** 149 (1992) 92.

[111] V. Holba, R. Kosicka, ***Collect. Czech. Chem. Commun.,*** 62 (1997) 849.

[112] E. A. Jenne, ***ACS Adv. Chem. Ser.***, 73 (1968) 337.

[113] H. Shindo, P. Huang, Appl. Clay Sci. 1 (1985) 71.

[114] W.R.Chen, Y. Ding, C. T. Johnston, B. J. Teppen, S. A. Boyd, H. Li, ***Environ. Sci. Technol.,*** 44 (2010) 4486.

[115] H. Zhang, W. R. Chen, H. C. Huang, ***Environ. Sci. Technol.***, 42(2008) 5548.

[116] J. Klausen, S. B. Haderlein, R. P. Schwarzenbach, ***Environ. Sci. Technol.,*** 31 (1997) 2642.

[117] C. S. McArdell, A. T. Stone, J. Tian, ***Environ. Sci. Technol.,*** 32 (1998) 2923.

[118] D. Wang, J. Y. Shin, M. A. Cheney, G. Sposito, T. G. Spiro, ***Environ. Sci. Technol.,*** 33 (1999) 3160.

[119] F. Li, C. Liu, C. Liang, X. Li, L. Zhang, ***J. Hazard. Mater.,*** 154(2008) 1098.

[120] H. Li, L. S. Lee, D. G. Schulze, C. A. Guest, ***Environ. Sci. Technol.,*** 37(2003)2686.

[121] L. Ukrainczyk, M. B. McBride, ***Environ. Toxicol. Chem.,*** 12 (1993) 2015.

[122] W. G. Sunda, D. J. Kieber, ***Nature,***367 (1994)62.

[123] Y. Li, D. Wei, Y. Du, ***Chemosphere***, 119 (2015) 282.

[124] A. K. Singh, N. Sen, S. K. Chatterjee, ***Indian Journal of Chemistry,*** 55A (2016) 1059.

[125] J. S. Sabirova, L. F. F. Cloetens, L. Vanhaecke, I. Forrez, W. Verstraete, N. Boon, ***Microbiol. Biotechnol***.1 (2008) 507.

[126] H. Li, L. S. Lee, D. G. Schulze, C. A. Guest, ***Environ. Sci. Technol.,*** 37 (2003)2686.

[127] L. Ukrainczyk, M. B. McBride, ***Environ. Toxicol. Chem.,*** 12 (1993) 2015.

[128] J. Han, M. Wang, S. Cao, P. Fang, S. Lu, R. Chen, R. Guo, ***J. Mater. Chem. A,*** 1 (2013) 13197.

[129] M. L. Chacon-Patino, C. Blanco-Tirado, J. P. Hinestroza, M. Y. Combariza, ***Green Chem.,*** 15 (2013) 2920.

[130] J. D. Andres, E. Brillas, J. A. Garrido, J. F. Perez Benito, ***J. Chem. Soc., Perkin Trans.,*** 2 (1988) 107.

[131] R. Sumichrast, V. Holba, ***Collect. Czech. Chem.Commun.,*** 58 (1993) 1777.

[132] M. Saeed, M.Ilyas, M. Siddique, A.Ahmad, ***Arab. J. Sci. Eng.,*** 38 (2013) 1739.

[133] J. Q. Jiang, B. Lloyd, ***Water Res.,*** 36 (2002) 1397.

[134] V. K. Sharma, ***Adv. Environ. Res.,***6(2002) 143.

[135] M. C. Day, J. Selbin, Theoretical inorganic chemistry. ***New York, NY: Reinhold,*** (1964).

[136] E. P. Kelson, P. P. Phengsy, ***Int. J. Chem. Kinet.,*** 32 (2000) 760.

[137] M. Martinez, M. Pitarque, R. Van Eldik, ***Journal of the Chemical Society, Dalton Transactions,*** (1996) 2665.

[138] G. Svehla, ***Vogel's quantitative inorganic analysis 7th ed.,*** (2002) 197.

[139] K. Sharanabasamma, M. A. Angadi, S. M. Tuwar, ***Ind. Eng. Chem. Res.*** 48 (2009) 10381.

[140] S. A. Farokhi, S. T. Nandibewoor, ***Tetrahedron***, 59 (2003) 7595.

[141] M. D. Meti, S. T. Nandibewoor, S. A. ***Turkish Journal of Chemistry,*** 38(2014) 477.

[142] A. Goel, R. Sharma, ***Journal of Chemical Engineering and Materials Science,*** 3 (2012) 1.

[143] S. Hussaina, B. S. Agrawal, S. B. Pakhare, ***International Journal of Chemical Research,*** 2 (2011) 8.

[144] Y. Nakajima, Y. Sato, T. Konishi, ***Chemical& Pharmaceutical Bulletin,*** 55 (2007) 1222.

[145] T. P. Jose, S. T. Nandibewoor, S. M. Tuwar, ***J.Sulfur. Chem,*** 27 (2006) 25.

[146] T. P. Jose, S. T. Nandibewoor, S. M. Tuwar, ***J. Solution Chem,*** 35 (2006) 51.

[147] V. N. Singh, M. P. Singh, B. B. L. Saxena, ***Indian J Chem.,*** 8 (1970) 529.

[148] J. M. Leal, B. Garcia, P. L. Domingo, ***Coord. Chem Rev.,*** 173 (1998) 79.

[149] T. P. Jose, M. A. Angadi, M. S. Salunke, S. M. Tuwar, ***J. Mol. Struct.,*** 892 (2008) 121.

[150] N. Nath, and L.P. Singh, ***J. Indian Chem. Soc***., 62 (1985) 108.

[151] H. J. El-Aila, **Journal of Dispersion Science and Technology**, 25 (2004) 157.

[152] M. M. Al-Subu, W. J. Jondi, A. A. Amer, M. M. Hannoun, M. J. Musmar, ***Chem. Heterocyclic Compounds,*** 4 (2003) 559.

[153] N. Diab, I. Abu-Shqair, M. Al-Subu, R. Salim, ***International Journal of Chemistry,*** 34 (2013) 1388.

[154] P. T. Speakman, W. A. Waters, ***J. Chem. Soc.,*** (1955) 40.

[155] G. Dasgupta, M. K. Mahanti, ***Bull. Soci. Chim. Fr.,*** 4 (1986)492.

[156] E. A. Prill, S.M. Mcelvain, ***Org. Synth. Coll.*** 2 (1943) 419.

[157] M. B. Patgar, S. T. Nandibewoor, S. A. Chimatadar, ***Cogent Chemistry,*** 1 (2015) 1.

[158] A. I. Vovk, I. V. Muraveva, V. P. Kukhar, V. F. Baklan, ***Russ. J. Gen. Chem.,*** 70 (2000) 1108.

[159] V. N. Singh, M. P. Singh, B. B. L. Saxena, ***Indian J. Chem.,*** 8 (1970) 529.

[160] H. Yao, M. Zhang, W. Zeng, X. Zeng, Z. Zhang, ***Spectro. Chim. Acta. Part A,***117 (2014) 645.

[161] A. Kumar, P. Kumar, P. Ramamurthy, ***Polyhedron,*** 18 (1999) 773.

[162] R. S. Shettar, S. T. Nandibewoor, ***J. Mol. Catal. A,*** 234 (2005) 137.

[163] Y. Hu, G. Li, Z. Zhang, ***Luminescence,*** 26 (2011) 313.

[164] J. E. Weder, C. T. Dillon, T. W. Hambley, B. J. Kennedy, P. A. Lay, J. R. Biffin, H. L. Regtop, N. M. Davies, ***Coord. Chem. Rev.,*** 232 (2010) 95.

[165] A. M. Bagoji, P. A. Magdum, S. T. Nandibewoor, ***J. Solution Chem.,*** (2016).

[166] R. N. Hegde, N. P. Shetti, S. T. Nandibewoor, ***Polyhedron,*** 28 (2009) 3499.

[167] K. S. Byadagi, R. V. Hosahalli, S. T. Nandibewoor, S. A. Chimatadar, ***Z. Phys. Chem.,*** 226 (2012) 233.

[168] K. Byadagi, M. Meti, S. T. Nandibewoor, S. Chimatadar, ***Ind. Eng. Chem. Res.,*** 52 (2013) 9011.

[169] S. D. Lamani, P. N. Naik, S. T. Nandibewoor, ***Solution Chem.,*** 39 (2010) 1291.

[170] U. R. Bagwan, A. L.Harihar, S. D. Lamani, I. N. Shaikh, A. B. Teradale, ***Research Journal of Pharmaceutical, Biological and Chemical Sciences,*** 8 (2017) 1015.

[171] M. A. Angadi, S. T. Tuwar, ***J. Solution Chem.,*** 39 (2010) 165.

[172] S. A. Chimatadar, T. Basavaraj, A. Kiran, Thabaj, S. T. Nandibewoor. ***Journal of Molecular Catalysis A: Chemical,*** 267 (2007) 65.

[173] Y. Hu, G. Li, Z. Zhang, ***Luminescence,*** 26 (2011) 313.

[174] L. Malatesta, ***Gazz. Chim. Ital.,*** 71 (1941) 467.

[175] A. Balikungeri, M. Pelletier, D. Monnier, ***Inorg. Chim. Acta,*** 22 (1977) 7; 29 (1978)141.

[176] M.W. Lister, ***Candian J. Chem.,*** 31 (1953) 638; ***ibid.,*** 39(1961) 2330.

[177] G.I. Rozovskii, ***Tovarnye. Zn. Alc.*** (1971); ***Chem. Abstr.,*** 74 (1971) 55808c.

[178] S. D. Kulkarni, S. T. Nandibewoor, ***Transit. Met. Chem.,*** 31 (2006) 1034.

[179] J. E. Weder, C. T. Dillon, T. W. Hambley, B. J. Kennedy, P. A. Lay, J. R. Biffin, H. L. Regtop, N. M. Davies, ***Coord. Chem. Rev.,*** 232 (2002) 95.

[180] B. Reddy, B. Sethuram,T. N. Rao, ***Indian J. Chem.,*** 23A (1984) 593.

[181] W. Levason, M. D. Spicer, ***Coord. Chem. Rev.,*** 76 (1987) 45.

[182] A. Balikungeri, M. Pelletier, D. Monnie, ***Inorg. Chim. Acta.,*** 22 (1977) 7.

[183] D. S. Munavalli, P. N. Naik, G. G. Ariga, S. T. Nandibewoor, C. Munavalli, ***Cogent Chemistry***, 1 (2015) 1068510.

[184] http://shodhganga.inflibnet.ac.in/bitstream/10603/95148/9/09_chapter%203.pdf visited in July (2018).

[185] N. P. Shetti, R. N. Hegde, S. T. Nandibewoor, ***Journal of Molecular Structure***, 930 (2009) 180.

[186] S. D. Kulkarni, S. T. Nandibewoor, ***Transition Metal Chemistry,*** 31 (2006) 1034.

[187] R. N. Hegde, N. P. Shetti, S. T. Nandibewoor, ***Polyhedron,*** 28 (2009) 3499.

[188] K. S. Byadagi, R. V. Hosahalli, S. T. Nandibewoor,S. A. Chimatadar , ***Z. Phys. Chem.,***226 (2012) 233.

[189] S. D. Lamani, P. N. Naik, S. T. Nandibewoor, ***J. Solution Chem.,*** 39(2010) 1291.

[190] W. Niu, Y. Zhu, K. Hu, C. Tong, H. Yang, ***Int. J.Chem. Kinet.,*** 28 **(**1996) 899.

[191] G. I. Rozovoskii, A. K. Misyavichyus, A. Y. Prokopchik, ***Kinet. Catal.,*** 16 (1975) 337.

Chapter – 2

Instrumentation and Materials

The present chapter includes the instrumental details of all the characterization and analytic tools, details of the reagents, chemicals and their solutions with other specifics occupied in the kinetic study of degradation processes. Two following sections are present in this chapter:

SECTION – I

2.1. Chemicals

The details of the reagents, chemicals and their solutions used in kinetic study of the different oxidation reactions are as follows:

2.1.1. Levofloxacin ($C_{18}H_{20}FN_3O_4$)

Levofloxacin sample (Cipla Limited) was used as supplied and the solution of desired concentration was prepared by dissolving appropriate quantity of the drug in doubly distilled water. Freshly prepared solution of levofloxacin was always employed.

2.1.2. Ciprofloxacin ($C_{17}H_{18}FN_3O_3$)

The solution of ciprofloxacin (KORES India Limited) was prepared by dissolving the requisite amount of its salt in doubly distilled water to obtain the solution of desired concentration. The drug was used as received. Freshly prepared solution of ciprofloxacin was always employed.

2.1.3. Ofloxacin ($C_{18}H_{20}FN_3O_4$)

Standard solution of ofloxacin (KORES India Limited) was prepared by dissolving the calculated quantity of pure drug in 0.1 M H_2SO_4. The acid present in the substrate solution is also taken into account in the calculation of the total acid present in each case of the proposed reaction. Solution of ofloxacin was always prepared freshly before experiment.

2.1.4. Moxifloxacin ($C_{21}H_{24}FN_3O_4$)

Solution of required concentration of moxifloxacin (Cipla Limited) was prepared by dissolving the known amount of drug in doubly distilled water. Moxifloxacin solution was always prepared freshly and the drug was used as received.

2.1.5. Sodium Thiosulphate Solution ($Na_2S_2O_3.5H_2O$)

The solution of sodium thiosulphate (A.R.) was prepared by dissolving known quantities in appropriate volume of double distilled water. These were standardized against standard solution of copper sulphate pentahydrate iodometrically [1]. Freshly prepared solutions of sodium thiosulphate were always used as these were reportedly deteriorated on standing at ambient temperature.

2.1.6. Potassium Permanganate ($KMnO_4$)

The solution of permanganate was made by dissolving the required quantity of $KMnO_4$ (BDH AnalaR) crystals in double-distilled water. Commercially available potassium permanganate generally contains impurity. In order to make standard potassium permanganate solution it is standardized by titrating against oxalic acid [2]. Freshly prepared & standardized permanganate solutions were always used in kinetics experiments.

2.1.7. Perchloric Acid ($HClO_4$)

Stock solution of perchloric acid was prepared by diluting 70% guaranteed reagent grade (Merck) perchloric acid. Perchloric acid solution was standardized by titrating a known aliquot of perchloric acid solution against sodium hydroxide solution using phenolphthalein as an indicator.

2.1.8. Sodium Perchlorate ($NaClO_4$)

Sodium perchlorate solutions of required concentration were prepared by neutralizing perchloric acid with sodium carbonate (A.R.) to the pH ~6.8. The dissolved CO_2 in the solution was expelled on heating before making up the required volume.

2.1.9. Sodium Fluoride (NaF)

Solution of sodium fluoride (Merck) was prepared by dissolving the requisite amount of the salt in doubly distilled water.

2.1.10. Sodium Sulphate (Na_2SO_4)

Solution of sodium sulphate (BDH AnalaR) was prepared by dissolving requisite quantity of the salt in doubly distilled water to obtain the solution of desired concentration.

2.1.11. Sulphuric Acid (H_2SO_4)

The solution of sulphuric acid (Merck) was prepared by dissolving the required volume of sulphuric acid in doubly distilled water. Then the solution was standardized against pre standardized sodium hydroxide solution using phenolphthalein as an indicator. The standardized solution was kept stoppered as a stock solution.

2.1.12. Potassium Hexacyanoferrate(III) [$K_4Fe(CN)_6$]

A stock solution of oxidant, hexacyanoferrate(III) was prepared by dissolving $K_3[Fe(CN)_6]$ (BDH) in double distilled water and standardized the solution iodometrically [3].

2.2.13. Copper Sulphate Pentahydrate (CuSO4.5H2O)

Copper sulphate (A.R., E. Merck) solution was prepared by dissolving the requisite quantity of copper sulphate in doubly distilled water and sufficient acetic acid was added to check the hydrolysis of copper sulphate in the solution.

2.1.14. Sodium Nitrate ($NaNO_3$)

The solution of sodium nitrate (Merck) was prepared by dissolving the required amount of the salt in doubly distilled water. The solution is quite stable and does not show any deterioration even on long standing at ambient temperature.

2.1.15. Sodium Hydroxide (NaOH)

The solution of sodium hydroxide was prepared by dissolving approximately weighed pellets of NaOH (BDH Analar) in doubly distilled water. The solution was standardized by titration the known aliquot sample against the standard oxalic acid solution to the phenolphthalein end point [4, 5]. However, sodium hydroxide solution was always used after standardizing as these solutions deteriorate on standing at ambient temperature.

2.1.16. Potassium Periodate (KIO_4)

The solution of potassium periodate (Merck) was prepared by dissolving the required amount of the salt in doubly distilled water.

2.1.17. Potassium Bisulphate ($KHSO_4$)

Potassium bisulphate solution of required concentration was prepared bydissolving requisite amount of $KHSO_4$ in doubly distilled water.

2.1.18. Diperiodatocuprate(III)

A stock solution of oxidant, DPC was prepared by dissolving copper sulphate (3.54 g), potassium meta periodate (6.8 g), potassium persulphate (2.2 g) and KOH (9.0 g) in 250cm^3water. The mixture was heated to boil on a hotplate with constant stirring till it turns to dark redand the boiling was continued for another 20 min for the completion of the reaction. Then mixture was cooled, filtered through sintered glass crucible (G-4). Filtrate was diluted to 250 cm^3 with distilled water. The obtained solution obtained was found fairly stable at room temperature for several months in the presence of periodate. The complex was characterized by UV-Visible spectrum, which exhibits strong broad absorption band at 415 nm. The aqueous solution of DPC was standardized by standard method [6].

2.1.19. 2, 4 – Dinitrophenylhydrazine ($C_6H_3(NO_2)_2NHNH_2$)

The reagent was prepared by means of Brady's method. Requisite amount of 2, 4 – dinitro phenyl hydrazine was mixed with 10 ml conc. HCl and 12.5 ml water, warming on a water bath, then diluted with deionized water. This reagent is more suitable for water soluble aldehydes.

2.1.20. Phenolphthalein Indicator ($C_{20}H_{14}O_4$)

Phenolphthalein (BDH, AnalaR) was used as an end point indicator for acid base titration.

2.1.21. Nessler's Reagent [$K_2(HgI_4)$]

The reagent was prepared by dissolving 100gm of mercury (II) iodide and 70gm of potassium iodide in 100 ml of deionized water. The resulting solution was then added to a solution of 160 gm of sodium hydroxide in 700 ml deionized water with stirring. This solution was diluted up to one litre with deionized water. The precipitate was allowed to settle for three days and the supernatant liquid was pouring out and kept in a brown bottle.

All other reagent viz. hydrochloric acid, potassium hydroxide, potassium nitrate, manganese chloride etc. were either of (BDH, AnalaR) grade or (E. Merck) guaranteed reagent grade. Their solutions were prepared by dissolving requisite quantities in known volumes of doubly distilled water and details regarding the preparation of their solutions are given in the respective chapters.

Kinetic procedure and methodology [7] adopted for the monitoring of kinetics and analysis of the kinetic results is given in concerned chapters. All glass vessels employed both for storing reagents solutions and also for kinetics were either of pyrex or coring make.

SECTION – II

2.2. Instrumental Techniques

This section describes the basic theories and principles of the main analytical methods and characterization techniques. This section also deals with the details of various instrumental techniques such as electron microscopy, XRD, Zeta sizer, LC-MS, FT-IR spectroscopy, UV-Visible spectroscopy etc. adopted for characterization and studies the degradation of fluoroquinolones in the presence of acid/alkaline medium.

2.2.1. Ultraviolet-Visible Spectrophotometer

Ultraviolet–visible spectroscopy or ultraviolet-visible spectrophotometry (UV-Vis or UV/Vis) refers to absorption spectroscopy or reflectance spectroscopy in the ultraviolet-visible spectral region. This system uses light in the visible and adjacent ranges. The absorption or reflectance in the visible range directly affects the identify color of the chemicals involved. Atoms and molecules undergo electronic transitions in this region of the electromagnetic spectrum. Fluorescence spectroscopy is reciprocal to absorption spectroscopy, in that absorption measures transitions from the ground state to the excited state, while fluorescence deals with transitions from the excited state to the ground state [8].

Non-bonding electrons (n-electrons) or π-electrons containing molecule scan absorb energy in the ultraviolet or visible light form to excite these electrons to higher anti-bonding molecular orbitals [9]. There are four possible types of transitions (π-π*, n-π*, σ-σ*, and n-σ*), and they can be ordered as follows: σ-σ* > n-σ* > π-π* > n-π*.

UV/Vis spectroscopy is commonly used in analytical chemistry for the quantitative evaluation of various analytes, such as biological macromolecules, highly conjugated organic compounds, and transition metal ions. Spectroscopic analysis is generally implemented in solutions but solids and gases may also be studied. The Beer-Lambert law states that the absorbance of a solution is directly proportional to the concentration of the absorbing species in the solution and the path length [10]. Thus, for a fixed path length, UV/Vis spectroscopy can be used to determine the concentration of the absorber in a solution. The reaction, occurring in solution, must present color or brightness shifts from reactants to products in order to use UV/Vis for this application. The rate constant of a particular reaction can be determined by measuring the UV/Vis absorbance spectrum at specific time intervals.

In this research work, a double beam 3000^{+} LABINDIA, UV-Vis spectrophotometer with a cell of 1.0 cm path length in the spectral range 200-800 nm, was used for optical characterization of various oxidants and kinetic study of the degradation of fluoroquinolones. A Peltier accessory (temperature-Controller) model PTC-2 is attached with the UV-Visible spectrophotometer is used for the kinetic study. Quartz cuvettes used as sample cell so that light beam travels a distance of 1 cm through the sample. Spectra were plotted between wavelength v/s absorbance [11, 12].

2.1.2. Fourier Transform Infrared Spectrophotometer

Fourier-transform infrared spectroscopy (FTIR) [13] is a technique used to obtain an infrared spectrum ofabsorption or transmittance of a solid, liquid or gas. An FTIR spectrometer simultaneously compiles high-spectral-resolution data over a

broad spectral range. This confers a significant advantage over a dispersive spectrometer, which measures intensity over a narrow range of wavelength at a time.

FTIR provides quantitative and qualitative study for organic and inorganic samples. FTIR determines chemical bonds in a molecule by generating an infrared absorption spectrum. The spectra provide a profile of the sample, a distinctive molecular fingerprint to screen and scan samples for many different components. It is a useful analytical tool for characterizing covalent bonding data and detecting functional groups.

Infrared spectroscopy is the analysis of interactions between matter and electromagnetic fields in the IR region. The electromagnetic waves mainly couple with the molecular vibrations in this spectral region. By absorbing IR radiation, a molecule can be excited to a higher vibrational state. The probability of an appropriate absorbed IR frequency depends on the actual interaction between this frequency and the molecule. Primarily, a frequency will be actively absorbed if its photon energy corresponds with the vibrational energy levels of the molecule. IR spectroscopy is a very powerful technique which gives finger print information on the chemical composition of the sample.

ALPHA-T model, Bruker, Germany spectrometer was used for getting spectra between wavelength and transmittance in 400-4000 cm^{-1} range with a resolution of 4 cm^{-1}. For preparation of pellet of sample first pellet holder, pestle, mortar, dies etc. were washing with alcohol and then 1:4 ratio dried sample and KBr grind with a pestle and mortar. Place just enough grinded samples to cover the bottom in pellet dies and press at 0-10 Tones. Then carefully remove the pressed sample from die and place in the FTIR sample holder for FTIR analysis. The pressed disc should be nearly clear if properly made [14, 15].

2.1.3. Liquid Chromatography – Mass Spectroscopy

Liquid chromatography mass spectrometry (LC-MS) offers a highly sensitive detection technique that ionizes the sample components using various methods, then separates the resulting ions in vacuum based on their mass-to charge ratios and measures the intensity of each ion. Since the mass spectra provided by MS can indicate the concentration level of ions that have a given mass, it is extremely helpful for qualitative analysis.

LC-MS is a dissolution technique used to separate the specific components of a mixture. This technique includes mass transfer between a sample and a polar mobile phase as well as a non-polar stationary phase. The tool is normally a column packed with the porous medium built of a granular solid material (i.e., stationary phase), such as silica and polymers, on this position the sample is injected and the solvent (i.e., mobile phase) passes to move the sample. After the inject sample, it is adsorbed on the stationary phase, and the solvent passes through the column to isolate the compounds one by one, based on their relative affinity to the packing objects and the solvent. The component with the most affinity to the stationary phase is the last to isolate. Due to the high affinity resemble to more time to travel to the end of the column [16].

The combined technique between MS and HPLC is HPLC-MS or more ordinarily LC-MS. Experimental error reduced through combining the two analytical methods and improves accuracy. This device is very effective in applications that involve a large number of compounds, such as environmental contaminants [17].

In this research work, LC-MS technique was used to detect intermediates and end products during antibacterial agent's degradation process. The molecular ions of unknown products were easily recognized by mass/charge ratio. Increasing fragmentation voltage of LC-MS yielded more fragments to facilitate product

identification. In this study, for LC-ESI-MS analysis Waters, Micromass Q-TOF micro was used with separation Module: Waters Alliance 2795; LC Column: Unisol YVR C18; Ionization: Electro spray Positive (ES+); Acquisition: MRM, unit resolution; Injection Volume: 20 micro liters; Flow rate: 0.5 ml/min and for Mass spectrometer, Desolvation Gas: 550Lts/Hr; Cone Gas: 30 Lts/Hr; Desolvation Temperature:300 °C; Source Temperature: 110 °C; Capillary Voltage: 3000 V; Cone Voltage: 30 V; Collision energy 4ev; Gases used N_2 and Argon; Mobile Phase used: 20/80:H_2O:MeOH; N_2 supply pressure is 6-7 bar (90-100psi), Argon is 5-6 bar etc. parameters were used. The characterization was done from SAIF/CIL, Panjab University, Chandigarh [18].

2.1.4. Ultrasonic Processor

Ultrasonic processor model EI-250UP with 250 watts (average) and 20+/-3 KHz frequency and microprocessor based timer 0 to 30 minutes was used to prepare the sample for characterization of the synthesized colloidal manganese dioxide by Transmission Electron Microscopy (TEM) analysis.

2.1.5. Transmission Electron Microscopy

Transmission Electron Microscopy (TEM) is a fundamental characterization apparatus for precisely illustrates nano materials to access quantitative measures of particle or fragment size, size distribution, and configuration. TEM illustrations are the transmission of a focused beam of electrons through a sample, forming an image in an analogous approach to a light microscope. However, electrons are used rather than light to illuminate the sample; TEM imaging technique has significantly high resolution than light-based imaging techniques [19].

In this technique, samples are prepared for imaging by drying nano particles on a thin layer of carbon coated copper grid. Materials with electron densities that are significantly higher than amorphous carbon are easily imaged. A thin specimen is imaged by an electron beam, which is irradiated through the sample at uniform

current density [20]. The typical acceleration voltage in an operational TEM is 80-200 KV. A thermionic (tungsten or lanthanum hexa boride filament) or field emission (tungsten filament) electron guns are used for electrons pouring. The illumination aperture and the area of specimen illuminated are controlled by a set of condenser lenses which are used either image or diffraction pattern formation of the specimen. Electron diffraction patterns are identified the crystallographic structure of the material. A three or four stage lens system amplified the electron intensity distribution behind the specimen and read on a fluorescent screen [20]. The illustration is captured on a photographic plate or CCD camera. A detailed description of TEM can be found elsewhere [21]. Transmission electron microscopy is an essential analytical tool in the physical, chemical and biological sciences. TEMs has utilization in many fields such as cancer research, virology, materials science, pollution, nano technology and semiconductor research [22].

Transmission electron microscope Model- Tecnai G^2 20 (FEI) S-Twin with 200 kV energy range has been used in this research work. The Tecnai G^2 hold a wide range of techniques including high resolution TEM diffraction and chemical analysis with on BF/DF axis detectors provide the Z-contrast imaging. The high angle, annular dark field detector illustrates atomic resolution dark field TEM images. The apparatus produce a point resolution of 0.24 nm, line resolution of 0.14 nm and TEM resolution of 1.0 nm. EDAX generates the elemental configuration of the material and these facilities avail by the Malaviya National Institute of Technology Jaipur, Jaipur (Rajasthan).

2.1.6. Zetasizer

The Zeta sizer nano range of instruments measures two characteristics of particles or molecules such as particles size and Zeta potential in a liquid medium. It is applicable over wide range of concentrations. Size of particle determined by calculating the random variation in the intensity of light scattered due to their random

motion from a suspension or solution, known as dynamic light scattering (DLS) technique. Random motion of particles linked to their size so larger particles move slower than small particles. The speed of Brownian motion is also analyzed by the temperature, thus precision temperature control is essential for accurate size measurement. To measure the diffusion speed, the speckle pattern composed by illuminating the particles with a laser is observed. The intensity changes are evaluated with a digital auto correlator which generates a correlation function and curve measure size distribution [23].

In this research work Zetasizer ver. 7.11 (Malvern), UK was used to analyze the average size and zeta potential of the colloidal solution of manganese dioxide. This analysis was done in the laboratory of Malaviya National Institute of Technology Jaipur, Jaipur (Rajasthan). For this analysis, sonicated sample poured in the disposable folded capillary cell then the cell was placed in the zetasizer instrument and obtained the electronic output of average size. To determine the zeta potential, the sonicated sample pours in dip cell of the instrument [24].

2.1.7. Electronic Balance

Citizen electronic balance (model- CX 220) was used for weighing reagents. It has motorised internal calibration feature with power supply A/C Adaptor 230 V or 115 V / +/-20% 50-60 Hz. The weighing range of balance is 0.0001 mg and 220 g respectively.

2.1.8. Magnetic Stirrer with Hot Plate

For preparation of required solutions for this study, magnetic stirrer with the hot plate (MSW-313, MAC) used at 600 rpm (range 0-1200 rpm) with temperature range (0-100 ℃) and stirrer work on 220/230 volts AC supply.

2.3. References

[1] I. M. Kolthoff, R. Belcher, Volumetric Analysis, ***Inter Science, New York*** (1957).

[2] A. I. Vogel, Vogel's- Textbook of Macro and Semi micro Qualitative Inorganic Analysis, ***John Wiley and Sons, New York*** (1967).

[3] G. H. Jeffery, J. Bassett, J. Mendham, R. C. Denny, Vogel's text book of quantitative chemical analysis, 5thedn. ELBS, ***Longman, Essex***, (1996) 339.

[4] A. I. Vogel, A Text Book of Quantitative Inorganic Analysis, ***Longmans***, 2 (1961) 240.

[5] C. J. Battaglia, J. O. Edwards, ***Inorg. Chem***., 4 (1965) 552.

[6] G. H. Jeffery, Bassett J, Mendham J, Denney RC. Vogel's Textbook of Quantitative Chemical. Analysis, 5th edn. ***ELBS, Longman, Essex, UK,*** (1996) 455.

[7] M. Latshaw, ***J. Am. Chem. Soc.***, 47 (1925) 793.

[8] D. A. Skoog, F. J. Holler, S. R. Crouch, ***Principles of Instrumental Analysis*** (6th ed.) (2007).

[9] http://pharmaxchange.info/press/2011/12/ultraviolet-visible-uv-vis-spectroscopy-principle/, visited in ***April, 2018***.

[10] http://pharmaxchange.info/press/2012/04/ultraviolet-visible-uv-vis-spectroscopy-%e2%80%93-derivation-of-beer-lambert-law, visited in ***April, 2018.***

[11] https://www.chemguide.co.uk/analysis/uvvisible/spectrometer.html, visited in ***May, 2018.***

[12] X. Xiong, B. Sun, J. Zhang, N. Gao, J. Shen, J. Li, X. Guan, ***Water Res.,*** 62 (2014) 53.

[13] P. Griffiths, J. A. Hasseth, Fourier Transform Infrared Spectrometry (https://books.google.com/?id=C_c0GVe8MX0C&printsec=frontcover) (2nd ed.). Wiley-Blackwell. ISBN 0-471-19404-2 visited in ***May 2007.***

[14] http://web.mst.edu/~tbone/Subjects/TBone/chem224/FTIR%20Procedure.pdf, visited in ***May, 2018.***

[15] T. Zhang, Y. Chen, Y. Wang, J. L. Roux, Y. Yang, J. -P. Croue, *Environ**. Sci. Technol.,*** 48 (2014) 5868.

[16] https://www.chemyx.com/support/knowledge-base/applications/basic-principles-hplc-ms-lc-ms/, visited in ***May, 2018.***

[17] S. Parasuraman, R. Anish, S. Balamurugan, S. Muralidharan, K. J. Kumar, V. Vijayan, ***Pharmaceutical Methods,*** 5 (2014) 47.

[18] A. J. Watkinson, E. J. Murby, S. D. Costanzo, ***Water Res.,*** 41 (2007) 4164.

[19] Transmission electron microscopy analysis of nanoparticles ***(nanocomposix.com.),*** 1.1 (2012) 4878.

[20] L. Reimer, Transmission electron microscopy: physics of image formation and microanalysis; ***Springer–Verlag, Berlin: New York,*** (1989).

[21] D. B. Williams, C. B. Carter, Transmission electron microscopy: A textbook for material science, ***Plenum Press, New York,*** (1996).

[22] https://en.wikipedia.org/wiki/Transmission_electron_microscopy, visited in ***Sep., 2018.***

[23] http://149.171.168.221/partcat/wp-content/uploads/Malvern-Zetasizer-LS.pdf, visited in ***Feb., 2018.***

[24] file:///C:/Users/pc-4/Downloads/Zetasizer%20range.pdf, visited in ***May, 2018.***

Chapter – 3

Soluble Colloidal Manganese Dioxide: Formation, Characterization and Application in Oxidative Kinetic study of Ciprofloxacin

3.1. Introduction

Manganese dioxide (MnO_2) is one of the most important natural oxidants with an oxidation potential of 1.23 V [1]. Due to its importance such as the low toxicity, low cost, electrochemical behaviour, environmental compatibility and ease of handling, many researchers have been developed different methods for preparation of soluble colloidal MnO_2 [2-4]. Various approaches such as self-reacting micro emulsion, precipitation, room temperature solid reactions, sono chemical reduction and hydrothermal methods have been developed to prepare nano scale MnO_2 [5-10]. Soluble colloidal MnO_2 has been prepared by the reduction of $KMnO_4$ by $Na_2S_2O_3$, $Mn(ClO_4)$, $MnSO_4$ and HCOOH [11-13]. Perez-Benito et al. [14-16] has also been reported a method for preparation of perfectly transparent dark brown water soluble colloidal manganese dioxide sols by the permanganate-thiosulphate reaction in aqueous neutral conditions. The formed soluble colloidal MnO_2 has been characterized by different instrumental techniques and determined by iodometric method [17, 18]. The oxidation of organic reductants by MnO_2 in aqueous media has received considerable attention. MnO_2 is the most effective and vital oxidizing agent and offers the potential for degrading various organic pollutants [19]. The presence of manganese(IV) in the aqueous solution in colloidal form and as negatively charged species has been described in the literature [20, 21], and due to its insolubility the oxidizing ability has been establish to be limited under normal conditions [22]. In fact, manganese oxides have been presented to be capable of oxidizing a wide range of organic pollutants [23–26]. The elimination of micro pollutants such as synthetic hormones, anti-inflammatory drugs, antibacterial agents, bisphenol A, phenols, sulfides, 2-mercaptobenzothiazole (2MBT), and sulfadiazine, have been obtained by MnO_2 [27-32]. The kinetics and mechanism of oxidation of simple organic reactants like aspartic acid, oxalic acid, lactic acid, mandelic acid, amino acid, D-fructose, D-glucose, Cystein and glutathione [21,33-39] etc by colloidal MnO_2 have been studied.

Ciprofloxacin (CIP) {1-cyclopropyl-6-fluoro-1,4-dihydro-4-oxo-7-(piperazine-1- yl)-quinolone-3-carboxylic acid} is a second generation fluoroquinolone antimicrobial agent with a wide spectrum of activity against many gram positive and gram negative aerobic and anaerobic bacteria. CIP possess two relevant ionisable functional groups: a basic piperazinyl group and a carboxylic group which are required for antimicrobial activity. The fluoroquinolones have become an increasingly popular class of antibiotics for use in a variety of infections so they are excessively used in the world. Most of them are partially metabolized and excreted by humans and animals and spilled into water. The presence and accumulation of fluoroquinolone antibiotics in aquatic environments, requires development of the various oxidation processes for the transformation of fluoroquinolones in water. The literature survey reveals that the oxidation of CIP by many oxidants such as hexacyanoferrate(III), chloramine-B, Cl_2, ClO_2, $CeSO_4$, Fe(VI) [40-47] have been carried out in either alkaline or acidic medium. Studies reveal that the piperazine moiety of CIP is the predominant oxidative site for oxidation [48-50]. Literature survey revealed that the kinetics and mechanism of degradation of different antibiotics by MnO_2 in aqueous acidic/alkaline medium have been studied earlier [51-54]. But the reaction involving CIP and colloidal MnO_2 in aqueous acidic medium has yet not been studied. Therefore, the objective of this study is to undertake the formation of colloidal MnO_2 and complete research of the kinetic and mechanistic aspects of the oxidation of CIP by formed MnO_2 in aqueous acidic medium.

3.2. Experimental Details

3.2.1. Chemicals

The method of preparation and standardization of the reagents are given in chapter 2 (Experimental). All chemicals used were of analytical grade and twice distilled water, second distillation being from alkaline permanganate solution in an all glass still, was used in all preparation and kinetic studies. Always freshly prepared and standardized MnO_2 solutions were used in the kinetics.

3.2.2. Preparation of MnO_2

For the formation of water soluble MnO_2, the required volume of $Na_2S_2O_3$ solution (20 cm^3, 2.0 × 10^{-2} mol dm^{-3}) was added to a standard solution of $KMnO_4$ (10 cm^3, 0.1mol dm^{-3}) and the reaction mixture was diluted by the required volume of water in 2 dm^{-3} standard flask [16].

$$8MnO_4^- + 3S_2O_3^{2-} + 2H^+ \rightarrow 8MnO_2 + 6SO_4^{2-} + H_2O \quad (3.1)$$

The dark brown and perfectly transparent solution was obtained and stable for several weeks. The absorption spectrum of the reaction mixture consists of one broad band covering the whole visible region of the spectrum with λ_{max} 390 nm. The formation and particle size of colloidal $MnO_2$was analyzed at different concentration of $Na_2S_2O_3$.The application of Beer's law of MnO_2 at 390 nm had been verified giving ε = 15660dm^3 mol^{-1} cm^{-1} [13].

3.2.3. Characterization

A Peltier accessory (temperature-Controlled) attached to a double beam, UV-Visible spectrophotometer (U.V.3000$^+$ LABINDIA, Mumbai) with U.V. path length 1.0 cm in the spectral range 200-800 nm, was used for the primary characterization of synthesized colloidal MnO_2 and kinetic analysis. Transmission electron microscopy (TEM) was used to study the morphology of colloidal MnO_2. Samples for TEM analysis were prepared by drop-coating MnO_2 suspension on carbon coated copper grid. The film on the TEM grid was allowed to stand for 2 minutes, following then the extra solution was removed using a blotting paper and the grid allowed drying prior to measurement on TEM (Model-Tecnai G^2 20 (FEI) S-Twin) instrument. Additionally, the presence of metal in the sample was analyzed by energy dispersive X-ray (EDX) spectrometer. Stability and average size of colloidal MnO_2 has been investigated by zeta sizer and zeta potential (Zetasizer ver. 7.11, Malvern). Spectrum of colloidal MnO_2 and oxidation product were recorded from Fourier Transform Infrared (FT-IR) Spectrophotometer (ALPHA-T, Bruker, Germany) in the range of 400-4000 cm^{-1} by mixing the sample with dried KBr (in 1:20 weight ratio) with a

resolution of 4 cm^{-1}. LC-ESI-MS, (Q-TOF Micromass, WATERS Company, UK), was used for oxidation product analysis over a mass scan range of 50 – 1000 m/z.

3.2.4. Kinetic Measurements

In all the kinetic runs, the oxidation of CIP by colloidal MnO_2 was carried out under pseudo first order condition. The required concentrations of reactants (CIP, $HClO_4$, and $NaClO_4$) were taken in the Erlenmeyer flask and the reaction was initiated by addition of required concentration of colloidal MnO_2 at 35ºC. The progress of the reaction was followed by monitoring the absorbance of MnO_2 at 390 nm in UV-Visible spectrophotometer at different time intervals **(Figure 3.1)**. All the kinetics runs were followed up to 80% completion of the reaction. The pseudo first order rate constants (k_{obs}) were evaluated from plots of log (absorbance) versus time.

3.3. Results and Discussion

3.3.1. Characterization of MnO_2

Formation of colloidal MnO_2 by reduction of permanganate ions by the sodium thiosulfate was studied by UV–Vis spectroscopy. The effect of different concentrations of sodium thiosulfate on the formation and particle size of nano particles were also investigated **(Figure 3.2)**. At lower $[Na_2S_2O_3]$ (1.75×10^{-4} mol dm^{-3}), a weak absorption peak at 390 nm was observed, indicating that due to insufficient reduction relatively low concentration of MnO_2 were produced. As the $[Na_2S_2O_3]$ increases up to 2.0×10^{-4} mol dm^{-3},intensity of absorption peak at 390 nm increases after that absorption peak becomes lower, indicating the precipitation of colloidal MnO_2 at higher $[Na_2S_2O_3]$. However, the maximum absorption peak was obtained at 2.0×10^{-4} mol dm^{-3}, suggesting the optimum concentration of $Na_2S_2O_3$ for formation of colloidal MnO_2. The resulting solution was dark reddish brown and perfectly transparent and stable for several weeks.

The surface elemental composition of the synthesized MnO_2nano particles was characterized by the energy dispersive X-ray (EDX) spectrometer. The EDX

pattern indicates the predominant presence of Mn and O peaks and Mn and O element content in the samples **(Figure 3.3)** confirming the colloidal MnO_2 formation which also reported in earlier studies [55, 56]. TEM analysis was carried out to determine the size and shape of colloidal MnO_2; the images show that the formed particles were needle shape **(Figure 3.4A)** with average size 20.59 nm at $[Na_2S_2O_3]$ 2.0 $\times 10^{-4}$ mol dm^{-3}. Whereas, at higher $[Na_2S_2O_3]$, TEM results **(Figure 3.4B)**, suggesting that too many reducing agent cause aggregation of formed particle. It is possible due to the interaction between capping molecules bound to the surface of particles and secondary reduction process on the surface of the performed nuclei [35]. The results are well consistent with U.V. spectra in figure 3.2. The selected area electron diffraction (SAED) arrangement **(Figure 3.4A inset)** of the colloidal MnO_2 was also recorded. The ring like diffraction shows crystalline particles nature [17]. Zeta sizer (dynamic light scattering) and zeta potential has been described the size distribution and the stability of synthesized colloidal MnO_2 respectively. The zeta potential of colloidal MnO_2 was found to be -41.1 mV with average size 20.59 nm **(Figure 3.5A and B)** suggesting that the surface of the particle was negatively charged that dispersed in the medium. To investigate the chemical structure of the particles, the FT-IR analysis was performed. Two absorption bands located at around 3400 and 1623 cm^{-1} correspond to O–H and H–O–H **(Figure 3.6)** [57].

The oxidation state of manganese species in the colloidal solution was also determined iodometrically at 390 nm based on previous report [58]. The determined oxidation state of Mn species in MnO_2 was (+4.16), was confirming the MnO_2 [59].

3.3.2. Stoichiometry and product analysis

The stoichiometry of the MnO_2 – CIP reaction was determined by carrying out the reaction with an excess of MnO_2 over CIP in acid perchlorate medium at 35˚C for 12 h. The excess of MnO_2 was determined spectrophotometrically and the results are correspond to the stoichiometry as represented by equation (3.2)

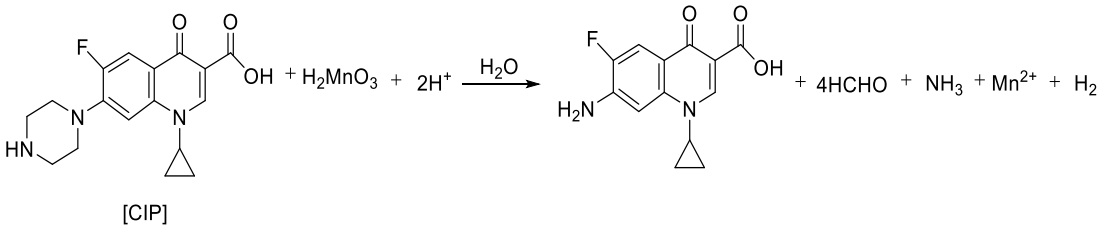

(3.2)

The product {7-amino-1-cyclopropyl-6-fluoro-1, 4-dihydro-4-oxo-quinolone-3-carboxylic acid} was extracted from the reaction mixture with ether and identified with the help of TLC and characterized by FT-IR and LC-MS analysis. FT-IR analysis confirmed the presence of $–NH_2$ group in the oxidation product **(Figure 3.7)**. The IR spectrum shows a peak at 3375.45 cm^{-1} which is due to –NH stretching of the $–NH_2$ group and the remaining peaks are of the parent compound. LC-MS analysis of CIP oxidation reaction indicates the formation of product with molecular ion of m/z 263 **(Figure 3.8)**. The m/z 263 corresponds to fully dealkylation of the piperazine ring [60]. It is worth noting, that oxidation of piperazine moiety of CIP between oxidized centres and nitrogen atoms lead to distinctive mass loss m/z = 69. This was attributed to ring opening, dealkylation and deamination process, which finally yielded 7-amino fluoroquinolone product. Formaldehyde was determined by spot test as a by-product and other product ammonia was distinguished by Nesseler's reagent test.

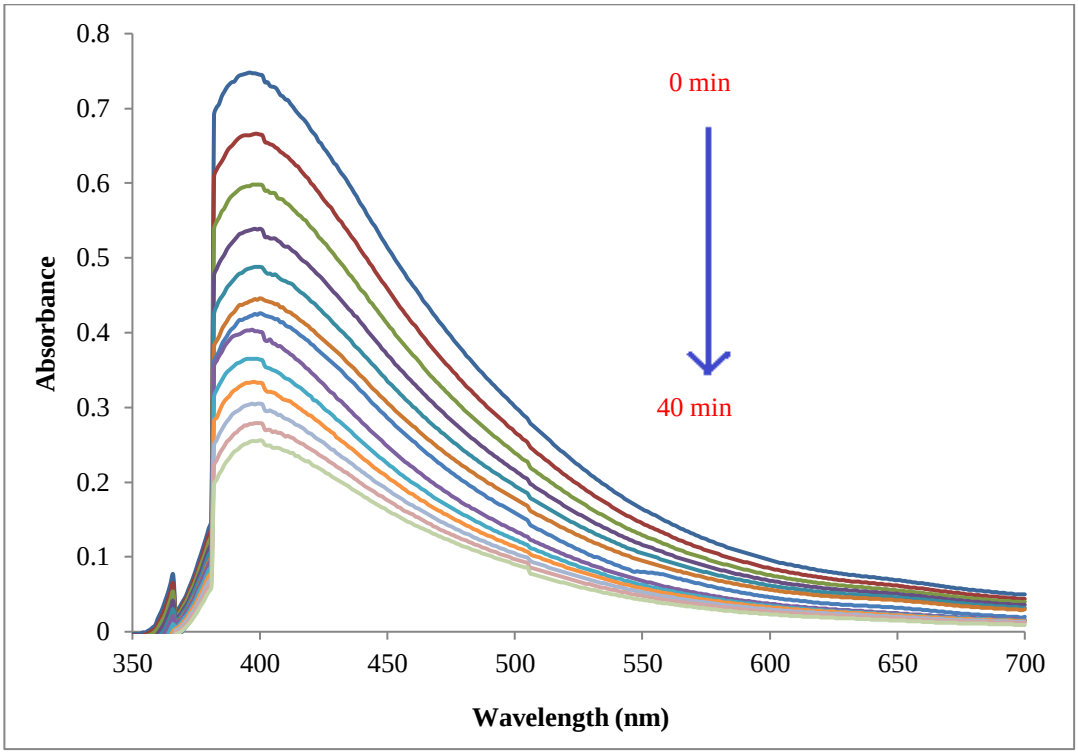

Figure 3.1: UV-visible spectral change during the oxidation of CIP by colloidal MnO_2 in acidic medium.

$[MnO_2] = 5.0 \times 10^{-5}$ mol dm^{-3}; $[CIP] = 5.0 \times 10^{-4}$ mol dm^{-3};

$[H^+] = 2.0 \times 10^{-4}$ mol dm^{-3}; $I = 4.0 \times 10^{-4}$ mol dm^{-3};

Temperature = 35 ˚C.

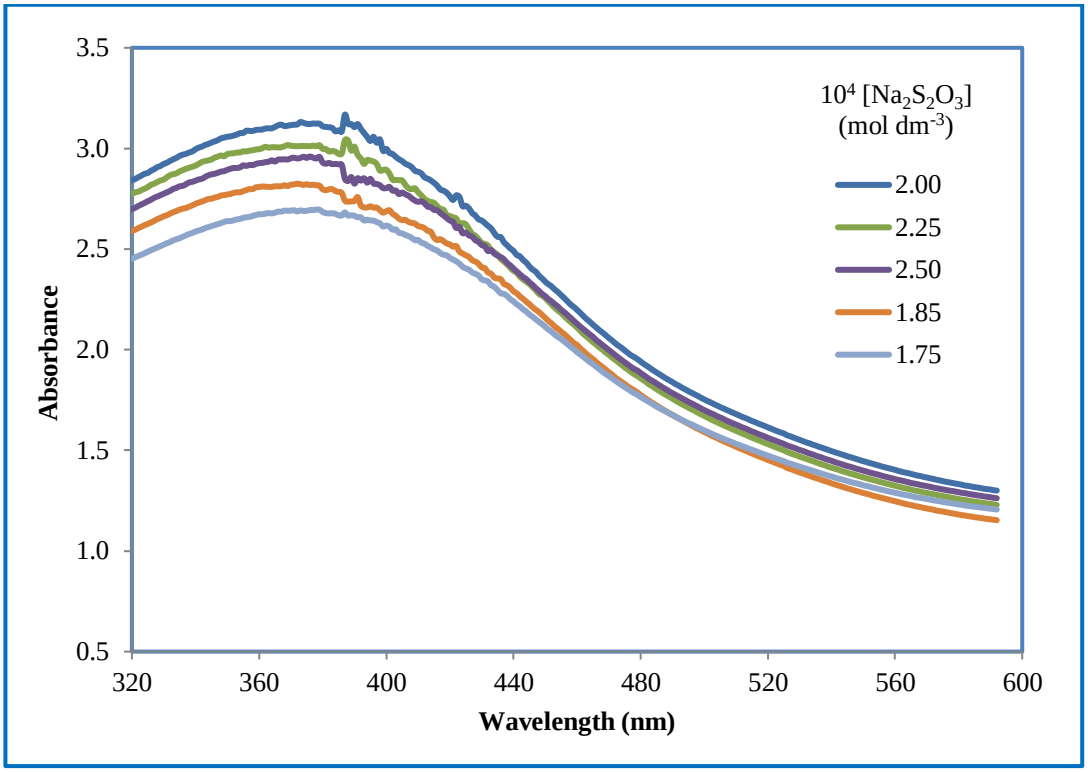

Figure 3.2: UV-visible spectra of the mixtures containing a fixed amount of $KMnO_4$ (2.0×10^{-4} mol dm^{-3}) and varying amounts of $Na_2S_2O_3$ at 35˚C.

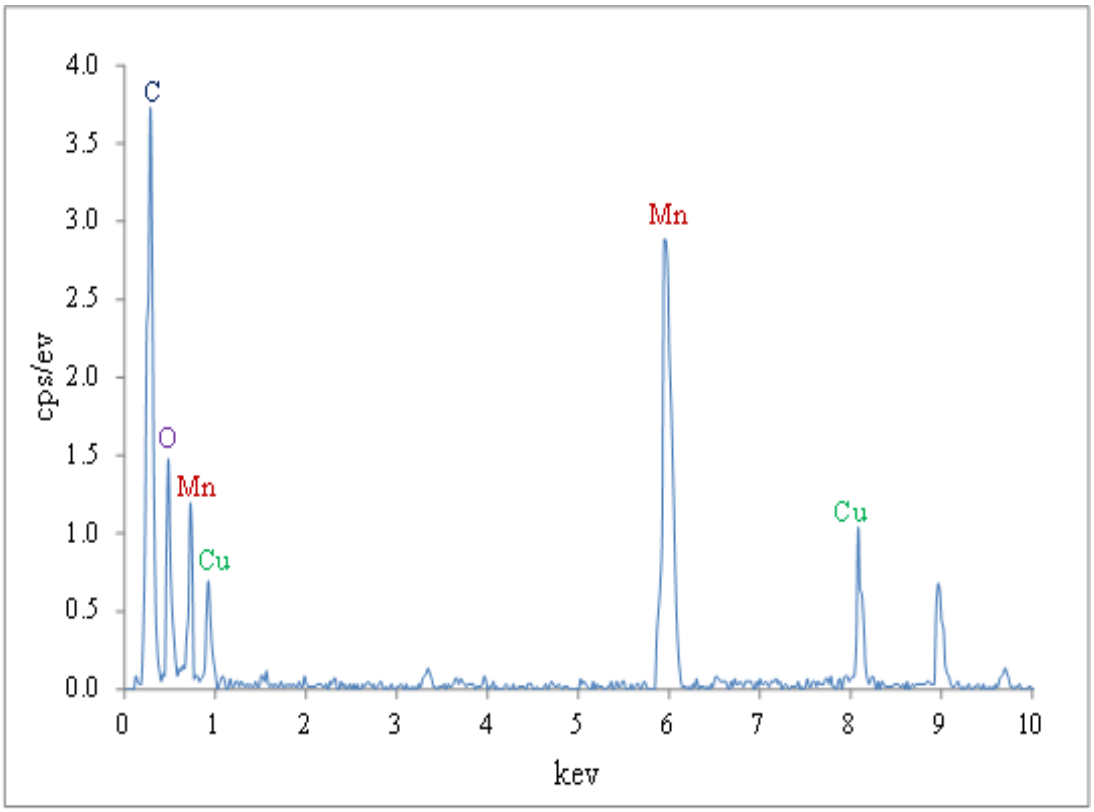

Figure 3.3: EDX analysis of synthesized colloidal MnO_2.

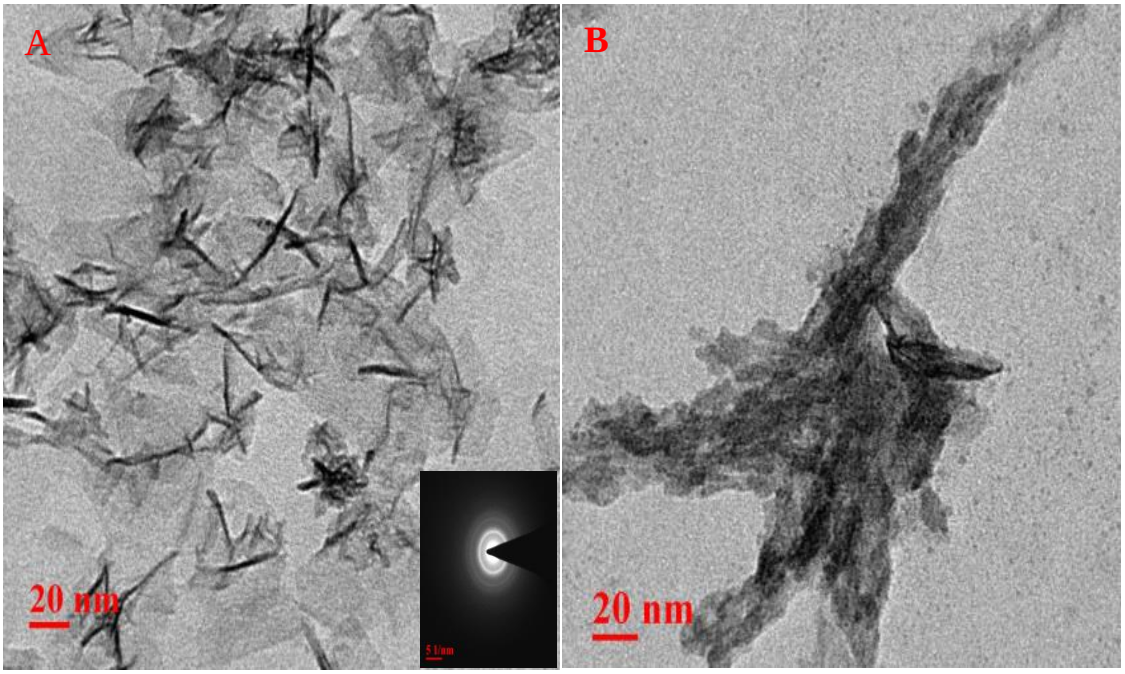

Figure 3.4: (A) TEM of synthesized colloidal MnO_2 at optimum conditions and inset SAED pattern. (B) TEM of synthesized colloidal MnO_2 at higher [$Na_2S_2O_3$].

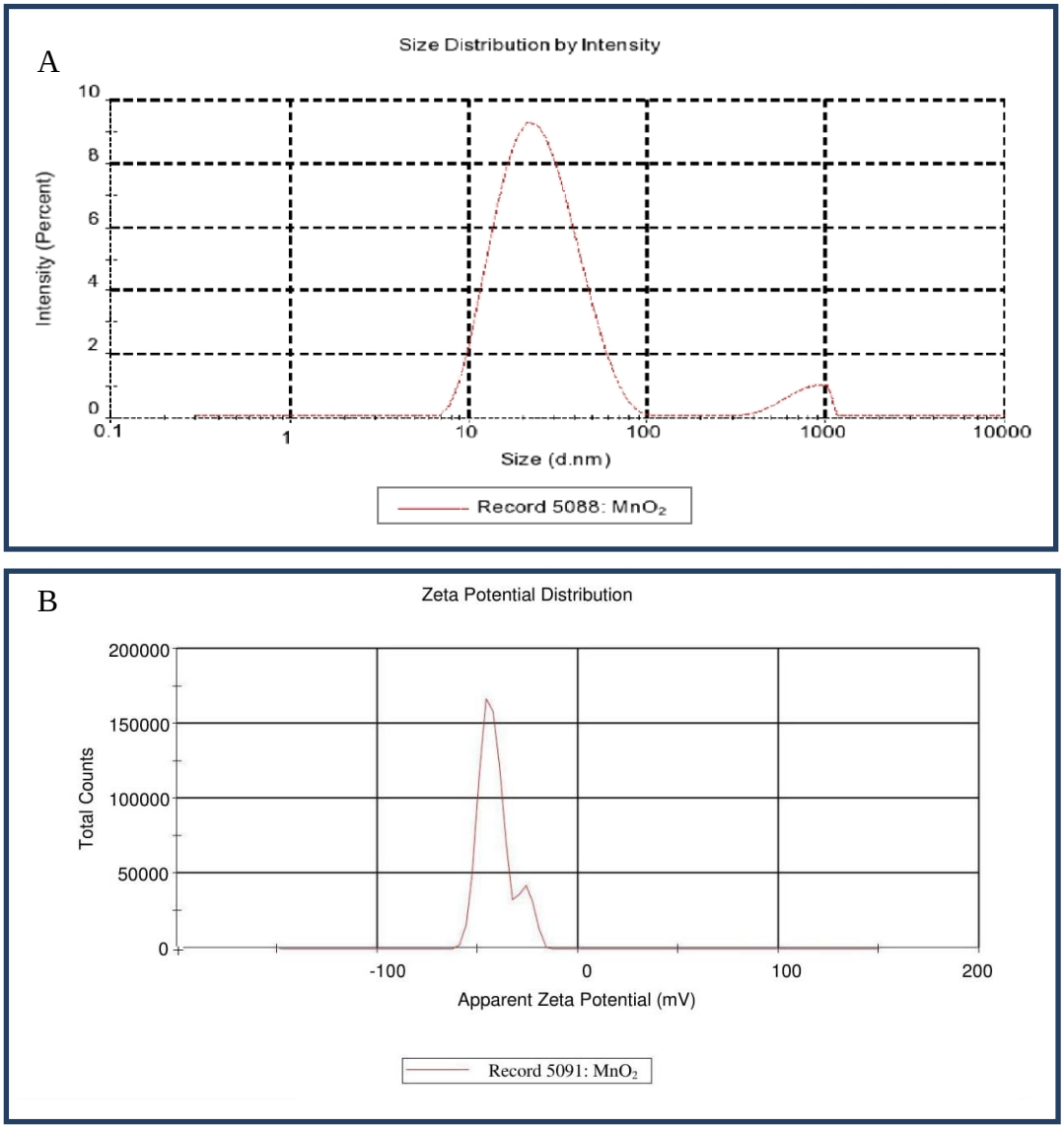

Figure 3.5: (A) Zeta sizer and (B) Zeta potential of synthesized colloidal MnO_2.

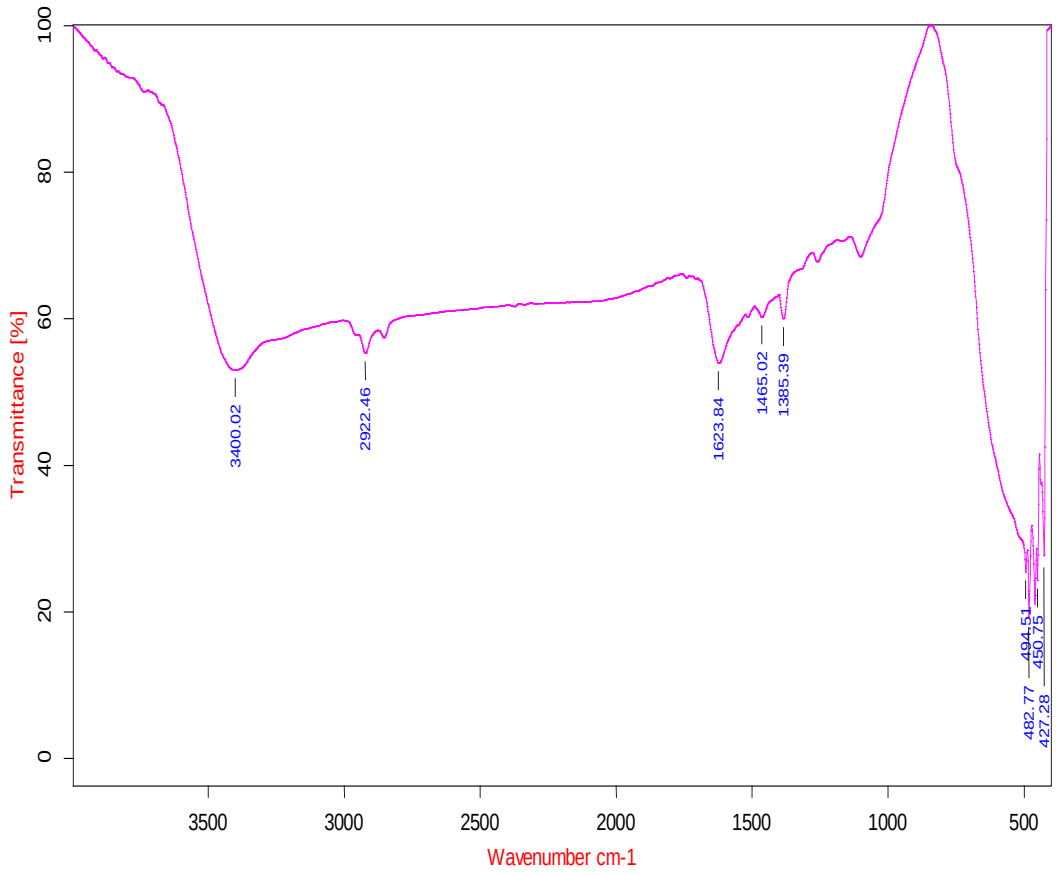

Figure 3.6: FT-IR spectra of synthesized colloidal MnO_2.

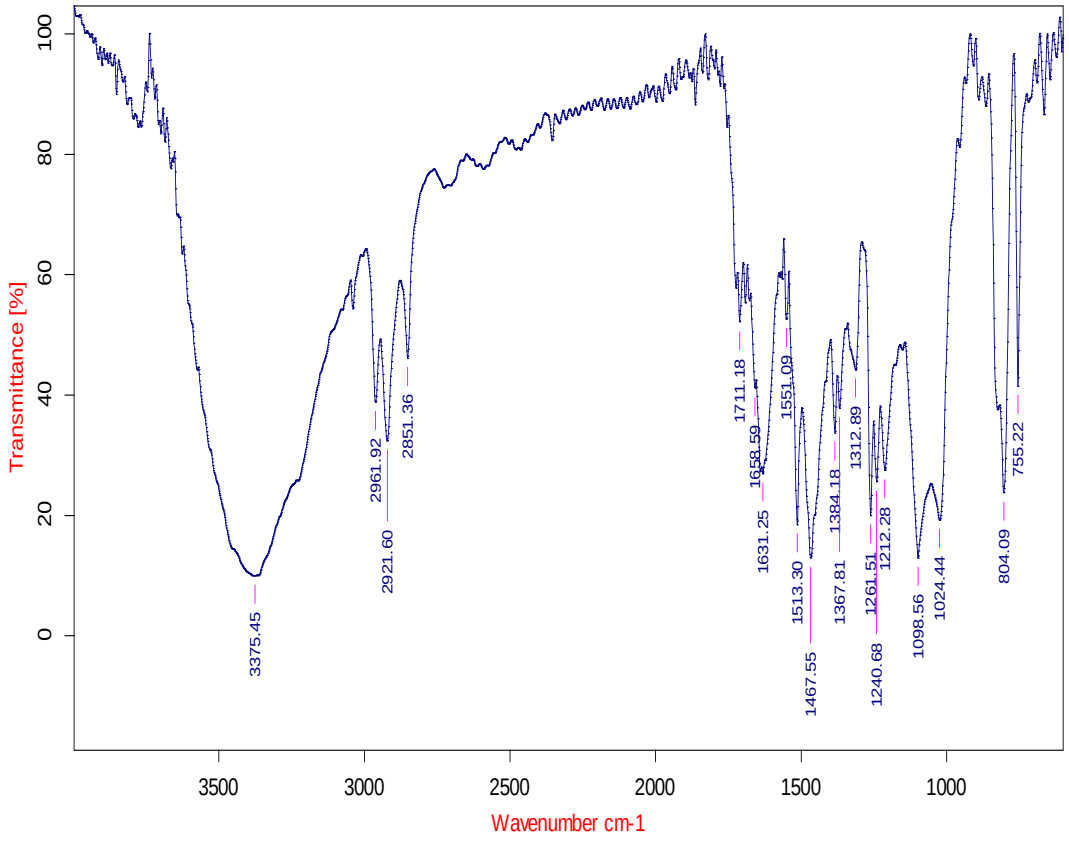

Figure 3.7: FTIR spectra of the oxidation product of CIP by MnO_2 in aqueous acidic medium.

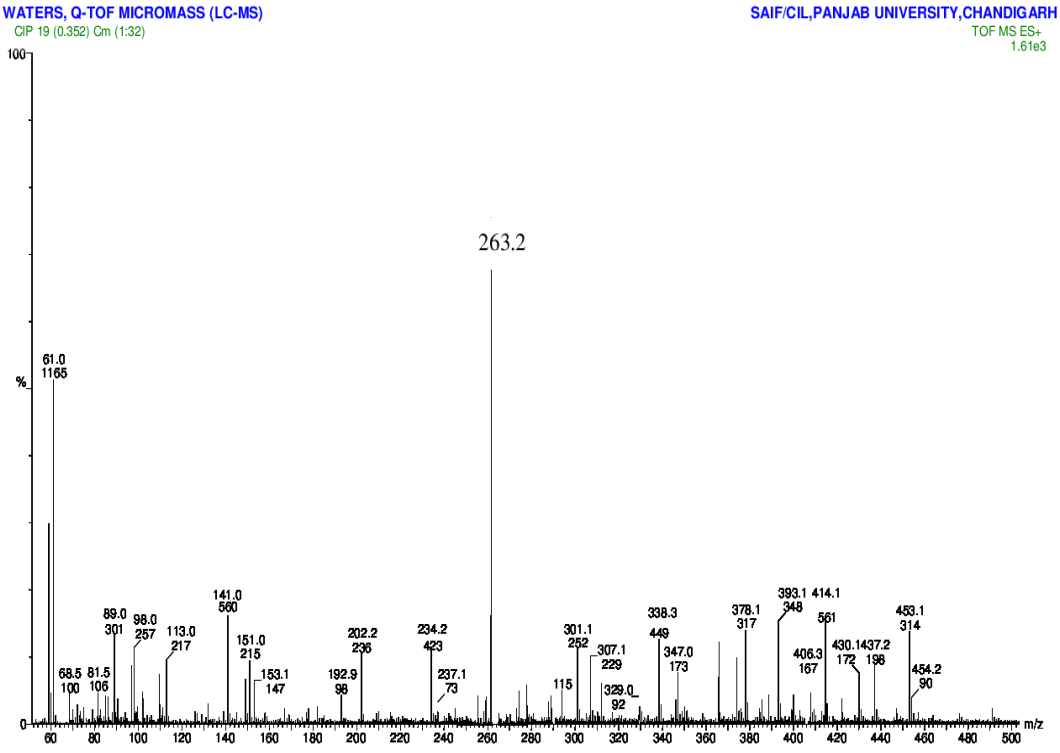

Figure 3.8: LC-ESI-MS spectra of oxidation product of ciprofloxacin.

3.3.3. Kinetics of CIP oxidation by colloidal MnO_2

3.3.3.1. MnO_2 dependence

The concentration of MnO_2 was varied from 0.75×10^{-5} mol dm^{-3} to 7.5×10^{-5} mol dm^{-3} at two different concentration of CIP (5.0×10^{-4} mol dm^{-3} and 8.0×10^{-4}mol dm^{-3}) but fixed $[H^+] = 2.0\times10^{-4}$ mol dm^{-3} and $I = 4.0\times10^{-4}$ mol dm^{-3} (adjusted by sodium perchlorate) at 35°C. Pseudo first order rate constants (k_{obs}) calculated from pseudo first order plots **(Figure3.9)** (r^2 =1.0), were to be independent of MnO_2 concentration indicates reaction is first order with respect to MnO_2.Results are given in **Tables 3.1, 3.2.**

3.3.3.2. Ciprofloxacin dependence

The concentration of CIP was varied from 1.0×10^{-4} mol dm^{-3} to 1.0×10^{-3} mol dm^{-3} at fixed concentration of other reaction ingredients viz. $[MnO_2] = 5.0 \times 10^{-5}$ mol dm^{-3}, $[H^+] = 2.0 \times 10^{-4}$ mol dm^{-3}, $I = 4.0 \times 10^{-4}$ mol dm^{-3} at three temperatures viz. 30 °C, 35°C, 40°C respectively. The rate of reaction initially increases and tends towards a limiting value with higher concentration of the CIP ($r^2 \leq 0.908$) showing fractional order dependence with respect to CIP **(Figure 3.10)**. Results are given in **Tables 3.3, 3.4 and 3.5.**

3.3.3.3. Hydrogen ion dependence

Hydrogen ion concentration was varied from 1.0×10^{-4} mol dm^{-3} to 4.0×10^{-4} mol dm^{-3} employing perchloric acid at fixed $[MnO_2] = 5.0 \times 10^{-5}$ mol dm^{-3}, [CIP] = 5.0×10^{-4} mol dm^{-3} and $I = 4.0 \times 10^{-4}$ mol dm^{-3}at 35 °C. The rate of reaction is increases with increasing concentration of H^+ (r^2 = 1.0) **(Figure 3.11)**. Results are given in **Tables 3.6.**

3.3.3.4. Ionic strength dependence

Ionic strength was varied from 3.0×10^{-4} to 9.0×10^{-4} mol dm^{-3} employing sodium perchlorate keeping constant concentration of $[MnO_2] = 5.0 \times 10^{-5}$ mol dm^{-3}, [CIP] = 5.0×10^{-4} mol $dm^{-3}$and $[H^+] = 2.0 \times 10^{-4}$ mol dm^{-3} at 35 °C. However, rate of

reaction remains unaffected by the change in ionic strength **(Table 3.7)**. The negligible effect of ionic strength on the rate of reaction suggests that the reaction is either between two neutral species or a neutral and a charged species [61].

3.3.3.5. Sodium fluoride dependence

The concentration of sodium fluoride was varied from 1.0×10^{-4} to 2.0×10^{-3} mol dm^{-3}at fixed constant concentration of other reactants $[MnO_2] = 5.0 \times 10^{-5}$ mol dm^{-3}, [CIP] = 5.0×10^{-4} mol dm^{-3}, $[H^+] = 2.0 \times 10^{-4}$ mol dm^{-3} and I = 4.0×10^{-4} mol dm^{-3} at 35 °C. The rate of reaction is retards and then attains a limiting rate at higher concentration of fluoride ion ($r^2 = 0.764$) **(Figure 3.12)**. Results are given in **Table 3.8**.

3.3.3.6. Test for free radical

The formation of free radical was confirmed by the addition of acrylonitrile in the reaction mixture. After 5 h diluted with methanol, while precipitate was formed, indicating the presence of free radical during the progress of reaction.

TABLE: 3.1

VARIATION OF MANGANESE DIOXIDE

[CIP] = 5.0 × 10^{-4} mol dm^{-3} **Temp. = 35°C**

[H^+] = 2.0 × 10^{-4} mol dm^{-3} **I = 4.0 × 10^{-4} mol dm^{-3}**

10^5 [MnO_2], mol dm^{-3}	**0.75**	**1.0**	**2.0**	**3.0**	**4.0**	**5.0**	**6.0**	**7.5**
Time in minutes				**Absorbance**				
0	0.117	0.145	0.302	0.455	0.626	0.783	0.940	1.170
5	0.092	0.114	0.237	0.359	0.495	0.610	0.733	0.923
10	0.072	0.089	0.186	0.282	0.389	0.479	0.575	0.724
15	0.057	0.070	0.146	0.221	0.305	0.376	0.452	0.569
20	0.045	0.055	0.115	0.174	0.240	0.295	0.355	0.447
25	0.035	0.043	0.090	0.136	0.188	0.232	0.279	0.351
30	0.028	0.034	0.071	0.107	0.148	0.182	0.219	0.275
35	0.022	0.027	0.056	0.084	0.116	0.143	0.172	0.216
10^4 (k_{obs}), mol dm^{-3}	8.05	8.10	7.90	8.01	8.10	8.00	7.91	8.11

Figures in parentheses denote time in minutes.

TABLE: 3.2

VARIATION OF MANGANESE DIOXIDE

[CIP] = 8.0 × 10^{-4} mol dm^{-3} **Temp. = 35ºC**

[H^+] = 2.0 × 10^{-4} mol dm^{-3} **I = 4.0 × 10^{-4} mol dm^{-3}**

10^5 [MnO_2], mol dm^{-3}	**0.75**	**1.0**	**2.0**	**3.0**	**4.0**	**5.0**	**6.0**	**7.5**
Time in minutes				**Absorbance**				
0	0.117	0.145	0.302	0.455	0.626	0.783	0.940	1.170
30	0.097	0.118	0.245	0.374	0.513	0.635	0.764	0.962
60	0.080	0.097	0.200	0.306	0.417	0.520	0.625	0.787
90	0.066	0.079	0.162	0.251	0.339	0.426	0.512	0.644
120	0.054	0.065	0.132	0.205	0.275	0.348	0.419	0.527
150	0.045	0.053	0.107	0.168	0.224	0.285	0.343	0.432
180	0.037	0.043	0.087	0.137	0.182	0.233	0.281	0.353
210	0.030	0.036	0.071	0.112	0.148	0.191	0.230	0.289
240	0.025	0.029	0.058	0.092	0.120	0.156	0.188	0.237
10^4 (k_{obs}), mol dm^{-3}	10.9	11.2	11.1	11.0	11.1	11.2	10.9	11.0

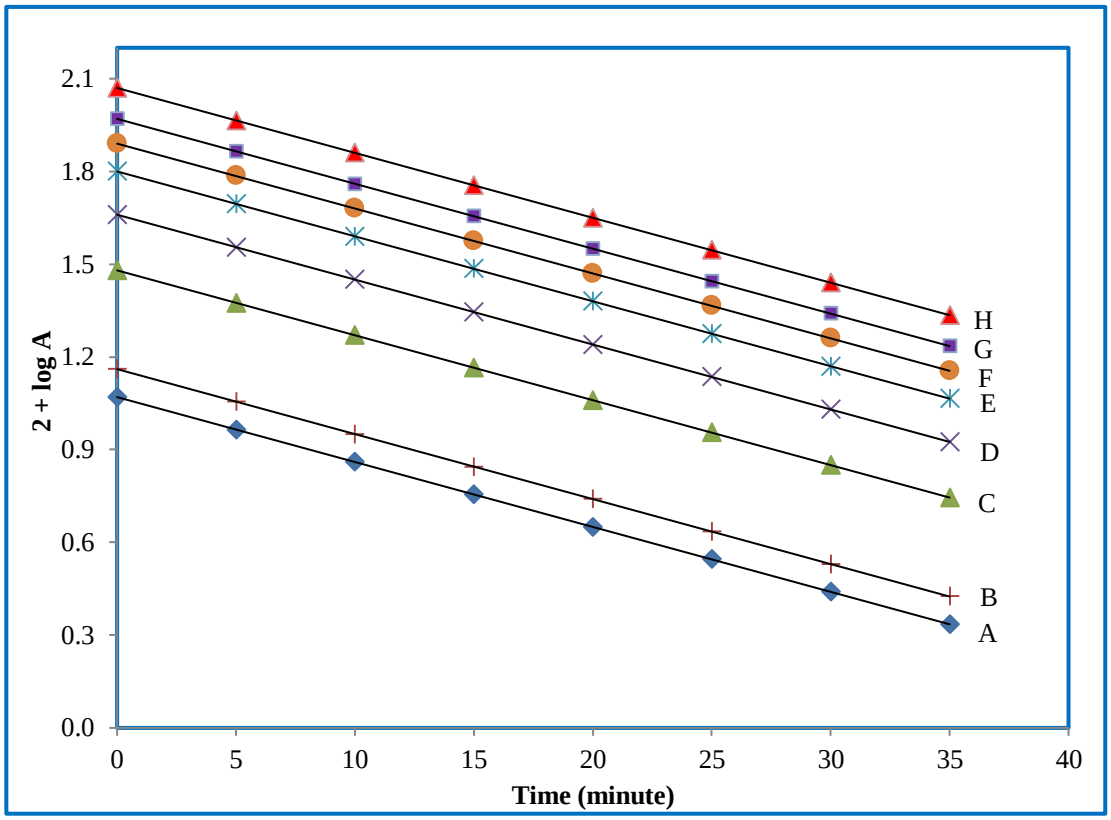

Figure 3.9: Variation of manganese dioxide.

[CIP] = 5.0×10^{-4} mol dm^{-3}; Temp. = 35°C;

$[H^+] = 2.0 \times 10^{-4}$ mol dm^{-3}; I = 4.0×10^{-4} mol dm^{-3};

$[MnO_2]$ = (A) 0.75×10^{-5} mol dm^{-3}; (B) 0.5×10^{-5} mol dm^{-3};

(C) 1.0×10^{-5} mol dm^{-3}; (D) 2.0×10^{-5} mol dm^{-3};

(E) 3.0×10^{-5} mol dm^{-3}; (F) 4.0×10^{-5} mol dm^{-3};

(G) 5.0×10^{-5} mol dm^{-3}; (H) 7.5×10^{-5} mol dm^{-3}.

(Ref. Tables: 3.1)

TABLE: 3.3

VARIATION OF CIPROFLOXACIN

$[MnO_2] = 5.0 \times 10^{-5}$ mol dm^{-3} **Temp. = 30ºC**

$[H^+] = 2.0 \times 10^{-4}$ mol dm^{-3} **I = 4.0×10^{-4} mol dm^{-3}**

10^4 [CIP], mol dm^{-3}	**1.0**	**3.0**	**5.0**	**7.0**	**9.0**	**10.0**
Time in minutes			**Absorbance**			
0	(0)0.776	(0)0.775	(0)0.777	0.773	0.776	0.775
6	(30)0.614	(12)0.612	(8)0.620	0.632	0.621	0.619
12	(60)0.486	(24)0.483	(16)0.494	0.515	0.497	0.493
18	(90)0.385	(36)0.381	(24)0.395	0.419	0.397	0.393
24	(120)0.304	(48)0.300	(32)0.315	0.342	0.318	0.313
30	(150)0.241	(60)0.237	(40)0.251	0.278	0.254	0.250
36	(180)0.190	(72)0.187	(48)0.201	0.227	0.204	0.199
42	(210)0.151	(84)0.147	(56)0.160	0.185	0.162	0.158
10^4 (k_{obs}), mol dm^{-3}	1.31	3.32	4.70	5.81	6.22	6.30

Figures in parentheses denote time in minutes.

TABLE: 3.4

VARIATION OF CIPROFLOXACIN

$[MnO_2] = 5.0 \times 10^{-5}$ mol dm^{-3} **Temp. = 35 ºC**

$[H^+] = 2.0 \times 10^{-4}$ mol dm^{-3} **I = 4.0×10^{-4} mol dm^{-3}**

10^4 [CIP], mol dm^{-3}	**1.0**	**3.0**	**5.0**	**7.0**	**9.0**	**10.0**
Time in minutes			**Absorbance**			
0	(0)0.776	(0)0.774	(0)0.777	0.775	0.776	0.774
4	(16)0.605	(6)0.628	(5)0.611	0.621	0.614	0.612
8	(32)0.471	(12)0.508	(10)0.480	0.497	0.485	0.483
12	(48)0.367	(18)0.411	(15)0.378	0.397	0.383	0.381
16	(64)0.286	(24)0.332	(20)0.297	0.318	0.303	0.300
20	(80)0.223	(30)0.268	(25)0.234	0.254	0.240	0.237
24	(96)0.174	(36)0.217	(30)0.184	0.203	0.189	0.187
28	(112)0.135	(42)0.176	(35)0.145	0.163	0.150	0.147
10^4 (k_{obs}), mol dm^{-3}	2.61	5.90	8.05	9.32	9.81	9.90

Figures in parentheses denote time in minutes.

TABLE: 3.5

VARIATION OF CIPROFLOXACIN

$[MnO_2] = 5.0 \times 10^{-5}$ mol dm^{-3} **Temp. = 40 ºC**

$[H^+] = 2.0 \times 10^{-4}$ mol dm^{-3} **I = 4.0×10^{-4} mol dm^{-3}**

10^4 [CIP], mol dm^{-3}	**1.0**	**3.0**	**5.0**	**7.0**	**9.0**	**10.0**
Time in minutes			**Absorbance**			
0	(0)0.774	(0)0.777	0.775	0.774	0.777	0.776
5	(10)0.600	(4)0.624	0.629	0.613	0.607	0.606
10	(20)0.463	(8)0.502	0.509	0.484	0.474	0.472
15	(30)0.358	(12)0.403	0.413	0.383	0.371	0.369
20	(40)0.277	(16)0.324	0.334	0.302	0.290	0.287
25	(50)0.214	(20)0.260	0.271	0.239	0.226	0.224
30	(60)0.165	(24)0.209	0.219	0.189	0.177	0.175
35	(70)0.128	(28)0.168	0.178	0.149	0.138	0.136
10^4 (k_{obs}), mol dm^{-3}	4.31	9.10	11.72	13.11	13.70	14.05

Figures in parentheses denote time in minutes.

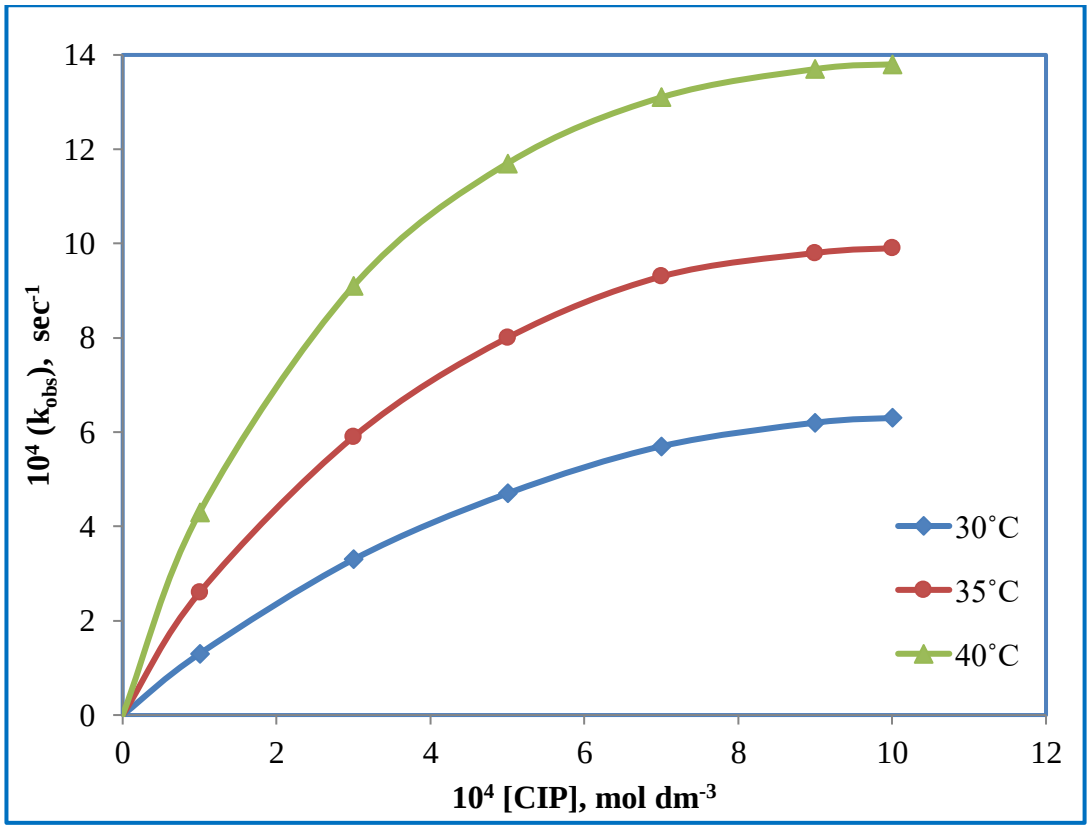

Figure 3.10: Variation of ciprofloxacin at different temperatures.

$[MnO_2] = 5.0 \times 10^{-5}$ mol dm^{-3};

$[H^+] = 2.0 \times 10^{-4}$ mol dm^{-3};

$I = 4.0 \times 10^{-4}$ mol dm^{-3}.

(Ref. Table: 3.3, 3.4 and 3.5)

TABLE: 3.6

VARIATION OF HYDROGEN ION

$[MnO_2] = 5.0 \times 10^{-5}$ mol dm^{-3} **Temp. = 35 ºC**

[CIP] = 5.0×10^{-4} mol dm^{-3} **I = 4.0×10^{-4} mol dm^{-3}**

10^4 [H^+], mol dm^{-3}	**1.0**	**1.5**	**2.0**	**2.5**	**3.0**	**3.5**	**4.0**
Time in minutes			**Absorbance**				
0	(0)0.775	(0)0.774	(0)0.776	(0)0.775	0.776	0.774	0.776
3	(10)0.611	(7)0.603	(5)0.611	(4)0.611	0.625	0.603	0.582
6	(20)0.480	(14)0.469	(10)0.480	(8)0.480	0.504	0.469	0.436
9	(30)0.378	(21)0.365	(15)0.378	(12)0.378	0.406	0.365	0.327
12	(40)0.297	(28)0.283	(20)0.297	(16)0.297	0.327	0.283	0.245
15	(50)0.234	(35)0.220	(25)0.234	(20)0.234	0.264	0.220	0.184
18	(60)0.184	(42)0.171	(30)0.184	(24)0.184	0.212	0.171	0.138
21	(70)0.145	(49)0.133	(35)0.145	(28)0.145	0.171	0.133	0.103
10^4 (k_{obs}), mol dm^{-3}	4.05	6.11	8.01	10.20	12.11	14.30	16.05

Figures in parentheses denote time in minutes.

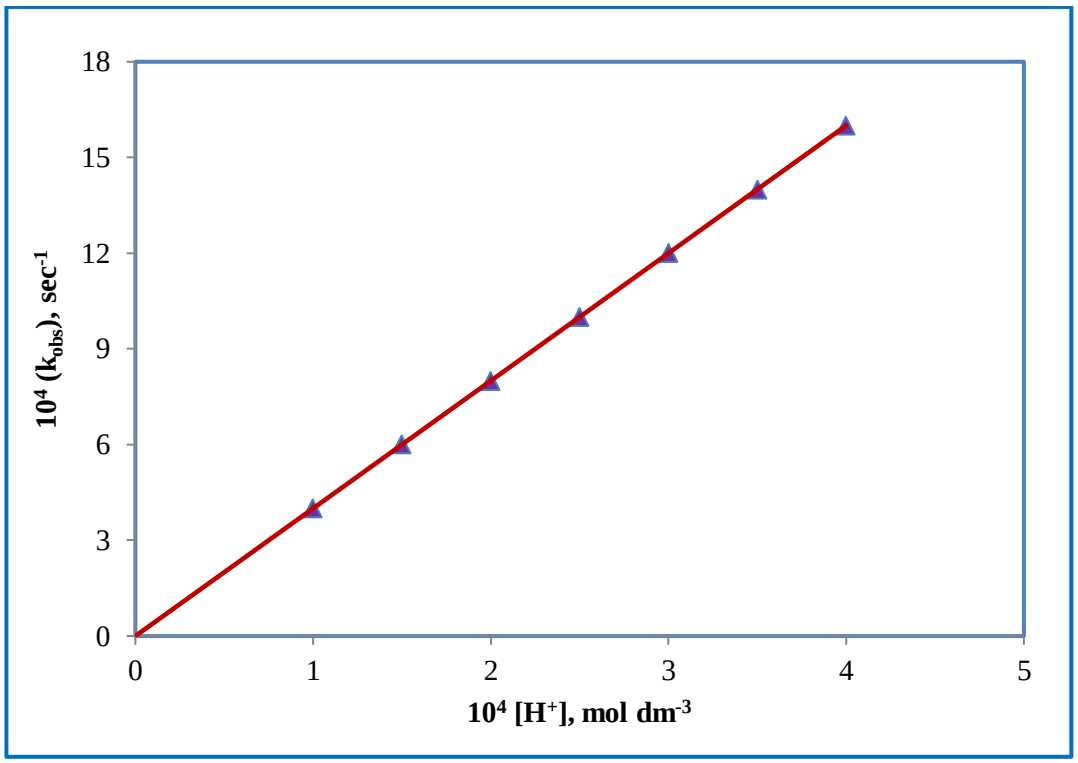

Figure 3.11: Variation of hydrogen ion.

$[MnO_2] = 5.0 \times 10^{-5}$ mol dm^{-3}; $[CIP] = 5.0 \times 10^{-4}$ mol dm^{-3};

$I = 4.0 \times 10^{-4}$ mol dm^{-3}; Temp. = 35 °C.

(Ref. Table: 3.6)

TABLE: 3.7

VARIATION OF IONIC STRENGTH

$[MnO_2] = 5.0 \times 10^{-5}$ mol dm^{-3} **Temp. = 35ºC**

[CIP] = 5.0×10^{-4} mol dm^{-3} **$[H^+] = 2.0 \times 10^{-4}$ mol dm^{-3}**

10^4 $[NaClO_4]$, mol dm^{-3}	**1.0**	**2.0**	**3.0**	**4.0**	**5.0**	**6.0**	**7.0**
Time in minutes			**Absorbance**				
0	0.775	0.777	0.774	0.776	0.775	0.774	0.777
5	0.610	0.611	0.612	0.611	0.609	0.612	0.610
10	0.482	0.480	0.479	0.481	0.482	0.479	0.481
15	0.375	0.378	0.377	0.376	0.374	0.377	0.375
20	0.295	0.297	0.295	0.296	0.296	0.295	0.297
25	0.235	0.234	0.235	0.233	0.234	0.235	0.235
30	0.186	0.184	0.185	0.187	0.187	0.185	0.186
35	0.144	0.145	0.146	0.147	0.144	0.146	0.145
10^4 (k_{obs}), mol dm^{-3}	7.95	8.05	8.10	8.11	7.95	8.08	8.05

TABLE: 3.8

VARIATION OF SODIUM FLUORIDE

$[MnO_2] = 5.0 \times 10^{-5}$ mol dm^{-3} **Temp. = 35ºC**

[CIP] = 5.0×10^{-4} mol dm^{-3} **$[H^+] = 2.0 \times 10^{-4}$ mol dm^{-3}**

10^4 [NaF], mol dm^{-3}	**0.0**	**1.0**	**2.5**	**5.0**	**7.5**	**10.0**	**15.0**	**20.0**
Time in minutes	**Absorbance**							
0	(0)0.776	(0)0.777	(0)0.775	(0)0.776	0.777	0.775	(0)0.776	(0)0.777
12	(5)0.611	(6)0.610	(7)0.616	(10)0.600	0.599	0.617	(13)0.624	(16)0.605
24	(10)0.480	(12)0.479	(14)0.489	(20)0.463	0.462	0.490	(26)0.502	(32)0.471
36	(15)0.378	(18)0.377	(21)0.388	(30)0.358	0.357	0.389	(39)0.403	(48)0.367
48	(20)0.297	(24)0.296	(28)0.308	(40)0.277	0.275	0.309	(52)0.324	(64)0.286
60	(25)0.234	(30)0.296	(35)0.245	(50)0.214	0.212	0.245	(65)0.261	(80)0.223
72	(30)0.184	(36)0.183	(42)0.194	(60)0.165	0.164	0.195	(78)0.210	(96)0.174
84	(35)0.145	(42)0.144	(49)0.154	(70)0.128	0.127	0.155	(91)0.169	(112)0.135
10^4 (k_{obs}), mol dm^{-3}	8.05	6.71	5.50	4.32	3.61	3.24	2.80	2.62

Figures in parentheses denote time in minutes.

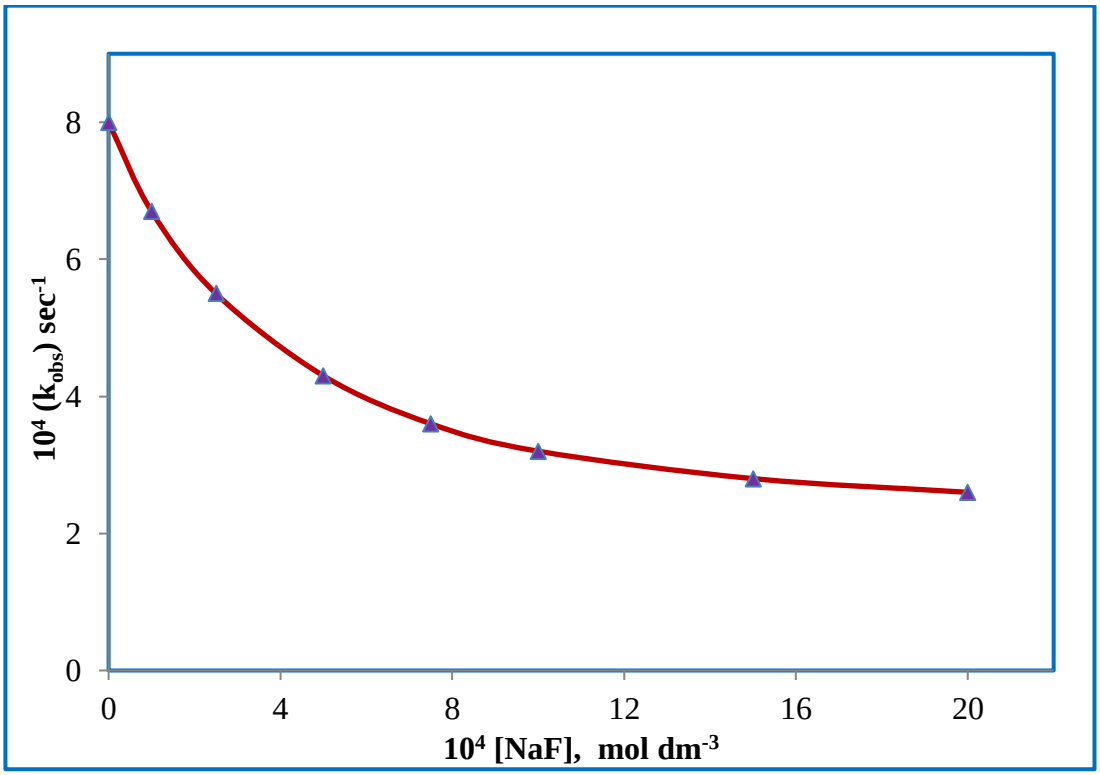

Figure 3.12: Variation of sodium fluoride.

$[MnO_2] = 5.0 \times 10^{-5}$ mol dm^{-3}; $[CIP] = 5.0 \times 10^{-4}$ mol dm^{-3};

$[H^+] = 2.0 \times 10^{-4}$ mol dm^{-3}; $I = 4.0 \times 10^{-4}$ mol dm^{-3};

Temp. = 35 °C.

(Ref. Table: 3.8)

The reaction of MnO_2 and CIP occurs via H_2MnO_3, a soluble species of Mn(IV) in solution, the complex dependence of CIP can account for an intermediate complex between H_2MnO_3 and CIP. Such an intermediate complex is not a unique proposition as the complexation between H_2MnO_3 and malonic acid has earlier been reported [62]. The rate being first order dependence of H^+ ion concentration, a reaction mechanism consisting of steps (3.3) to (3.5) can be proposed.

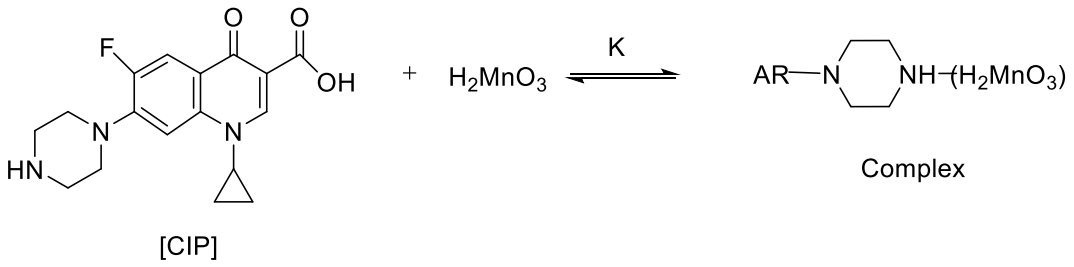

(3.3)

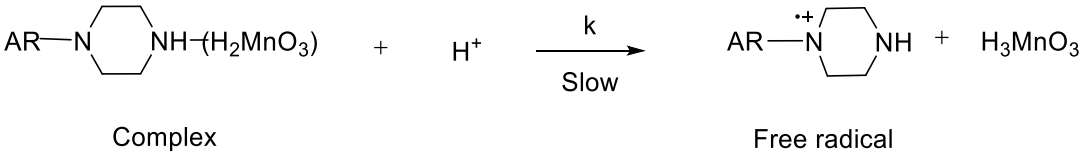

(3.4)

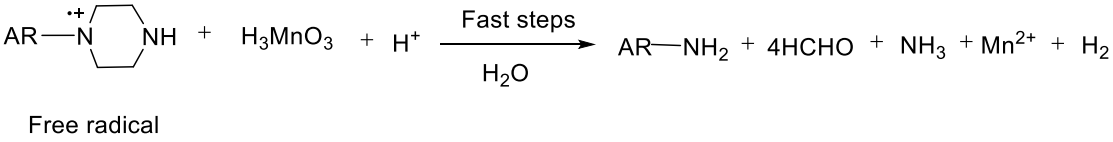

(3.5)

Here, AR =

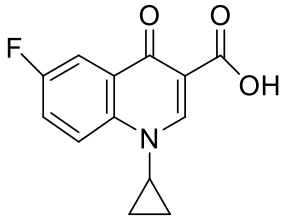

Scheme 3.1

The proposed mechanism leads to the rate law (3.6) and (3.7)

$$-\frac{d[Mn(IV)}{dt} = \frac{kK[Mn(IV)][CIP][H^+]}{1+K[CIP]} \quad (3.6)$$

$$k_{obs} = \frac{kK[CIP][H^+]}{1+K[CIP]} \quad (3.7)$$

The double reciprocal plot between $(k_{obs})^{-1}$ and $[CIP]^{-1}$ was made from equation (3.7) that yield straight line with non zero intercept (r^2 =0.999) **(Figure 3.13)**. The rate constant k, of the slow step of scheme 3.1 was obtained from the intercept of the plots $(k_{obs})^{-1}$ versus $[CIP]^{-1}$ at 30˚C, 35˚C, 40˚C respectively. The energy of activation was determined by the plot of log kversus 1/T **(Figure 3.14) (Table 3.9)** [63]. The equilibrium constant (K) in scheme 3.1 were calculated from the intercept and slope of the plot $(k_{obs})^{-1}$ versus $[CIP]^{-1}$ at 30˚C, 35˚C, 40˚C respectively. Thermodynamic quantities **(Table 3.9)** were calculated from the Van't Hoff plots i.e. log K versus 1/T **(Figure 3.15).**

Since one electron transfer process is more facile than the two electron transfer process, the decomposition of complex give a free radical species of drug, which on further fast interactions converts to end product. These results are also consistent with the observed stoichiometry of the reaction.

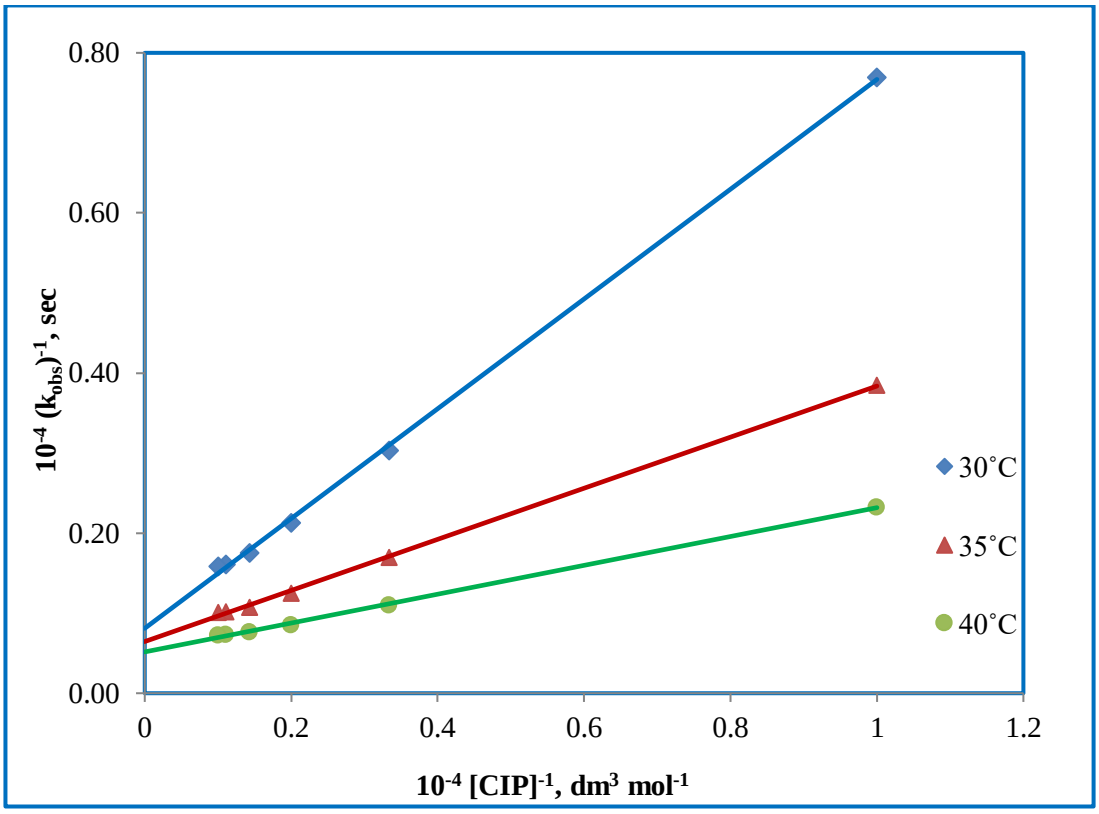

Figure 3.13: Plot of $(k_{obs})^{-1}$ verses $[CIP]^{-1}$ at different temperatures.

$[MnO_2] = 5.0 \times 10^{-5}$ mol dm^{-3};

$[H^+] = 2.0 \times 10^{-4}$ mol dm^{-3};

$I = 4.0 \times 10^{-4}$ mol dm^{-3}.

TABLE: 3.9

ACTIVATION PARAMETERS AND THERMODYNAMIC QUANTITIES EVALUATED FROM SCHEME 3.1.

Temperature (Kelvin)	**10^2 k** (sec^{-1})	**Activation Parameters**	**10^{-2} K** ($dm^3\ mol^{-1}$)	**Thermodynamic Quantities** (From K)
303	12.35	E_a= 33.89 ($kJ\ mol^{-1}$)	11.81	ΔH = 68.93 ($kJ\ mol^{-1}$)
308	15.50	$\Delta H^{\#}$ = 31.33 ($kJ\ mol^{-1}$)	20.22	ΔS = 223.21 ($JK^{-1}\ mol^{-1}$)
313	19.38	$\Delta S^{\#}$ = – 159.30 ($JK^{-1}\ mol^{-1}$)	28.67	ΔG = 1.17 ($kJ\ mol^{-1}$)
		$\Delta G^{\#}$ = 80.32 ($kJ\ mol^{-1}$)		

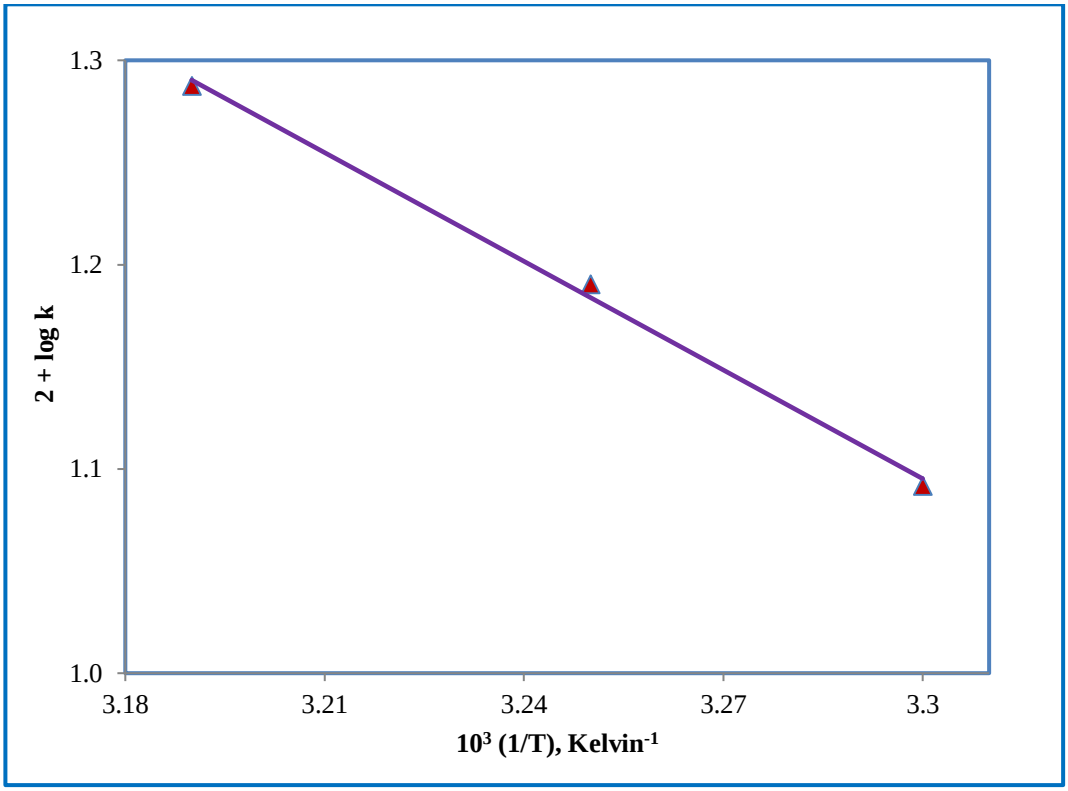

Figure 3.14: Plot of log k versus 1/T.

(Ref. Table: 3.9)

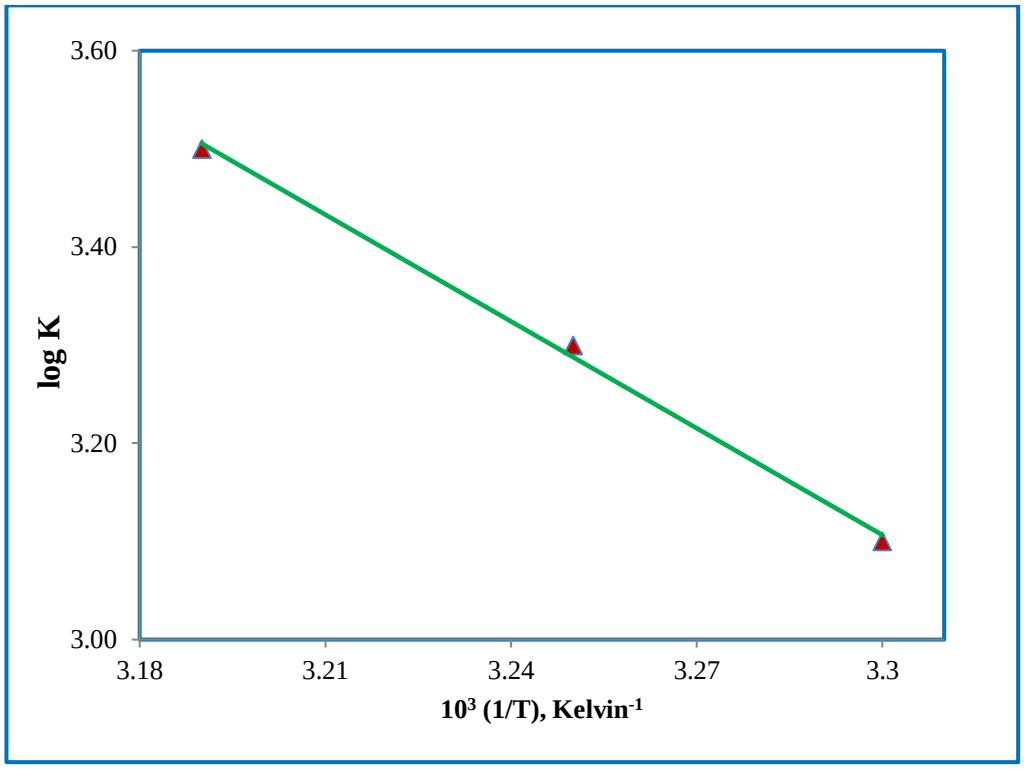

Figure 3.15: Plot of log K versus 1/T.

(Ref. Table: 3.9)

3.4. F^- ion inhibition

The rate of reaction retards by F^- ion, the simple explanation for such inhibition is the complexation of H_2MnO_3 by F^-ions yielding unreactive species of the type $H_2MnO_3F^-$. Such retarding effect has earlier been reported to the formation of complexes of intermediate Mn(IV) by these ions [64]. The rate law gives by equation (3.8) accounts for inhibition by F^-ion.

$$k'_{F^-} = \left[\frac{k_{Mn} + k_{F^-} \cdot k_{F^-}[F^-]}{1 + k_{F^-}[F^-]} \right] \tag{3.8}$$

Where k_{Mn} and k'_{F^-} are the rate constants in the absence and presence of fluoride.

$$k'_{F^-} = \frac{k_{F^-} + (k_{Mn} - k_{F^-})}{k_{F^-}[F^-]} \tag{3.9}$$

A plot of k'_{F^-} versus $\left(\frac{k_{Mn} - k_{F^-}}{[F^-]} \right)$ according to equation (3.9) yielded a straight line with non zero intercept ($r^2 = 0.995$) **(Figure.16)** and the value of K_{F^-} calculated from the slope was 24.44×10^2 dm^3 mol^{-1} at 35°C [62]. Through the value of K_{F^-} appears to be high in view of strong retarding effect of F^- ion. Nevertheless, inhibition by fluoride ions does indicate indirectly a pre-equilibrium step involving an intermediate complex between Mn(IV) species and drug in the reaction mechanism. Furthermore, if inhibition is due to the shift in pre-equilibrium without involving $H_2MnO_3F^-$directly in the oxidation of drug given by the equation (3.10)

$$k'_{F^-} = \frac{k_{Mn}}{1 + k_{F^-}[F^-]} \tag{3.10}$$

A plot of $[k'_{F^-}]^{-1}$ versus $[F^-]$ according to equation (3.10) yielded a curve instead of a straight line ($r^2 = 0.942$) **(Figure 3.17)** describing to a reaction pathway that involves $H_2MnO_3F^-$and CIP. Thus $H_2MnO_3F^-$species that in all probability accounts for inhibition of the rate in H_2MnO_3-CIP reaction.

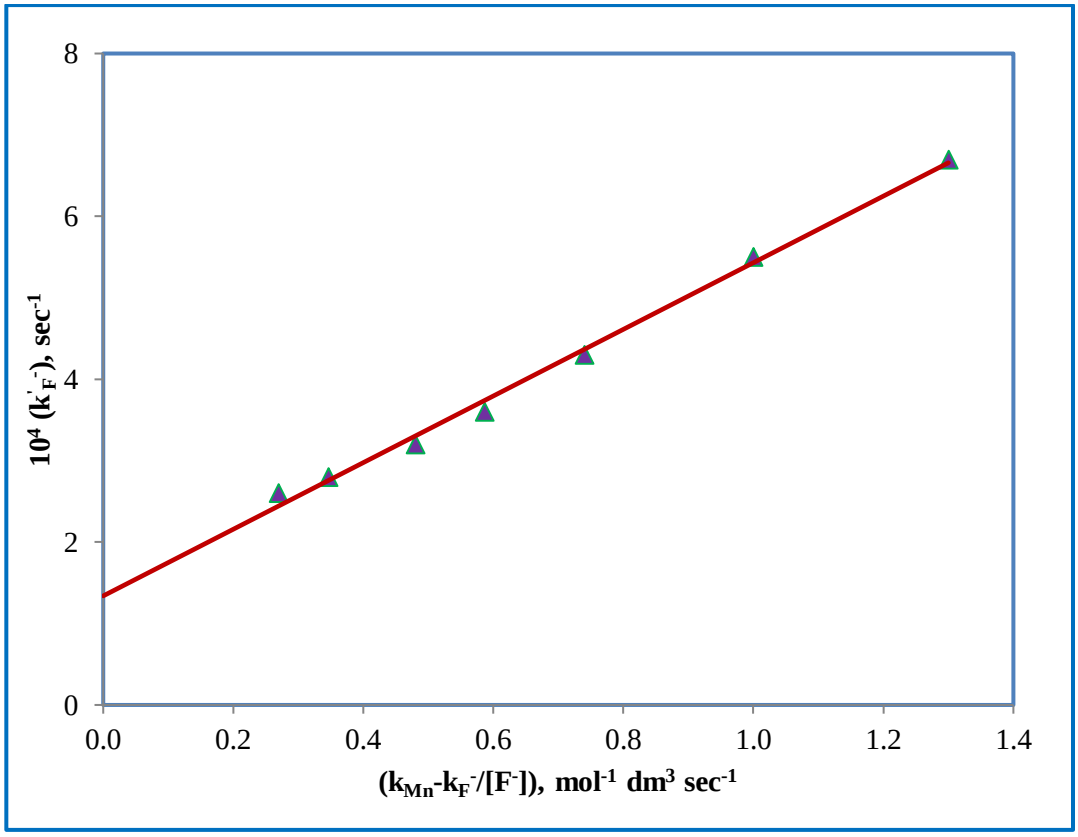

Figure 3.16: Plot of k'_{F^-} **versus** $\left(\frac{k_{Mn}-k_{F^-}}{[F^-]}\right)$**.**

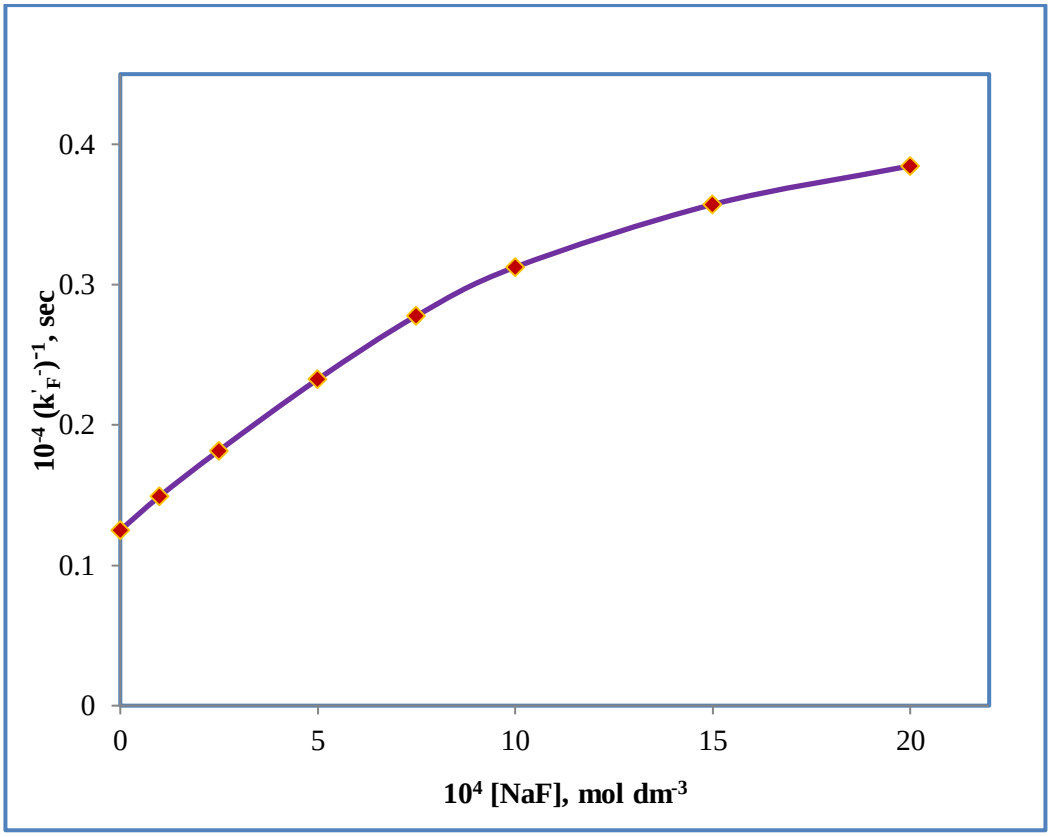

Figure 3.17: Plot of **$[k'_F]^{-1}$ versus $[F^-]$.**

3.5. Conclusion

The present study reports highly stable needle shaped colloidal nano sized MnO_2 was formed by simple laboratory equipment in ambient condition. The nano sized colloid MnO_2 was characterized by UV-Visible spectrophotometer, transmission electron microscopy (TEM) and Fourier transform infrared (FTIR) spectrophotometer. A kinetic and mechanistic study of CIP oxidation by colloidal MnO_2 has been investigated in aqueous acidic medium. The reaction follows first order kinetics with respect to MnO_2 and H^+ion under first order reaction conditions. Mechanism illustrate the reactive species of MnO_2 that H_2MnO_3. Since dealkylated products are obtained in the present study, it is evident that the products of the title reaction have antimicrobial activity after oxidation. Thus the degradation of fluoroquinolones plays an important role in the field of waste water treatment. The kinetic results have also been used to evaluate various activation parameters associated with the degradation of CIP by MnO_2 in aqueous acidic medium.

3.6. References

[1] H. Zhang, W. R. Chen, H. C. Huang, ***Environ. Sci. Technol***., 42 (2008) 5548.

[2] T. C. Sharma, A. Lal, V. Saksena, ***Bull. Chem. Soc. Jpn***., 49 (1976) 2881.

[3] Basak, M. A. Malati, ***J. Inorg. Nucl. Chem***., 39 (1977) 1081.

[4] F. Kienzle, ***Tetrahedron Lett.***, 24 (1983) 2213.

[5] C. Xu, B. Li, H. Du, F. Kang, Y. Zeng, ***J. Power Sources,*** 180 (2008) 664.

[6] V. Subramanian, H. Zhu, B. Wei, ***Chem. Phys. Lett.,*** 453 (2008) 242.

[7] A. Yuan, X. Wang, Y. Wang, J. Hu, ***Electrochim. Acta,*** 54 (2009) 1021.

[8] A. Zolfaghari, F. Ataherian, M. Ghaemi, A. Gholami, ***Electrochim. Acta,*** 52 (2007) 2806.

[9] D. Yan, P. Yan, S. Cheng, J.T. Chen, R.F. Zhuo, J.J. Feng, G.A. Zhang, Cryst. ***Growth Des.***, 9 (2009) 218.

[10] A. Abulizi , G. H. Yang , K. Okitsu , J. J. Zhu. UltrasonicsSonochemistry xxx (2014) xxx–xxx.

[11] C. LumePereira,S. Baral, A. Henglein, E. Janata,***J. Phys. Chem.,***89 (1985) 5772.

[12] O. Horvath, K. Strohmayer, ***J. Photochem. Photobiol. A,***116 (1998) 69.

[13] M. A. Islam, M. M. Rahman, ***Colloidal Journal,*** 75 (2013) 591.

[14] J. F. Perez-Benito, C. Arias, ***J. Colloid Interface Sci.,*** 149(1992) 92.

[15] J. F. Perez-Benito, C. Arias, E. Amat, ***J. Colloid Interface Sc.,,*** 77 (1996) 228.

[16] J. F. Perez-Benito, E. Brillas, R. Pouplana, ***Inorg. Chem.,*** 28(1989) 390.

[17] M. Altaf, D. Jaganyi, ***J. Solution Chem.,*** (2014).

[18] M. Saeed. M.Ilyas,M. Siddique. A. Ahmad, ***Arab. J. Sci. Eng.,*** 38 (2013) 1739.

[19] G. Chen, L. Zhao, Y. Dong, ***J. Hazard. Mater.,*** 193 (2011) 128.

[20] F. Freeman, L. Y. Chang, J. C. Kappos, L. Sumarta, ***J. Organo. Met. Chem.,*** 52 (1987)1460.

[21] F. Mata-Perez, J. F. Perez-Benito, ***Can. J. Chem.,*** 63(1985) 988.

[22] Qamruzzaman, A. Nasar, ***J. Ind. Eng. Chem.,*** 20(2014) 897.

[23] J. Klausen, S. B. Haderlein, R. P. Schwarzenbach, ***Environ. Sci. Technol.,*** 31 (1997) 2642.

[24] C. S. McArdell, A. T. Stone, J. Tian, ***Environ. Sci. Technol.,*** 32 (1998) 2923.

[25] D. Wang,J. Y. Shin,M. A. Cheney, G. Sposito, T. G. Spiro, ***Environ. Sci. Technol.,*** 33 (1999) 3160.

[26] F. Li, C. Liu, C. Liang, X. Li, L. Zhang, ***J. Hazard. Mater.,*** 154 (2008) 1098.

[27] J. Gao, G. D. Sheng, Y. P. Qiu, ***Chem. J. Chin. Univ.,*** 33 (2012) 948.

[28] K. Lin, W. Liu, J. Gan, ***Environ. Sci. Technol.,*** 43 (2009) 3860.

[29] A. K. Singh, N. Sen, S. K. Chatterjee, M. A. B. H. Susan, ***Colloid Polym. Sci.,*** (2016) DOI 10.1007/s00396-016-3921-8

[30] J. Wan, L. Zhou, H. Deng, F. Zhan, R. Zhang. ***Journal of Molecular Catalysis A: Chemical***, 407 (2015) 67.

[31] F. Kennedy,Rubert, A. Joel, Pedersen. ***Environ. Sci. Technol.,*** 40 (2006) 7216.

[32] P. Mahamallik, S. Saha, A.Pal,***Chemical Engineering Journal,***(2015)

[33] M. Akram, M. Altaf, Kabir-ud-din,***Indian Journal of Chemistry,*** 46 (2007) 1427.

[34] Kabir-Ud-Din, W. Fatma, Z. Khan, ***Colloids and Surfaces A: Physicochemical and Engineering Aspects,*** 234 (2004) 159.

[35] Z. Khan, Raju, M. Akram, Kabir-Ud-Din,***Int. J. Chem. Kinet.,*** 36 (2004) 359.

[36] Kabir-Ud-Din, S. M. S. Iqubal,***Colloid Journal,*** 72 (2010) 195.

[37] Kabir-ud-Din, M.Altaf, M.Akram,***Journal of Dispersion Science and Technology,*** 29 (2008) 809.

[38] Z. Khan, P. Kumar, Kabir-Ud-Din,***Colloids and Surfaces A: Physicochemical and Engineering Aspects,*** 248 (2004)25.

[39] Kabir-Ud-Din, N. H. Zaidi, M. Akram, Z. Khan, 284 (2006) 1387.

[40] J. Herszage, M. D. S. Afonso, G. Luther, ***Environ. Sci. Technol.,*** 37 (2003) 3332.

[41] N. Diab, I. Abu-Shqair, M. Al-Subu, R. Salim, ***International Journal of Chemistry,*** 34 (2013) 1388.

[42] N. Nanda, S. Dakshayani, Puttaswamy, ***Oxid. Commun.,***34 (2011) 44.

[43] M. C. Dodd, A. D. Shah, U. V. Gunten, C. H. Huang,***Environ. Sci. Technol.,*** 39 (2005) 7065.

[44] P. Wang, H.Y. Liang, C. H. Ching-Hua,***Water Res.,*** 44 (2010) 5989.

[45] K. Basavaiah, P. Nagegowda, B. C. Somashekar, V. Ramakrishna,***Science Asia,*** 32 (2006) 403.

[46] B. Yang, R. S. Kookana, M. Williams, G. G. Ying,J. Du, H. Doan, A. Kumar. ***J. Hazard. Mater.,***320 (2016) 296.

[47] Z. Zhou, J. Q. Jiang,***Chemosphere,*** S119 (2015) 95.

[48] K. A. Thabaj, S. D. Kulkarni, S. A. Chimatadar, S. T. Nandibewoor,***Polyhedron,*** 26 (2007) 4877.

[49] H. C. Zhang, C. H. Haung,***Environ. Sci. Technol.,*** 39 (2005) 4474.

[50] X. Xiao, S. P. Sun, M. B. McBride, A. T. Lemley,***Environ. Sci. Pollut. Res.,***20 (2013) 10.

[51] L. Hu, H. M. Martin, T. J. Strathmann,***Environ. Sci. Technol.,*** 44 (2010) 6416.

[52] L. Hu, A. M. Stemig, K. H. Wammer, T. J. Strathmann, ***Environ. Sci. Technol.,*** 45 (2011) 3635.

[53] G. Chen, L. Zhao, Y. H. Dong, ***J. Hazard. Mater.,*** 193 (2011) 128.

[54] A. K. Singh, N. Sen, S. K. Chatterjee,***Indian J. of Chem.,*** 55A (2016)1059.

[55] H. Q. Wang, G. F. Yang, Q. Y. Li, X. X. Zhong, F. P. Wang, Z. S. Li, Y. H. Li, ***New. J. Chem.,*** 35 (2011) 469.

[56] D. Jaganyi, M. Altaf, I. Wekesa, ***Appl. Nano. Sci.,*** 3 (2013) 329.

[57] G. Tazwar, A. Jain, V. Devra. ***Chem. Pap.,*** 71 (2017) 1749.

[58] Y. Huang, Y. Lin, W. Li. ***Electro. chim. Acta.,*** 99 (2013) 161.

[59] M. A. Islam, M. M. Rahman, ***Russian Journal of Physical Chemistry A,*** 89 (2015) 706.

[60] M. Akram, M. Altaf, Kabir-Ud-Din,***Colloids Surf. B,*** 82 (2011) 217.

[61] K. J. Laidler, Chemical Kinetics. ***Pearson Education, (Singapore) Pte. Ltd, Indian Branch, Delhi, India, 3rdedn.,*** 183 (2004) 198.

[62] I. Rao, S. K. Mishra, P. D. Sharma, ***Transition Met. Chem.,*** 18 (1993) 182.

[63] A. Jain, S. Jain, V. Devra. ***International Journal of Pharmaceutical Sciences and Drug Research,*** 7 (2015) 205.

[64] J. Lurie (Ed.), Handbook of Analytical Chemistry, ***Mir Publishers, Moscow,*** (1975) 292.

Chapter – 4

Oxidative Degradation of Levofloxacin by Water-Soluble Manganese Dioxide in Aqueous Acidic Medium: A Kinetic Study

4.1. Introduction

In the past few decades, there has been great concern on pharmaceuticals waste which is a key source of impurities in the aquatic ecosystem, ground water and soil, which leads to the bacterial resistance against antibiotics even at their low concentrations [1]. Fluoroquinolones are anthropogenic contaminants which are comprehensively used as pharmaceuticals for both human and veterinary purposes [2, 3]. Levofloxacin (LEV), (-)-(S)-9-fluoro-2,3-dihydro-3-methyl-10-(4-methyl-1-piperazinyl)-7-oxo-7-Hpyrido-[1,2,3-de]-1,4-benzoxazine-6-carboxylic acid hemihydrates, is one of the commonly used third-generation fluoroquinolone antimicrobials, being the active S isomer isolated from racemic ofloxacin and is twice as active as the parent drug. LEV has broad-spectrum activity against various bacteria, including Gram-positive and Gram-negative microorganisms [4, 5]. It has been widely used for the treatment of infectious diseases, such as community-acquired pneumonia and acute exacerbation of chronic bronchitis due to its effective antibacterial activity and low frequency of adverse effects on oral administration [6]. Waste water discharge from conventional waste water treatment plants is the main source of LEV in the aquatic environment [7, 8]. Removal of LEV residue from aquatic environment is, therefore, considered as a priority and serves as an important study. The oxidative study of LEV has been effectuated by various oxidants such as alkali permanganate [9], acidic chloramine-T [10], ozone and hydroxyl radicals [11], aqueous chlorine [12], acidic permanganate [13] and hexacyanoferrate(III) [14] etc. Many other degradation and transformation studies are also available in the literature [15-17].

Manganese dioxide (MnO_2) is one of the most active and important oxidative components, showing high potency in degrading various organic pollutants such as antibacterial agents [18, 19]. Perez-Benito et al. found first time that water-soluble manganese dioxide can be prepared from reduction of aqueous potassium permanganate by sodium thiosulfate under neutral condition [20] the prepared MnO_2 was used in the oxidation of organic acids[21-23] by MnO_2. MnO_2 exhibits considerable activity in oxidation–reduction reactions due to the

presence of different oxidation states of manganese ions [24]. It has been reported in several studies that the intermediate (Mn(IV)) could be H_2MnO_4, H_2MnO_3, or a water-soluble colloidal MnO_2 [25, 26]. Water-soluble colloidal MnO_2 has the advantage over water-insoluble forms as conventional UV–visible spectrophotometer can be used to monitor their reactions with organic and inorganic subtracts.

A literature survey confessed that the kinetics and mechanism of degradation of some antibiotics by MnO_2 in aqueous acidic/alkaline medium have been studied earlier [27, 28]. But yet lack of literature on the oxidative degradation of LEV by MnO_2 in aqueous acidic medium has been reported, so the title reaction prompted us to understand the mechanism of the reaction.

4.2. Experimental details

4.2.1. Chemicals

The method of preparation and standardization of the reagents are given in chapter 2 (Experimental). All chemicals used were of analytical reagent grade, commercially available, and were used without further purification. Always freshly prepared and standardized MnO_2solutions were used in the kinetics. The method of preparation and characterization of manganese dioxide are given in chapter 3.All the solutions were prepared by using double distilled water.

4.2.2. Kinetic Measurements

The reaction was initiated by mixing the solutions of MnO_2 and LEV which also contained the required concentration of H_2SO_4 and Na_2SO_4 at 25˚C. The progress of the reaction was followed by spectrophotometrically at 390 nm **(Figure 4.1)**, that there was no interference from other species in the reaction mixture at this wave length. Initial rates were calculated employing plane mirror method. The pseudo-first-order plots were also made in which reaction conditions allowed. Results in triplicate were reproducible to within ±6%.

4.3. Stoichiometry and Product Analysis

The stoichiometry of the reaction was resolved with various ratio of reactants and constant concentration of H_2SO_4 and Na_2SO_4 at room temperature in a closed vessel were kept for 12 h. After completion of the reaction, unreacted concentration of MnO_2 was suggested that one mole of LEV was oxidized by one mole of MnO_2, exhibiting 1:1 ratio for the consumption of reductant to oxidant **(Table 4.1).**

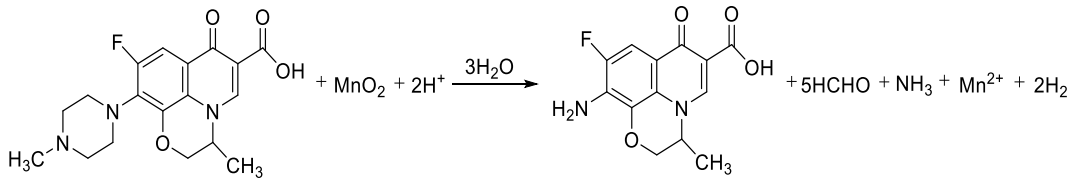

Levofloxacin

(4.1)

The product was extracted from the reaction mixture with ether. The product 10-amino-9-fluoro-2,3-dihydro-3-methyl-7-oxo-7H-pyrido-[1,2,3-de]-1,4-benzoxazine-6-carboxylic acid was identified with the help of TLC and characterized by FT-IR and LC-MS analysis. FT-IR analysis confirmed the presence of $–NH_2$ group in the oxidation product **(Figure 4.2)**. The IR spectrum display a peak at 3412.70 cm^{-1} for –NH stretching of the $–NH_2$ group and the other peaks are of the parent compound. LC-MS analysis of LEV oxidation reaction indicates the formation of product with molecular ion of m/z 279 **(Figure 4.3)**. The m/z 279 corresponds to fully dealkylation of the piperazine ring [30]. It is worth noting, that oxidation of piperazine moiety of LEV between oxidized centers and nitrogen atoms lead to distinctive mass loss m/z = 83. This was attributed to ring opening, dealkylation and deamination process, which finally yielded 7-amino fluoroquinolone product. The by-product formaldehyde was identified by spot test [31]. The other product ammonia was detected by Nesseler's reagent test [32].

TABLE: 4.1

Stoichiometry of manganese dioxide and levofloxacin in aqueous acidic medium

[MnO_2] **mol dm^{-3}**	**[LEV]** **mol dm^{-3}**	$\frac{\Delta[LEV]}{\Delta[MnO_2]}$
0.0005	0.0002	1:1
0.0005	0.0003	1:1
0.0005	0.0004	1:0.98
0.0006	0.0004	1:0.98

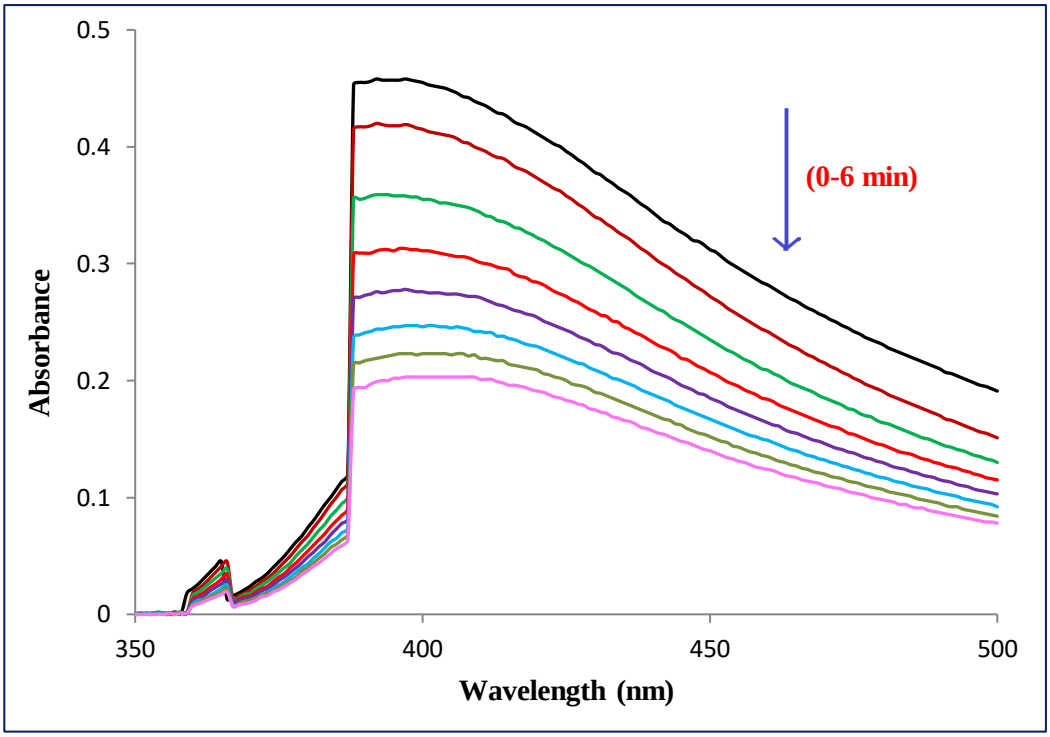

Figure 4.1: Spectral changes during the oxidation of LEV by MnO_2 in acidic medium.

$[MnO_2] = 3.0 \times 10^{-5}$ mol dm^{-3}; $[LEV] = 5.0 \times 10^{-5}$ mol dm^{-3};

$[H^+] = 2.0 \times 10^{-4}$ mol dm^{-3}; $I = 5.0 \times 10^{-4}$ mol dm^{-3};

Temp. = 25°C.

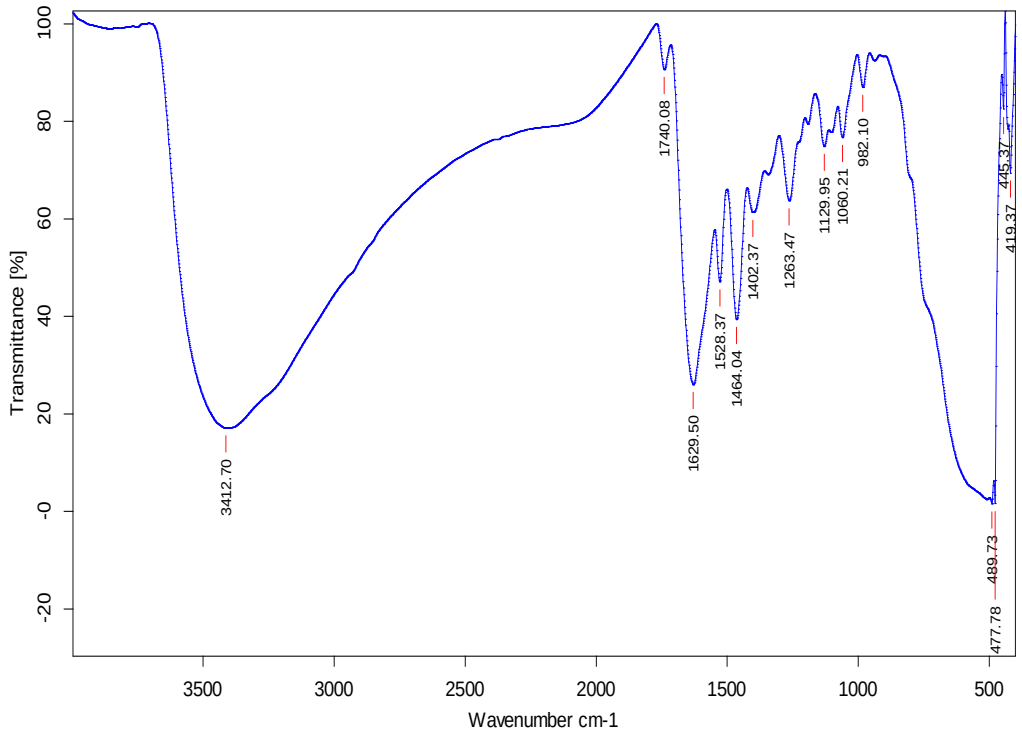

Figure 4.2: FTIR spectra of the oxidative product of levofloxacin by manganese dioxide in aqueous acidic medium.

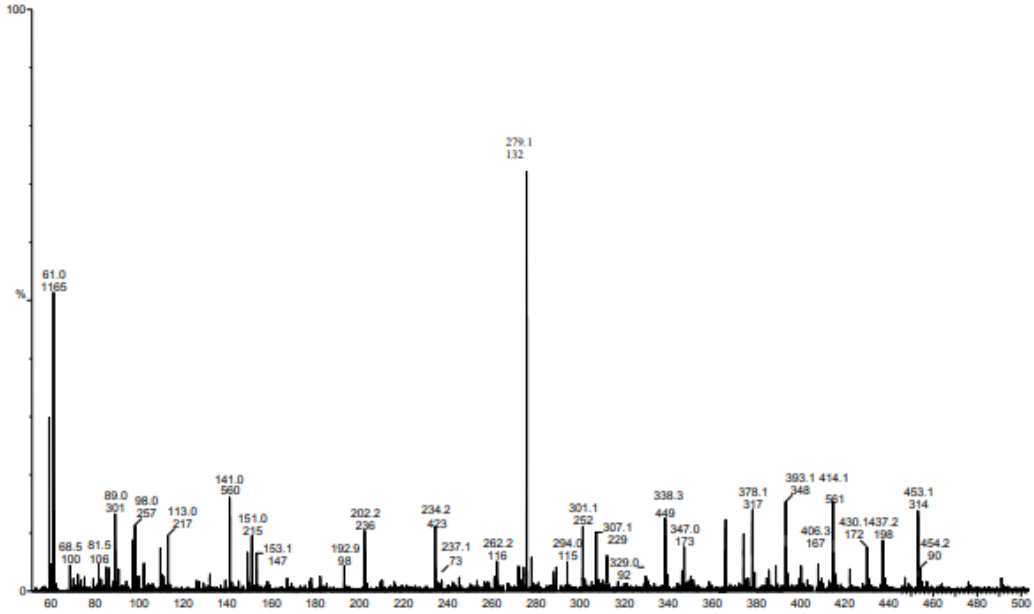

Figure 4.3: LC-ESI-MS spectra of oxidation product of levofloxacin.

4.4. Results

4.4.1. Effect of manganese dioxide concentration

The concentration of MnO_2 was varied in the range (0.75 to 7.5) × 10^{-5} mol dm^{-3} at two but fixed concentration of LEV to be 5.0 × 10^{-5} and 6.0 × 10^{-5} mol dm^{-3}, $[H_2SO_4]$ = 2.0 × 10^{-4} mol dm^{-3} and $[Na_2SO_4]$ = 3.0 × 10^{-4} mol dm^{-3} at 25°C. Initial rates (k_i mol dm^{-3} s^{-1}) were calculated employing plane mirror method and a plot of initial rate (k_i) versus $[MnO_2]$ was made that yielded a straight line passing through the origin ascribing first order dependence with respect to MnO_2 ($r^2 \geq 0.998$) **(Figure 4.4)**. Second order plots were also made by making plots of log $([LEV]_t/[MnO_2]_t)$ against time ($r^2 \geq 0.985$) **(Figure 4.5)**. Second order rate constants have good agreement, calculated from initial rates as well as second order plots **(Table 4.2 and 4.3)**.

4.4.2. Effect of levofloxacin concentration

The concentration of LEV was varied from (1.0 to 10.0) × 10^{-5} mol dm^{-3} at two but fixed concentration of MnO_2 viz. 2.0 × 10^{-5} and 3.0 × 10^{-5} mol dm^{-3}, $[H_2SO_4]$ = 2.0 × 10^{-4} mol dm^{-3} and $[Na_2SO_4]$ = 3.0 × 10^{-4} mol dm^{-3} at 25°C. Initial rates (k_i mol dm^{-3} s^{-1}) were calculated and a plot of initial rate (k_i mol dm^{-3} s^{-1}) against [LEV] was made, a straight line passing through the origin was obtained confirming first order dependence with respect to LEV ($r^2 \geq 0.998$) **(Figure 4.6)**. Certain reactions were also undertaken under pseudo first order conditions ($[LEV] >> [MnO_2]$) under identical experiment conditions varying from (1.0 to 10.0) × 10^{-4} mol dm^{-3}, pseudo first order plots were made and pseudo first order rate constants (k_{obs}, s^{-1}) evaluated from these plots were found to increase proportionately with the increasing concentration of LEV(r^2 = 0.999) **(Figure 4.7)**. Results are given in **Table 4.6 and 4.7.** Second order rate constants have good agreement, calculated from initial rates as well as second order plots **(Table 4.4 and 4.5)**.

TABLE: 4.2

VARIATION OF MANGANESE DIOXIDE

[LEV] = 5.0 × 10^{-5} mol dm^{-3} **Temp. = 25°C**

[H^+] = 2.0 × 10^{-4} mol dm^{-3} **I = 5.0 × 10^{-4} mol dm^{-3}**

10^5 [MnO_2], mol dm^{-3}	**0.75**	**1.0**	**2.0**	**3.0**	**4.0**	**5.0**	**6.0**	**7.5**
Time in minutes				**Absorbance**				
0	0.117	0.146	0.302	0.456	(0)0.626	(0)0.783	(0)0.940	(0)1.175
10	0.097	0.116	0.251	0.360	(15)0.501	(20)0.517	(20)0.642	(20)0.861
20	0.081	0.094	0.204	0.282	(30)0.392	(40)0.392	(40)0.454	(40)0.658
30	0.069	0.075	0.166	0.235	(45)0.329	(60)0.313	(60)0.345	(60)0.501
40	0.056	0.061	0.136	0.185	(60)0.282	(80)0.251	(80)0.266	(80)0.392
50	0.047	0.047	0.110	0.157	(75)0.235	(100)0.219	(100)0.204	(100)0.313
60	0.038	0.039	0.094	0.125	(90)0.196	(120)0.188	(120)0.172	(120)0.235
70	0.028	0.031	0.072	0.106	(105)0.158	(140)0.172	(140)0.141	(140)0.188
80	0.022	0.028	0.060	0.094	(120)0.141	(160)0.157	(160)0.125	(160)0.157
$10^9(k_i)$,mol dm^{-3} s^{-1}	**3.16**	**4.16**	**8.66**	**12.0**	**17.0**	**20.5**	**24.0**	**30.8**
k´, dm^3 mol^{-1} s^{-1}	**7.50**	**8.10**	**8.80**	**7.29**	**7.67**	**-**	**-**	**-**

Figures in parentheses denote time in minutes.

TABLE: 4.3

VARIATION OF MANGANESE DIOXIDE

[LEV] = 6.0 × 10^{-5} mol dm^{-3} **Temp. = 25ºC**

[H^+] = 2.0 × 10^{-4} mol dm^{-3} **I = 5.0 × 10^{-4} mol dm^{-3}**

10^5 [MnO_2], mol dm^{-3}	**0.75**	**1.0**	**2.0**	**3.0**	**4.0**	**5.0**	**6.0**	**7.5**
Time in minutes				**Absorbance**				
0	0.117	0.146	0.302	(0)0.456	(0)0.626	(0)0.783	(0)0.940	(0)1.175
10	0.100	0.113	0.233	(15)0.329	(15)0.485	(20)0.548	(20)0.705	(20)0.908
20	0.083	0.085	0.180	(30)0.251	(30)0.376	(40)0.393	(40)0.564	(40)0.736
30	0.067	0.064	0.141	(45)0.196	(45)0.282	(60)0.290	(60)0.454	(60)0.564
40	0.055	0.047	0.110	(60)0.149	(60)0.204	(80)0.219	(80)0.360	(80)0.454
50	0.044	0.036	0.081	(75)0.117	(75)0.157	(100)0.172	(100)0.290	(100)0.219
60	0.033	0.027	0.063	(90)0.078	(90)0.110	(120)0.141	(120)0.219	(120)0.157
70	0.023	0.022	0.053	(105)0.067	(105)0.094	(140)0.125	(140)0.157	(140)0.149
80	0.016	0.019	0.044	(120)0.063	(120)0.078	(160)0.110	(160)0.133	(160)0.141
$10^9(k_i)$, mol dm^{-3} s^{-1}	**3.80**	**5.00**	**10.0**	**14.4**	**18.9**	**24.5**	**29.0**	**36.0**
k´, dm^3 mol^{-1} s^{-1}	**8.44**	**8.06**	**8.92**	**7.29**	**8.83**	**8.06**	**-**	**-**

Figures in parentheses denote time in minutes.

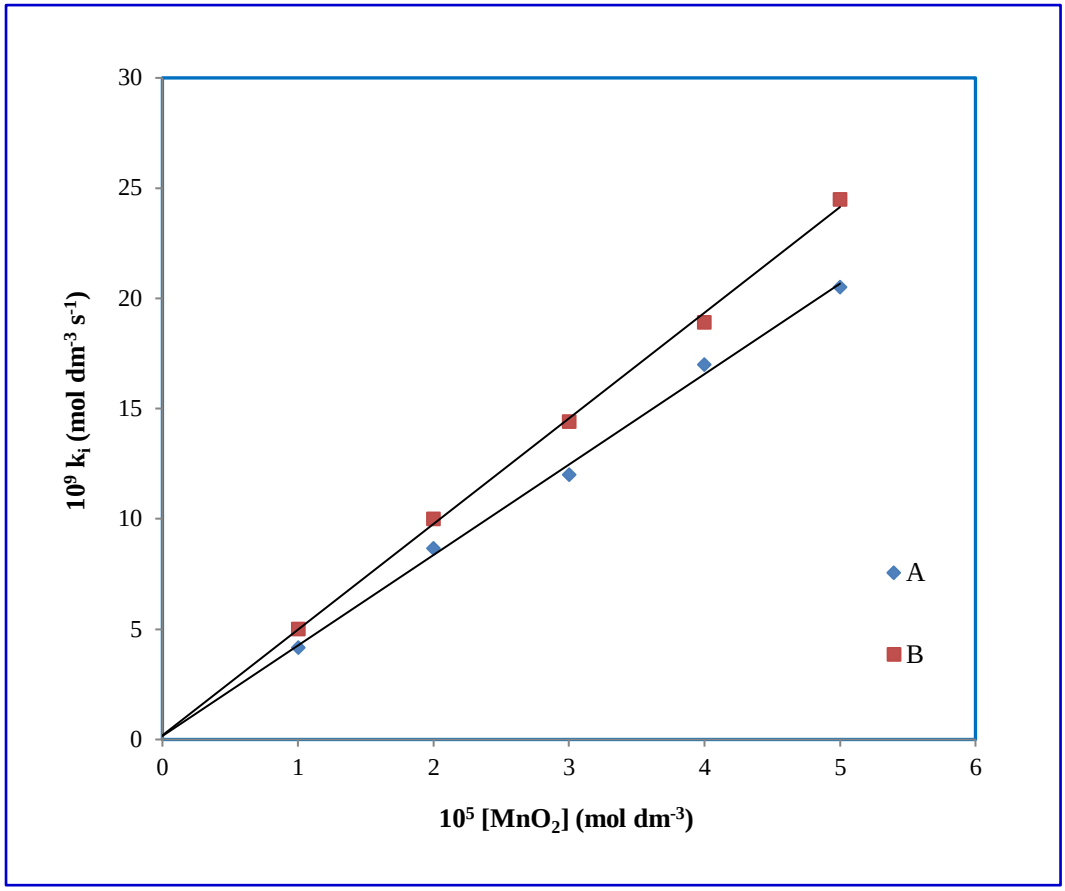

Figure 4.4: Variation of manganese dioxide

$[H^+]$ = 2.0 × 10^{-4} mol dm^{-3}; I = 5.0 × 10^{-4} mol dm^{-3};

Temp. = 25°C

[LEV] = (A) 5.0 × 10^{-5} mol dm^{-3}; (B) 6.0 × 10^{-5} mol dm^{-3}.

(Ref. Tables: 4.2 and 4.3)

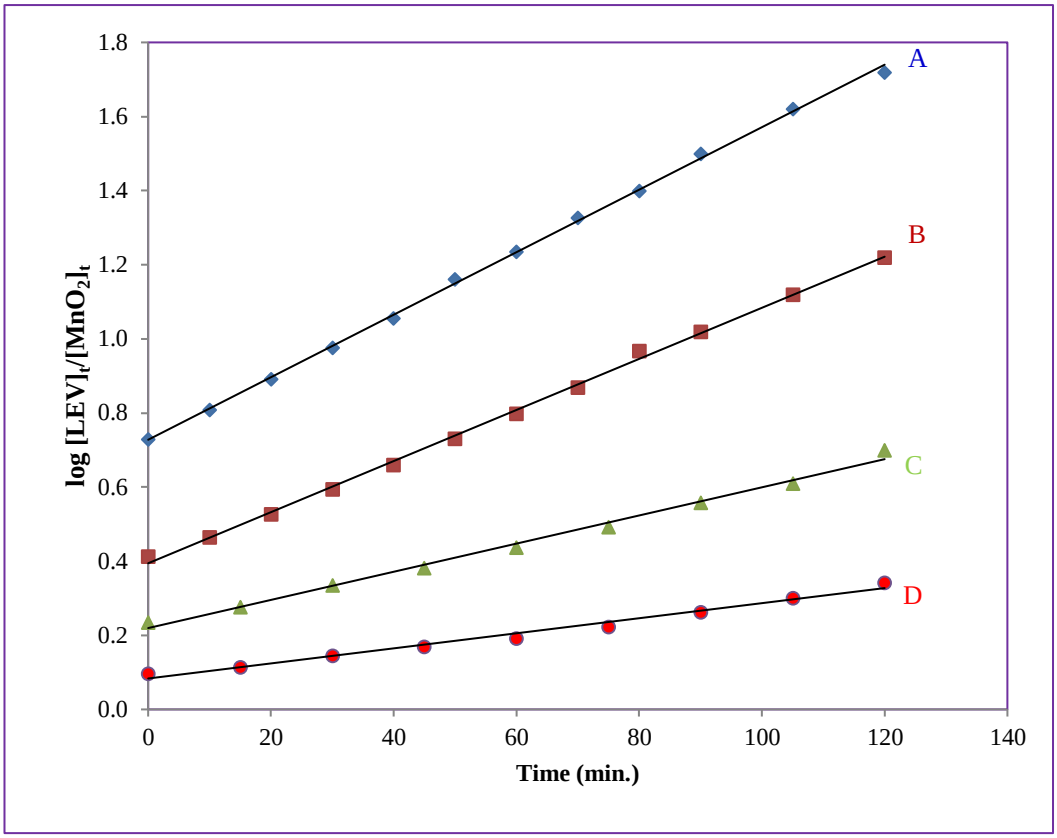

Figure 4.5: Second order plots

[LEV] = 5.0×10^{-5} mol dm^{-3}; Temp. = 25°C;

$[H^+]$=2.0×10^{-4} mol dm^{-3}; I = 5.0×10^{-4} mol dm^{-3};

$[MnO_2]$ = (A) 1.0×10^{-5} mol dm^{-3}; (B) 2.0×10^{-5} mol dm^{-3};

(C) 3.0×10^{-5} mol dm^{-3}; (D) 4.0×10^{-5} mol dm^{-3}.

(Ref. Table: 4.2)

TABLE: 4.4
VARIATION OF LEVOFLOXACIN

$[MnO_2] = 2.0 \times 10^{-5}$ mol dm^{-3} **Temp. = 25°C**

$[H^+] = 2.0 \times 10^{-4}$ mol dm^{-3} **I = 5.0×10^{-4} mol dm^{-3}**

10^5[LEV], mol dm^{-3}	1.0	2.5	4.0	5.0	6.0	7.0	8.0	9.0	10.0
Time in minutes	**Absorbance**								
0	0.302	0.302	0.302	(0)0.302	(0)0.302	(0)0.302	(0)0.302	(0)0.302	(0)0.302
20	0.226	0.220	0.215	(15)0.251	(15)0.235	(15)0.232	(15)0.222	(8)0.222	(8)0.210
40	0.172	0.167	0.160	(30)0.202	(30)0.179	(30)0.177	(30)0.169	(16)0.172	(16)0.157
60	0.128	0.122	0.119	(45)0.163	(45)0.141	(45)0.141	(45)0.122	(24)0.125	(24)0.111
80	0.098	0.093	0.091	(60)0.133	(60)0.110	(60)0.102	(60)0.085	(32)0.094	(32)0.078
100	0.085	0.073	0.067	(75)0.112	(75)0.081	(75)0.061	(75)0.055	(40)0.063	(40)0.049
120	0.062	0.056	0.044	(90)0.092	(90)0.063	(90)0.063	(90)0.034	(48)0.036	(48)0.030
140	0.031	0.021	0.018	(105)0.083	(105)0.050	(105)0.047	(105)0.020	(56)0.022	(56)0.013
160	0.022	0.018	0.015	(120)0.062	(120)0.042	(120)0.038	(120)0.014	(64)0.016	(64)0.005
$10^9(k_i)$, sec^{-1}	**1.80**	**4.00**	**7.00**	**8.66**	**10.0**	**11.7**	**13.3**	**15.2**	**17.0**
k´, dm^3 mol^{-1} s^{-1}	**7.70**	**8.11**	**7.68**	**8.80**	**8.92**	**7.67**	**7.95**	**8.33**	**8.05**

Figures in parentheses denote time in minutes.

TABLE: 4.5

VARIATION OF LEVOFLOXACIN

$[MnO_2] = 3.0 \times 10^{-5}$ mol dm^{-3} **Temp. = 25ºC**

$[H^+] = 2.0 \times 10^{-4}$ mol dm^{-3} **I = 5.0×10^{-4} mol dm^{-3}**

10^5[LEV], mol dm^{-3}	**1.0**	**2.5**	**4.0**	**5.0**	**6.0**	**7.0**	**8.0**	**9.0**	**10.0**
Time in minutes					**Absorbance**				
0	0.456	0.456	0.456	(0)0.456	(0)0.456	(0)0.456	(0)0.456	(0)0.456	(0)0.456
20	0.367	0.335	0.319	(15)0.368	(15)0.329	(15)0.329	(10)0.360	(10)0.329	(10)0.329
40	0.281	0.261	0.222	(30)0.282	(30)0.251	(30)0.241	(20)0.282	(20)0.163	(20)0.238
60	0.238	0.219	0.199	(45)0.232	(45)0.188	(45)0.188	(30)0.219	(30)0.172	(30)0.175
80	0.187	0.165	0.143	(60)0.188	(60)0.152	(60)0.141	(40)0.172	(40)0.128	(40)0.125
100	0.161	0.145	0.122	(75)0.155	(75)0.119	(75)0.094	(50)0.141	(50)0.094	(50)0.083
120	0.122	0.112	0.107	(90)0.125	(90)0.085	(90)0.069	(60)0.110	(60)0.067	(60)0.0.47
140	0.110	0.092	0.078	(105)0.106	(105)0.067	(105)0.047	(70)0.094	(70)0.047	(70)0.025
160	0.104	0.082	0.070	(120)0.094	(120)0.063	(120)0.039	(80)0.078	(80)0.039	(80)0.011
$10^9(k_i)$, sec^{-1}	**2.50**	**6.00**	**9.70**	**12.0**	**14.4**	**16.7**	**19.2**	**21.7**	**23.8**
k´,dm^3 mol^{-1} s^{-1}	**8.33**	**8.00**	**8.10**	**7.29**	**7.29**	**8.60**	**8.00**	**8.33**	**8.06**

Figures in parentheses denote time in minutes.

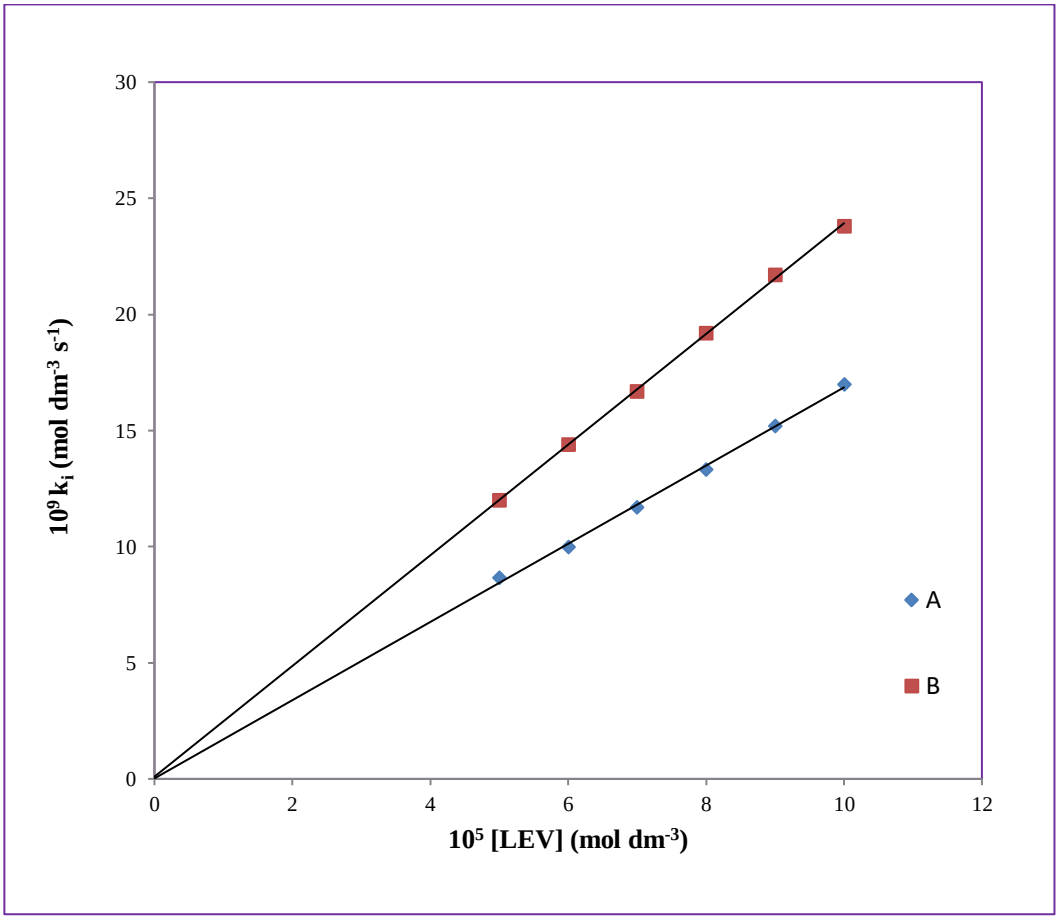

Figure 4.6: Variation of levofloxacin

$[H^+]$ = 2.0 × 10^{-4} mol dm^{-3}; I = 5.0 × 10^{-4} mol dm^{-3};

Temp. = 25ºC

$[MnO_2]$ = (A) 2.0 × 10^{-5} mol dm^{-3}; (B) 3.0 × 10^{-5} mol dm^{-3}.

(Ref. Table: 4.4 and 4.5)

TABLE: 4.6

VARIATION OF LEVOFLOXACIN

$[MnO_2]$ = 2.0 × 10^{-5} mol dm^{-3} **Temp. = 25ºC**

$[H^+]$ = 2.0 × 10^{-4} mol dm^{-3} **I = 5.0 × 10^{-4} mol dm^{-3}**

10^4 [LEV], mol dm^{-3}	**1**	**2**	**3**	**4**	**5**	**6**	**8**	**10**
Time in minutes				**Absorbance**				
0	(0)0.302	(0)0.302	(0)0.302	(0)0.302	(0)0.302	(0)0.302	0.302	0.302
0.5	(5)0.237	(2)0.250	(2)0.226	(1)0.251	(1)0.238	(1)0.229	0.248	0.237
1.0	(10)0.186	(4)0.207	(4)0.169	(2)0.208	(2)0.187	(2)0.174	0.204	0.186
1.5	(15)0.146	(6)0.171	(6)0.126	(3)0.173	(3)0.147	(3)0.132	0.168	0.146
2.0	(20)0.115	(8)0.142	(8)0.095	(4)0.143	(4)0.116	(4)0.100	0.138	0.115
2.5	(25)0.090	(10)0.117	(10)0.071	(5)0.119	(5)0.091	(5)0.076	0.114	0.090
3.0	(30)0.071	(12)0.097	(12)0.053	(6)0.099	(6)0.072	(6)0.058	0.093	0.071
3.5	(35)0.056	(14)0.081	-	(7)0.082	(7)0.056	-	0.077	0.056
4.0	(40)0.044	(16)0.067	-	(8)0.068	-	-	0.063	-
4.5	-	(18)0.055	-	(9)0.056	-	-	0.052	-
$10^3(k_{obs})$, sec^{-1}	**-**	**1.58**	**2.43**	**3.12**	**4.00**	**4.77**	**6.39**	**7.90**
k´, dm^3 mol^{-1} s^{-1}	**8.05**	**7.90**	**8.10**	**7.80**	**8.00**	**7.95**	**7.99**	**7.90**

Figures in parentheses denote time in minutes

TABLE: 4.7

VARIATION OF LEVOFLOXACIN

$[MnO_2] = 3.0 \times 10^{-5}$ mol dm^{-3} **Temp. = 25ºC**

$[H^+] = 2.0 \times 10^{-4}$ mol dm^{-3} **I = 5.0×10^{-4} mol dm^{-3}**

10^4[LEV], mol dm^{-3}	**1**	**2**	**3**	**4**	**5**	**6**	**8**	**10**
Time in minutes				**Absorbance**				
0	(0)0.455	(0)0.455	(0)0.455	(0)0.455	(0)0.455	(0)0.455	0.455	0.455
0.5	(5)0.357	(2)0.377	(2)0.342	(1)0.378	(1)0.356	(1)0.337	0.374	0.357
1.0	(10)0.281	(4)0.312	(4)0.257	(2)0.313	(2)0.278	(2)0.250	0.308	0.281
1.5	(15)0.220	(6)0.258	(6)0.193	(3)0.260	(3)0.217	(3)0.185	0.253	0.220
2.0	(20)0.173	(8)0.214	(8)0.145	(4)0.216	(4)0.170	(4)0.137	0.208	0.173
2.5	(25)0.136	(10)0.177	(10)0.109	(5)0.179	(5)0.133	(5)0.102	0.171	0.136
3.0	(30)0.107	(12)0.147	(12)0.082	(6)0.149	(6)0.104	(6)0.076	0.141	0.107
3.5	(35)0.084	(14)0.121	-	(7)0.123	(7)0.081	-	0.116	0.084
4.0	(40)0.066	(16)0.100	-	(8)0.102	-	-	0.095	-
4.5	(45)0.052	(18)0.083	-	(9)0.085	-	-	0.078	-
$10^3(k_{obs})$, sec^{-1}	**-**	**1.57**	**2.39**	**3.12**	**4.05**	**4.78**	**6.40**	**7.88**
k´, dm^3 mol^{-1} s^{-1}	**8.06**	**7.84**	**7.95**	**7.81**	**8.10**	**7.97**	**8.00**	**7.88**

Figures in parentheses denote time in minutes

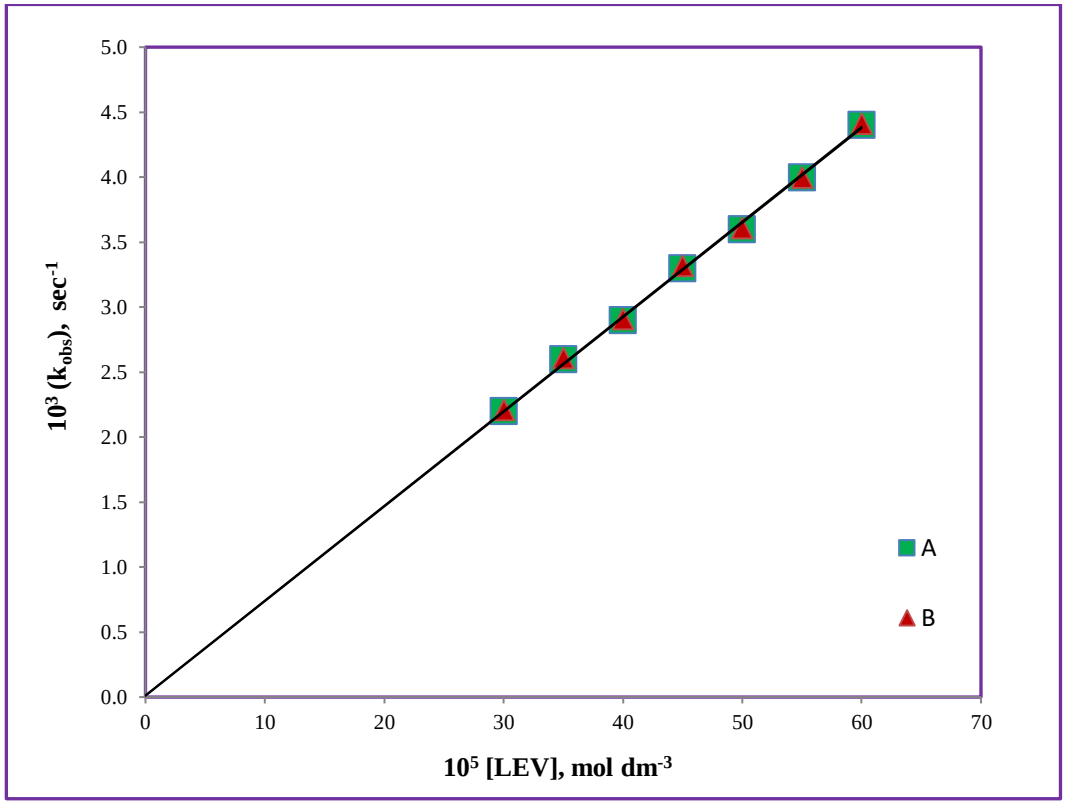

Figure 4.7: Variation of levofloxacin

$[H^+]$ = 2.0 × 10^{-4} mol dm^{-3}; I = 5.0 × 10^{-4} mol dm^{-3};

Temp. = 25ºC

$[MnO_2]$ = (A) 2.0 × 10^{-5} mol dm^{-3}; (B) 3.0 × 10^{-5} mol dm^{-3};

(Ref. Table: 4.6 and 4.7)

4.4.3. Effect of hydrogen ion

The effect of concentration variation of $[H^+]$ ion on the rate of reaction was studied in the concentration range (0.08–0.75) × 10^{-4} mol dm^{-3} at fixed concentration of LEV, MnO_2, ionic strength and $[SO_4^{2-}]$ = 1.0 × 10^{-4} mol dm^{-3} at three temperatures viz. 20ºC, 25ºC, 30ºC respectively. Pseudo-first-order rate constant (k_{obs}) was found to be increased with increase in $[H^+]$ ($r^2 \geq 0.999$) **(Figure 4.8).** Results are given in **Tables 4.8, 4.9 and 4.10**. The energy of activation (E_a) of the reaction which is calculated by plotting the graph between log k_{obs} (s^{-1}) versus 1/T was found to be 30.54 kJ mol^{-1} and enthalpy of the reaction was 28.07 kJ mol^{-1} **(Figure 4.9)**. The obtained parameters show good agreement with the oxidation of LEV by chlorine [12].

4.4.4. Effect of ionic strength and dielectric constant

At constant concentration of reactants, the ionic strength was varied by varying concentration of sodium sulphate (0.3–3.0) × 10^{-4} mol dm^{-3} at 25˚C. Ionic strength had negligible effect on the rate of reaction. At constant acidity and other constant conditions, as the t-butyl alcohol content increases from 0 to 50% (v/v) in the reaction, change in dielectric constant had negligible effect on the rate of reaction. Results are given in **Tables 4.11.**

The negligible effect of ionic strength and dielectric constant on the rate of reaction suggests that the reaction is either between two neutral species or a neutral and a charged species [33].

TABLE: 4.8

VARIATION OF HYDROGEN ION

$[MnO_2] = 3.0 \times 10^{-5}$ mol dm^{-3} **$[LEV] = 5.0 \times 10^{-4}$ mol dm^{-3}**

$I = 2.0 \times 10^{-4}$ mol dm^{-3} **Temp. = 20^{o}C**

10^4 [H^+], mol dm^{-3}	**0.3**	**0.5**	**1.0**	**1.5**	**1.8**	**2.0**	**2.3**	**2.5**	**3.0**
Time in minutes	**Absorbance**								
0	(0)0.455	(0)0.455	(0)0.455	(0)0.455	0.455	0.455	0.455	0.455	0.455
1	(10)0.380	(4)0.376	(2)0.371	(2)0.337	0.380	0.373	0.364	0.354	0.337
2	(20)0.318	(8)0.310	(4)0.303	(4)0.250	0.317	0.306	0.292	0.275	0.250
3	(30)0.265	(12)0.256	(6)0.247	(6)0.185	0.265	0.251	0.234	0.214	0.185
4	(40)0.222	(16)0.211	(8)0.201	(8)0.137	0.221	0.206	0.187	0.167	0.137
5	(50)0.185	(20)0.175	(10)0.164	(10)0.102	0.185	0.169	0.150	0.130	0.102
6	(60)0.155	(24)0.144	(12)0.134	(12)0.075	0.154	0.139	0.120	0.101	0.075
7	(70)0.129	(28)0.119	(14)0.109	-	0.129	0.114	0.096	0.079	-
8	(80)0.108	(32)0.098	(16)0.089	-	0.108	0.093	0.077	-	-
9	(90)0.090	(36)0.081	-	-	0.090	0.077	-	-	-
$10^3(k_{obs})$, sec^{-1}	**0.5**	**0.8**	**1.7**	**2.5**	**3.0**	**3.3**	**3.7**	**4.2**	**5.0**

Figures in parentheses denote time in minutes.

TABLE: 4.9

VARIATION OF HYDROGEN ION

$[MnO_2] = 3.0 \times 10^{-5}$ mol dm^{-3} **$[LEV] = 5.0 \times 10^{-4}$ mol dm^{-3}**

$I = 2.0 \times 10^{-4}$ mol dm^{-3} **Temp. = 25ºC**

10^4 [H^+], mol dm^{-3}	**0.3**	**0.5**	**1.0**	**1.5**	**1.8**	**2.0**	**2.3**	**2.5**	**3.0**
Time in minutes	**Absorbance**								
0	(0)0.455	(0)0.455	(0)0.455	0.455	0.455	0.455	0.455	0.455	0.455
1	(5)0.380	(4)0.358	(2)0.358	0.380	0.369	0.358	0.347	0.337	0.317
2	(10)0.318	(8)0.281	(4)0.282	0.317	0.299	0.282	0.265	0.250	0.222
3	(15)0.265	(12)0.221	(6)0.222	0.265	0.242	0.222	0.202	0.185	0.155
4	(20)0.222	(16)0.174	(8)0.174	0.221	0.196	0.175	0.155	0.137	0.108
5	(25)0.185	(20)0.137	(10)0.137	0.185	0.159	0.137	0.118	0.102	0.075
6	(30)0.155	(24)0.108	(12)0.108	0.154	0.129	0.108	0.090	0.075	0.048
7	(35)0.129	(28)0.085	(14)0.085	0.129	0.105	0.085	-	-	-
8	(40)0.108	-	-	0.108	0.085	-	-	-	-
$10^3(k_{obs})$, sec^{-1}	**0.6**	**1.0**	**2.2**	**3.1**	**3.5**	**4.0**	**4.6**	**5.2**	**6.1**

Figures in parentheses denote time in minutes.

TABLE: 4.10

VARIATION OF HYDROGEN ION

$[MnO_2] = 3.0 \times 10^{-5}$ mol dm^{-3} **$[LEV] = 5.0 \times 10^{-4}$ mol dm^{-3}**

$I = 2.0 \times 10^{-4}$ mol dm^{-3} **Temp. = 30^{o}C**

10^4 [H^+], mol dm^{-3}	**0.3**	**0.5**	**1.0**	**1.5**	**1.8**	**2.0**	**2.3**	**2.5**	**3.0**
Time in minutes	**Absorbance**								
0	(0)0.455	(0)0.455	(0)0.455	(1)0.455	(1)0.455	(1)0.455	0.455	0.455	0.455
0.5	(4)0.376	(3)0.360	(2)0.337	(2)0.362	(2)0.349	(2)0.337	0.385	0.378	0.363
1.0	(8)0.310	(6)0.285	(4)0.250	(3)0.288	(3)0.268	(3)0.250	0.325	0.314	0.290
1.5	(12)0.256	(9)0.225	(6)0.185	(4)0.230	(4)0.206	(4)0.185	0.275	0.260	0.232
2.0	(16)0.211	(12)0.178	(8)0.137	(5)0.183	(5)0.158	(5)0.137	0.232	0.216	0.185
2.5	(20)0.175	(15)0.141	(10)0.102	(6)0.146	(6)0.122	(6)0.102	0.196	0.180	0.148
3.0	(24)0.144	(18)0.112	(12)0.075	(7)0.116	(7)0.093	(7)0.075	0.166	0.149	0.118
3.5	(28)0.119	(21)0.088	-	(8)0.092	-	-	0.140	0.124	0.094
4.0	(32)0.098	-	-	(9)0.073	-	-	0.119	0.103	0.075
$10^3(k_{obs})$, sec^{-1}	**0.8**	**1.3**	**2.5**	**3.8**	**4.4**	**5.0**	**5.6**	**6.2**	**7.5**

Figures in parentheses denote time in minutes

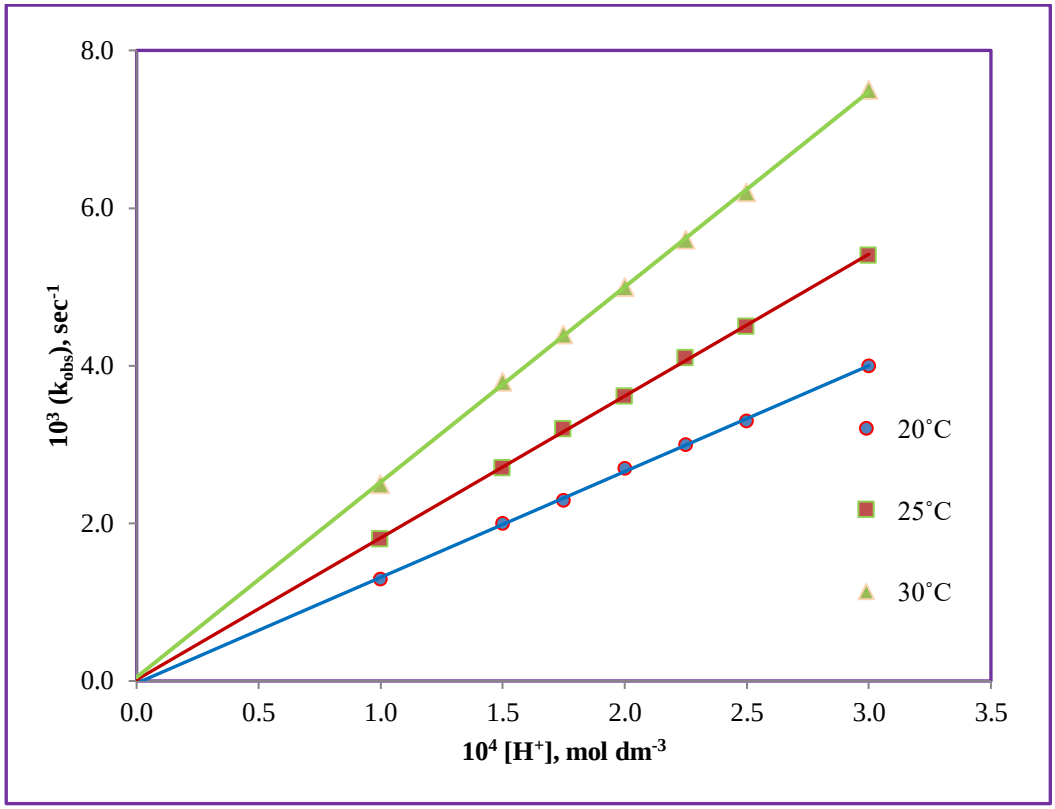

Figure 4.8: Variation of hydrogen ion at different temperatures

[LEV] = 5.0×10^{-4} mol dm^{-3}; I = 2.0×10^{-4} mol dm^{-3};

[MnO_2] = 3.0×10^{-5} mol dm^{-3}.

(Ref. Table: 4.8, 4.9, 4.10)

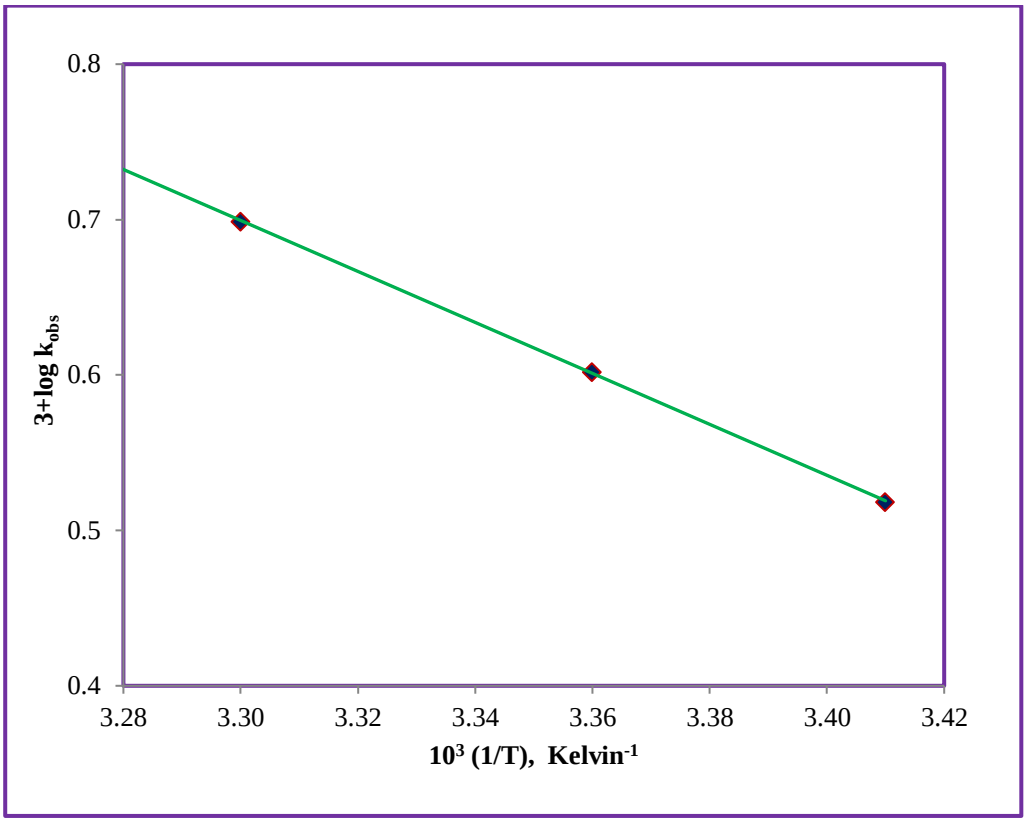

Figure 4.9: Plot of log k_{obs} versus 1/T

(Ref. Table: 4.9)

TABLE: 4.11

VARIATION OF SODIUM SULPHATE

$[MnO_2] = 3.0 \times 10^{-5}$ mol dm^{-3} **$[LEV] = 5.0 \times 10^{-4}$ mol dm^{-3}**

$[H^+] = 2.0 \times 10^{-4}$ mol dm^{-3} **Temp. = 25ºC**

10^4 $[Na_2SO_4]$, mol dm^{-3}	**0.3**	**0.5**	**1.0**	**1.5**	**2.0**	**2.5**	**3.0**
Time in minutes				**Absorbance**			
0	0.455	0.455	0.455	0.455	0.455	0.455	0.455
1	0.356	0.358	0.360	0.358	0.356	0.360	0.358
2	0.278	0.282	0.284	0.282	0.278	0.284	0.282
3	0.217	0.222	0.225	0.222	0.217	0.225	0.222
4	0.170	0.175	0.178	0.175	0.170	0.178	0.175
5	0.133	0.137	0.141	0.137	0.133	0.141	0.137
6	0.104	0.108	0.111	0.108	0.104	0.111	0.108
7	0.081	0.085	0.088	0.085	0.081	0.088	0.085
8	0.063	0.067	0.070	0.067	0.063	0.070	0.067
$10^3(k_{obs})$,sec^{-1}	**4.1**	**4.0**	**3.9**	**4.0**	**4.1**	**3.9**	**4.0**

4.4.5. Effect of added product

The effect of externally added Mn(II) on the rate of reactionwas studied by varying concentration of $MnCl_2$ (1.0×10^{-5} to 10.0×10^{-5} mol dm^{-3}) keeping otherexperimental conditions constant. The results indicates thatthe rate of reaction is unaffected by the addition of Mn(II).

4.4.6. Test for free radical

The formation of free radical was confirmed by the addition of acrylonitrile in the reaction mixture. After 5 h thereaction mixture was diluted with methanol then precipitate was formed which is indicating the presence of free radical during the progress of reaction.

4.5. Mechanism

On the basis of above results, the mechanism of oxidationof LEV by MnO_2 in acid aqueous media is given in scheme. Scheme illustrates the mechanism of reaction betweenMnO_2 and LEV in acid aqueous medium. The reaction of MnO_2 and LEV occurs to form an intermediate complex(C_1) in the fast equilibrium step, and the complex (C_1) reacts with the H^+ ions to form another complex (C_2) in thesecond equilibrium step. The complex (C_2) is involved inthe rate-determining step to form a free radical cation and$HMnO_2$. This free radical cation again reacts with $HMnO_2$in the fast step and converts into dealkylated product ofLEV and gives Mn^{2+}, HCHO, NH_3 as end products.

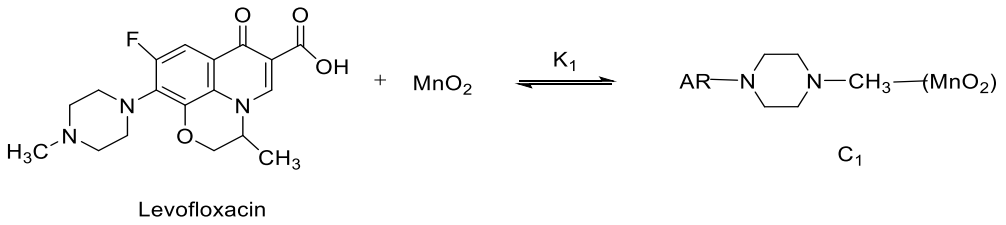

(4.2)

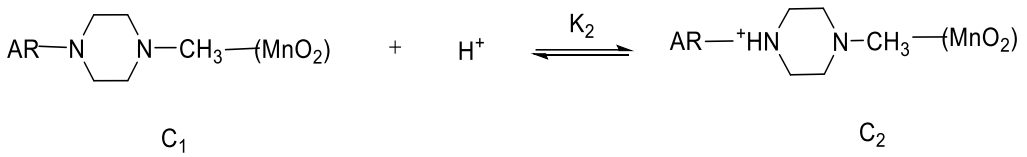

(4.3)

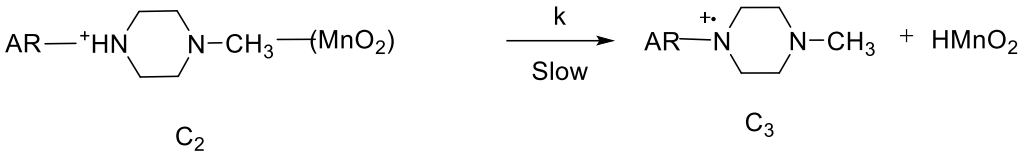

C_2 C_3

(4.4)

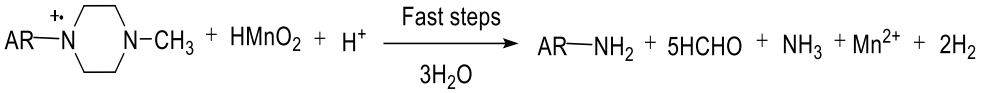

C_3

(4.5)

Here, AR = 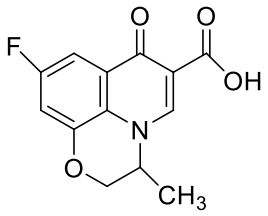

Scheme 4.1

On the basis of above mechanism, the following rateequations can be proposed:

$$Rate = kK_1K_2[MnO_2][LEV][H^+] \tag{4.6}$$

$$\frac{Rate}{[MnO_2]} = k_{obs} = kK_1K_2[LEV][H^+] \tag{4.7}$$

$$\frac{k_{obs}}{[LEV]} = k' = kK_1K_2[H^+] \tag{4.8}$$

Where k′ is second order rate constant.

$$\frac{1}{k'} = \frac{1}{kK_1K_2[H^+]} \tag{4.9}$$

It is further interesting to mention that the stoichiometry of the reaction was further justified kinetically when reactions were carried out in stoichiometric conditions. The plots of $[MnO_2]_t^{-1}$ versus time were made ($r^2 \geq 0.999$) **(Table 4.12; Figure 4.10)** and the rate constants evaluated from these plots agree with the second-order plots **(Table 4.13)**.

TABLE: 4.12

VARIATION OF LEVOFLOXACIN AND MANGANESE DIOXIDE

$[H^+] = 2.0 \times 10^{-4}$ mol dm^{-3} $I = 5.0 \times 10^{-4}$ mol dm^{-3}

Temp. = 25°C

10^5 [LEV], mol dm^{-3}	**2.0**	**3.0**	**4.0**	**5.0**
10^5 [MnO_2], mol dm^{-3}	**2.0**	**3.0**	**4.0**	**5.0**
Time in minutes		**Absorbance**		
0	0.302	0.456	0.626	0.783
20	0.241	0.340	0.423	0.521
40	0.206	0.270	0.320	0.392
60	0.178	0.224	0.261	0.313
80	0.157	0.191	0.215	0.262
100	0.139	0.167	0.186	0.224
120	0.126	0.149	0.165	0.196
140	0.116	0.134	0.148	0.174
160	0.107	0.121	0.133	0.157
k´, dm^3mol^{-1} s^{-1}	**8.32**	**8.33**	**8.34**	**8.33**

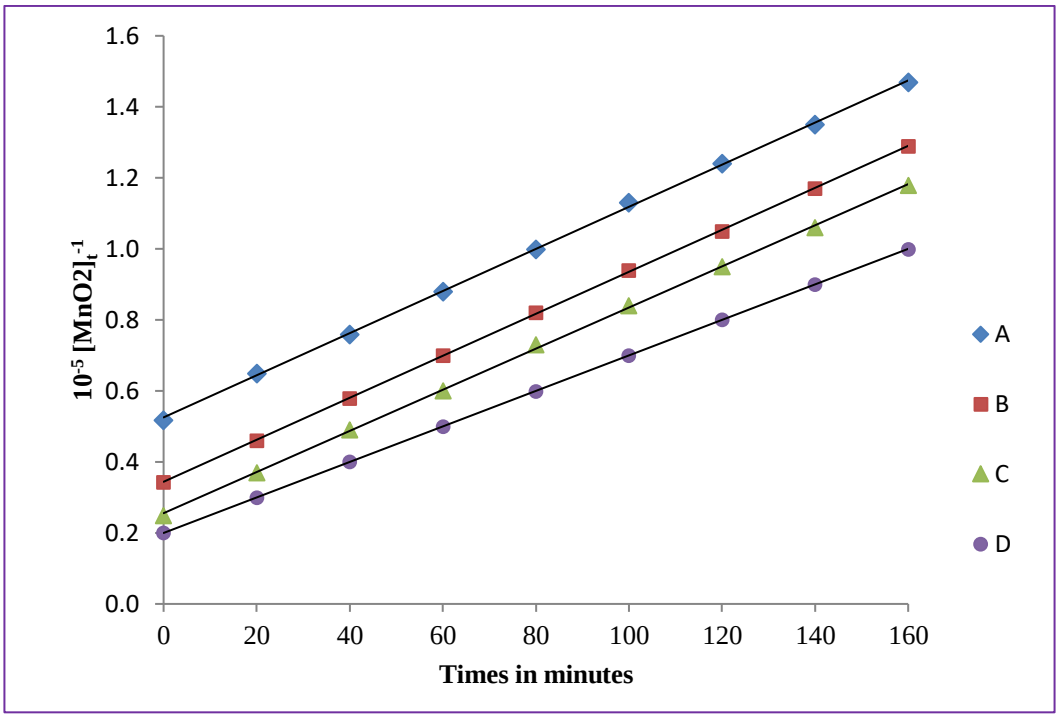

Figure 4.10 A plot of $[MnO_2]_t^{-1}$ versus time.

$[H^+]$ = 2.0 ×10^{-4} mol dm^{-3}; Temp. = 25°C;

I = 5.0 × 10^{-4} mol dm^{-3};

$[MnO_2]$ and [LEV] = (A) 2.0 × 10^{-5} mol dm^{-3}; (B) 3.0 × 10^{-5} mol dm^{-3};

(C) 4.0 × 10^{-5} mol dm^{-3}; (D) 5.0 × 10^{-5} mol dm^{-3}.

(Ref. Table: 4.12)

TABLE 4.13

Second order rate constants from stoichiometric plots in MnO_2 and levofloxacin reaction in aqueous acidic medium. $[H^+] = 2.0 \times 10^{-4}$ mol dm^{-3}, $I = 5.0 \times 10^{-4}$ mol dm^{-3}, Temperature = 25°C

10^5 $[MnO_2]$, mol dm^{-3}	10^5 [LEV], mol dm^{-3}	k´, mol^{-1} dm^3 s^{-1}
2.0	2.0	8.32
3.0	3.0	8.33
4.0	4.0	8.34
5.0	5.0	8.33

TABLE 4.14

Initial rate (k_i), pseudo first order rate constants (k_{obs}) and second order rate constant (k′) in the reaction of LEV with MnO_2 in aqueous acidic medium at temperature = 25°C and I = 5.0×10^{-4} mol dm^{-3}.

10^5 [MnO_2] (mol dm^{-3})	10^5 [LEV] (mol dm^{-3})	10^4 [H^+] (mol dm^{-3})	10^4[SO_4^{2-}] (mol dm^{-3})	$10^9 k_i$ (mol dm^{-3} s^{-1})	$10^3 k_{obs}$±S.D. (s^{-1})	k′±S.D. (dm^3 mol^{-1} s^{-1})
0.75	5.0	0.5	1.0	3.16	-	7.50±.21(8.43)
1.0	5.0	0.5	1.0	4.16		8.10±.26(8.33)
2.0	5.0	0.5	1.0	8.66	-	8.80±.53(8.66)
3.0	5.0	0.5	1.0	12.0	-	7.29±.79(8.00)
4.0	5.0	0.5	1.0	17.0	-	7.67±1.0(8.33)
5.0	5.0	0.5	1.0	20.5	-	- (8.33)
6.0	5.0	0.5	1.0	24.0		- (8.10)
7.5	5.0	0.5	1.0	30.8		- (8.20)
0.75	6.0	0.5	1.0	3.80		8.44±.32 (8.11)
1.0	6.0	0.5	1.0	5.00	-	8.06±.20(8.33)
2.0	6.0	0.5	1.0	10.0	-	8.92±.60(8.33)
3.0	6.0	0.5	1.0	14.4	-	7.29±.80(8.02)
4.0	6.0	0.5	1.0	18.9	-	8.83±.53(7.90)
5.0	6.0	0.5	1.0	24.5	-	8.06±.20(8.10)
6.0	6.0	0.5	1.0	29.0		- (8.20)
7.5	6.0	0.5	1.0	36.0		- (8.30)
2.0	1.0	0.5	1.0	1.80	-	7.70±1.0(8.50)
2.0	2.5	0.5	1.0	4.00	-	8.11±.27(8.70)
2.0	4.0	0.5	1.0	7.00	-	7.68±.90(8.43)
2.0	7.0	0.5	1.0	11.7	-	7.67±.87(8.33)
2.0	8.0	0.5	1.0	13.3	-	7.95±1.1(8.33)
2.0	9.0	0.5	1.0	15.2	-	8.33±.41(8.40)
2.0	10.0	0.5	1.0	17.0	-	8.05±.20(8.50)

3.0	1.0	0.5	1.0	2.50	-	8.33±.38(8.00)
3.0	2.5	0.5	1.0	6.00	-	8.00±.10(8.30)
3.0	4.0	0.5	1.0	9.70	-	8.10±.30(8.00)
3.0	7.0	0.5	1.0	16.7	-	8.60±.70(7.94)
3.0	8.0	0.5	1.0	19.2	-	8.00±.17(7.99)
3.0	9.0	0.5	1.0	21.7	-	8.33±.40(8.02)
3.0	10.0	0.5	1.0	23.8	-	8.06±.20(7.90)
2.0	2.0	0.5	1.0	-	-	8.33±.40
3.0	3.0	0.5	1.0	-	-	8.33±.41
4.0	4.0	0.5	1.0	-	-	8.33±.40
2.0	20.0	0.5	1.0	-	1.58±.10	7.90±.10
2.0	30.0	0.5	1.0	-	243±.11	8.10±.11
2.0	40.0	0.5	1.0	-	3.12±.13	7.80±.13
2.0	50.0	0.5	1.0	-	4.00±.14	8.00±.14
2.0	60.0	0.5	1.0	-	4.77±.11	7.95±.11
2.0	80.0	0.5	1.0	-	6.39±.12	7.99±.12
2.0	100.0	0.5	1.0	-	7.90±.13	7.90±.13
3.0	20.0	0.5	1.0	-	1.57±.09	7.84±.09
3.0	30.0	0.5	1.0	-	2.39±.10	7.95±.10
3.0	40.0	0.5	1.0	-	3.12±.13	7.81±.13
3.0	50.0	0.5	1.0	-	4.05±.14	8.10±.14
3.0	60.0	0.5	1.0	-	4.78±.11	7.97±.11
3.0	80.0	0.5	1.0	-	6.40±.12	8.00±.12
3.0	100.0	0.5	1.0	-	7.88±.13	7.88±.13
3.0	5.0	0.08	1.0	-	0.06±.06	-
3.0	5.0	0.13	1.0	-	1.00±.08	-
3.0	5.0	0.25	1.0	-	2.00±.10	-
3.0	5.0	0.38	1.0	-	3.00±.15	-
3.0	5.0	0.44	1.0	-	3.50±.18	-
3.0	5.0	0.50	1.0	-	4.00±.20	-

3.0	5.0	0.56	1.0	-	4.50±.27	-
3.0	5.0	0.63	1.0	-	5.00±.30	-
3.0	5.0	0.75	1.0	-	6.00±.36	-
3.0	5.0	0.5	0.15	-	4.00±.20	-
3.0	5.0	0.5	0.25	-	4.10±.18	-
3.0	5.0	0.5	0.50	-	4.05±.20	-
3.0	5.0	0.5	0.75	-	4.11±.21	-
3.0	5.0	0.5	0.88	-	4.00±.20	-
3.0	5.0	0.5	1.00	-	4.10±.19	-
3.0	5.0	0.5	1.13	-	4.05±.22	-
3.0	5.0	0.5	1.25	-	4.10±.20	-
3.0	5.0	0.5	1.50	-	4.00±.21	-

Result in parenthesis shows the values of second order rate constants which derived from initial rates.

(S.D.= Standard Deviation)

4.6. Conclusion

A kinetic and mechanistic study of LEV oxidation by MnO_2 has been first time investigated in aqueous acidic medium. The reaction follows first-order kinetics with respect to MnO_2, LEV and H^+ ion under first-order reaction conditions. The experiment illustrates the reactive species of MnO_2 that is H_2MnO_3. Since dealkylated products are obtained in the present study, it is evident that the products of the title reaction have antimicrobial activity after oxidation. Thus, the oxidation study with fluoroquinolones has importance in the field of waste water treatment. The kinetic results have also been used to evaluate various activation parameters associated with the degradation of LEV by MnO_2 in aqueous acidic medium.

4.7. References

[1] E. S. Elmolla, M. Chaudhari, ***Desalination***,252 (2010) 46.

[2] S. Kusari, D. Prabakaram, L. Lamshoft, M. Spiteller, ***Environ. Pollut.,*** 157 **(**2009) 2722.

[3] M. Sturini, A. Speltini, F. Maraschi, ***Water. Res.,*** 46 (2012) 5575.

[4] D. Croisier, M. Etienne, E. Bergoin, ***Antimicrob. Agents. Chemother.,*** 48 **(**2004) 1699.

[5] P. M. Roblin, M. R. Hammerschlag, ***Antimicrob. Agents. Chemother.,*** 471 **(**2003) 447.

[6] R. C. J. Owens, P. G.Ambrose, ***Med. Clin. North. Am.,*** 84 (2000) 1447.

[7] K. Kummerer, ***J. Environ. Manage.,*** 90 (2009) 2354.

[8] D. Fatta-Kassinos, M. Merics, A. Nikolaou,***Anal. Bianal. Chem.,*** 399 (2011) 251.

[9] A. A. P.Khan, A. Mohammad, S. Bano, A. Husain, K. S. Siddiqi, ***Transition Met. Chem.,*** 35 (2010) 117.

[10] A. A. P.Khan, A. M. Asiri, N. Azum, ***Ind. Eng. Chem. Res.,***51 (2012)4819.

[11] N. H. E.Najjar, E. Touffet, M. Deborde, R. Journel, N. K. V.Leitner.***Chemosphere,***93 (2013) 604.

[12] R. M.Kulkarni, M. S.Hanagadakar, R. S.Malladi, ***Asian J. Research Chem.,***6 (2013) 1124.

[13] A. Jain,G. Tazwar, V. Devra, ***Int. J. Res. Pharm. Sci.,*** 5 (2015) 1.

[14] M. B.Patgar, S. T. Nandibewoor, S. A. Chimatadar, ***Cogent Chemistry,***1 (2015) 1.

[15] M. S.Gudaganatti, M. S.Hanagadakar, R. M.Kulkarni, S. Malladi, R. K.Nagarale, ***Progress in Reaction Kinetics Mechanism,*** 37 (2012) 366.

[16] G. Gupta, A. Kaur, A. S. K. Sinha, S. K. Kansal, ***Materials Research Bulletin,*** 88 (2017) 148.

[17] M. S.Yahvya, M. E.Karbane, N. Oturan, K. E. Kacemi, M. A. Outran, ***Environmental Technology,*** 37 (2016) 1276.

[18] H. Zhang, W. R. Chen, C. H. Haung, ***Environ. Sci. Technol.,*** 42 (2008) 5548.

[19] H. C.Zhang, C. H. Haung, ***Environ. Sci. Technol.,*** 39 (2005) 4474.

[20] J. F.Perez-Benito, E. Brillas, R. Pouplana, ***Inorg. Chem.,*** 28 (1989) 390.

[21] J. F.Perez-Benito, C. Arias, ***J. Colloid Interface. Sci.,*** 149 (1992) 92.

[22] J. F.Perez-Benito, C. Arias, E. Amat, ***J. Colloid Interface Sci.,*** 177 (1996) 228.

[23] J. F. Perez-Benito, ***J. Colloid Interface Sci.,*** 284 (2002) 130.

[24] A. T. Stone, J. J. Morgan, ***Environ. Sci. Technol.,*** 18 (1984) 617.

[25] F. Mata-Perez, J. F. Perez-Benito, ***Can. J. Chem.,*** 63 (1985) 988.

[26] F. Freeman, C. O. Fuselier, C. R. Armstead, C. E. Dalton, P. A. Davidson, E. M. Karchefski, D. E. Krochman, M. N. Johnson, N. K. Jones, ***J. Am. Chem. Soc.,*** 103 (1981) 1154.

[27] G. Chen, L. Zhao, Y. H. Dong, ***J. Hazard. Mater.***193 (2011) 128.

[28] A. K. Singh, N. Sen, S. K. Chatterjee, ***Indian J. of Chem.,*** 55A (2016) 1059.

[29] M. Akram, M. Altaf, K. Ud-Din, ***Colloids Surf. B***, 82 (2011) 217.

[30] L. Yuan, W. Dongbin, D. Yuguo, ***Chemosphere,*** 119 (2015) 282.

[31] F. Fiegl, Spot Tests in Organic analysis. ***Elsevier: New York,*** (1975) 435.

[32] A. I. Vogel, A Textbook of Practical Organic chemistry including Qualitative Organic Analysis. ***3rd ed. Longman,*** (1973) 332.

[33] K. J.Laidler, Chemical Kinetics. Pearson Education, (Singapore) Pte. Ltd, Indian Branch, Delhi, ***India, 3rdedn .,*** 183 (2004) 198.

Chapter – 5

Oxidation of Ciprofloxacin by Hexacyanoferrate(III) in Presence of Cu(II) as A Catalyst: A Kinetic Study

5.1. Introduction

A large number of the clinically prescribed antibacterial drugs are discharged into waste water systems, which indicates the presence of different antibacterial agents into aquatic environment [1]. Fluoroquinolones have been detected at various concentration ranges from dm^{-3} to ng dm^{-3} in waste water [2]. Antibacterial resistant bacteria have been detected in waste water effluents from sewage treatment plant and in drinking water. Recent research has verified the ubiquing of numerous antibacterial compounds in the aquatic environment [3]. These antibacterial have emerged as a new class of pollutants because of their adverse effects on human health [4]. The oxidative transformation of fluoroquinolone antibacterial agents in water treatment process definitely plays a major role in this concern. Ciprofloxacin (CIP) {1-cyclopropyl-6-fluoro-1,4-dihydro-4-oxo-7-(piperazine-1-yl)-quinolone-3-carboxylic acid} is a second generation fluoroquinolone antimicrobial agent with a wide spectrum of activity against many gram positive and gram negative aerobic and anaerobic bacteria. CIP is a member of fluoroquinolone group and is used world-wide as a human and veterinary medicine [5]. There are studies on the modified pharmacological and toxicological properties of these drugs in the form of metallic complexes [6-8]. To properly assess the risk of CIP in aqueous solution and better understand its environmental fate and the transformation of fluoroquinolone pharmaceuticals in water systems, oxidative kinetic study could be helpful in effective removal of CIP from environmental water.

In recent years the use of transition metal ion such as Ru(II)/Ru(III), Os(IV)/Os(VIII), Pd(II)/Pd(IV), Mn(IV)/Mn(II), Cr(IV)/Cr(III), Ir(IV)/Ir(VI) and Cu(II)/Cu(I) as catalyst in various redox processes have attracted considerable interest [9-11]. It has been shown [12] that metal ion act as catalyst by one of several different paths, such as formation of complexes with reactants or oxidation of the substrate itself or through the formation of free radicals. The Cu(II) generally forms an activated complex with the substrate before converting into final product [13]. The mechanism of the catalysis depends on the nature of substrate, oxidant and experimental conditions.

Hexacyanoferrate(III) (HCF(III)) has been widely used to oxidize various organic and inorganic compounds in basic, acidic and neutral medium [14-15]. HCF(III) is a one electron oxidant with a redox potential of +0.45V for the $[Fe(CN)_6]^{-3}$/ $[Fe(CN)_6]^{-4}$ couple in alkaline medium leading to its reduction to hexacyanoferrate(II) a stable product [16-18]. In most of the oxidations, HCF(III) is mainly used as hydrogen atom abstractor [19] and free radical generator [20]. HCF(III) is a transition metal complex, consisting of a central iron ion, surrounded by six negative cyanide ions, or ligands, in an octahedral arrangement. A literature survey revealed that the kinetics and mechanism of oxidation of CIP by different oxidants such as ClO_2, Ozone free chlorine and permanganate [21-24]. However, the reaction of CIP with HCF(III) have not been investigated in detail and thus is the focus of this study and title reaction is undertaken to understand the mechanism of the reaction and active species involved in Cu(II) catalyzed reaction.

5.2. Experimental

5.2.1. Chemicals and Reagents

The methods of preparation of the reagents are given in chapter 2 (Experimental section). However, all other reagents were either of AnalaR grade or guaranteed reagent grade and were used as supplied without any further treatment. A fresh solution of hexacyanoferrate(III) was prepared before running the experiment every time. All the glass vessels and apparatus used in this work were of corning or Pyrex makes. Doubly distilled water was used in complete study.

5.2.2. Kinetic Procedure

All kinetic measurements were conducted under pseudo first order conditions, where [CIP] was always in excess over [HCF(III)], at a constant ionic strength in alkaline medium and temperature of 40±1ºC. The reaction was initiated by mixing the thermostatted solutions of HCF and CIP which also contained the required concentration of Cu(II), NaOH and $NaNO_3$. The progress of the reaction was followed by observing the absorbance of $[Fe(CN)_6]^{3-}$ in the

reaction mixture at 420nm in a placed in the cell compartment of an UV-Visible spectrophotometer, that there was no interference from other species in the reaction mixture at this wavelength. The U.V. spectra indicates gradual disappearance of HCF(III) band with time as a result of its reduction to HCF(II) **(Figure 5.1)**.The application of Beer's law of HCF(III) at 420 nm had been verified giving ε =1050 dm^3 mol^{-1} cm^{-1} [26], pseudo-first-order rate constant (k_{obs}) was calculated from the plot of the logarithm of absorbance versus time. The pseudo first order plot was linear up to 80% completion of the reaction and k_{obs} value was reproducible within ±6%.

5.2.3. Stoichiometry and product analysis

The stoichiometry of the reaction was determined with various ratio of reactants in the presence of Cu(II) as catalyst and constant concentration of NaOH and $NaNO_3$ were kept for 24 h at 40ºC in a closed vessel. The results indicated that one mole of CIP reacts with two mole of HCF as given in the following **equation (5.1)**

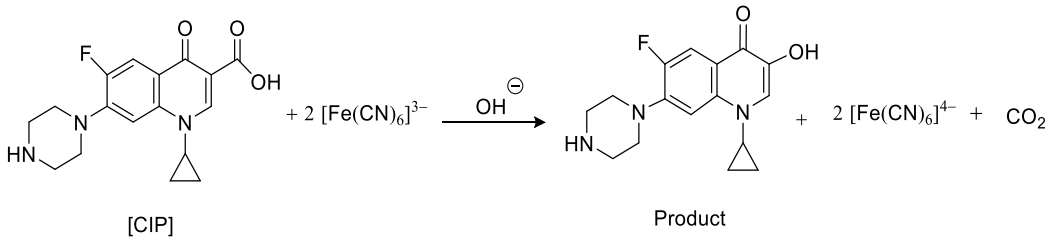

(5.1)

The remaining reaction mixture was acidified, concentrated and extracted with ether. The main product {1-cyclopropyl-3-hydroxy-6-fluoro-1, 4-dihydro-7-(piperazine-1-yl)-quinolin-4-one}, was identified with the help of TLC and characterized by FT-IR and LC-MS analysis. FT-IR spectra of product show carbonyl stretching of 7-oxo group at 1640.35 cm^{-1} and a broad peak at 3472.09 cm^{-1} is due to OH-stretching and the carbonyl stretching of acid is disappear **(Figure 5.2)**. LC-MS analysis of CIP oxidation reaction indicates the formation of product with molecular ion of m/z 304 amu **(Figure 5.3)**. The molecular ion of CIP is m/z 332, the m/z 304 corresponds to decarboxylation of quinolones ring and yield {1-cyclopropyl-3-hydroxy-6-fluoro-1,4-dihydro-7-(piperazine-1-yl)-quinolin-4-one}as oxidation product. The product was also short written asm-28,

indicating the net mass loss of product from the parent CIP. The liberated $CO_2$was identified by the lime water test.

5.3. Results

5.3.1. Hexacyanoferrate(III) dependence

The oxidant HCF(III) concentration in Cu(II) catalyzed reaction was varied from 1.0×10^{-4} mol dm^{-3} to 1.0×10^{-3} mol dm^{-3} at fixed concentration of [CIP] = 1.0×10^{-2} mol dm^{-3}, [Cu(II)] = 1.0×10^{-3} mol dm^{-3}, [OH^-] = 1.0 mol dm^{-3} and I = 2.0 mol dm^{-3} at 40 ºC. The plot of log absorbance versus time was linear **(Figure 5.4)** indicating that the reaction is first order with respect to [HCF(III)]. The observed pseudo first order rate constant (k_{obs}) was independent of the concentration of HCF(III). Results are given in **Tables 5.1, 5.2 and 5.3**.

5.3.2. Ciprofloxacin dependence

The effect of different concentration variation of CIP in Cu(II) catalyzed reaction on the rate of reaction was studied in the range 0.5×10^{-2} mol dm^{-3} to 5.0×10^{-2} mol dm^{-3} at fixed concentration of [HCF] = 1.0×10^{-3} mol dm^{-3}, [Cu(II)] = 1.0×10^{-3} mol dm^{-3}, [OH^-] = 1.0 mol dm^{-3} and I = 2.0 mol dm^{-3} at 35˚C, 40˚C, 45˚C temperatures respectively. The rate of reaction increases with increasing concentration of CIP. A plot of log k_{obs} versus log [CIP] was linear with a slope of 0.73, thus indicating a fractional-order dependence on CIP concentration. Results are given in **Tables 5.4, 5.5 and 5.6**.

5.3.3. Hydroxyl ion dependence

The effect of concentration variation of sodium hydroxide in Cu(II) catalyzed reaction on rate of reaction was studied in the concentration range 0.2 mol dm^{-3} to 1.4 mol dm^{-3} at fixed concentration of [HCF] = 1.0×10^{-3} mol dm^{-3}, [CIP] = 1.0×10^{-2} mol dm^{-3}, [Cu(II)] = 1.0×10^{-3} mol dm^{-3} and I = 2.0 mol dm^{-3} at three temperatures viz. 35˚C, 40˚C, 45˚C respectively. Pseudo first-order rate constant (k_{obs}) was found to be increased with increase in [OH^-]. A plot of log k_{obs} versus log [OH^-] was linear with a fractional slope of 0.64. Results are given in **Tables 5.7, 5.8 and 5.9**.

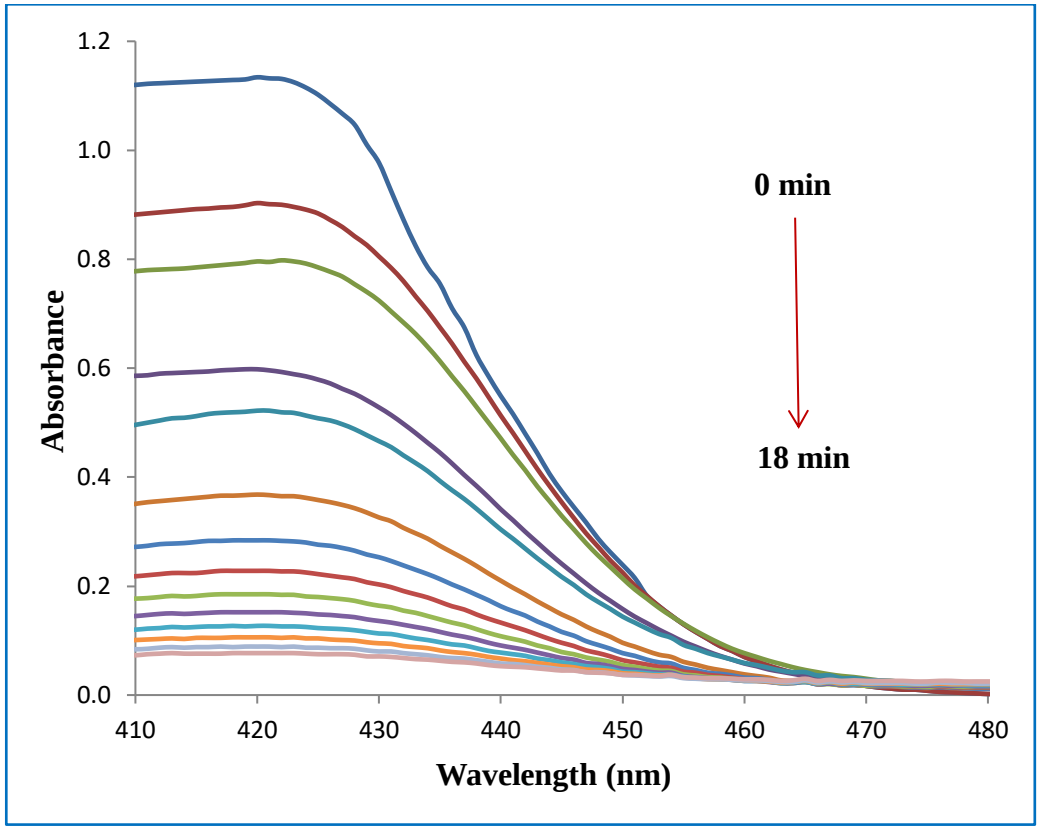

Figure 5.1: Spectral changes during the Cu(II) catalyzed oxidation of ciprofloxacin by hexacyanoferrate(III) in alkaline medium.

[HCF(III)] = 1.0×10^{-3} mol dm^{-3}; $[OH^-]$ = 1.0 mol dm^{-3};

[CIP] = 1.0×10^{-2} mol dm^{-3}; I = 2.0 mol dm^{-3};

[Cu(II)] = 1.0×10^{-3} mol dm^{-3}; Temp. = 40°C.

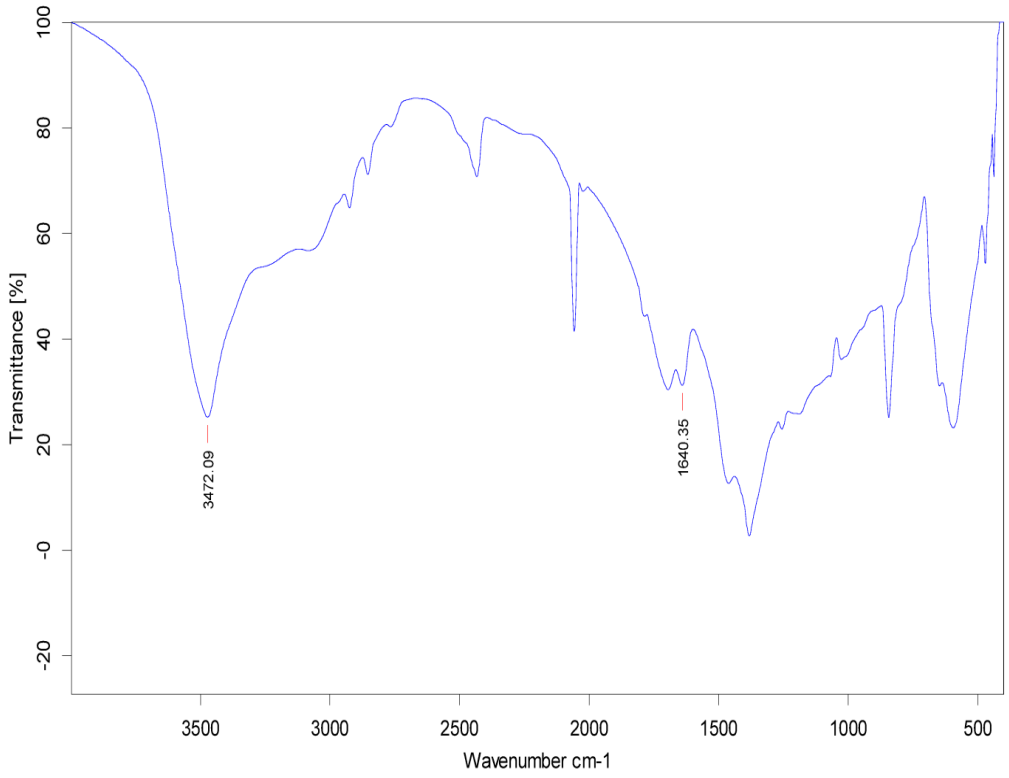

Figure 5.2: FTIR spectra of the oxidative product of ciprofloxacin by hexacyanoferrate(III) in aqueous alkaline medium.

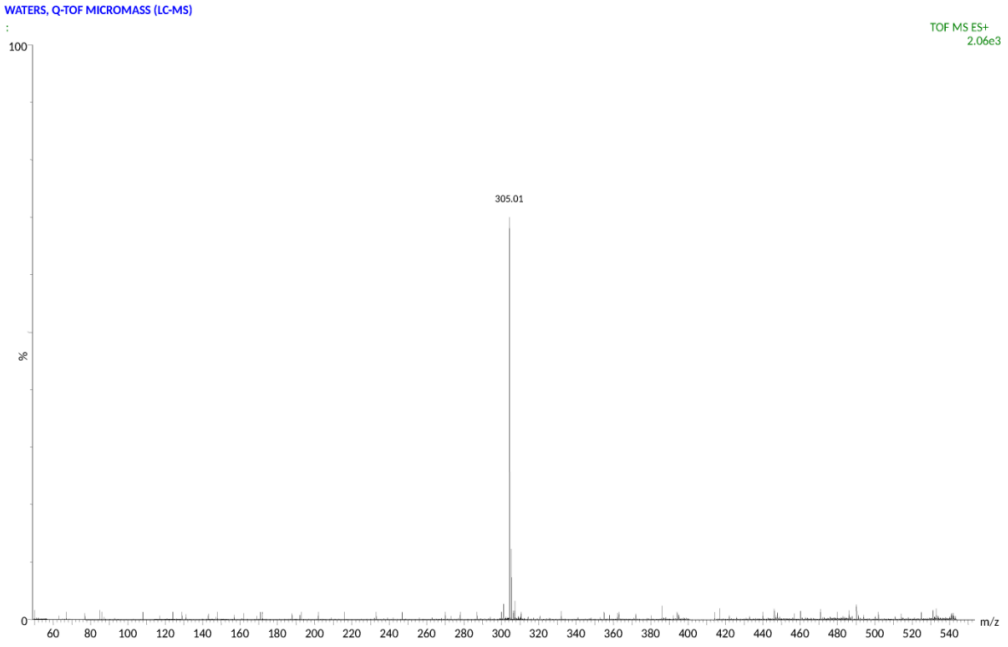

Figure 5.3: LC-ESI-MS spectra of oxidation product of ciprofloxacin.

TABLE: 5.1

VARIATION OF HEXACYANOFERRATE(III)

[CIP] = 1.0 x 10^{-2} mol dm^{-3} **Temp. = 40°C**

[OH^-] = 1.0 mol dm^{-3} **I = 2.0 mol dm^{-3}**

[Cu] = 1.0 x 10^{-3} mol dm^{-3}

10^4[HCF(III)], mol dm^{-3}	**1.0**	**2.5**	**5.0**	**7.5**	**10.0**
Time in minutes			**Absorbance**		
0	0.150	0.300	0.560	0.841	1.135
2	0.112	0.223	0.416	0.622	0.841
4	0.083	0.166	0.308	0.461	0.624
6	0.062	0.123	0.229	0.357	0.461
8	0.046	0.092	0.170	0.253	0.342
10	0.035	0.068	0.126	0.187	0.254
12	0.026	0.051	0.094	0.138	0.188
$10^4(k_{obs})$, sec^{-1}	**24.50**	**24.70**	**24.85**	**25.05**	**25.00**

TABLE: 5.2

VARIATION OF HEXACYANOFERRATE(III)

[CIP] = 2.0 x 10^{-2} mol dm^{-3} **Temp. = 40°C**

[OH^-] = 1.0 mol dm^{-3} **I = 2.0mol dm^{-3}**

[Cu] = 1.0 x 10^{-3} mol dm^{-3}

10^4[HCF(III)], mol dm^{-3}	**1.0**	**2.5**	**5.0**	**7.5**	**10.0**
Time in minutes			**Absorbance**		
0	0.150	0.300	0.560	0.841	1.135
2	0.108	0.215	0.401	0.601	0.811
4	0.078	0.154	0.287	0.430	0.579
6	0.056	0.110	0.206	0.307	0.414
8	0.040	0.079	0.148	0.220	0.296
10	0.029	0.057	0.106	0.157	0.211
12	0.021	0.041	0.076	0.112	0.181
$10^4(k_{obs})$, sec^{-1}	**27.50**	**27.75**	**27.80**	**28.00**	**28.02**

TABLE: 5.3

VARIATION OF HEXACYANOFERRATE(III)

[CIP] = 3.0 x 10^{-2} mol dm^{-3} **Temp. = 40°C**

[OH^-] = 1.0 mol dm^{-3} **I = 2.0mol dm^{-3}**

[Cu] = 1.0 x 10^{-3} mol dm^{-3}

10^4 [HCF(III)], mol dm^{-3}	**1.0**	**2.5**	**5.0**	**7.5**	**10.0**
Time in minutes			**Absorbance**		
0	0.150	0.300	0.560	0.841	1.135
2	0.104	0.208	0.387	0.580	0.783
4	0.072	0.144	0.268	0.400	0.541
6	0.050	0.100	0.185	0.276	0.373
8	0.035	0.069	0.128	0.190	0.258
10	0.024	0.048	0.089	0.131	0.178
12	0.017	0.033	0.061	0.090	0.123
$10^4(k_{obs})$, sec^{-1}	**30.55**	**30.60**	**30.75**	**31.00**	**30.90**

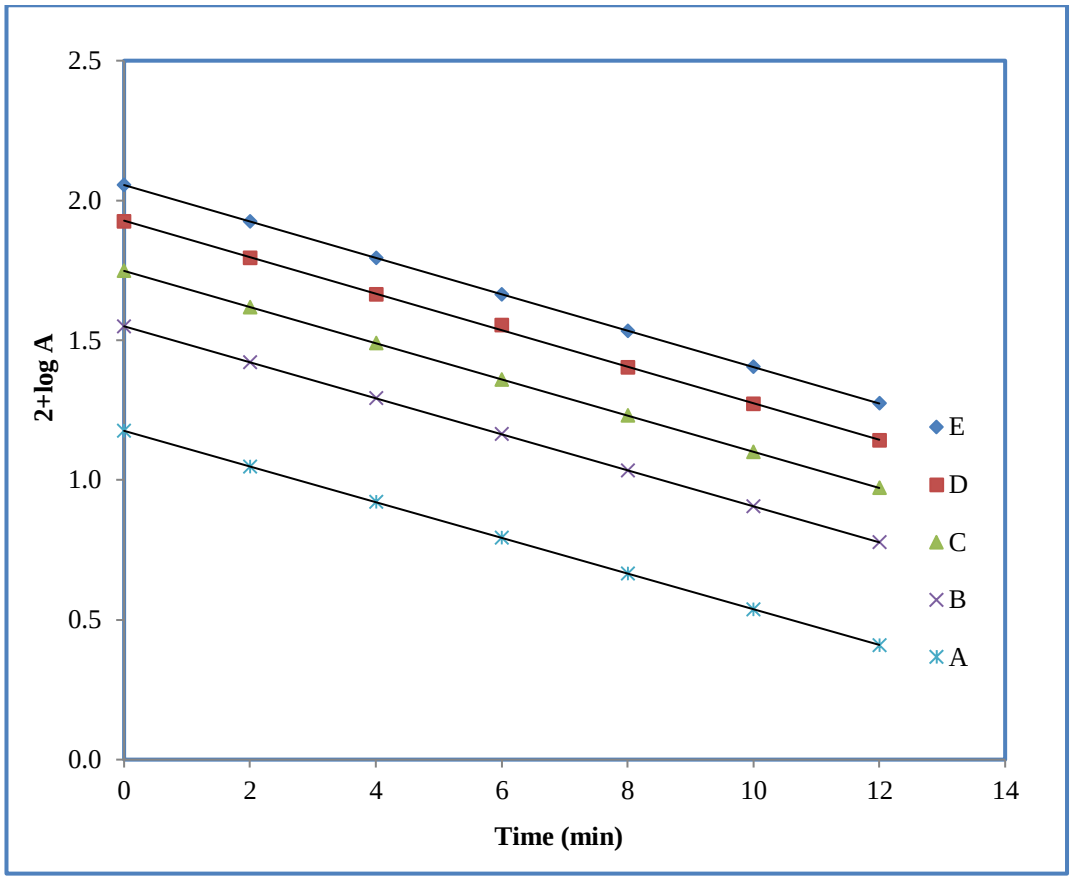

Figure 5.4: First order plots of the variation of hexacyanoferrate(III) concentration.

[CIP] = 1.0×10^{-2} mol dm^{-3}; [OH^-] = 1.0 mol dm^{-3};

[Cu(II)] = 1.0×10^{-3} mol dm^{-3}; I = 2.0 mol dm^{-3};

Temp. = 40ºC;

[HCF(III)] = (A) 1.0×10^{-4} mol dm^{-3} (B) 2.5×10^{-4} mol dm^{-3}

(C) 5.0×10^{-4} mol dm^{-3} (D) 7.5×10^{-4} mol dm^{-3}

(E) 10.0×10^{-4} mol dm^{-3}.

(Ref. Table 5.1)

TABLE: 5.4
VARIATION OF CIPROFLOXACIN

[HCF(III)] = 1.0 x 10^{-3} mol dm^{-3} **Temp. = 35°C**
[OH^-] = 1.0 mol dm^{-3} **I = 2.0 mol dm^{-3}**
[Cu] = 1.0 x 10^{-3} mol dm^{-3}

10^2 [CIP], mol dm^{-3}	**0.5**	**0.75**	**1.0**	**2.0**	**3.0**	**4.0**	**5.0**
Time in minutes				**Absorbance**			
0	(0)1.135	(0)1.135	(0)1.135	1.135	1.135	1.135	1.135
1	(4)0.892	(2)0.955	(2)0.912	0.945	0.902	0.874	0.860
2	(8)0.702	(4)0.804	(4)0.733	0.787	0.716	0.673	0.652
3	(12)0.552	(6)0.676	(6)0.590	0.655	0.569	0.518	0.494
4	(16)0.434	(8)0.569	(8)0.474	0.546	0.452	0.399	0.374
5	(20)0.341	(10)0.479	(10)0.381	0.454	0.359	0.307	0.284
6	(24)0.268	(12)0.403	(12)0.306	0.378	0.285	0.236	0.215
7	(28)0.211	(14)0.339	(14)0.246	0.315	0.226	0.182	0.163
8	(32)0.166	(16)0.285	(16)0.198	0.262	0.180	0.140	0.124
10^4 (k_{obs}), sec^{-1}	**10.0**	**14.4**	**18.2**	**30.5**	**38.4**	**43.6**	**46.2**

Figures in parentheses denote time in minutes.

TABLE: 5.5
VARIATION OF CIPROFLOXACIN

[HCF(III)] = 1.0 x 10^{-3} mol dm^{-3} **Temp. = 40°C**
[OH^-] = 1.0 mol dm^{-3} **I = 2.0 mol dm^{-3}**
[Cu] = 1.0 x 10^{-3} mol dm^{-3}

10^2 [CIP], mol dm^{-3}	**0.5**	**0.75**	**1.0**	**2.0**	**3.0**	**4.0**	**5.0**
Time in minutes				**Absorbance**			
0	(0)1.135	(0)1.135	(0)1.135	(0)1.135	1.135	1.135	1.135
0.5	(2)0.956	(2)0.886	(2)0.841	(1)0.893	0.976	0.956	0.948
1.0	(4)0.805	(4)0.692	(4)0.623	(2)0.703	0.839	0.805	0.793
1.5	(6)0.678	(6)0.541	(6)0.462	(3)0.553	0.722	0.678	0.662
2.0	(8)0.571	(8)0.422	(8)0.342	(4)0.436	0.621	0.571	0.553
2.5	(10)0.481	(10)0.330	(10)0.254	(5)0.343	0.534	0.481	0.462
3.0	(12)0.405	(12)0.257	(12)0.188	(6)0.270	0.459	0.406	0.386
3.5	(14)0.341	(14)0.201	(14)0.139	(7)0.212	0.395	0.342	0.323
4.0	(16)0.287	(16)0.157	(16)0.103	(8)0.167	0.340	0.288	0.270
10^4 (k_{obs}), sec^{-1}	**14.3**	**20.6**	**25.0**	**39.8**	**50.3**	**57.2**	**60.0**

Figures in parentheses denote time in minutes.

TABLE: 5.6
VARIATION OF CIPROFLOXACIN

[HCF(III)] = 1.0 x10^{-3} mol dm^{-3} **Temp. = 45°C**
[OH^-] = 1.0 mol dm^{-3} **I = 2.0 mol dm^{-3}**
[Cu] = 1.0 x 10^{-3} mol dm^{-3}

10^2 [CIP], mol dm^{-3}	**0.5**	**0.75**	**1.0**	**2.0**	**3.0**	**4.0**	**5.0**
Time in minutes				**Absorbance**			
0	(0)1.135	(0)1.135	(0)1.135	1.135	1.135	1.135	1.135
0.5	(2)0.875	(1)0.951	(1)0.744	0.972	0.941	0.922	0.910
1.0	(4)0.675	(2)0.797	(2)0.488	0.833	0.780	0.749	0.586
1.5	(6)0.520	(3)0.667	(3)0.320	0.714	0.647	0.609	0.470
2.0	(8)0.401	(4)0.559	(4)0.210	0.611	0.536	0.495	0.377
2.5	(10)0.309	(5)0.468	(5)0.137	0.524	0.445	0.402	0.302
3.0	(12)0.238	(6)0.392	(6)0.320	0.449	0.369	0.327	0.243
3.5	(14)0.184	(7)0.329	(7)0.259	0.384	0.306	0.265	0.243
4.0	(16)0.142	(8)0.275	(8)0.210	0.329	0.253	0.216	0.195
10^4 (k_{obs}), sec^{-1}	**21.7**	**29.5**	**35.2**	**51.6**	**62.5**	**69.2**	**73.5**

Figures in parentheses denote time in minutes.

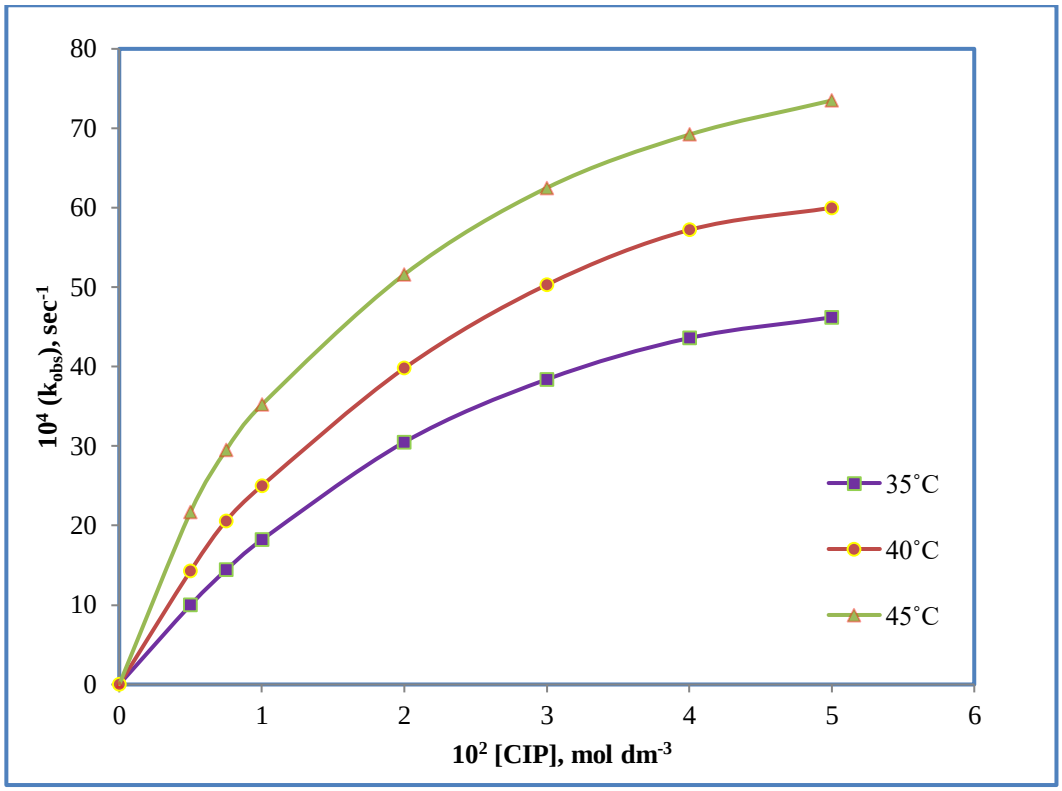

Figure 5.5: Variation of ciprofloxacin at different temperature.

[HCF(III)] = 1.0×10^{-3} mol dm^{-3}; $[OH^-] = 1.0$ mol dm^{-3};

[Cu(II)] = 1.0×10^{-3} mol dm^{-3}; I = 2.0 mol dm^{-3}.

(Ref. Table: 5.4, 5.5, 5.6)

TABLE: 5.7
VARIATION OF HYDROXYL ION

[HCF(III)] = 1.0 x 10^{-3} mol dm^{-3} **Temp. = 35°C**

[CIP] = 1.0 x 10^{-2} mol dm^{-3} **I = 2.0 mol dm^{-3}**

[Cu] = 1.0 x 10^{-3} mol dm^{-3}

10^2 [CIP], mol dm^{-3}	**0.2**	**0.4**	**0.6**	**0.8**	**1.0**	**1.2**	**1.4**
Time in minutes				**Absorbance**			
0	(0)1.135	(0)1.135	(0)1.135	1.135	1.135	1.135	1.135
3	(10)0.863	(5)0.886	(5)0.817	0.891	0.853	0.843	0.835
6	(20)0.656	(10)0.692	(10)0.507	0.700	0.642	0.626	0.615
9	(30)0.499	(15)0.540	(15)0.423	0.550	0.482	0.465	0.452
12	(40)0.379	(20)0.422	(20)0.304	0.432	0.363	0.345	0.333
15	(50)0.288	(25)0.329	(25)0.219	0.339	0.273	0.256	0.245
18	(60)0.219	(30)0.257	(30)0.157	0.226	0.205	0.190	0.180
10^4 (k_{obs}), sec^{-1}	**4.55**	**8.25**	**10.97**	**13.45**	**15.65**	**16.55**	**17.05**

Figures in parentheses denote time in minutes.

TABLE: 5.8
VARIATION OF HYDROXYL ION

[[HCF(III)] = 1.0 x 10^{-3} mol dm^{-3} **Temp. = 40°C**

[CIP] = 1.0 x 10^{-2} mol dm^{-3} **I = 2.0 mol dm^{-3}**

[Cu] = 1.0 x 10^{-3} mol dm^{-3}

10^2 [CIP], mol dm^{-3}	**0.2**	**0.4**	**0.6**	**0.8**	**1.0**	**1.2**	**1.4**
Time in minutes				**Absorbance**			
0	(0)1.135	(0)1.135	(0)1.135	1.135	1.135	1.135	1.135
2	(7)0.830	(3)0.886	(3)0.815	0.871	0.841	0.823	0.822
4	(14)0.607	(6)0.692	(6)0.586	0.669	0.624	0.597	0.596
6	(21)0.444	(9)0.541	(9)0.421	0.514	0.462	0.433	0.432
8	(28)0.325	(12)0.422	(12)0.302	0.394	0.343	0.314	0.313
10	(35)0.238	(15)0.330	(15)0.217	0.303	0.254	0.228	0.226
12	(42)0.174	(18)0.257	(18)0.156	0.232	0.188	0.165	0.164
10^4 (k_{obs}), sec^{-1}	**7.45**	**13.75**	**18.37**	**22.05**	**25.00**	**26.80**	**27.00**

Figures in parentheses denote time in minutes.

TABLE: 5.9
VARIATION OF HYDROXYL ION

[HCF(III)] = 1.0 x 10^{-3} mol dm^{-3} **Temp. = 45°C**
[CIP] = 1.0 x 10^{-2} mol dm^{-3} **I = 2.0 mol dm^{-3}**
[Cu] = 1.0 x 10^{-3} mol dm^{-3}

10^2 [CIP], mol dm^{-3}	**0.2**	**0.4**	**0.6**	**0.8**	**1.0**	**1.2**	**1.4**
Time in minutes				**Absorbance**			
0	(0)1.135	(0)1.135	(0)1.135	1.135	1.135	1.135	1.135
1	(4)0.892	(2)0.909	(2)0.861	0.944	0.923	0.911	0.904
2	(8)0.700	(4)0.728	(4)0.653	0.785	0.750	0.730	0.719
3	(12)0.550	(6)0.583	(6)0.495	0.630	0.595	0.575	0.565
4	(16)0.432	(8)0.467	(8)0.376	0.511	0.475	0.450	0.448
5	(20)0.340	(10)0.374	(10)0.285	0.428	0.387	0.367	0.345
6	(24)0.267	(12)0.300	(12)0.216	0.332	0.312	0.297	0.275
7	(28)0.210	(14)0.240	(14)0.164	0.285	0.242	0.225	0.210
10^4 (k_{obs}), sec^{-1}	**10.05**	**18.50**	**24.65**	**30.08**	**34.52**	**36.75**	**38.00**

Figures in parentheses denote time in minutes.

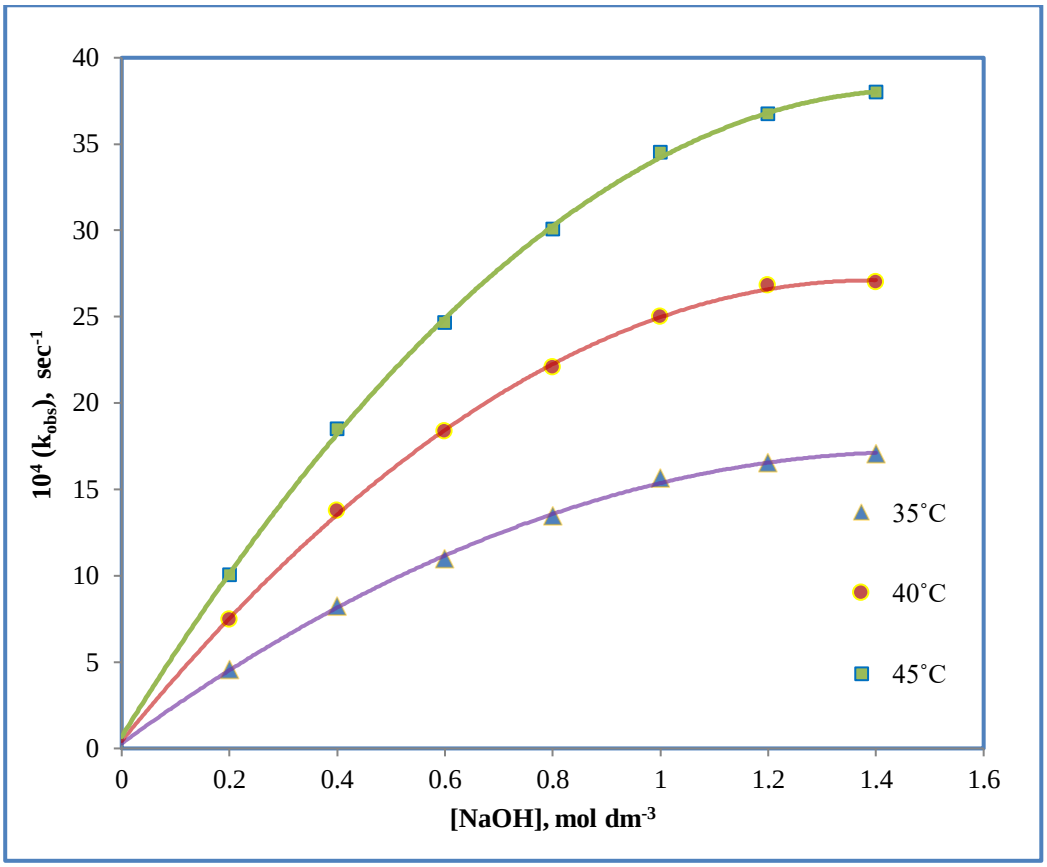

Figure 5.6: Variation of hydroxyl ion at different temperature.

[HCF] = 1.0 × 10^{-3} mol dm^{-3}; [CIP] = 1.0× 10^{-2} mol dm^{-3};

[Cu(II)] = 1.0 × 10^{-3} mol dm^{-3}; I = 2.0 mol dm^{-3}.

(Ref. Table: 5.7, 5.8, 5.9)

5.3.4. [Cu(II)] ion dependence

The concentration of copper sulphate was varied from 0.25 $\times 10^{-3}$ mol dm^{-3} to 2.0 $\times$ 10^{-3} mol dm^{-3} at three different concentration of CIP viz. 0.5 $\times$ 10^{-2} mol dm^{-3}, 1.0 $\times$ 10^{-2} mol dm^{-3}, 2.0$\times 10^{-2}$ mol dm^{-3} respectively at constant [HCF]=1.0$\times 10^{-3}$ mol dm^{-3}, [OH^-] = 1.0 mol dm^{-3} and I = 2.0 mol dm^{-3}at 40˚C temperature. The rate constant (k_{obs}) increases with increasing Cu(II) ion concentration. A plot of rate constant(k_{obs}) against [Cu(II)] yields a straight line with zero intercept indicating the unit order with respect to Cu(II). Results are given in **Tables 5.10, 5.11 and 5.12**.

5.3.5. Effect of Ionic Strength and Dielectric Constant

At constant concentration of [HCF] = 1.0 $\times$ 10^{-3} mol dm^{-3}, [CIP] = 1.0 $\times$ 10^{-2} mol dm^{-3}, [Cu(II)] = 1.0 $\times$ 10^{-3} mol dm^{-3} and [OH^-] = 1.0 mol dm^{-3} the ionic strength was varied by varying concentration of sodium nitrate 0.25 mol dm^{-3} to 2.0 mol dm^{-3}at 40˚C temperature. Ionic strength had negligible effect on the rate of reaction. At constant acidity and other constant conditions, as the t-butyl alcohol content increase from 0 to 50% (v/v) in the reaction, change in dielectric constant had negligible effect on the rate of reaction. Results are given in **Table 5.13**.

5.3.6. Effect of Initially Added Product

The initial added products, hexacyanoferrate(II) was studied in the range of 1.0 $\times$ 10^{-4} mol dm^{-3} to 10.0 $\times$ 10^{-4} mol dm^{-3} while other reactants concentration and conditions constant, [HCF] = 1.0 $\times$ 10^{-3} mol dm^{-3}, [CIP] = 1.0 $\times$ 10^{-2} mol dm^{-3}, [Cu(II)] = 1.0 $\times$ 10^{-3}mol dm^{-3} , [OH^-] = 1.0 mol dm^{-3} and I = 2.0 mol dm^{-3} at 40˚C temperature, the rate of reaction was unaffected. Results are given in **Table 5.14.**

5.3.7. Test for Free Radicals

The formation of free radical was confirmed by the addition of acrylonitrile in the reaction mixture. After 5 hours then diluted with methanol, white precipitate was formed, indicating the presence of free radical during the progress of reaction [27, 28].

TABLE: 5.10
VARIATION OF COPPER SULPHATE

[HCF(III)] = 1.0 x 10^{-3} mol dm^{-3} **Temp. = 40°C**
[CIP] = 0.5 x 10^{-2} mol dm^{-3} **I = 2.0 mol dm^{-3}**

10^3 [$CuSO_4$], mol dm^{-3}	**0.25**	**0.5**	**0.75**	**1.0**	**1.25**	**1.5**	**1.75**	**2.0**
Time in minutes				**Absorbance**				
0	(0)1.135	(0)1.135	(0)1.135	1.135	1.135	1.135	(0)1.135	(0)1.135
2	(10)0.867	(5)0.866	(3)0.896	0.920	0.867	0.819	(1)0.938	(1)0.920
4	(20)0.662	(10)0.661	(6)0.707	0.746	0.662	0.591	(2)0.774	(2)0.745
6	(30)0.506	(15)0.504	(9)0.558	0.605	0.505	0.426	(3)0.640	(3)0.604
8	(40)0.386	(20)0.385	(12)0.440	0.490	0.386	0.307	(4)0.528	(4)0.490
10	(50)0.295	(25)0.293	(15)0.347	0.397	0.294	0.222	(5)0.437	(5)0.397
12	(60)0.225	(30)0.224	(18)0.274	0.322	0.225	0.160	(6)0.361	(6)0.322
14	(70)0.172	(35)0.171	(21)0.216	0.261	0.172	0.115	(7)0.298	(7)0.261
10^4 (k_{obs}), sec^{-1}	**4.50**	**9.02**	**13.15**	**17.50**	**22.50**	**27.22**	**31.85**	**35.05**

Figures in parentheses denote time in minutes.

TABLE: 5.11
VARIATION OF COPPER SULPHATE

[HCF(III)] = 1.0 x 10^{-3} mol dm^{-3} **Temp. = 40°C**
[CIP] = 1.0 x 10^{-2} mol dm^{-3} **I = 2.0 mol dm^{-3}**

10^3 [$CuSO_4$], mol dm^{-3}	**0.25**	**0.5**	**0.75**	**1.0**	**1.25**	**1.5**	**1.75**	**2.0**
Time in minutes	**Absorbance**							
0	(0)1.135	(0)1.135	(0)1.135	(0)1.135	1.135	1.135	1.135	1.135
1	(8)0.848	(4)0.841	(3)0.803	(2)0.841	0.943	0.906	0.872	0.841
2	(16)0.634	(8)0.623	(6)0.568	(4)0.623	0.784	0.724	0.670	0.623
3	(24)0.474	(12)0.461	(9)0.402	(6)0.462	0.652	0.578	0.514	0.461
4	(32)0.354	(16)0.342	(12)0.284	(8)0.342	0.542	0.462	0.395	0.342
5	(40)0.265	(20)0.253	(15)0.201	(10)0.254	0.450	0.369	0.303	0.253
6	(48)0.198	(24)0.187	(18)0.142	(12)0.188	0.374	0.280	0.233	0.188
10^4 (k_{obs}), sec^{-1}	**6.05**	**12.50**	**19.22**	**25.00**	**30.82**	**37.50**	**44.00**	**50.02**

Figures in parentheses denote time in minutes.

TABLE: 5.12
VARIATION OF COPPER SULPHATE

[HCF(III)] = 1.0 x 10^{-3}mol dm^{-3} **Temp. = 40°C**
[CIP] = 2.0 x 10^{-2} mol dm^{-3} **I = 2.0 mol dm^{-3}**

10^3 [$CuSO_4$], mol dm^{-3}	**0.25**	**0.5**	**0.75**	**1.0**	**1.25**	**1.5**	**1.75**	**2.0**
Time in minutes				**Absorbance**				
0	(0)1.135	(0)1.135	(0)1.135	1.135	1.135	1135	1.135	1.135
1	(5)0.878	(3)0.842	(2)0.843	0.928	0.885	0.841	0.804	0.760
2	(10)0.679	(6)0.624	(4)0.625	0.759	0.689	0.623	0.569	0.509
3	(15)0.525	(9)0.463	(6)0.464	0.621	0.537	0.461	0.403	0.341
4	(20)0.406	(12)0.343	(8)0.345	0.508	0.419	0.342	0.286	0.228
5	(25)0.314	(15)0.254	(10)0.256	0.415	0.326	0.253	0.202	0.153
6	(30)0.243	(18)0.189	(12)0.190	0.340	0.254	0.188	0.143	0.102
10^4 (k_{obs}), sec^{-1}	**8.55**	**16.62**	**24.82**	**33.50**	**41.55**	**50.00**	**57.50**	**66.85**

Figures in parentheses denote time in minutes.

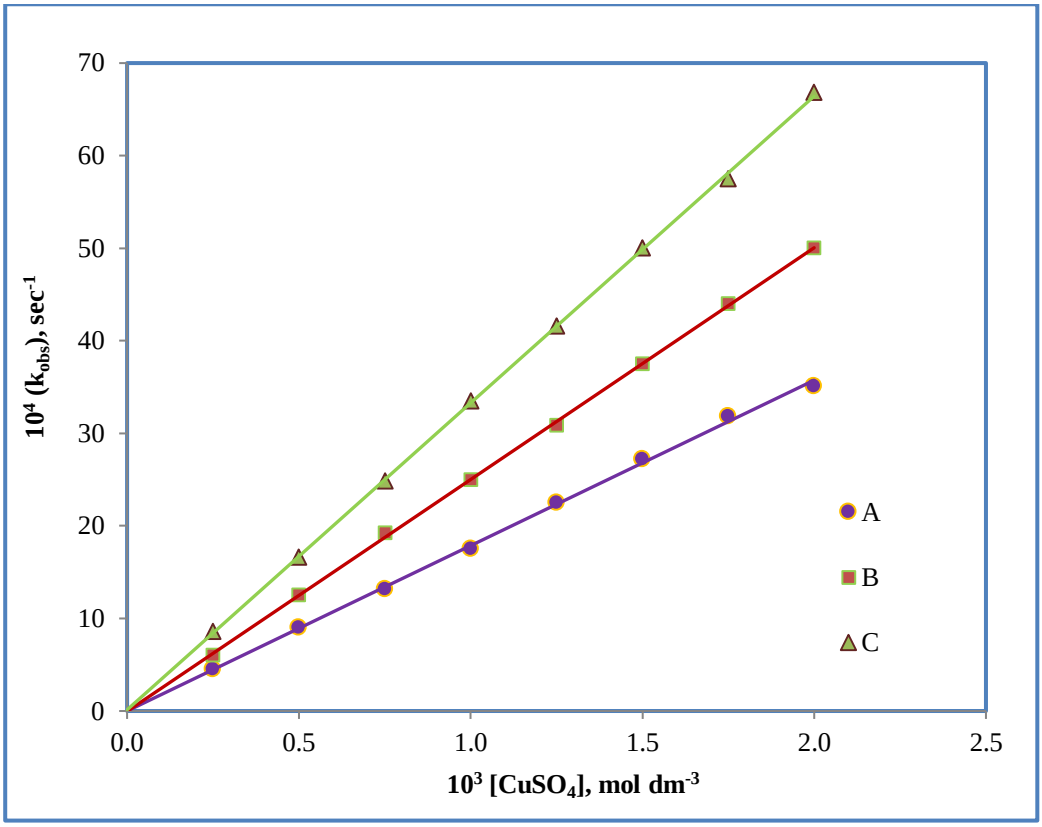

Figure 5.7: Variation of copper sulphate ion at different concentration of ciprofloxacin.

[HCF(III)] = 1.0×10^{-3} mol dm^{-3}; I = 2.0 mol dm^{-3};

[OH^-] = 1.0 mol dm^{-3}; Temp. = 40 ºC;

[CIP] = (A) 0.5×10^{-2} mol dm^{-3}; (B) 1.0×10^{-2} mol dm^{-3};

(C) 2.0×10^{-2} mol dm^{-3}.

(Ref. Table: 5.10, 5.11, 5.12)

TABLE: 5.13

VARIATION OF SODIUM NITRATE

[HCF(III)] = 1.0 x 10^{-3} mol dm^{-3} **Temp. = 40°C**

[CIP] = 2.0 x 10^{-2} mol dm^{-3} **[Cu(II)] = 1.0 x 10^{-3} mol dm^{-3}**

[$NaNO_3$], mol dm^{-3}	**0.25**	**0.5**	**0.75**	**1.0**	**1.25**	**1.5**	**1.75**	**2.0**
Time in minutes				**Absorbance**				
0	1.133	1.136	1.134	1.133	1.135	1.137	1.133	1.136
2	0.839	0.841	0.843	0.842	0.840	0.846	0.845	0.844
4	0.630	0.624	0.626	0.625	0.623	0.628	0.629	0.626
6	0.461	0.462	0.460	0.461	0.460	0.465	0.459	0.464
8	0.342	0.343	0.345	0.344	0.345	0.347	0.346	0.346
10	0.254	0.254	0.256	0.255	0.252	0.256	0.251	0.252
12	0.187	0.188	0.189	0.189	0.186	0.190	0.185	0.186
10^4 (k_{obs}), sec^{-1}	**25.05**	**25.00**	**25.11**	**25.09**	**25.02**	**25.10**	**25.10**	**25.07**

TABLE: 5.14

EFFECT OF HCF(II) ION

[HCF(III)] = 1.0 x 10^{-3}mol dm^{-3} **Temp. = 40°C**

[CIP] = 1.0 x 10^{-2} mol dm^{-3} **I = 2.0 mol dm^{-3}**

[OH^-] = 1.0 mol dm^{-3}

10^4 [Mn(II)]	**1.0**	**3.0**	**5.0**	**7.0**	**10.0**
Time in minutes			**Absorbance**		
0	1.134	1.133	1.132	1.134	1.135
2	0.844	0.842	0.846	0.843	0.841
4	0.622	0.625	0.628	0.626	0.624
6	0.463	0.465	0.465	0.464	0.462
8	0.340	0.344	0.347	0.345	0.343
10	0.256	0.255	0.256	0.253	0.254
12	0.187	0.189	0.190	0.187	0.188
10^4 (k_{obs}), sec^{-1}	**25.10**	**25.09**	**25.11**	**25.05**	**25.00**

5.4. Discussion

Cu(II) is known to be a catalyst in many redox reactions, particularly in alkaline medium [29] and catalysis has usually been explained by assuming the intermediate complex formed by an interaction of anionic form of CIP and Cu(II). This intermediate complex reacts with the oxidant in rate determining step, since order with respect to HCF(III) and Cu(II) is one each and less than unit order with respect to [CIP]. Furthermore, rate also increases with increasing of hydroxyl ion with fractional first order dependence. Thus a mechanism consisting of scheme and also accounting for all experimental observations can be proposed in scheme 5.1.

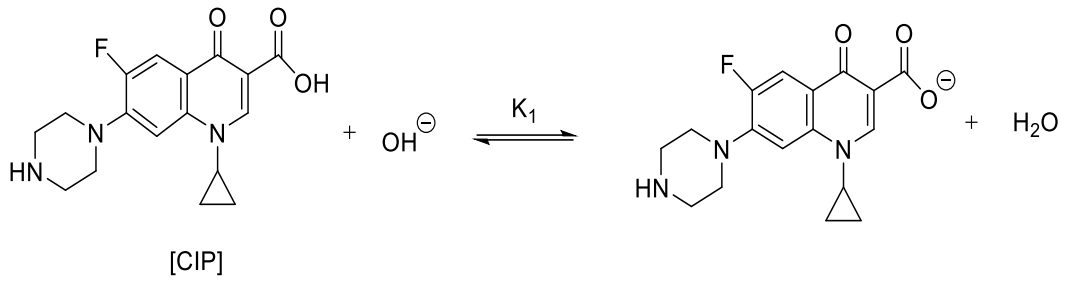

[CIP]

(5.2)

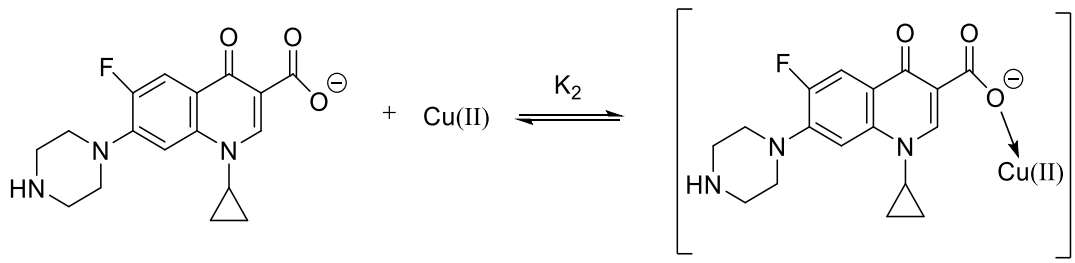

Complex

(5.3)

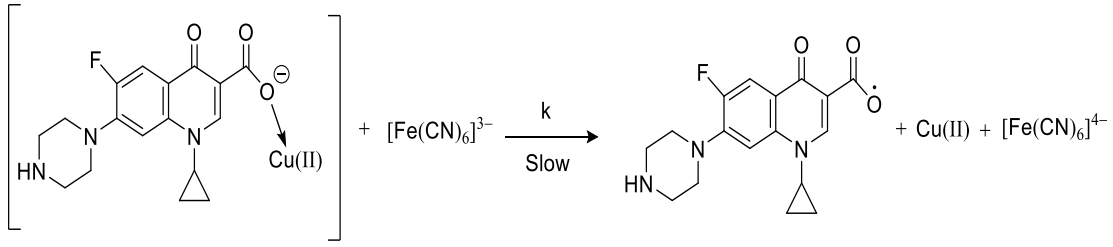

Complex Free radical

(5.4)

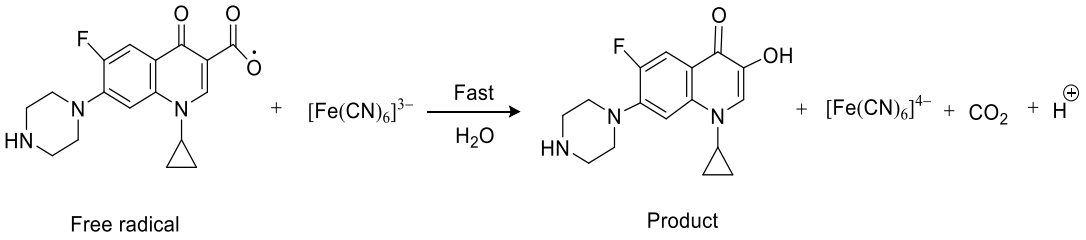

(5.5)

Scheme 5.1

In most of the oxidation reactions, HCF(III) resembles Cu(II) oxidation reactions [30-32], which involves free radical formation and rapidly oxidises it. However, our experimental results are contrary to that expected. The HCF(III)–HCF(II) system has the redox potential +0.45V which has higher redox potential than Cu(II)-Cu(I) couple (-0.34V), has a better possibility for the rapid oxidation of the free radical with HCF(III) in the alkaline medium.

The probable structure of the complex is given below:

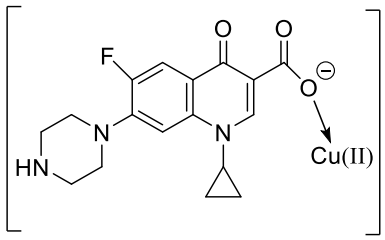

Complex

The formation of the complex is proven kinetically by the non zero intercept of Cu(II)/k_{obs} versus 1/[CIP] **(Figure. 5.8)**.

Following rate equation can be derived from the **scheme 5.1**:

$$Rate = \frac{-d[HCF]}{dt} = k[C][HCF] \tag{5.6}$$

$$K_1 = \frac{[CIP^-]}{[CIP]_F[OH^-]_F} \tag{5.7}$$

$$[CIP^-] = K_1[CIP]_F[OH^-]_F$$

$$K_2 = \frac{[C]}{[CIP^-][Cu(II)]_F}$$

$$[C] = K_2[CIP^-][Cu(II)]_F$$

$$[C] = K_1K_2[CIP]_F[OH^-]_F[Cu(II)]_F \quad (5.8)$$

Substituting equation (5.8) into equation (5.6) leads to,

$$Rate = kK_1K_2[CIP]_F[OH^-]_F[Cu(II)]_F[HCF] \quad (5.9)$$

The total concentration of CIP is given by,

$$[CIP]_T = [CIP]_F + [CIP^-] + [C] \quad (5.10)$$

where 'T' and 'F' stand for total and free concentrations.

Substituting equations (5.7) and (5.8) into equation (5.10) and rearrangement gives,

$$[CIP]_T = [CIP]_F + K_1[CIP]_F[OH^-]_F + K_1K_2[CIP]_F[OH^-]_F[Cu(II)]_F \quad (5.11)$$

$$[CIP]_T = [CIP]_F\{1 + K_1[OH^-]_F + K_1K_2[OH^-]_F[Cu(II)]_F\} \quad (5.12)$$

Therefore,

$$[CIP]_F = \frac{[CIP]_T}{1 + K_1[OH^-]_F + K_1K_2[OH^-]_F[Cu(II)]_F} \quad (5.13)$$

In view of low $[Cu(II)]_F$, the third denominator term $K_1\ K_2\ [OH^-]\ [Cu(II)]$ in the above equation can be neglected. Therefore, equation (5.13) can be simplified to the following,

$$[CIP]_F = \frac{[CIP]_T}{1 + K_1[OH^-]_F} \quad (5.14)$$

The concentration of Cu(II) can be calculated as,

$$[Cu(II)]_T = [Cu(II)]_F + [C] \quad (5.15)$$

$$[Cu(II)]_T = [Cu(II)]_F\{1 + K_1K_2[CIP]_F[OH^-]_F\} \quad (5.16)$$

$$[Cu(II)]_F = \frac{[Cu(II)]_T}{1 + K_1K_2[CIP]_F[OH^-]_F} \quad (5.17)$$

Regarding to the concentration of OH^-,

$$[OH^-]_F = [OH^-]_T \quad (5.18)$$

Substituting equations (5.14), (5.17) and (5.18) into equation (5.19) (and omitting 'T' and 'F' subscripts) leads to,

$$Rate = \frac{kK_1K_2[CIP][OH^-][Cu(II)][HCF]}{\{1 + K_1[OH^-]\}\{1 + K_1K_2[CIP][OH^-]\}} \quad (5.19)$$

$$Rate = \frac{kK_1K_2[CIP][OH^-][Cu(II)][HCF]}{1 + K_1[OH^-] + K_1K_2[CIP][OH^-] + K_1^2K_2[CIP][OH^-]^2} \quad (5.20)$$

The term $K_1^2\ K_2\ [CIP][OH^-]^2$ in the denominator of equation (5.20) is negligibly small compared to unity in view of the low concentration of CIP used.

Therefore equation (5.20) can be written as,

$$Rate = \frac{kK_1K_2[CIP][OH^-][Cu(II)][HCF]}{1 + K_1[OH^-] + K_1K_2[CIP][OH^-]} \quad (5.21)$$

Under Pseudo-first order condition, the rate-law can be expressed by equation (5.22),

$$Rate = \frac{-d[HCF]}{dt} = k_{obs}[HCF] \quad (5.22)$$

Therefore, comparing equation (5.21) and (5.22), the following relationship is obtained,

$$k_{obs} = \frac{Rate}{[HCF]} = \frac{kK_1K_2[CIP][OH^-][Cu(II)]}{1 + K_1[OH^-] + K_1K_2[CIP][OH^-]} \quad (5.23)$$

Equation (5.21) can be rearranged to the following forms, which is suitable for verification,

$$\frac{[Cu(II)]}{k_{obs}} = \left[\frac{1}{kK_1K_2[OH^-]} + \frac{1}{kK_1}\right]\frac{1}{[CIP]} + \frac{1}{k} \quad (5.24)$$

$$\frac{[Cu(II)]}{k_{obs}} = \left[\frac{1}{kK_1K_2[CIP]}\right]\frac{1}{[OH^-]} + \frac{1}{kK_2[CIP]} + \frac{1}{k} \quad (5.25)$$

According to equation (5.24) the plot of [Cu(II)]/k_{obs} versus 1/ [CIP] **(Figure 5.8)** is linear with positive intercept and slope at three different temperatures. The rate constant k, of the slow step, scheme 1 was obtained from the intercept of the plots [Cu(II)]/k_{obs} versus 1/ [CIP] **(Table 5.15)**. The energy of activation was determined by the plot of log k versus 1/T **(Figure 5.9)** from which activation parameters were calculated **(Table 5.15)**. Also, the values of the equilibrium constants associated with the mechanistic scheme (5.1) ($K_1$and K_2) are evaluated from the intercept and slope of the plots of [Cu(II)]/k_{obs} versus 1/ [CIP] and [Cu(II)]/k_{obs} versus 1/ [OH^-] **(Figure 5.10)(Table 5.15)**. The value of equilibrium constantK_1 is in good agreement with earlier work [11] at 40˚C. Van't Hoff plots were drawn for the variations of K_1 and K_2 with temperature i.e. log K_1versus 1/T **(Figure 5.11)** and log K_2 versus 1/T **(Figure 5.12)** and thermodynamic quantities were calculated **(Table 5.15)**.

The entropy of activation ($\Delta S^{\neq}$) tends to be more negative for reaction of an inner-sphere nature, where as the reactions of positive $\Delta S^{\neq}$ values proceed via an outer-sphere mechanism [33-35]. The obtained large negative values of $\Delta S^{\neq}$ **(Table 5.15)** express that the mechanism is one-electron transfer of inner-sphere nature which indicate that there is a decrease in the randomness during the reaction process. This leads to the formation of intermediate complex and such activated complex is more arranged than the reactants due to loss of degree of freedom. Whether, the positive value of $\Delta H^{\neq}$ indicates that the complex formation is endothermic and the value of $\Delta G^{\neq}$ suggests enhanced formation of the intermediate with raising temperature as well as to the non-spontaneity of the complex formation.

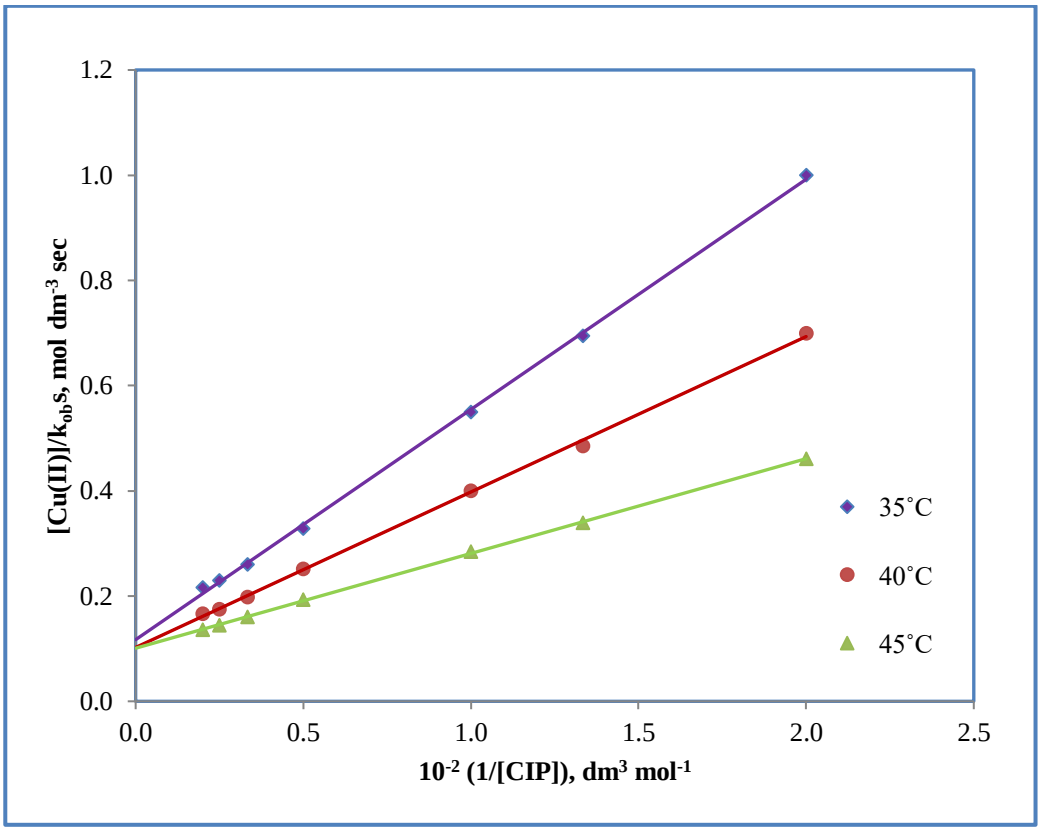

Figure 5.8: Plots of [Cu(II)]/k_{obs} versus 1/[CIP] at different temperature.

[HCF(III)] = 1.0×10^{-3} mol dm^{-3}; [OH^-] = 1.0 mol dm^{-3};

[Cu(II)] = 1.0×10^{-3} mol dm^{-3}; I = 2.0 mol dm^{-3}.

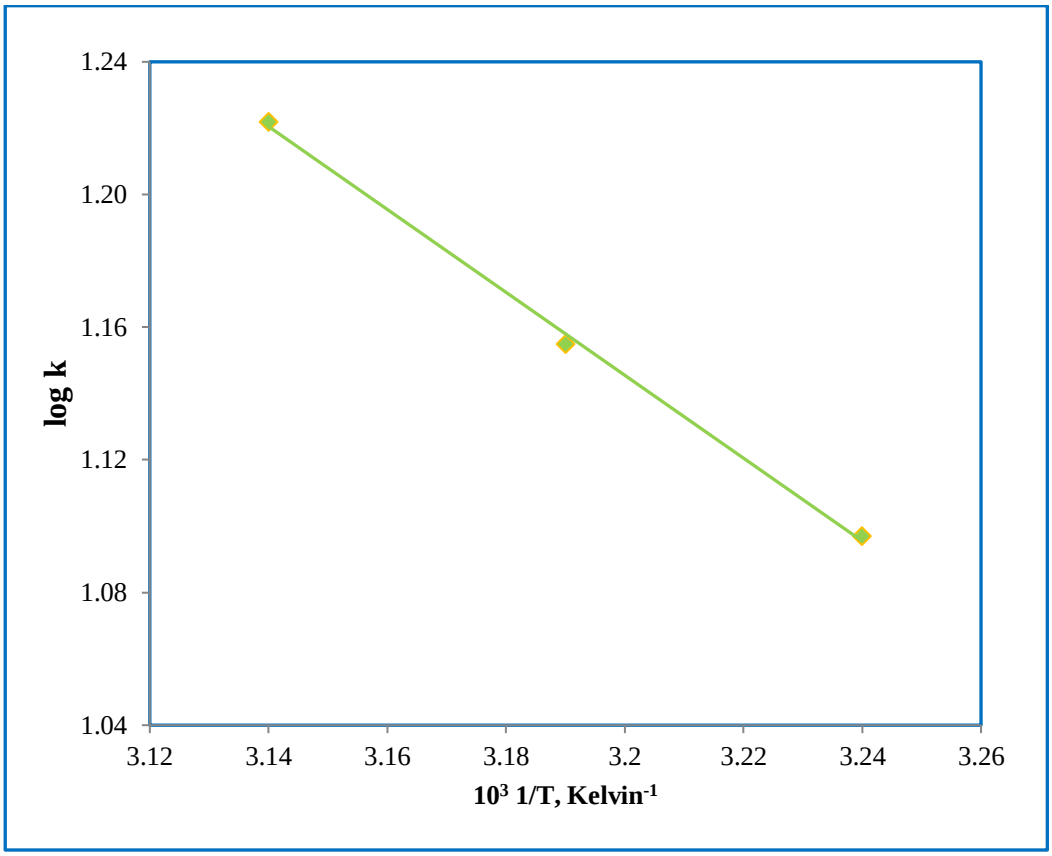

Figure 5.9: Plot of log k versus 1/T.

(Ref. Table: 5.15)

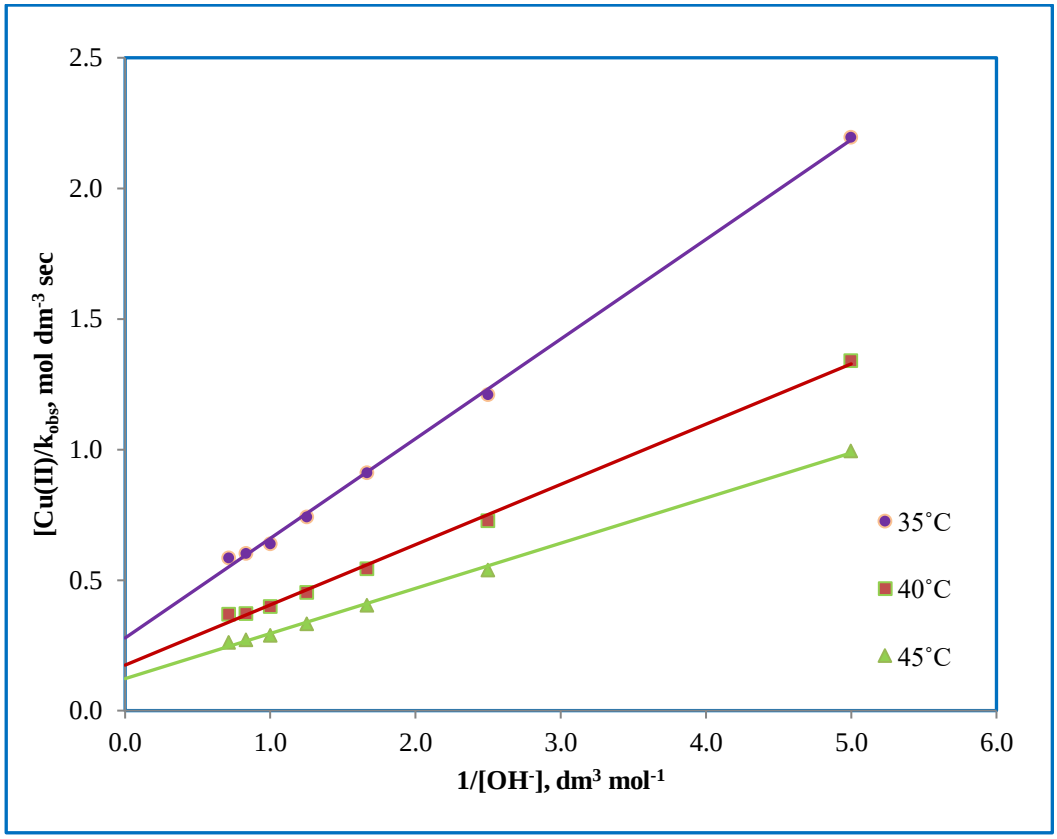

Figure 5.10: Plots of [Cu(II)]/k_{obs} versus 1/[OH^-] at different temperature.

[HCF(III)] = 1.0×10^{-3} mol dm^{-3}; [CIP] = 1.0×10^{-2} mol dm^{-3};

[Cu(II)] = 1.0×10^{-3} mol dm^{-3}; I = 2.0 mol dm^{-3}.

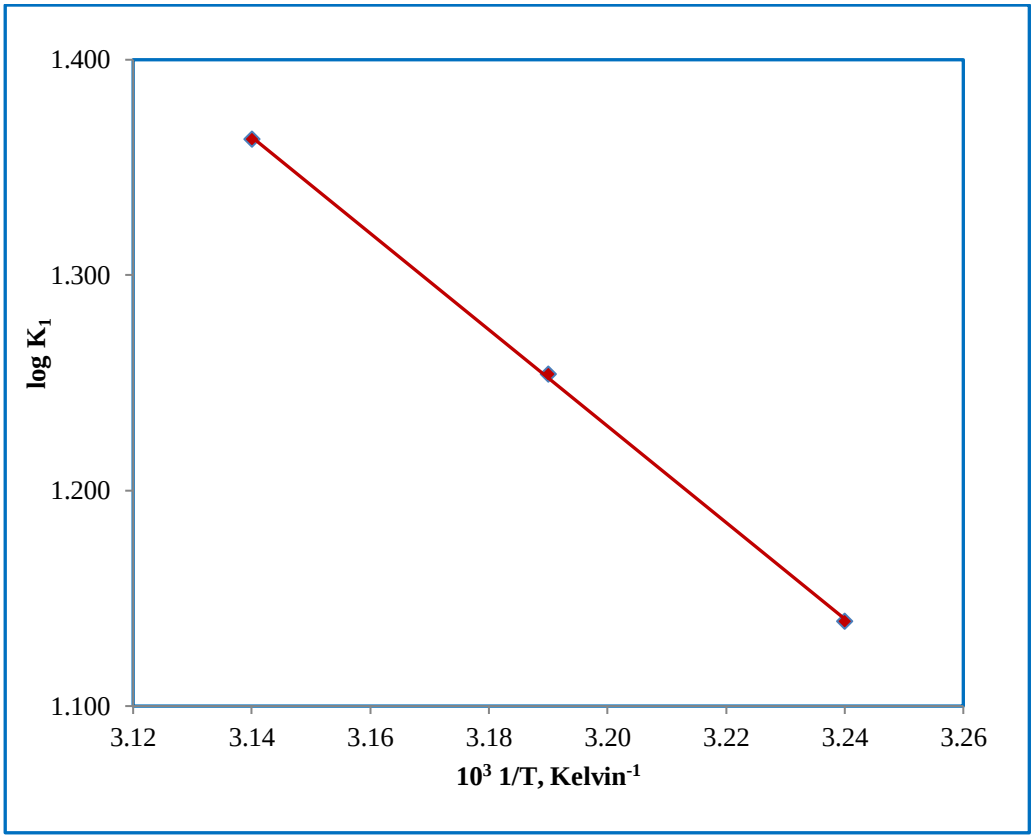

Figure 5.11: Plot of log K_1 versus 1/T.

(Ref. Table: 5.15)

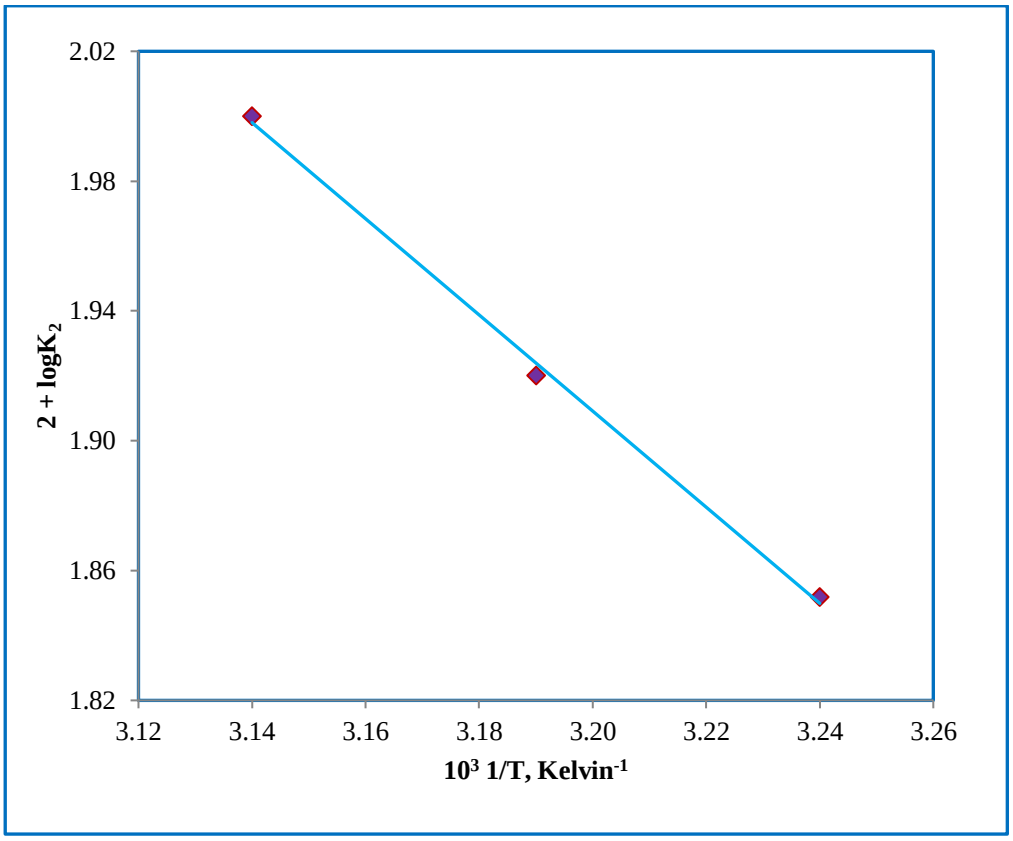

Figure 5.12: Plot of log K_2 versus 1/T.

(Ref. Table: 5.15)

TABLE: 5.15

ACTIVATION PARAMETERS AND THERMODYNAMIC QUANTITIES EVALUATED FROM SCHEME 5.1.

Temperature (Kelvin)	**k (dm^3 $mol^{-1}sec^{-1}$)**	**Activation Parameters**	**K_1 (dm^3 mol^{-1})**	**Thermodynamic Quantities (From K_1)**	**10 K_2 (dm^3 mol^{-1})**	**Thermodynamic Quantities (From K_2)**
308	12.5	E_a= 23.93 ($kJ\ mol^{-1}$)	13.79	ΔH = 40.19 ($kJ\ mol^{-1}$)	7.11	ΔH = 25.74 ($kJ\ mol^{-1}$)
313	14.3	$\Delta H^{\#}$= 21.33 ($kJ\ mol^{-1}$)	17.95	ΔS =– 181.52 ($JK^{-1}\ mol^{-1}$)	9.05	ΔS = - 220.57 ($JK^{-1}\ mol^{-1}$)
318	16.7	$\Delta S^{\#}$ = – 202 ($JK^{-1}\ mol^{-1}$)	23.08	ΔG = 97.11 ($kJ\ mol^{-1}$)	10.00	ΔG = 94.78 ($kJ\ mol^{-1}$)
		$\Delta G^{\#}$ = 84.56 ($kJ\ mol^{-1}$)				

5.5. Conclusion

Cu(II) catalyzed oxidation of ciprofloxacin by hexacyanoferrate(III) in aqueous alkaline medium was found to be first order with respect to oxidant and fractional order with respect to substrate and alkali. The reaction pathway involves complex formation and free radical mechanism. The observed stoichiometry indicates that, the oxidation of one mole of CIP requires two moles of HCF(III). The major product of reaction obtained by the decarboxylation of quinolones moiety and hence, it may retain the antibacterial activity. The overall sequence illustrate here is persistent with all experimental findings, product, mechanistic and kinetic studies.

5.6. References

[1] R. M. Kulkarni, M. S. Hanagadakar, R. S. Malladi, M. S. Gudaganatti, H. S. Biswal, S. T. Nandibewoor, ***Indian J. Chem. Technol.,*** 21 (2014) 38.

[2] M. S. Gudaganatti, M. S. Hanagadakar, R. M. Kulkarni, R. S. Malladi, R. K. Nagarale, ***Prog. React. Kinet.,*** 37 (2012) 366.

[3] R. M. Kulkarni, R. S. Malladi, M. S. Hanagadakar, M. R. Doddamani, U. K. Bhat, ***Desalination and Water Treatment,*** 57 (2016) 16111.

[4] R. M. Kulkarni, M. S. Hanagadakar, R. S. Malladi, H. S. Biswal, E. M. Cuerda-correa, ***Desalination and Water Treatment,*** 57 (2016) 10826.

[5] H. Zhang, C. H. Haung, ***Environ. Sci. Technol.,*** 39 (2005) 4474.

[6] M. Ruyz, L. Perello, R. Ortiz R, A. Castineiras, C. Maichle- Mossmer, E. J. Canton, ***Inorg. Biochem.,*** 59 (1995) 801.

[7] I. Turel, I. Leban, N. Bukovec, ***J. Inorg. Biochem.,*** 66 (1997) 241.

[8] M. P. Lopez-Gresa, R. Oritz, L. Parello, J. Latorre, M. Liu-Gonzalez, S. Perez-Priede, E. Canton, ***J. Inorg. Biochem.*** 92 (2002) 65.

[9] A. K. Das, ***Coord. Chem. Rev.,*** 213 (2001) 307.

[10] N. Diab, I. Abu- Shquair, M. Al-Sunei, R. Salim, ***Int. J. of Chemistry***, 4 (2013) 1388.

[11] M. D. Meti, K. S. Bayadgi, S. T. Nandibewoor, S. A. Chimatadar, ***Montash. Chem.,*** 1 (2014) 1561.

[12] A. K. Singh, S. Srivastava, J. Srivastava,R. Srivastava, P. Singh, ***J. Mol. Catal. A: Chem***., 278 (2007) 72.

[13] R. M. Kulkarni, M. S. Hanagadakar, R. S. Malladi, B. Santhakumari, S. T. Nandibewoor, ***Prog. React. Kinet.,*** 41 (2016) 245.

[14] E. P. Kelson, P. P. Phengsy, ***Int. J. Chem. Kinet.,*** 32 (2000) 760.

[15] A. I. Vovk, I. V. Muraveva, V. P. Kukhar, ***Russ. J. Gen. Chem.,*** 70 (2000) 1108.

[16] G. Dasgupta, K. Mahanti, ***Bull. Soc. Chim. Fr.,*** 4 (1986) 492.

[17] S. A. Farokhi, S. T. Nandibewoor, ***Tetrahedrone,*** 59 (2003) 7595.

[18] A. Nowdari, K. K. Adari,N. R. Gollapalli, V. Parvataneni, ***Eur. J. Chem.,*** 6 (2009) 93.

[19] M. Martinez, M. Pitarque, R. V. Eldik, ***J. Chem. Soc. Dalton. Trans.,*** (1966) 2665.

[20] M. B. Patgar, S. T. Nandibewoor, S. A. Chimatadar, ***Cogent Chemistry,*** 1 (2015) 1.

[21] P. Wang, Y. L. He, C. H. Huang, ***Water Res.,*** 44 (2010) 5989.

[22] E. Guinea, E. Brillas, F. Centellas, P. Canizares, M. A. Radrigo, C. Saez, ***Water Res.,*** 43 (2009) 2131.

[23] M. C. Dodd, A. D. Shah, U. Vongunten, C. H. Huang, ***Environ. Sci. Technol.,*** 39 (2005) 7065.

[24] A. Jain, S. Jain, V. Devra, ***Int. J. of Phar. Sciences and Drug Research,*** 7 (2015)205.

[25] G. H. Jeffery, J. Bassett, J. Mendham, R. C. Denny. Vogel's text book of quantitative chemical analysis, 5thedn. ***ELBS, Longman, Essex,*** (1996) 339.

[26] A. Nowduri, A. B. Duggada, V. R. Kurimella, ***Int. J. of Scientific Research,*** 3 (2014) 131.

[27] A. A. P. Khan, A. Khan, A. M. Asiri, N. Azum, M. A. Rub, ***Journal of the Taiwan Institute of Chemical Engineers,*** 45 (2014) 127.

[28] A. M. Asiri, A. A. P. Khan,A. Khan, ***J. Mol. Liq.,*** 203 (2015) 1.

[29] B. S. Sateesh, V. Shastry, S. Shashidhar, ***Int. J. Res. Phy. Chem.,*** 3 2013) 18.

[30] M. P. Singh, S. Ghosh, ***Z. Phys. Chem.,*** 204 (1955) 1.

[31] J. K. Kochi, B. M. Graybill, M. Kurtz, ***J. Am. Chem. Soc.,*** 86 (1964) 5257.

[32] K. B. Wilberg,W. G. Nigh, ***J. Am. Chem. Soc.,*** 87 (1965) 3849.

[33] A. A. P. Khan, A. M. Asiri, N. Azum, M. A. Rub, A. Khan, A. O. Al-Youbi,***Ind. Eng. Chem. Res.,*** 51 (2012) 4819.

[34] A. A. P. Khan, A. Khan, A. M. Asiri, M. A. Rub, ***J. Ind. Eng. Chem.,*** 20 (2014) 3590.

[35] A. A. P. Khan, A. Khan, A. M. Asiri, S. A. Khan, ***J. Mol. Liq.,*** 218 (2014) 604.

Chapter – 6

Uncatalyzed and Cu(II) Catalyzed Oxidation of Ofloxacin in Aqueous Alkaline Medium: A Kinetic and Mechanistic Study

6.1. Introduction

Ofloxacin (OFL) [9-fluoro-2, 3-dihydro-3-methyl-10-(4-methyl-1-piperazinyl)-7-oxo-7H-pyrido-[1,2,3-de]-1,4-benzoxazine-6-carboxylicacid] belongs to the fluoroquinolone class of antibiotics [1]. The fluoroquinolones have become a more famous class of antibiotics for use in a variety of infections so they are excessively used in the world. Most of them are partially metabolized and excreted by humans, animals and spilled into water. The presence and accumulation of fluoroquinolone antibiotics in aquatic environments, requires development of the various oxidation processes for the transformation of fluoroquinolones in water. OFL have a basic piperazinyl group and a carboxylic group as an ionisable functional groups. The carboxylic group and the carbonyl groups are responsible for antimicrobial activity. These antibiotics connect with a number of other drugs, as well as many herbal and natural supplements. These interactions increase the anticoagulation, non-absorbable complexes formation and the possibility of toxicity.

The huge attention is being paid to various oxidizing agents in attacking distinct groups in simple and large molecules. Among these a potassium hexacyanoferrate(III) {HCF(III)} [2], a one electron oxidant with a redox potential of + 0.45V for the $[Fe(CN)_6]^{-3}$/ $[Fe(CN)_6]^{-4}$ couple in alkaline medium leading to its reduction to hexacyanoferrate(II) [3,4]. It has widely used as oxidizing agent for degradation of various organic and inorganic compounds in alkaline media. Literature survey [5,6] informed that alkaline HCF(III) ion act as an electron abstracting reagent in redox reactions. However Speakman and Wats [7] proposed various path of oxidation of aldehydes, ketone and nitroparaffins by HCF(III). Singh et al [8] suggested the oxidation of formaldehyde, acetone & ethyl methyl ketone by HCF(III) takes place via an electron transfer mechanism resulting in the free radical intermediate formation. Although, HCF(III) has a few advantage that become useful oxidizing agent for many organic substrate [9]. Especially, its stability over the full pH scale and being a balanced oxidant, its reactions with some nitrogen containing compounds are not facile and requires the presence of catalyst [10]. Transition metals have multiple oxidation states, so they are use as catalyst in many oxidation-reduction reactions. In recent years the

transition metal ion such as ruthenium, osmium, palladium, manganese, chromium, iridium and copper has attracted considerable interest as catalyst in various redox processes [11-14]. The mechanism of the catalysis depends on the nature of substrate, oxidant and experimental conditions. It has been observed [15] that metal ion act as catalyst by one of several different paths, such as formation of complexes with reactants or oxidation of the substrate itself or through the formation of free radicals. Although the oxidation of OFL by various oxidants has been carried out [16, 17], there is a lack of literature on the oxidation of this drug by HCF(III) in the absence and presence of catalyst Cu(II). Such studies have importance in understanding the mechanistic profile of OFL in redox reactions and provide an insight into the interaction of metal ion with the substrate and to determine the active species of HCF(III) and Cu(II) catalyst, a detailed study of the reaction becomes important. Hence, the present study aimed to establish the reactivity of OFL towards HCF(III) in both uncatalyzed and Cu(II) catalysed reaction and attempt to explore the mechanism on the basis of kinetic parameters. Furthermore, the oxidation products of the OFL are previously reported and the distribution of products appears to depend upon the nature and potentiality of the oxidants. This was the additional interest of undertaking the title study.

6.2. Experimental details

6.2.1. Chemicals and Reagents

The method of preparation and standardization of the reagents are given in chapter 2 (Experimental). All chemicals used were of analytical grade and twice distilled water, second distillation being from alkaline permanganate solution in an all glass still, was used in all preparation and kinetic studies. Always freshly prepared OFL (KORES India Limited) solutions were used in the kinetics.

6.2.2. Kinetic Procedure

Kinetic measurements were conducted in glass Stoppard flasks immersed in a thermostated water bath at 40±1ºC. Reaction mixture were prepared by

mixing the desired concentration of various reaction components, Fe(III) was the last to be added. The progress of the reaction was followed by measuring absorbance of $[Fe(CN)_6]^{3-}$ in the reaction mixture at 420 nm in a placed in the cell compartment of an U.V.3000^{+} UV-Visible spectrophotometer **(Figure 6.1)**. The application of Beer's law of HCF(III) at 420 nm had been verified giving ε =1050 $dm^3\,mol^{-1}\,cm^{-1}$ [18]. The pseudo first order plots in almost all the cases were linear up to 80% completion of the reaction and values of constants were reproducible within ±6%.

6.2.3. Stoichiometry and product analysis

The reaction mixture containing excess of HCF(III) over OFL were allowed for 12 h to react at 40^{o}C. The excess of HCF(III) concentration determined by measuring the absorbance at 420 nm. The stoichiometry of the reaction indicates **(equation 6.1)** that one mole of OFL reacts with two mole of HCF(III).

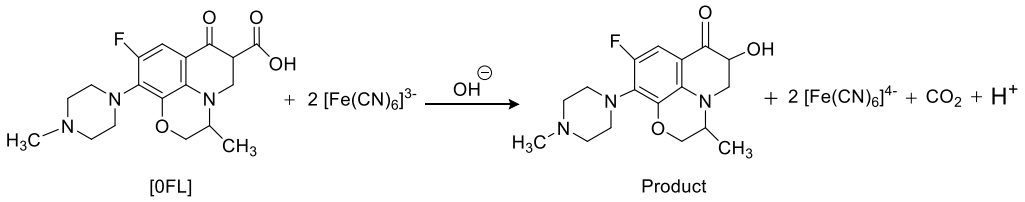

[0FL] Product

(6.1)

The remaining reaction mixture was extracted with ether. The main product, 9-fluoro-2,3-dihydro-6-hydroxy-3-methyl-10-(4-methylpiperazine-1-yl)-[1,4]oxazinoquinolon-7-one, was isolated, identified with the help of TLC and characterized by FT-IR and LC-MS analysis. The FT-IR spectra of pure OFL, the (C=O) band of acid group is appears at 1,718 cm^{-1} and the carbonyl stretching of 7-oxo group appears at 1,621 cm^{-1} **(Figure 6.2A)**. After oxidation, FT-IR spectra of product 9-fluoro-2,3-dihydro-6-hydroxy-3-methyl-10-(4-methylpiperazine-1-yl)-[1,4]-oxazino quinolon-7-one, show band at 1,619 cm^{-1}, was carbonyl stretching of 7-oxo group, a broad peak at 3,457 cm^{-1} is due to OH stretching and the carbonyl stretching of acid is disappear **(Figure 6.2B)**. LC-MS analysis of OFL oxidation product indicates the molecular ion of m/z 333 amu **(Figure 6.3)**. The m/z 333 corresponds to decarboxylation of quinolone ring and yield 9-fluoro-

2,3-dihydro-6-hydroxy-3-methyl-10-(4-methylpiperazine-1-yl)-[1,4]oxazino quinolon-7-one as oxidation product and the melting point of product was 205 ºC [19]. Fe (II) another product was confirmed by the spectral change during the oxidation reaction at 510 nm **(Figure 6.1)**.

6.3. Results

6.3.1. Hexacyanoferrate(III) dependence

The concentration of HCF(III) was varied in the range 1.0×10^{-4} to 1.0×10^{-3} mol dm^{-3}at fixed concentration of [OFL] = 1.0×10^{-3} mol dm^{-3}, [OH^-] = 1.0 mol dm^{-3} and I = 2.0 mol dm^{-3}at 40 ºC for uncatalysed reaction **(Figure 6.4)**. The variation of HCF(III) in presence of Cu(II) as catalyst were performed in same concentration of other reactants and conditions. Pseudo first order plots were made and pseudo first order rate constants were found to be independent of the initial concentration of HCF(III) in both uncatalyzed (k_{un})and catalyzed reaction (k_c) **(Figure 6.5).** Results are given in **Tables 6.1, 6.2.**

6.3.2. Ofloxacin dependence

The concentration of OFL was varied from 0.5×10^{-2} to 5.0×10^{-2} mol dm^{-3} at fixed concentration of [HCF] = 1.0×10^{-3} mol dm^{-3}, [OH^-] = 1.0 mol dm^{-3} and I = 2.0 mol dm^{-3} at 40ºC for uncatalyzed reaction **(Figure 6.6)**. The plot of pseudo first order rate constant (k_{un}) verses [OFL] yielded a straight line passing through the origin indicating first order dependence with respect to OFL. Results are given in **Table 6.3.** The concentration of OFL in Cu(II) catalyzed reaction was also varied from 0.5×10^{-2} to 5.0×10^{-2} mol dm^{-3} at three concentration of [OH^-] viz. 0.5, 1.0, 1.5 mol dm^{-3} respectively and fixed concentration of other reactants and constant conditions. The value of pseudo first order rate constant (k_c) increases at lower concentration of OFL then tends towards a limiting value at higher concentration of OFL **(Figure 6.7)**. The plot of log k_c verses log [OFL] shows the order with respect to the OFL was less than unity (0.663). Results are given in **Tables 6.4, 6.5 and 6.6**.

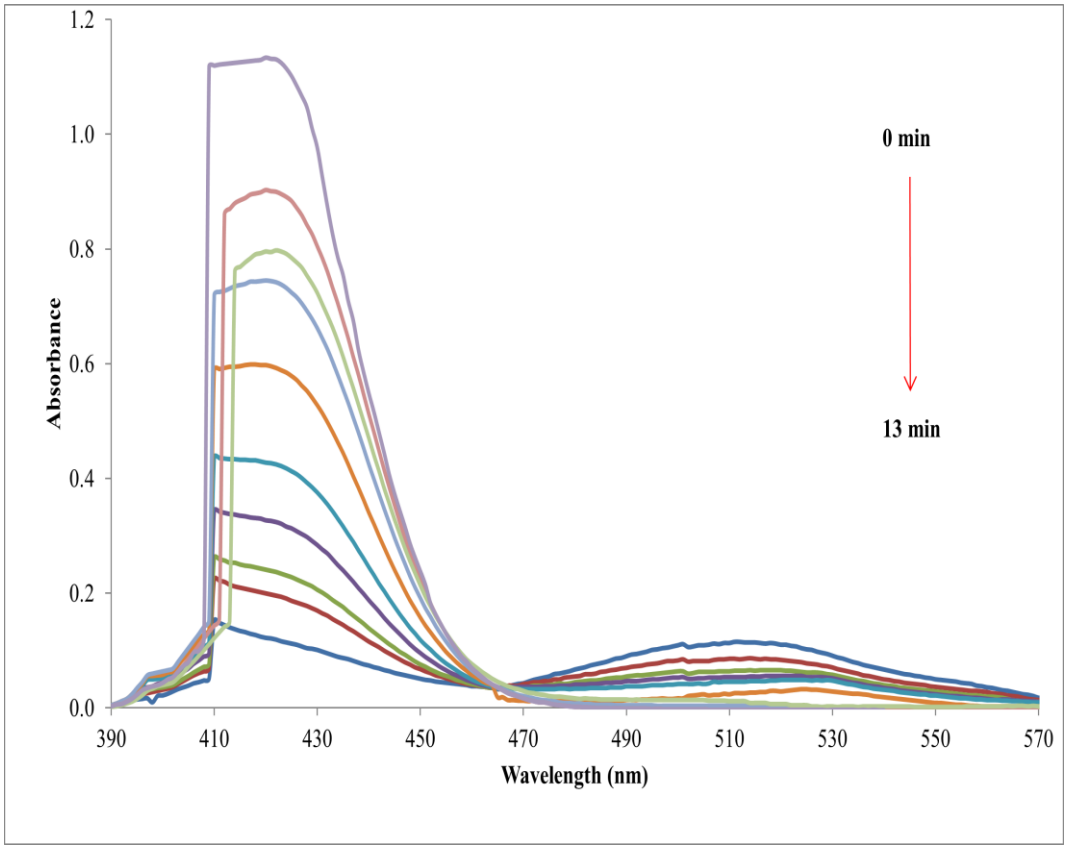

Figure 6.1: Spectral changes during the Cu(II) catalyzed oxidation of OFL by HCF(III) in alkaline medium

[HCF(III)] = 1.0×10^{-3} mol dm^{-3}; [OH^-] = 1.0 mol dm^{-3};

[OFL] = 1.0×10^{-2} mol dm^{-3}; I = 2.0 mol dm^{-3};

[Cu(II)] = 1.0×10^{-3} mol dm^{-3}; Temp. = 40 ºC.

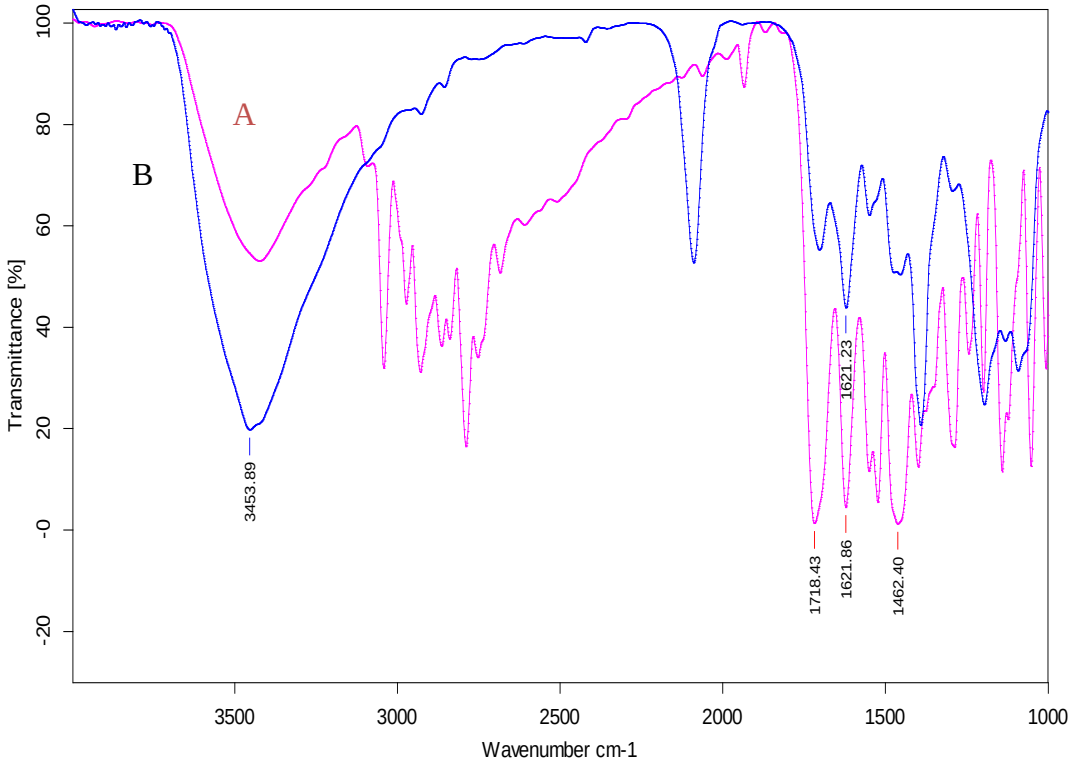

Figure 6.2: Comparative FT-IR spectra of (A) Pure ofloxacin (B) Oxidation product of ofloxacin by hexacyanoferrate(III) in aqueous alkaline medium.

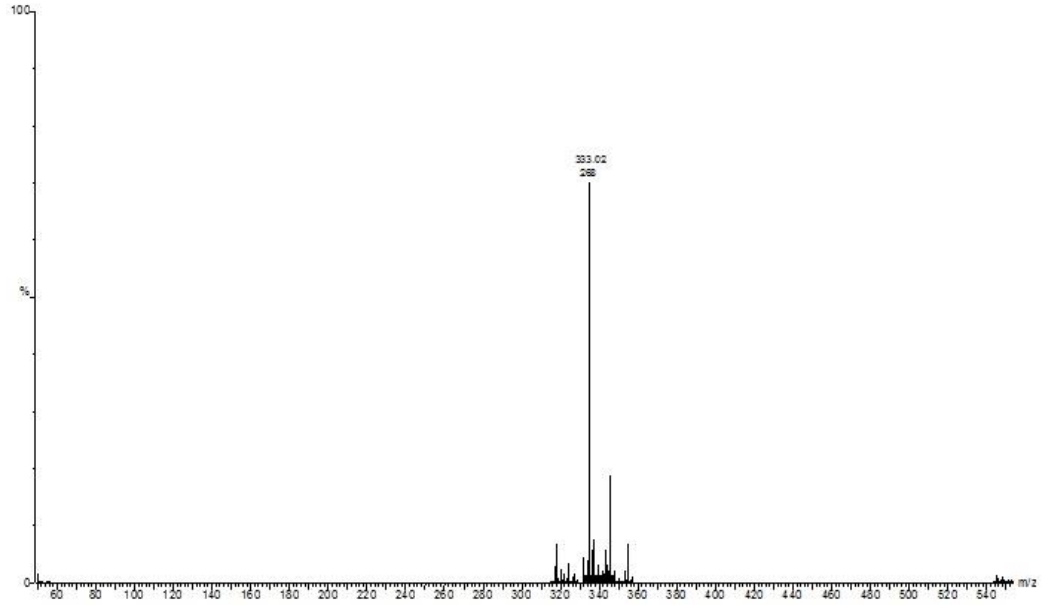

Figure 6.3: LC-ESI-MS spectra of oxidation product of ofloxacin.

6.3.3. Hydroxyl ion dependence

Hydroxyl ion concentration was varied employing NaOH from 0.25 to 2.0 mol dm^{-3}at fixed concentration of [HCF] = 1.0×10^{-3} mol dm^{-3}, [OFL] = 1.0×10^{-3} mol dm^{-3} and I = 2.0 mol dm^{-3}at three temperatures viz 35ºC, 40ºC, 45ºC respectively. The rate initially increases and tends towards a limiting value with increasing concentration of hydroxide ion concentration in uncatalyzed reaction **(Figure 6.8)**. Results are given in **Tables 6.7, 6.8 and 6.9**. Similarly in case of Cu(II) catalysed reaction the hydroxyl ion concentration was varied from 0.25 to 2.0 mol dm^{-3}employing sodium hydroxide at three different concentration of OFL viz 1.0×10^{-2}, 2.0×10^{-2}, 3.0×10^{-2} mol dm^{-3} respectively and fixed concentration of [HCF] = 1.0×10^{-3} mol dm^{-3}, [OFL] = 1.0×10^{-3} mol dm^{-3} and I = 2.0 mol dm^{-3} at 40 ºC. First order rate constants (k_c) increases with increasing concentration of hydroxyl ion **(Figure 6.9)**. Results are given in **Tables 6.10, 6.11, 6.12.**

6.3.4. [Cu(II)] ion dependence

The effect of copper(II) ion on rate of reaction studied by concentration of copper sulphate varied from 0.25×10^{-3} to 2.0×10^{-3} mol dm^{-3}at three different concentration of OFL viz. 1.0×10^{-2}, 2.0×10^{-2}, 3.0×10^{-2} mol dm^{-3} respectively and fixed concentration of [HCF] = 1.0×10^{-3} mol dm^{-3}, [OH^-] = 1.0 mol $dm^{-3}$and I = 2.0 mol dm^{-3}at 40 ºC.. The reaction rate increases with increasing concentration of Cu(II) ion. A plot of rate constant (k_c) against [Cu(II)] yields a straight line with non-zero intercept that confirms to a simultaneous uncatalyzed reaction **(Figure 6.10)**. Results are given in **Tables 6.13, 6.14, 6.15.**

6.3.5. Effect of ionic strength

Ionic strength in the reaction was varied employing sodium nitrite from 0.25 to 2.0 mol dm^{-3}at fixed concentration of [HCF] = 1.0×10^{-3} mol dm^{-3}, [OFL] = 1.0×10^{-3} mol dm^{-3} and [OH^-] = 1.0mol dm^{-3}at 40 ºC for uncatalyzed reaction and at 1.0×10^{-3}mol dm^{-3}concentration of Cu(II) for catalyzed reaction. For uncatalyzed reaction increase in ionic strength increases the rate of reaction indicating the reaction between two ions of similar charges. However the effect of

ionic strength did not exhibit in catalyzed reaction. Results are given in **Tables 6.16, 6.17.**

6.3.6. Effect of initially added product

The initially added products hexacyanoferrate(II) was studied in the range of 1.0×10^{-4} to10.0×10^{-4} mol dm^{-3} at fixed concentration of [HCF] = 1.0×10^{-3} mol dm^{-3}, [OFL] = 1.0×10^{-3} mol dm^{-3} and [OH^-] = 1.0 mol dm^{-3}at 40 ºC for uncatalyzed reaction and at 1.0×10^{-3} mol dm^{-3}concentration of Cu(II) for catalyzed reaction, the rate of reaction was unaffected in uncatalyzed as well as catalysed reaction. Results are given in **Tables 6.18, 6.19.**

6.3.7. Test for free radicals

The possible intervention of free radicals during the oxidation reactions was examined by a polymerization test. A known quantity of acrylonitrile had been added in the reaction mixture. After 2 hours diluting the reaction mixture with methanol, a white ppt was formed, indicating the intervention of free radicals in the reaction. The same experiment was repeated in the absence of OFL under similar conditions, the test was negative. This confirms that the reaction was routed through free radical pathway [20].

TABLE: 6.1

VARIATION OF HEXACYANOFERRATE(III)

[OFL] = 1.0 x 10^{-2}mol dm^{-3} **Temp. = 40°C**

[OH^-] = 1.0 mol dm^{-3} **I = 2.0mol dm^{-3}**

10^4 [HCF(III)], mol dm^{-3}	**1.0**	**2.5**	**5.0**	**7.5**	**10.0**
Time in minutes			**Absorbance**		
0	0.151	0.302	0.561	0.840	1.134
4	0.115	0.229	0.427	0.640	0.861
8	0.088	0.176	0.325	0.487	0.653
12	0.067	0.134	0.248	0.370	0.496
16	0.052	0.103	0.189	0.282	0.376
20	0.039	0.079	0.144	0.214	0.285
24	0.030	0.060	0.110	0.163	0.216
$10^4(k_{un})$, sec^{-1}	**11.13**	**11.16**	**11.32**	**11.40**	**11.51**

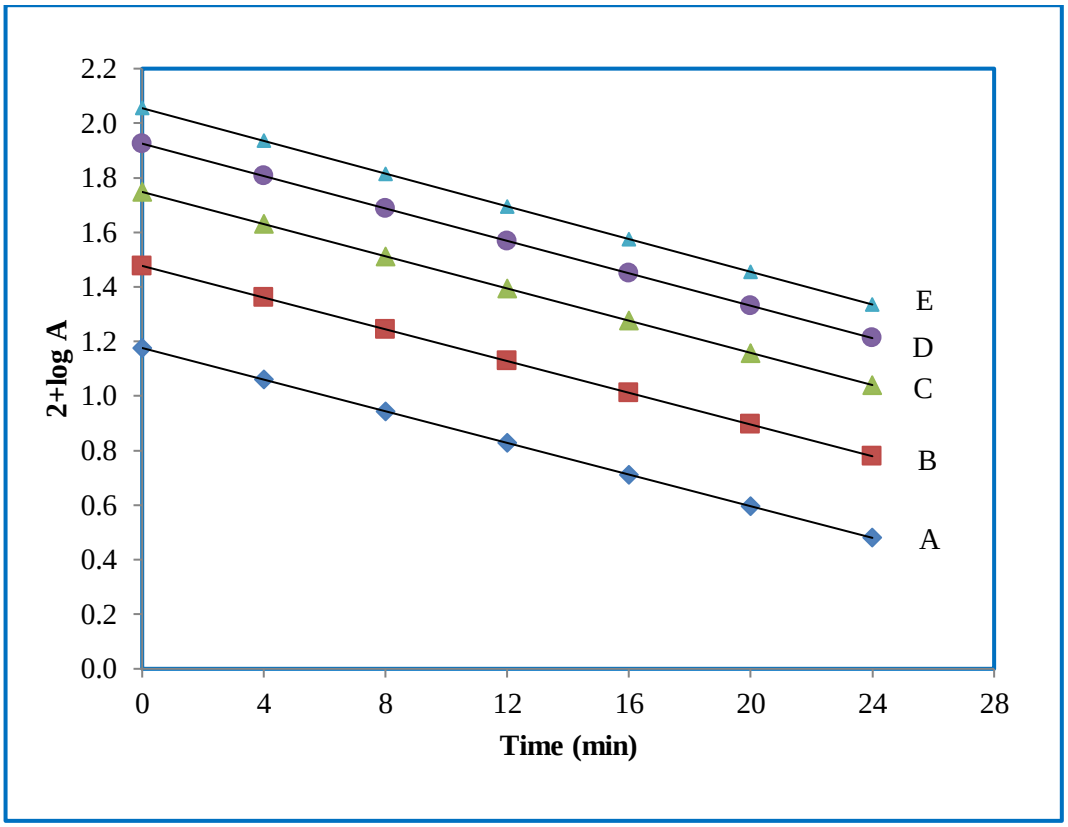

Figure 6.4: First order plots of the variation of hexacyanoferrate(III) concentration.

[OFL] = 1.0×10^{-2} mol dm^{-3}; [OH^-] = 1.0 mol dm^{-3};

I = 2.0 mol dm^{-3}; Temp. = 40°C;

[HCF(III)] = (A) 1.0×10^{-4} mol dm^{-3} (B) 2.5×10^{-4} mol dm^{-3}

(C) 5.0×10^{-4} mol dm^{-3} (D) 7.5×10^{-4} mol dm^{-3}

(E) 10.0×10^{-4} mol dm^{-3}.

(Ref. Table 6.1)

TABLE: 6.2
VARIATION OF HEXACYANOFERRATE(III)

[OFL] = 1.0 x 10^{-2}mol dm^{-3} **Temp. = 40°C**
[OH^-] = 1.0 mol dm^{-3} **I = 2.0 mol dm^{-3}**
[Cu] = 1.0 x 10^{-3} mol dm^{-3}

10^4[HCF(III)], mol dm^{-3}	**1.0**	**2.5**	**5.0**	**7.5**	**10.0**
Time in minutes			**Absorbance**		
0	0.152	0.302	0.559	0.840	1.134
2	0.115	0.230	0.430	0.646	0.871
4	0.088	0.176	0.330	0.496	0.668
6	0.068	0.135	0.253	0.380	0.513
8	0.052	0.104	0.194	0.292	0.394
10	0.040	0.080	0.149	0.224	0.302
12	0.031	0.061	0.114	0.172	0.232
14	0.024	0.047	0.088	0.132	0.178
10^4 (k_{cat}), sec^{-1}	**21.99**	**21.10**	**22.07**	**22.05**	**22.07**

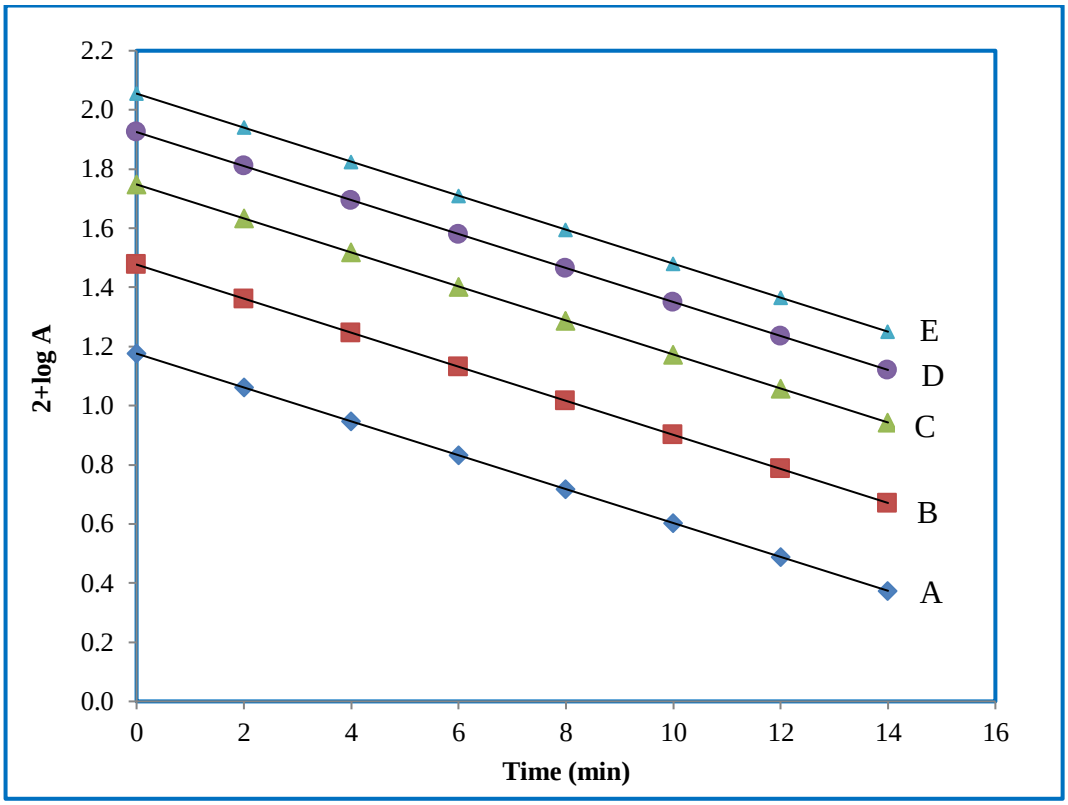

Figure 6.5: First order plots of the variation of hexacyanoferrate(III) concentration.

[OFL] = 1.0×10^{-2} mol dm^{-3}; [OH^-] = 1.0 mol dm^{-3};

[Cu(II)] = 1.0×10^{-3} mol dm^{-3}; I = 2.0 mol dm^{-3};

Temp. = 40ºC;

[HCF(III)] = (A) 1.0×10^{-4}mol dm^{-3} (B) 2.5×10^{-4} mol dm^{-3}

(C) 5.0×10^{-4}mol dm^{-3} (D) 7.5×10^{-4} mol dm^{-3}

(E) 10.0×10^{-4} mol dm^{-3}.

(Ref. Table 6.2)

TABLE: 6.3

VARIATION OF OFLOXACIN

[HCF(III)] = 1.0 x10^{-3}mol dm^{-3} **Temp. = 40 °C**

[OH$^-$] = 1.0 mol dm^{-3} **I = 2.0 mol dm^{-3}**

10^2 [OFL], mol dm^{-3}	**0.5**	**0.75**	**1.0**	**2.0**	**3.0**	**4.0**	**5.0**
Time in minutes				**Absorbance**			
0	1.135	1.134	(0)1.135	(0)1.136	(0)1.134	1.135	1.136
1	(7)0.869	(6)0.835	(4)0.861	(2)0.879	(2)0.784	0.889	0.831
2	(14)0.666	(12)0.614	(8)0.653	(4)0.680	(4)0.541	0.696	0.608
3	(21)0.510	(18)0.451	(12)0.496	(6)0.526	(6)0.374	0.545	0.445
4	(28)0.391	(24)0.332	(16)0.376	(8)0.407	(8)0.258	0.427	0.326
5	(35)0.299	(30)0.244	(20)0.285	(10)0.315	(10)0.178	0.335	0.239
6	(42)0.222	(36)0.199	(24)0.216	(12)0.235	(12)0.123	0.262	0.175
10^4 (k_{un}), sec^{-1}	**6.35**	**8.54**	**11.51**	**21.35**	**30.85**	**40.73**	**52.00**

Figures in parentheses denote time in minutes.

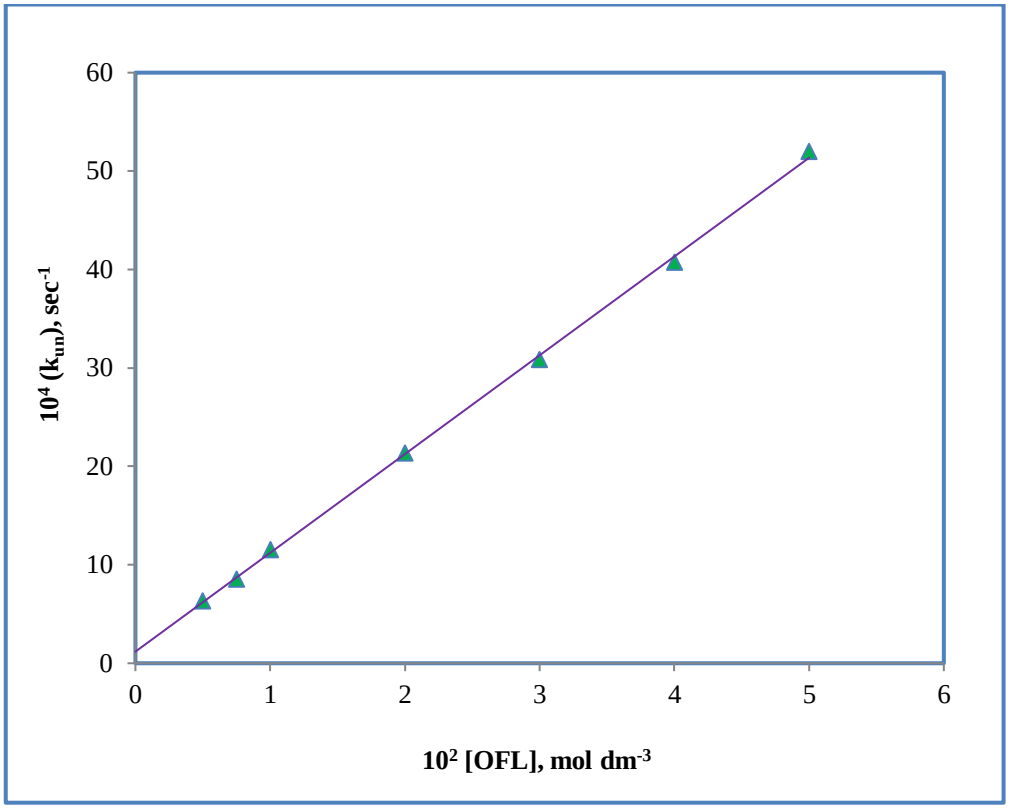

Figure 6.6: Variation of ofloxacin.

[HCF(III)] = 1.0×10^{-3} mol dm^{-3}; [OH^-] = 1.0 mol dm^{-3};

I = 2.0 mol dm^{-3}; Temp. = 40 °C

(Ref. Table: 6.3)

TABLE: 6.4
VARIATION OF OFLOXACIN

[HCF(III)] = 1.0 x 10^{-3}mol dm^{-3} **Temp. = 40°C**
[OH^-] = 0.5 mol dm^{-3} **I = 2.0 mol dm^{-3}**
[Cu] = 1.0 x 10^{-3} mol dm^{-3}

10^2 [OFL], mol dm^{-3}	**0.5**	**0.75**	**1.0**	**2.0**	**3.0**	**4.0**	**5.0**
Time in minutes				**Absorbance**			
0	(0)1.135	(0)1.134	(0)1.135	(0)1.136	1.132	1.133	1.135
1	(5)0.854	(4)0.847	(3)0.849	(2)0.817	0.904	0.897	0.889
2	(10)0.642	(8)0.632	(6)0.636	(4)0.588	0.720	0.710	0.705
3	(15)0.483	(12)0.472	(9)0.476	(6)0.423	0.574	0.529	0.507
4	(20)0.363	(16)0.352	(12)0.356	(8)0.305	0.457	0.410	0.387
5	(25)0.273	(20)0.263	(15)0.267	(10)0.219	0.364	0.318	0.296
6	(30)0.205	(24)0.196	(18)0.199	(12)0.158	0.290	0.247	0.226
10^4 (k_{cat}), sec^{-1}	**9.50**	**12.2**	**16.1**	**27.4**	**37.9**	**42.2**	**44.8**

Figures in parentheses denote time in minutes.

TABLE: 6.5
VARIATION OF OFLOXACIN

[HCF(III)] = 1.0 x 10^{-3}mol dm^{-3} **Temp. = 40°C**
[OH^-] = 1.0 mol dm^{-3} **I = 2.0 mol dm^{-3}**
[Cu] = 1.0 x 10^{-3} mol dm^{-3}

10^2 [OFL], mol dm^{-3}	**0.5**	**0.75**	**1.0**	**2.0**	**3.0**	**4.0**	**5.0**
Time in minutes				**Absorbance**			
0	(0)1.134	(0)1.135	(0)1.136	1.132	1.135	1.134	1.135
1	(4)0.823	(3)0.818	(2)0.871	0.905	0.899	0.892	0.885
2	(8)0.597	(6)0.589	(4)0.668	0.721	0.705	0.675	0.660
3	(12)0.433	(9)0.425	(6)0.513	0.575	0.464	0.412	0.405
4	(16)0.314	(12)0.306	(8)0.394	0.458	0.344	0.294	0.288
5	(20)0.227	(15)0.221	(10)0.302	0.0.365	0.256	00.210	0.204
6	(24)0.165	(18)0.159	(12)0.232	0.291	0.190	0.150	0.145
10^4 (k_{cat}), sec^{-1}	**13.4**	**18.2**	**22.1**	**37.8**	**49.7**	**56.3**	**57.2**

Figures in parentheses denote time in minutes.

TABLE: 6.6

VARIATION OF OFLOXACIN

[HCF(III)] = 1.0 x 10^{-3} mol dm^{-3} **Temp. = 40 °C**

[OH^-] = 1.5 mol dm^{-3} **I = 2.0 mol dm^{-3}**

[Cu] = 1.0 x 10^{-3} mol dm^{-3}

10^2 [OFL], mol dm^{-3}	**0.5**	**0.75**	**1.0**	**2.0**	**3.0**	**4.0**	**5.0**
Time in minutes				**Absorbance**			
0	(0)1.135	(0)1.136	(0)1.134	1.135	1.134	1.136	1.135
1	(3)0.848	(2)0.866	(2)0.817	0.868	0.849	0.829	0.802
2	(6)0.633	(4)0.661	(4)0.588	0.663	0.576	0.536	0.528
3	(9)0.473	(6)0.505	(6)0.423	0.507	0.411	0.368	0.360
4	(12)0.354	(8)0.386	(8)0.305	0.387	0.293	0.253	0.246
5	(15)0.264	(10).294	(10)219	0.296	0.208	0.174	0.167
6	(18)0.197	(12)0.225	(12)0.158	0.226	0.149	0.119	0.114
10^4 (k_{cat}), sec^{-1}	**16.2**	**22.5**	**27.4**	**44.8**	**56.5**	**62.6**	**63.8**

Figures in parentheses denote time in minutes.

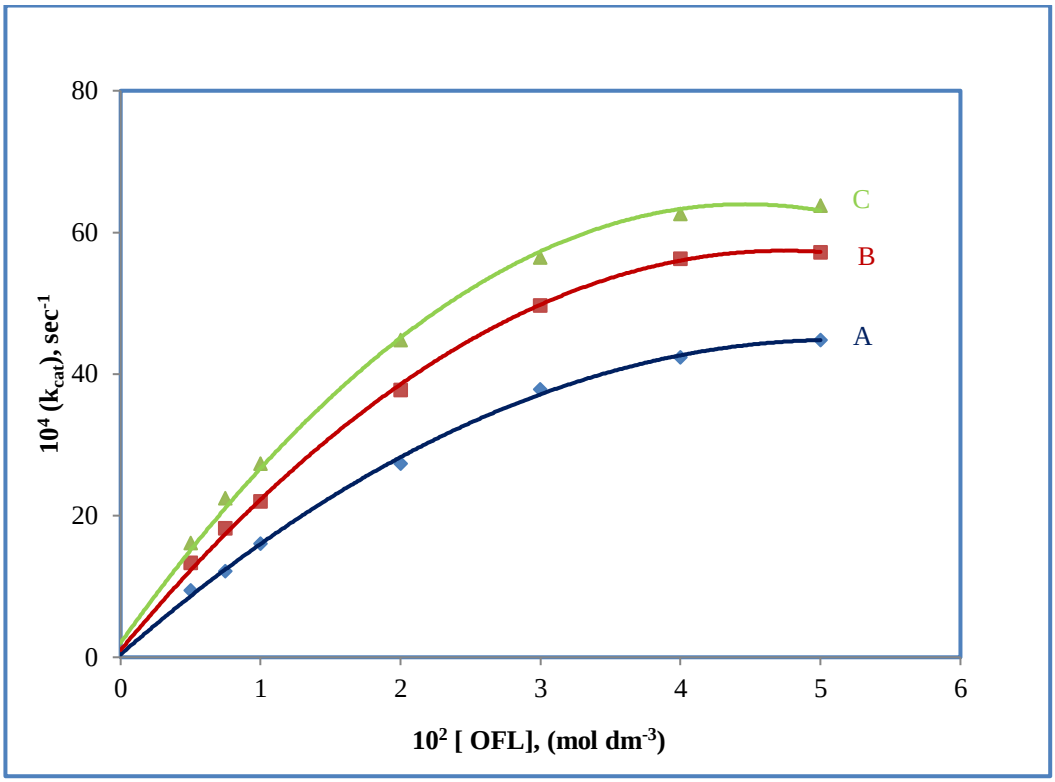

Figure 6.7: Variation of ofloxacin at different concentration of hydroxyl ion (A) 0.5mol dm^{-3}, (B) 1.0 mol dm^{-3}, (C) 1.5 mol dm^{-3}.

[HCF(III)] = 1.0×10^{-3} mol dm^{-3}; [Cu(II)] = 1.0×10^{-3} mol dm^{-3};

I = 2.0 mol dm^{-3}; Temp. = 40 ºC.

(Ref. Table: 6.4, 6.5, 6.6)

TABLE: 6.7
VARIATION OF HYDROXYL ION

[HCF(III)] = 1.0 x 10^{-3} mol dm^{-3} **Temp. = 35°C**
[OFL] = 1.0 x 10^{-2} mol dm^{-3} **I = 2.0 mol dm^{-3}**

$[OH^-]$, mol dm^{-3}	**0.25**	**0.5**	**0.75**	**1.0**	**1.25**	**1.5**	**1.75**	**2.0**
Time in minutes					**Absorbance**			
0	(0)1.135	(0)1.134	(0)1.134	(0)1.136	(0)1.135	1.134	1.135	1.136
4	(20)0.846	(10).866	(7)0.869	(6)0.856	(5)0.860	0.885	0.872	0.860
8	(40)0.630	(20)0.661	(14)0.666	(12)0.645	(10)0.651	0.690	0.669	0.651
12	(60)0.470	(30)0.505	(21)0.510	(18)0.486	(15)0.493	0.538	0.514	0.493
16	(80)0.350	(40)0.386	(28)0.391	(24)0.367	(20)0.374	0.420	0.395	0.374
20	(100)0.261	(50)0.294	(35)0.299	(30)0.276	(25)0.283	0.327	0.303	0.283
24	(120)0.195	(60)0.225	(42)0.223	(36)0.217	(30).225	0.240	0.233	0.215
$10^4(k_{un})$, sec^{-1}	**2.45**	**4.50**	**6.35**	**7.85**	**9.26**	**10.36**	**11.01**	**11.57**

Figures in parentheses denote time in minutes.

TABLE: 6.8
VARIATION OF HYDROXYL ION

[[HCF(III)] = 1.0 x 10^{-3} mol dm^{-3} **Temp. = 40°C**
[OFL] = 1.0 x 10^{-2} mol dm^{-3} **I = 2.0 mol dm^{-3}**

$[OH^-]$,mol dm^{-3}	**0.25**	**0.50**	**0.75**	**1.00**	**1.25**	**1.50**	**1.75**	**2.00**
Time in minutes	**Absorbance**							
0	(0)1.135	(0)1.135	(0)1.134	(0)1.136	(0)1.135	1.135	1.134	1.136
2	(12)0.851	(7)0.861	(5)0.860	(4)0.861	(3)0.881	0.938	0.923	0.923
4	(24)0.638	(14)0.653	(10)0.652	(8)0.653	(6)0.685	0.776	0.759	0.751
6	(36)0.478	(21)0.495	(15)0.494	(12)0.496	(9)0.532	0.642	0.621	0.611
8	(48)0.359	(28)0.376	(20)0.375	(16)0.376	(12)0.413	0.530	0.508	0.497
10	(60)0.269	(35)0.285	(25)0.284	(20)0.285	(15)0.321	0.439	0.415	0.404
12	(72)0.202	(42)0.216	(30)0.215	(24)0.216	(18)0.249	0.363	0.339	0.329
$10^4(k_{un})$, sec^{-1}	**4.01**	**6.58**	**9.24**	**11.51**	**14.05**	**15.85**	**16.77**	**17.20**

Figures in parentheses denote time in minutes.

TABLE: 6.9
VARIATION OF HYDROXYL ION

[HCF(III)] = 1.0 x 10^{-3} mol dm^{-3} **Temp. = 45°C**
[OFL] = 1.0 x 10^{-2} mol dm^{-3} **I = 2.0 mol dm^{-3}**

$[OH^-]$,mol dm^{-3}	**0.25**	**0.5**	**0.75**	**1.0**	**1.25**	**1.5**	**1.75**	**2.0**
Time in minutes	**Absorbance**							
0	(0)1.135	(0)1.134	(0)1.1.35	(0)1.136	1.135	1.135	1.135	1.135
2	(7)0.866	(4)0.866	(3)0.863	(3)0.810	0.879	0.860	0.846	0.838
4	(14)0.660	(8)0.661	(6)0.656	(6)0.578	0.680	0.652	0.631	0.618
6	(21)0.504	(12)0.505	(9)0.498	(9)0.412	0.527	0.494	0.471	0.456
8	(28)0.384	(16)0.386	(12)0.379	(12)0.294	0.408	0.374	0.351	0.337
10	(35)0.293	(20)0.294	(15)0.288	(15)0.210	0.316	0.284	0.262	0.249
12	(42)0.223	(24)0.225	(18)0.219	(18)0.150	0.245	0.215	0.195	0.183
$10^4(k_{un})$, sec^{-1}	**6.45**	**11.25**	**15.25**	**18.75**	**21.32**	**23.11**	**24.46**	**25.32**

Figures in parentheses denote time in minutes.

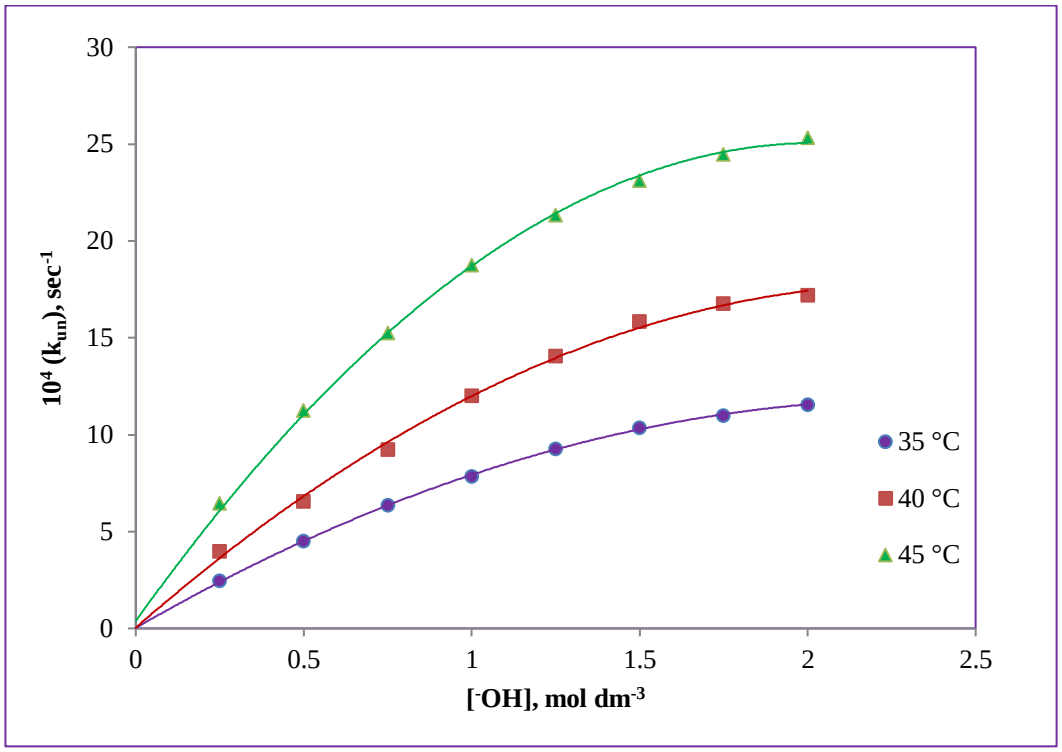

Figure 6.8: Variation of hydroxyl ion at different temperature.

[HCF] = 1.0×10^{-3} mol dm^{-3}; [OFL] = 1.0×10^{-2} mol dm^{-3};

[Cu(II)] = 1.0×10^{-3} mol dm^{-3}; I = 2.0 mol dm^{-3}.

(Ref. Table: 6.7, 6.8, 6.9)

TABLE: 6.10
VARIATION OF HYDROXYL ION

[HCF(III)] = 1.0 x 10^{-3} mol dm^{-3} **Temp. = 40°C**
[OFL] = 1.0 x 10^{-2} mol dm^{-3} **I = 2.0 mol dm^{-3}**
[Cu] = 1.0 x 10^{-3} mol dm^{-3}

[OH^-],mol dm^{-3}	**0**	**0.5**	**0.75**	**1.0**	**1.25**	**1.5**	**1.75**	**2.0**
Time in minutes	**Absorbance**							
0	(0)1.135	(0)1.137	(0)1.132	1.134	1.135	1.133	(0)1.136	(0)1.135
2	(5)0.848	(3)0.860	(3)0.814	0.871	0.840	0.817	(1)0.944	(1)0.922
4	(10)0.634	(6)0.652	(6)0.583	0.668	0.621	0.588	(2)0.784	(2)0.749
6	(15)0.474	(9)0.494	(9)0.418	0.513	0.460	0.423	(3)0.652	(3)0.608
8	(20).354	(12)0.375	(12)0.300	0.394	0.340	0.305	(4)0.542	(4)0.494
10	(25)0.265	(15)0.284	(15)0.215	0.302	0.252	0.219	(5)0.451	(5)0.401
12	(30)0.198	(18)0.215	(18)0.154	0.232	0.186	0.158	(6)0.375	(6)0.326
$10^4(k_{cat})$, sec^{-1}	**9.7**	**15.4**	**18.5**	**22.07**	**25.1**	**27.4**	**30.8**	**34.7**

Figures in parentheses denote time in minutes.

TABLE: 6.11
VARIATION OF HYDROXYL ION

[HCF(III)] = 1.0 x 10^{-3}mol dm^{-3} **Temp. = 40°C**
[OFL] = 2.0 x 10^{-2} mol dm^{-3} **I = 2.0 mol dm^{-3}**
[Cu] = 1.0 x 10^{-3} mol dm^{-3}

[OH^-], mol dm^{-3}	**0**	**0.5**	**0.75**	**1.0**	**1.25**	**1.5**	**1.75**	**2.0**
Time in minutes				**Absorbance**				
0	(0)1.135	(0)1.137	1.132	1.134	1.135	1.133	1.136	1.135
2	(4)0.851	(3)0.812	0.864	0.826	0.944	0.924	0.906	0.884
4	(8)0.638	(6)0.581	0.658	0.601	0.784	0.752	0.723	0.688
6	(12)0.478	(9)0.416	0.501	0.437	0.652	0.612	0.577	0.536
8	(16)0.359	(12)0.297	0.382	0.318	0.542	0.498	0.460	0.417
10	(20)0.269	(15)0.213	0.291	0.232	0.451	0.406	0.367	0.325
12	(24)0.202	(18)0.152	0.221	0.168	0.375	0.330	0.293	0.253
$10^4(k_{cat})$, sec^{-1}	**12.0**	**18.6**	**22.7**	**26.5**	**30.8**	**34.3**	**37.6**	**41.7**

Figures in parentheses denote time in minutes.

TABLE: 6.12
VARIATION OF HYDROXYL ION

[HCF(III)] = 1.0 x 10^{-3}mol dm^{-3} **Temp. = 40°C**
[OFL] = 3.0 x 10^{-2} mol dm^{-3} **I = 2.0 mol dm^{-3}**
[Cu] = 1.0 x 10^{-3} mol dm^{-3}

$[OH^-]$,mol dm^{-3}	**0**	**0.5**	**0.75**	**1.0**	**1.25**	**1.5**	**1.75**	**2.0**
Time in minutes					**Absorbance**			
0	(0)1.135	(0)1.137	(0)1.132	1.134	1.135	1.133	1.136	1.135
1	(3)0.857	(2)0.837	(2)0.779	0.917	0.900	0.869	0.843	0.821
2	(6)0.647	(4)0.617	(4)0.534	0.740	0.713	0.665	0.627	0.594
3	(9)0.489	(6)0.455	(6)0.367	0.598	0.566	0.509	0.466	0.429
4	(12)0.369	(8)0.335	(8)0.251	0.483	0.448	0.389	0.346	0.311
5	(15)0.279	(10)0.247	(10)0.173	0.390	0.356	0.298	0.257	0.225
6	(18)0.211	(12)0.182	(12)0.118	0.315	0.282	0.228	0.191	0.163
$10^4(k_{cat})$, sec^{-1}	**15.6**	**25.4**	**31.4**	**35.6**	**38.7**	**44.6**	**49.5**	**54.0**

Figures in parentheses denote time in minutes.

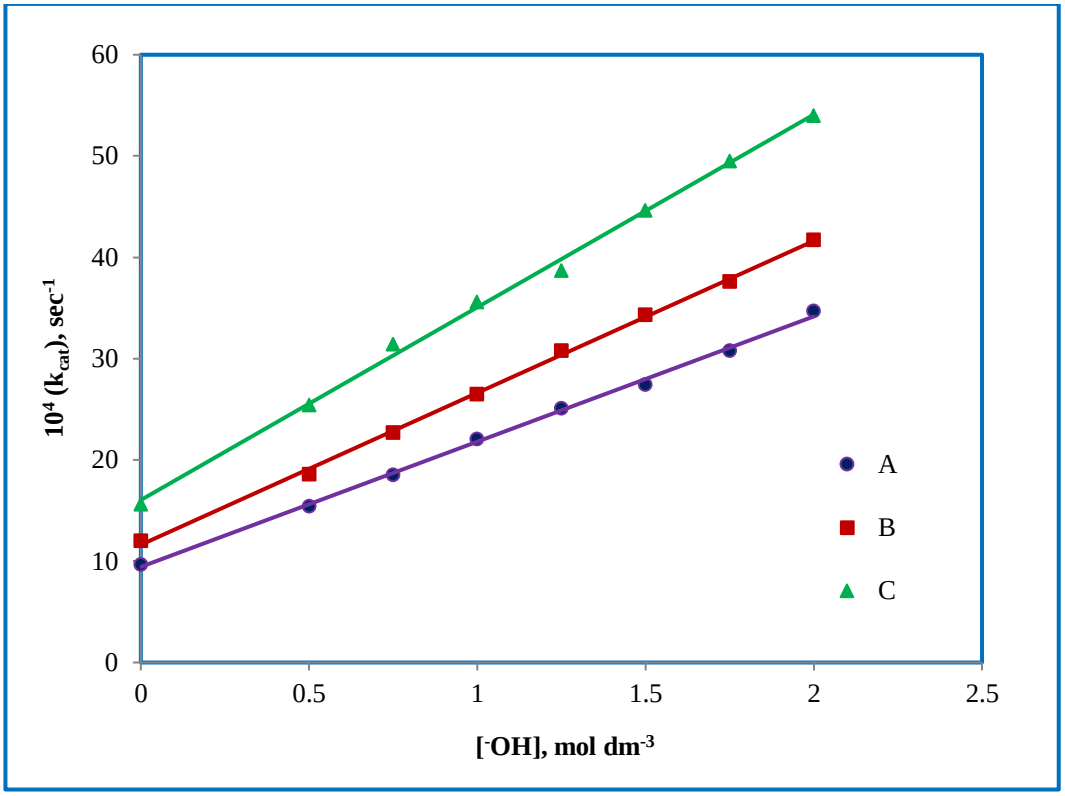

Figure 6.9: Variation of hydroxyl ion at different ofloxacin concentration (A) 1.0 × 10^{-2}; (B) 2.0 × 10^{-2}; (C) 3.0 × 10^{-2}/mol dm^{-3}.

[HCF] = 1.0 × 10^{-3} mol dm^{-3}; [Cu(II)] = 1.0 × 10^{-3}mol dm^{-3};

I = 2.0 mol dm^{-3}; Temp. = 40 ºC.

(Ref. Table: 6.10, 6.11, 6.12)

TABLE: 6.13

VARIATION OF Cu(II) ION

[HCF(III)] = 1.0 x 10^{-3} mol dm^{-3} **Temp. = 40°C**

[OFL] = 1.0 x 10^{-2} mol dm^{-3} **I = 2.0 mol dm^{-3}**

[OH^-] = 1.0 mol dm^{-3}

10^3 [Cu(II)], mol dm^{-3}	**0**	**0.25**	**0.5**	**0.75**	**1.0**	**1.25**	**1.5**	**1.75**	**2.0**
Time in minutes	**Absorbance**								
0	(0)1.135	(0)1.135	(0)1.135	1.135	1.135	1.135	1.135	(0)1.135	(0)1.135
2	(5)0.855	(3)0.865	(3)0.887	0.895	0.871	0.849	0.833	(1)0.962	(1)0.951
4	(10)0.520	(6)0.661	(6)0.611	0.706	0.668	0.635	0.611	(2)0.815	(2)0.797
6	(15)0.367	(9)0.590	(9)0.464	0.557	0.513	0.475	0.448	(3)0.691	(3)0.667
8	(20)0.239	(12)0.386	(12)0.329	0.439	0.394	0.355	0.329	(4)0.585	(4)0.559
10	(25)0.167	(15)0.385	(15)0.281	0.346	0.302	0.266	0.241	(5)0.496	(5)0.468
12	(30)0.109	(18)0.225	(18)0.177	0.273	0.232	0.199	0.177	(6)0.420	(6)0.393
10^4 (k_{cat}), sec^{-1}	**13.0**	**15.2**	**17.3**	**19.8**	**22.0**	**24.2**	**25.8**	**27.6**	**29.5**

Figures in parentheses denote time in minutes.

TABLE: 6.14
VARIATION OF Cu(II) ION

[HCF(III)] = 1.0 x 10^{-3} mol dm^{-3} **Temp. = 40°C**
[OFL] = 2.0 x 10^{-2} mol dm^{-3} **I = 2.0 mol dm^{-3}**
[OH^-] = 1.0 mol dm^{-3}

10^3 [Cu(II)], mol dm^{-3}	**0**	**0.25**	**0.5**	**0.75**	**1.0**	**1.25**	**1.5**	**1.75**	**2.0**
Time in minutes					**Absorbance**				
0	(0)1.138	(0)1.135	1.133	1.135	1.137	1.134	(0)1.135	(0)1.132	1.135
2	(3)0.878	(3)0.852	0.888	0.861	0.831	0.806	(1)0.942	(1)0.927	(1)0.915
4	(6)0.661	(6)0.594	0.694	0.654	0.608	0.573	(2)0.782	(2)0.757	(2)0.737
6	(9)0.573	(9)0.322	0.543	0.496	0.445	0.407	(3)0.650	(3)0.618	(3)0.594
8	(12)0.386	(12)0.311	0.424	0.376	0.326	0.289	(4)0.539	(4)0.504	(4)0.478
10	(15)0.219	(15)0.231	0.332	0.286	0.239	0.205	(5)0.448	(5)0.412	(5)0.386
12	(18)0.225	(18)0.162	0.259	0.217	0.175	0.146	(6)0.372	(6)0.336	(6)0.311
10^4 (k_{cat}), sec^{-1}	**15.0**	**18.3**	**20.5**	**23.2**	**26.1**	**28.5**	**31.2**	**33.8**	**36.0**

Figures in parentheses denote time in minutes.

TABLE: 6.15
VARIATION OF Cu(II) ION

[HCF(III)] = 1.0 x10^{-3}mol dm^{-3} **Temp. = 40°C**
[OFL] = 3.0 x10^{-2} mol dm^{-3} **I = 2.0 mol dm^{-3}**
[OH^-] = 1.0 mol dm^{-3}

10^3 [Cu(II)], mol dm^{-3}	**0**	**0.25**	**0.5**	**0.75**	**1.0**	**1.25**	**1.5**	**1.75**	**2.0**
Time in minutes					**Absorbance**				
0	(0)1.138	(0)1.135	(0)1.133	1.135	1.135	1.134	1.135	1.135	1.135
1	(3)0.821	(2)0.877	(2)0.844	0.813	0.942	0.923	0.904	0.888	0.866
2	(6)0.594	(4)0.678	(4)0.627	0.582	0.782	0.751	0.719	0.694	0.661
3	(9)0.429	(6)0.524	(6)0.467	0.417	0.649	0.611	0.573	0.543	0.505
4	(12)0.311	(8)0.405	(8)0.347	0.299	0.538	0.497	0.456	0.424	0.386
5	(15)0.225	(10)0.313	(10)0.258	0.214	0.447	0.404	0.363	0.332	0.294
6	(18)0.163	(12)0.241	(12)0.192	0.153	0.371	0.329	0.289	0.259	0.225
10^4 (k_{cat}), sec^{-1}	**18.1**	**21.5**	**24.7**	**27.8**	**31.1**	**34.4**	**38.2**	**40.9**	**45.0**

Figures in parentheses denote time in minutes.

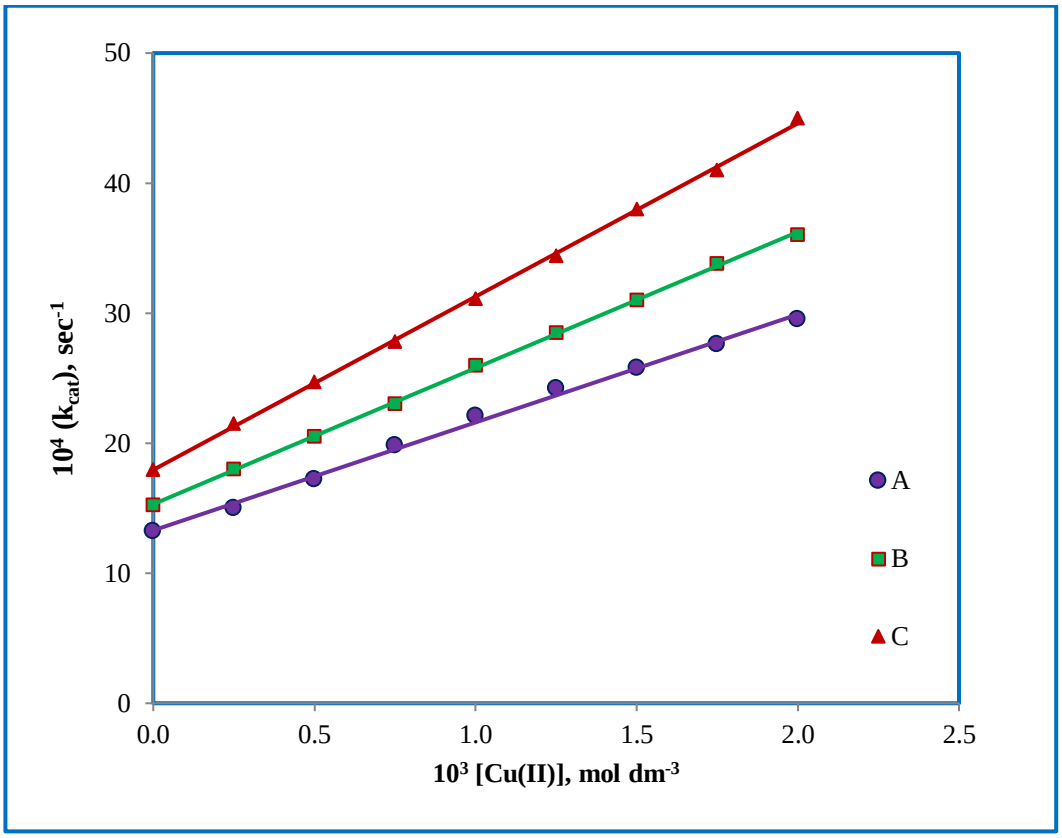

Figure 6.10: Variation of copper ion at different ofloxacin concentration (A) 1.0 × 10^{-2}; (B) 2.0 × 10^{-2}; (C) 3.0 × 10^{-2}/mol dm^{-3}.

[HCF] = 1.0 × 10^{-3} mol dm^{-3}; I = 2.0 mol dm^{-3};

[OH^-] = 1.0 mol dm^{-3}; Temp. = 40 ºC.

(Ref. Table: 6.13, 6.14, 6.15)

TABLE: 6.16

VARIATION OF SODIUM NITRATE

[HCF(III)] = 1.0 x 10^{-3}mol dm^{-3} **Temp. = 40°C**

[OFL] = 1.0 x 10^{-2} mol dm^{-3} **[OH^-] = 1.0 mol dm^{-3}**

[$NaNO_3$], mol dm^{-3}	**0.25**	**0.5**	**0.75**	**1.0**	**1.25**	**1.5**	**1.75**	**2.0**
Time in minutes				**Absorbance**				
0	1.133	1.136	1.134	1.135	1.133	1.136	1.135	1.134
4	0.859	0.862	0.860	0.861	0.863	0.859	0.861	0.860
8	0.652	0.654	0.652	0.653	0.652	0.652	0.653	0.652
12	0.494	0.497	0.495	0.496	0.496	0.494	0.496	0.495
16	0.373	0.377	0.375	0.376	0.375	0.373	0.376	0.375
20	0.282	0.286	0.284	0.285	0.287	0.282	0.285	0.284
24	0.212	0.217	0.215	0.216	0.214	0.212	0.216	0.215
10^4 (k_{un}), sec^{-1}	**11.49**	**11.52**	**11.50**	**11.51**	**11.52**	**11.49**	**11.51**	**11.50**

TABLE: 6.17
VARIATION OF SODIUM NITRATE

[HCF(III)] = 1.0 x 10^{-3}mol dm^{-3} **Temp. = 40°C**
[OFL] = 1.0 x 10^{-2} mol dm^{-3} **[OH^-] = 1.0 mol dm^{-3}**
[Cu(II)] =1.0 x 10^{-3} mol dm^{-3}

[$NaNO_3$], mol dm^{-3}	**0.25**	**0.5**	**0.75**	**1.0**	**1.25**	**1.5**	**1.75**	**2.0**
Time in minutes				**Absorbance**				
0	1.135	1.136	1.134	1.133	1.135	1.137	1.134	1.134
2	0.871	0.869	0.872	0.871	0.868	0.872	0.871	0.872
4	0.668	0.665	0.667	0.668	0.669	0.667	0.666	0.667
6	0.513	0.511	0.515	0.513	0.513	0.515	0.513	0.515
8	0.395	0.392	0.396	0.394	0.397	0.396	0.394	0.396
10	0.302	0.300	0.305	0.302	0.306	0.305	0.302	0.305
12	0.234	0.230	0.235	0.232	0.231	0.235	0.232	0.235
14	0.175	0.177	0.180	0.178	0.176	0.180	0.177	0.180
10^4 (k_{cat}), sec^{-1}	**22.09**	**22.10**	**22.11**	**22.07**	**22.00**	**22.10**	**22.08**	**22.11**

TABLE: 6.18

EFFECT OF HCF(II) ION

[HCF(III)] = 1.0 x 10^{-3}mol dm^{-3} **Temp. = 40 °C**

[OFL] = 1.0 x 10^{-2} mol dm^{-3} **I = 2.0 mol dm^{-3}**

[OH^-] = 1.0 mol dm^{-3}

10^4 [HCF(II)]	**1.0**	**3.0**	**5.0**	**7.0**	**10.0**
Time in minutes			**Absorbance**		
0	1.135	1.136	1.134	1.133	1.135
4	0.861	0.859	0.860	0.863	0.861
8	0.653	0.652	0.652	0.652	0.653
12	0.496	0.494	0.495	0.496	0.496
16	0.376	0.373	0.375	0.375	0.376
20	0.285	0.282	0.284	0.287	0.285
24	0.216	0.212	0.215	0.214	0.216
10^4 (k_{un}), sec^{-1}	**11.51**	**11.49**	**11.50**	**11.52**	**11.51**

TABLE: 6.19
EFFECT OF HCF(II) ION

[HCF(III)] = 1.0 x 10^{-3} mol dm^{-3} **Temp. = 40 °C**
[OFL] = 1.0 x 10^{-2} mol dm^{-3} **[OH^-] = 1.0 mol dm^{-3}**
[Cu(II)] =1.0 x 10^{-3} mol dm^{-3} **I =2.0 mol dm^{-3}**

10^4 [HCF(II)]	**1.0**	**3.0**	**5.0**	**7.0**	**10.0**
Time in minutes			**Absorbance**		
0	1.133	1.136	1.135	1.134	1.134
2	0.871	0.869	0.868	0.871	0.872
4	0.668	0.665	0.669	0.666	0.667
6	0.513	0.511	0.513	0.513	0.515
8	0.394	0.392	0.397	0.394	0.396
10	0.302	0.300	0.306	0.302	0.305
12	0.232	0.230	0.231	0.232	0.235
14	0.178	0.177	0.176	0.177	0.180
10^4 (k_{cat}), sec^{-1}	**22.07**	**22.10**	**22.00**	**22.08**	**22.11**

6.4. Discussion

6.4.1. Mechanism for uncatalyzed reaction

Variation of concentration of each of the oxidant HCF(III), substrate OFL, base and ionic strength, while mainly the other concentration constant shows that the reaction is first order in oxidant, substrate and with respect to alkali in fractional order. On the basis of stoichiometric and experimental results, a reaction mechanism can be prepared for which all the observed order in each constituent i.e. [Oxidant], [substrate] and [OH^-] and ionic strength may be well accounted for. In the present investigation, alkali combines first with OFL to give anionic form of OFL, in a pre-equilibrium step. The anionic form of OFL reacts with the HCF(III) species and give a free radical in a slow step. Then free radical react with another molecule of HCF(III) to give final products, as given in scheme-1.

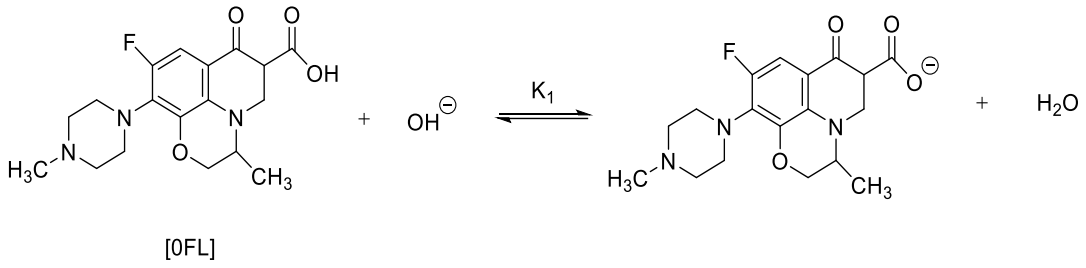

[0FL]

(6.2)

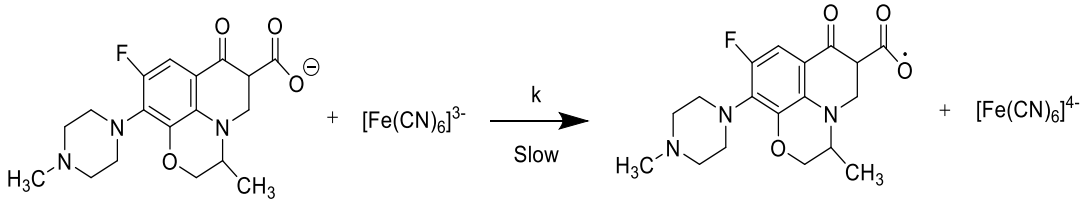

Free radical

(6.3)

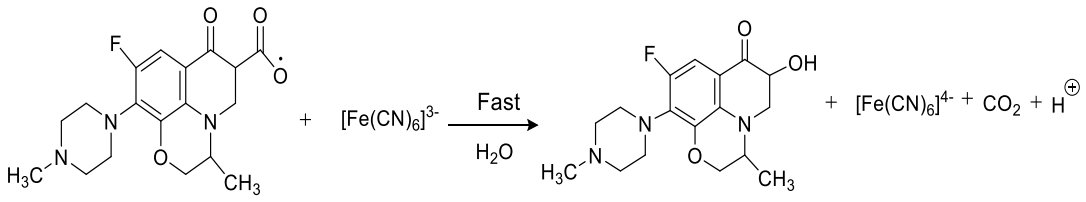

Free radical Product

(6.4)

Scheme 6.1

The proposed mechanism leads to the rate law (6.5) accounting for an experimental observations.

$$\frac{-d\left[Fe(III)\right]}{dt} = \frac{K_1 k\left[Fe(III)\right]\left[OH^-\right][OFL]}{1+K_1\left[OH^-\right]} \tag{6.5}$$

$$k_{un} = \frac{Rate}{\left[Fe(III)\right]} = \frac{K_1 k\left[OH^-\right][OFL]}{1+K_1\left[OH^-\right]} \tag{6.6}$$

$$\frac{k_{un}}{[OFL]} = k' = \frac{K_1 k\left[OH^-\right]}{1+K_1\left[OH^-\right]} \tag{6.7}$$

Rearrange the Eq. (6.7)

$$\frac{1}{k'} = \frac{1}{K_1 k\left[OH^-\right]} + \frac{1}{k} \tag{6.8}$$

Where k´ is observed second order rate constant.

A plot of 1/k´ verses 1/[OH^-] was made from the equation (6.8)at three different temperatures, that yielded at straight line with non zero intercept **(Figure 6.11)**. The intercept gives the value of slow step (k) and the ratio of intercept and gradient gives the value of K at three different temperatures.

The activation parameters of the reaction was calculated by plotting a graph between log k verses 1/T **(Figure 6.12)** and the thermodynamic quantities of the reaction are also determined by plotting a graph between log K verses 1/T **(Figure 6.13) (Table 6.20).** However energy of activation is closer to the value normally found in bimolecular reaction and entropy of activation indicates a more organized transition state.

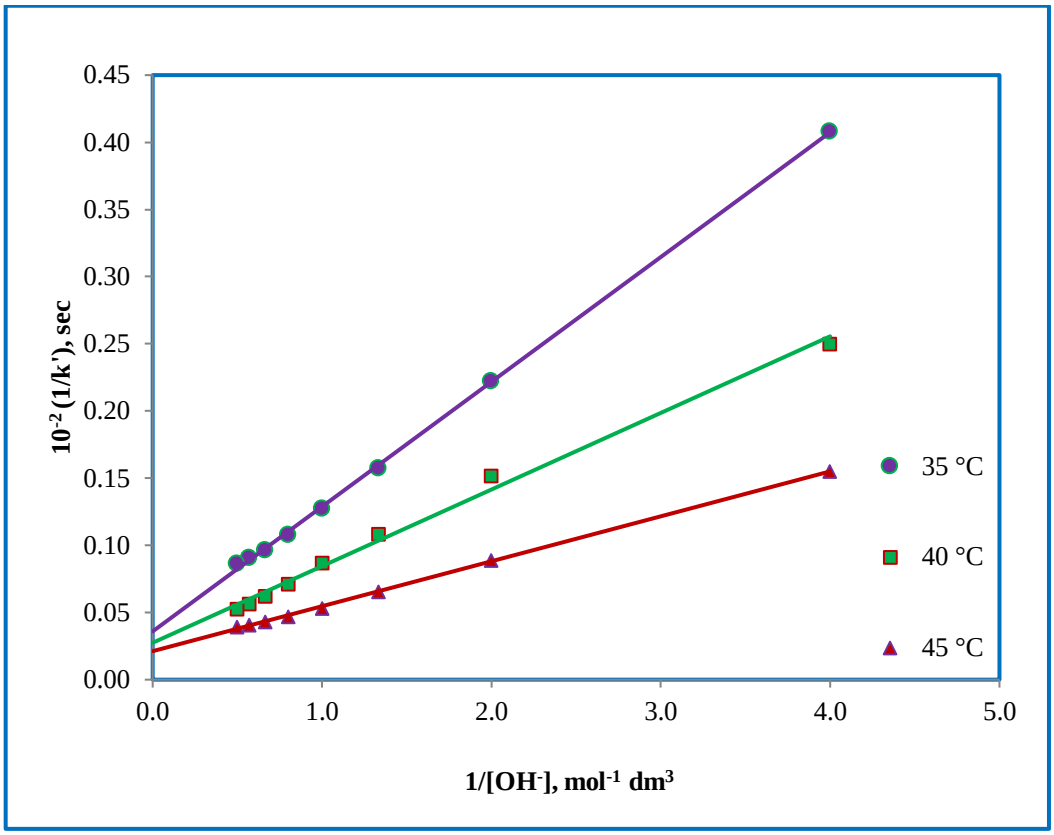

Figure 6.11: Plots of 1/k' versus 1/[OH$^-$] at different temperature.

[HCF] = 1.0 × 10^{-3}mol dm^{-3}; [OFL] = 1.0× 10^{-2} mol dm^{-3}; I = 2.0 mol dm^{-3}.

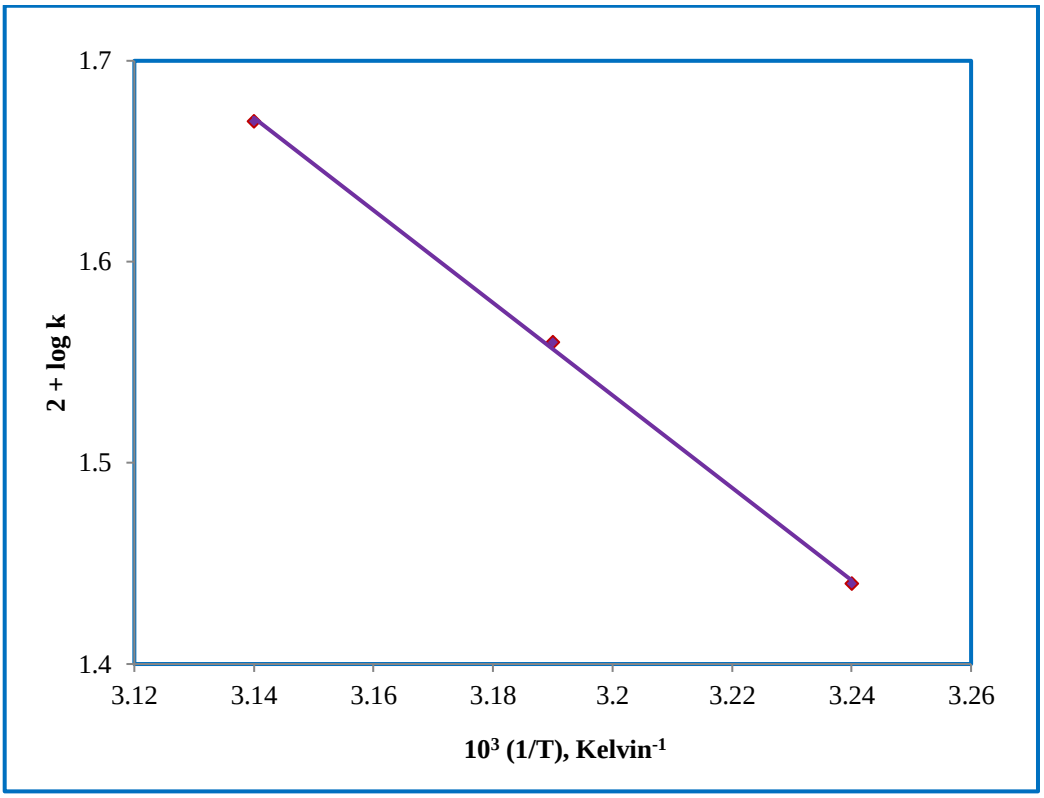

Figure 6.12: A plot of log k versus 1/T.

(Ref. Table: 6.20)

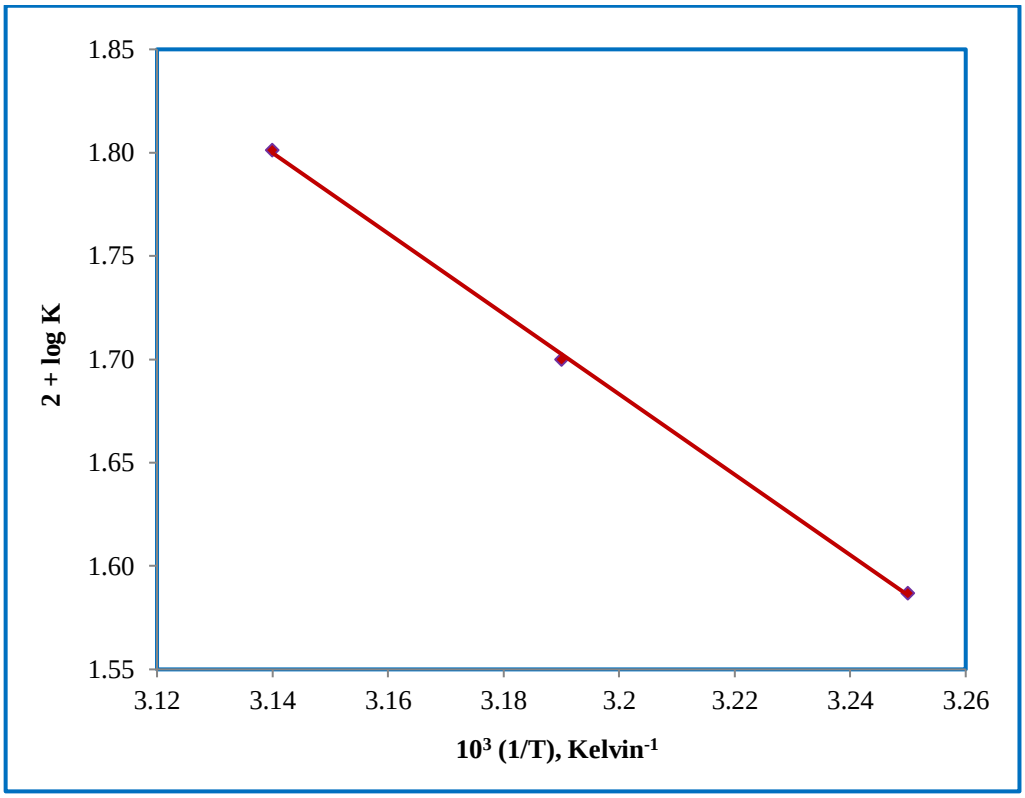

Figure 6.13: A plot of log K versus 1/T.

(Ref. Table: 6.20)

TABLE: 6.20

ACTIVATION PARAMETERS AND THERMODYNAMIC QUANTITIES EVALUATED FROM SCHEME 6.1.

Temperature (Kelvin)	**10^2 (k) (dm^3 $mol^{-1}sec^{-1}$)**	**Activation Parameters**	**10^2 (K) (dm^3 mol^{-1})**	**Thermodynamic Quantities (From K)**
308	27.86	E_a= 42.12 (kJ mol^{-1})	38.64	ΔH = 37.34 (kJ mol^{-1})
313	36.50	$\Delta H^{\#}$ = 39.42 (kJ mol^{-1})	48.07	ΔS = 118.48 (JK^{-1} mol^{-1})
318	47.17	$\Delta S^{\#}$ = – 126.95 (JK^{-1} mol^{-1})	63.28	ΔG = 2.91 (kJ mol^{-1})
		$\Delta G^{\#}$ = 79.41 (kJ mol^{-1})		

6.4.2. Mechanism for Cu(II) catalyzed reaction

Copper (II) is known to be a catalyst in many redox reactions, particularly in alkaline medium [14] and catalysis has usually been explained by assuming the intermediate complex formed by an interaction of anionic form of OFL and Cu(II). This intermediate complex reacts with the oxidant in rate determining step, since order with respect to HCF(III) and Cu(II) is one each, the order with respect to OFL is fractional. Furthermore, rate also increases with increasing concentration of hydroxyl ion. Thus a mechanism consisting of scheme 6.2 and also accounting for experimental observations can be proposed.

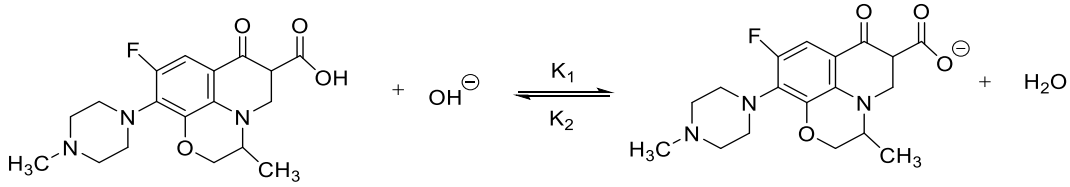

[0FL]

(6.9)

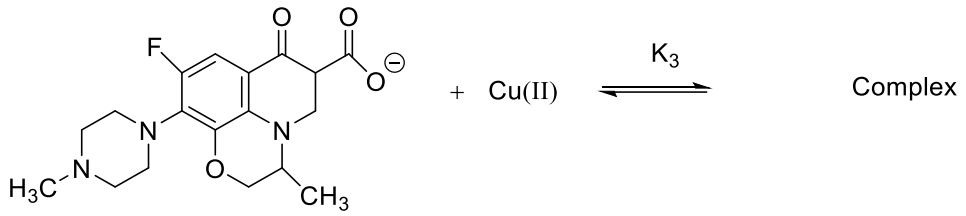

(6.10)

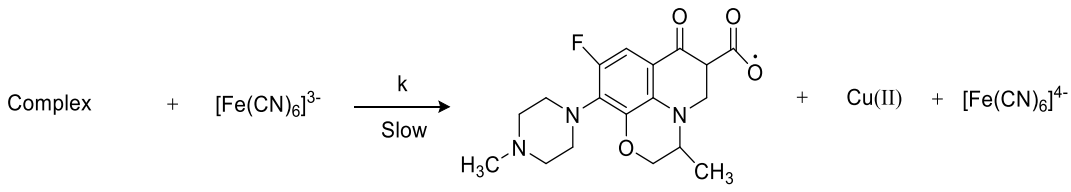

Free radical

(6.11)

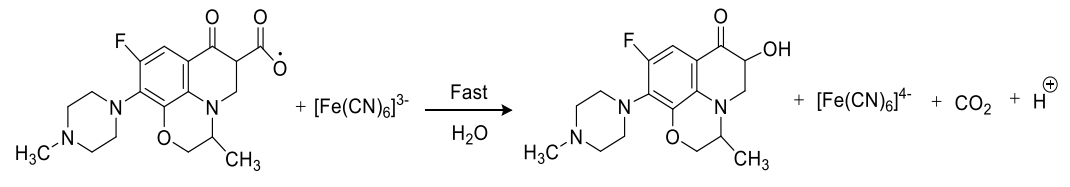

Free radical Product

(6.12)

Scheme 6.2

Following rate law can be derived from scheme 6.2:

$$\text{Rate} = \frac{-d\left[Fe(III)\right]}{dt} = \frac{K_1K_3k\left[Fe(III)\right]\left[Cu(II)\right]\left[OH^-\right][OFL]}{K_2 + K_3[OFL]} \tag{6.13}$$

$$k_c = \frac{K_1K_3k\left[Cu(II)\right]\left[OH^-\right][OFL]}{K_2 + K_3[OFL]} \tag{6.14}$$

Where k_c is observed first order rate constant for catalyzed reaction. Since effect of Cu (II) ion on the rate also indicates uncatalysed path, the rate law (6.14) accounting for this path can be written as equation (6.7)

$$k'' = k_{un} + \frac{K_1K_3k\left[Cu(II)\right]\left[OH^-\right][OFL]}{K_2 + K_3[OFL]} \tag{6.15}$$

Where k'' = k_{un} + k_c is the total observed first order rate constant.

A plot of (k''-k_{un}) verses [Cu(II)] made from equation (6.15) at three different concentrations of yields straight line passing through the origin **(Figure 6.14)**. The gradient (G) of the line from equation (6.15) at constant hydroxyl ion concentration can be represented by equation (6.16)

$$\text{Gradient (G)} = \frac{K_1K_3k\left[OH^-\right][OFL]}{K_2 + K_3[OFL]} \tag{6.16}$$

which on further rearrangement yields equation (6.17)

$$\frac{G}{\left[OH^-\right]} = \frac{K_1K_3k[OFL]}{K_2 + K_3[OFL]} \tag{6.17}$$

Taking reciprocal of both the sides of equation (6.17), equation (6.18) is obtained

$$\frac{\left[OH^-\right]}{G} = \frac{K_2}{K_1K_3k[OFL]} + \frac{1}{K_1k} \tag{6.18}$$

A plot of $[OH^-]/G$ verses $[OFL]^{-1}$ made from equation (6.15) also yielded a straight line with non-zero intercept **(Figure 6.15)**. The ratio of slope and intercept from figure 6.15 gives the value of K_2/K_3 to be 1.18×10^{-2}mol/ dm^3 at 2.0 mol dm-3 ionic strength at 40ºC. Similar plot of $(k''-k_{un})$ verses $[OH^-]$ made from equation 6.15at constant concentration of copper ion also yields a straight line passing through the origin **(Figure 6.16)** with the gradient of the line as represented by equation (6.19)

$$G' = \frac{K_1 K_3 k\left[Cu(II)\right][OFL]}{K_2 + K_3[OFL]} \qquad (6.19)$$

That on rearrangement further gives equation (6.20)

$$\frac{\left[Cu(II)\right]}{G'} = \frac{K_2}{K_1 K_3 k[OFL]} + \frac{1}{K_1 k} \qquad (6.20)$$

A plot of [Cu (II)]/G verses $[OFL]^{-1}$ was also made from equation (6.20) also yielded a straight line with non-zero intercept **(Figure 6.17).** The ratio of slope and intercept (K_2/K_3) from figure6.17 was calculated to be 1.01×10^{-2} mol dm^{-3}. Thus the value of K_2/K_3 obtained from hydroxyl and copper ions variations are in good agreement.

These values of K_2/K_3 were further substituted in equation (6.15) and $(k''-k_{un})$ were calculated. The agreement between $(k''-k_{un})_{cal.}$ and $(k''-k_{un})_{exp.}$ as collected in table 6.21 is an addition support to the mechanism and negation of ofloxacin as the reactive species of OFL.

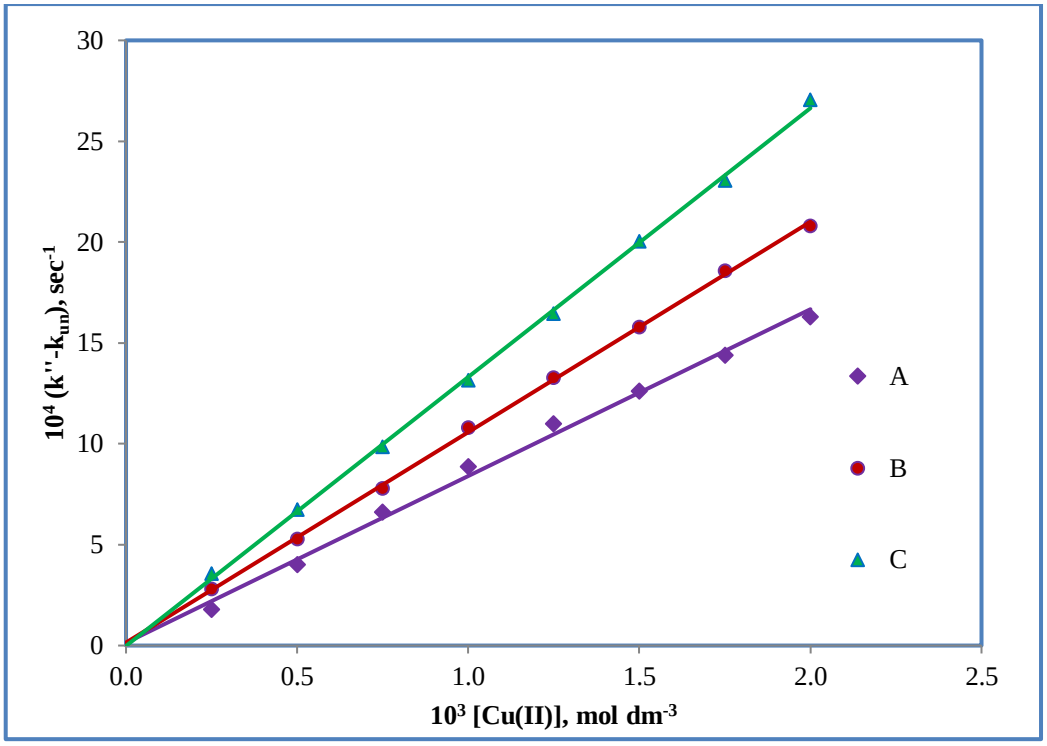

Figure 6.14: Plots of (k"-k_{un}) verses [Cu(II)] at different OFL concentrations (A) 1.0 × 10^{-2}; (B) 2.0 × 10^{-2}; (C) 3.0 × 10^{-2}/mol dm^{-3}.

[HCF] = 1.0 × 10^{-3} mol dm^{-3}; [OH^-] = 1.0 mol dm^{-3};

I = 2.0 mol dm^{-3}; Temp. = 40 ºC.

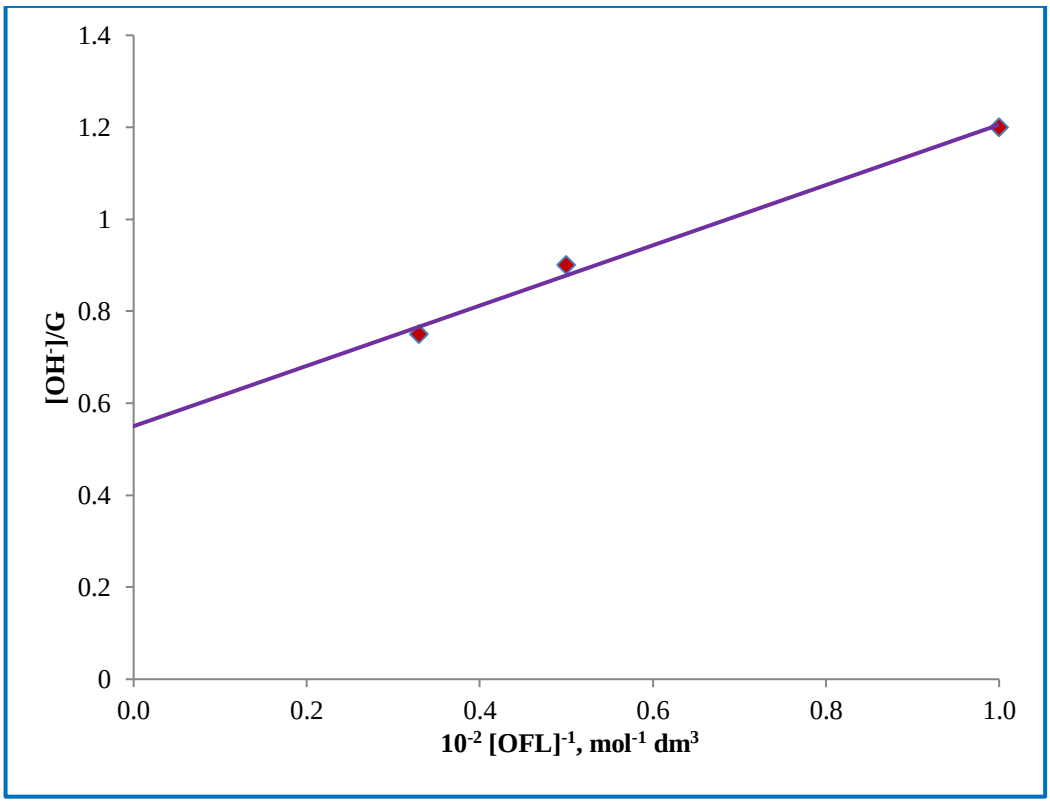

Figure 6.15: A plot of $[OH^-]/G$ verses $[OFL]^{-1}$ from variation of [Cu(II)] at different OFL concentrations.

(Reference Figure 6.14)

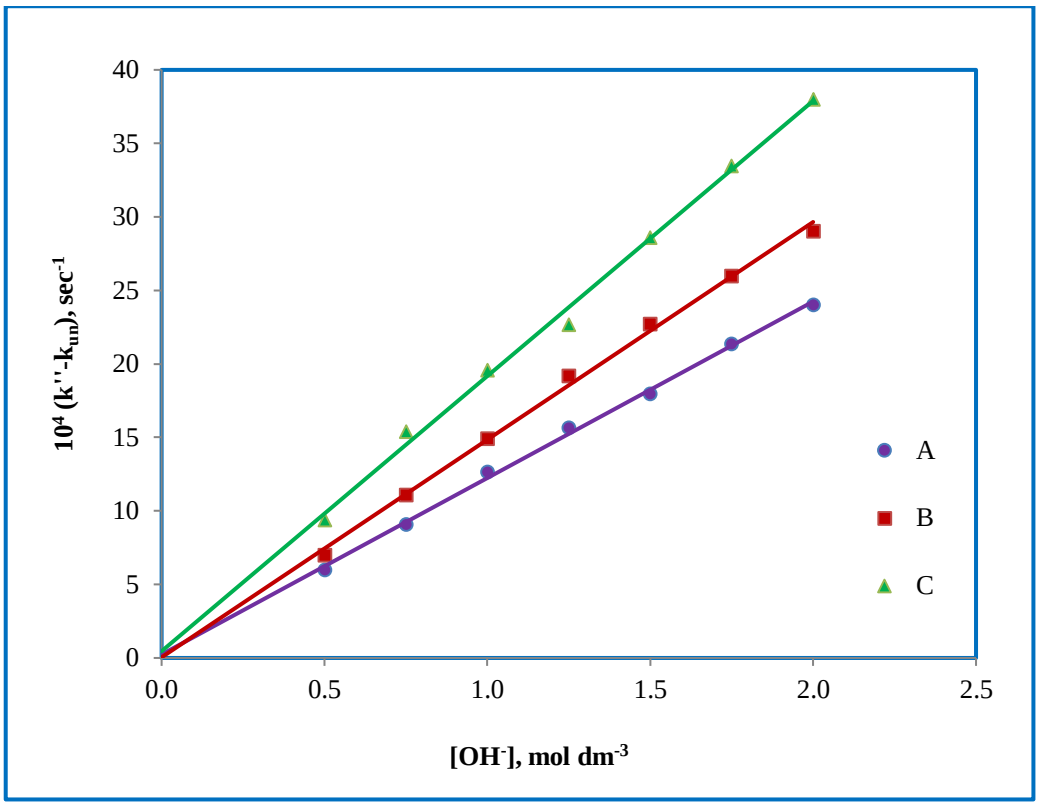

Figure 6.16: Plots of (k"-k_{un}) verses [OH^-] at different OFL concentrations (A) 1.0 × 10^{-2}; (B) 2.0 × 10^{-2}; (C) 3.0 × 10^{-2}/mol dm^{-3}.

[HCF] = 1.0 × 10^{-3} mol dm^{-3}; [Cu(II)] = 1.0 × 10^{-3} mol dm^{-3};

I = 2.0 mol dm^{-3}; Temp. = 40 ºC.

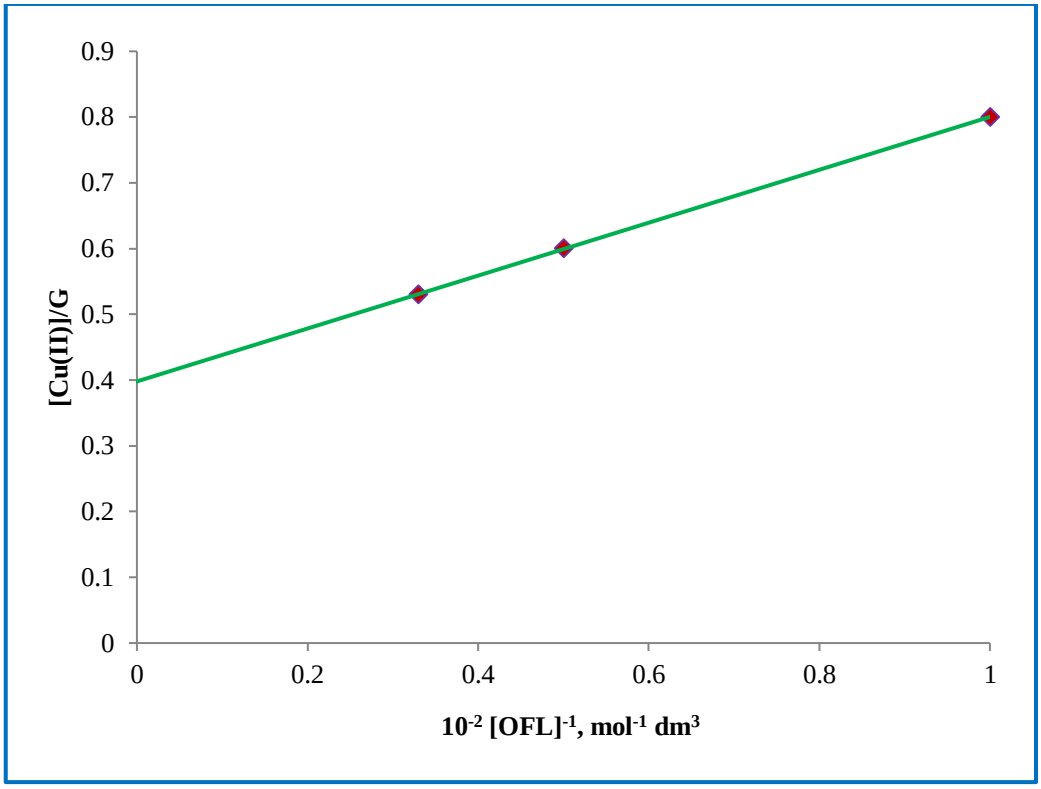

Figure 6.17: A plot of [Cu(II)]/G verses [OFL]$^{-1}$ from variation of [OH^{-}] at different OFL concentrations.

(Reference Figure 6.16)

Table 6.21: Experimental and calculated ($k''-k_{un}$) in the [OH^-] variation at different OFL concentration. [HCF (III)] = 1.0×10^{-3} mol dm^{-3}, [Cu (II)] = 1.0×10^{-3} mol dm^{-3}, [$NaNO_3$] = 1.0 mol dm^{-3}, Temp. = 40°C.

[OFL] mol dm^{-3}	1.0×10^{-2}		2.0×10^{-2}		3.0×10^{-2}	
[OH^-] mol dm^{-3}	$(k''-k_{un})_{exp.}$	$(k''-k_{un})_{cal.}$	$(k''-k_{un})_{exp.}$	$(k''-k_{un})_{cal.}$	$(k''-k_{un})_{exp.}$	$(k''-k_{un})_{cal.}$
0.50	5.97	6.22	6.99	7.56	9.37	9.43
0.75	9.07	9.33	11.09	11.34	15.37	14.15
1.00	12.64	12.45	14.89	15.13	19.57	18.87
1.25	15.67	15.56	19.19	18.91	22.67	23.58
1.50	17.97	18.67	22.69	22.69	28.57	28.30
1.75	21.37	21.78	26.47	26.47	33.47	33.02
2.00	25.67	24.90	30.26	30.26	37.97	37.74

6.5. Conclusion

The uncatalyzed and Cu(II) catalyzed oxidation of OFL by HCF(III) in aqueous alkaline media was investigated. The observed stoichiometry indicates that, the oxidation of one mole of OFL requires two moles of HCF(III). The observed major product obtained by the decarboxylation of quinolone moiety and hence, it may retain the antibacterial activity. The kinetic study indicates that in uncatalyzed reaction the outer sphere formation of $[Fe(CN)_6]^{4-}$ and free radical in slow step which is followed by the rapid reaction of free radical by $[Fe(CN)_6]^{3-}$ to give product where as in catalyzed reaction, a mechanism was proposed via the formation of an intermediate complex between OFL and HCF(III) in presence of Cu(II) as catalyst. The scheme 1 and scheme 2 are consistent with all experimental findings, including the product and kinetic studies.

6.6. References

[1] K. Kaur, A. Kumar, A. K. Malik, B. Singh,A. L. J. Rao, ***Critical Reviews in Analytical Chemistry,*** 38 (2008)2.

[2] G. Dasgupta, K. Mahanti, ***Bull. Soc. Chim.,*** 4 (1986) 492.

[3] S. A. Farokhi, S. T. Nandibewoor, ***Tetrahedrone***, 59 (2003) 7595.

[4] A. Nowdari, K. K. Adari, N. R. Gollapalli, V. Parvataneni, ***Eur. J. Chem.,***6 (2009) 93.

[5] E. P. Kelson, P. Phengsy, ***Int. J. Chem. Kinet.,*** 32 (2000)760.

[6] A. I. Vovk, I. V. Muraveva, V. P. Kukhar, V. F. Baklan, ***Russ. J. Gen. Chem.,*** 70 (2000) 1108.

[7] P. T. Speakman, W. A. J. Waters, ***J. Chem. Soc.,*** 40 (1955).

[8] V. N. Singh, M. C. Gangwar, B. B. L. Saxena, M. P. Singh, ***Can. J. Chem.,*** 47 (1969) 1051.

[9] M. M. Al-Subu, An-Najah, ***J. Res.,***7 (1992) 37.

[10] N. Nath, L. P. Singh, ***J. Indian Chem. Soc.,*** 62 (1985) 108.

[11] A. K. Das,***Coord. Chem. Rev***.,213 (2001)307.

[12] N. Diab, I. Abu-Shquair, M. Al-Subei, R. Salim, ***Int. J. of Chemistry***, 4 (2013) 1388.

[13] M. D. Meti, K. S. Bayadgi, S. T. Nandibewoor, S. A. Chimatadar, ***MontashChem***. 145 (2014) 1561.

[14] B. C. Sateesh, V. Shastry, S. Shashidhar, ***International Journal of Research in Physical Chemistry***, 3 (2013) 18.

[15] A. K. Singh, S. Srivastava, J. Srivastava, R. Srivastava, P. Singh, ***J. Mol. Catal. A: Chem.***, 278 (2007) 72.

[16] V. Devra, A. Jain,S. Jain, ***World Journal of Pharmaceutical Research***, 4 (2014) 963.

[17] U. Hubicka, P. Zmudzki, B. Z. Witek, P. Zajdel, M. Pawiowski, J. Krzek, ***Talanta***, 109 (2013) 91.

[18] A. Nowduri, A. B. Duggada, V. R. Kurimella, ***Int. J. of Scientific Research***, 3 (2014) 131.

[19] M. B. Patgar, S. T. Nandibewoor, S. A. Chimatadar, ***Cogent Chemistry***, 1 (2015) 1.

[20] R. V. Jagdeesh, Puttuswammy, ***Phys. Org. Chem***., 21 (2008) 844.

Chapter – 7

Kinetics and Mechanism of Oxidation of Moxifloxacin – A Fluoroquinolone Drug by Diperiodatocuprate(III) in Aqueous Alkaline Medium

7.1. Introduction

Fluoroquinolones are aclass of synthetic antibacterial agents with anincreasing popularity. These antibiotics display a broad spectrum of antibacterial activity including strong effects on gram-negative aerobic and anaerobic organisms as well as on gram-positive and a typical pathogens [1, 2]. Moxifloxacin (MF), 1-cyclopropyl-6-fluoro-1,4-dihydro-8-methoxy-7-[(4as,7as)-octa-hydro-6H-pyrrolo [3,4-b] pyridine-6-yl]-4-oxo-3-quinolone carboxylic acid monohydrochloride, is an antibacterial synthetic drug that belongs to the fourth generation of fluoroquinolones [3,5]. As a new generation of antibacterial Fluoroquinolone, MF has strong antibacterial activity, good clinical effects with little toxicity. The use of this newer generation Fluoroquinolone is increasing due to expand antibacterial spectrum which makes them useful in a broader range of applications [6]. But these are not fully metabolized in the body and are partially excreted in its pharmaceutically active form [7,8]. As a result of their excessive usage, antibacterial may enter into the environment through waste water and manure from animal husbandryetc [9,10]. The presence of antibacterial drugs in the aquatic environment that will become the source of potable supply, merits particular concern because of health recites. Effective removal of antibacterial drugs by water treatment process is important to minimize the potential health risks. For the removal of these Fluoroquinolone many studies are reported, in which oxidation process is commonly used for their degradation [11,12]. Recently, transition metals in their higher oxidation states can be stabilized by chelation with metal chelate such as diperiodatocuprate(III), diperiodatoargenate(III) and diperiodatonickelate(IV) [13-15], exhibits good oxidize properties with an appropriate pH value. Diperiodatocuprate(III) (DPC) is one-electrontransferoxidant for the substrate [16] and kinetic study of DPC are scanty because of its low solubility and stability in aqueous medium [17-25].A literature surveyrevealed that the kinetics and mechanism of oxidation of MF by different oxidants such as potassium permanganate and TiO_2 using various processes like electro-Fenton process, photolytic and photo catalyticetc, was carried out in both acidic and alkaline medium [26-30]. There are no reports on the oxidation of MF by DPC from kinetic and mechanistic points of view.

Copper(III) periodate complex as an oxidant shows multiple equlibria between different copper(III) species and it would be important to know which of the active species as an oxidant. Such studies are of importance in understanding the mechanistic pathways of oxidation of MF and to provide an insight into the interaction of metal ions with substrates. Hence, the present investigation is aimed to elucidate the reactivity of MF towards DPC, to arrive at a plausible mechanism and to understand the reactive species.

7.2. Experimental

7.2.1. Chemicals and Reagents

The method of preparation and standardization of the reagents are given in chapter 2 (Experimental). All reagents were of analyticalgrade and their solutions were prepared by dissolving the necessary amounts of the samples in doubly distilled water. Solution of diperiodatocuprate(III) was prepared freshly before running the experiment all the time. Doubly distilled water was employed throughout the work. The second distillation was from alkaline permanganate solution in a glass assembly.

7.2.2. Preparation of diperiodatocuprate(III)

The method of preparation and standardization of the reagents are given in chapter 2 (Chemicals). The complex was characterized by its UV-Visible spectrum, which exhibits strong broad absorption band at 415 nm. The aqueous solution of DPC was standardized bystandard method [31] and stable for several months.

7.2.3. Kinetic Procedure

The reactions were carried out in stoppered flask at 30±1ºC with all ingredients of the reaction mixture except DPC and the reaction was initiated by adding a known volume of DPC. Aliquot (2 ml) of the reaction mixture was withdrawn periodically. The progress of the reaction was followed by observing the absorbance of DPC in the reaction mixture at 415 nm in a placed in the cell compartment of an UV-Visible spectrophotometer, that there was no interference

from other species in the reaction mixture at this wave length. The U.V. spectra indicates gradually disappearance of Cu(III) band with time as a result of its reduction to Cu(II) **(Figure 7.1)**. The application of Beer's law of DPC concentration range 1.0×10^{-5} to 1.0×10^{-4} mol dm^{-3} at 415 nm had been verified giving Ɛ = 6230 dm^3 mol^{-1} cm^{-1} [32], pseudo-first-order rate constants (k_{obs}) were calculated from the plot of the logarithm of absorbance versus time. The pseudo first order plots were linear up to 80% completion of the reaction and k_{obs} value was reproducible within ±6%.

7.2.4. Stoichiometry and product analysis

The stoichiometry of the reaction determined by various sets of reaction mixtures containing different concentration of DPC and MF in aqueous alkaline medium at constant ionic strength for 12 h at 30˚C in a closed vessel to ensure the completion of the reaction. The excess of DPC wasestimated spectrophotometrically and the results correspond to the stoichiometry as represented by equation (7.1)

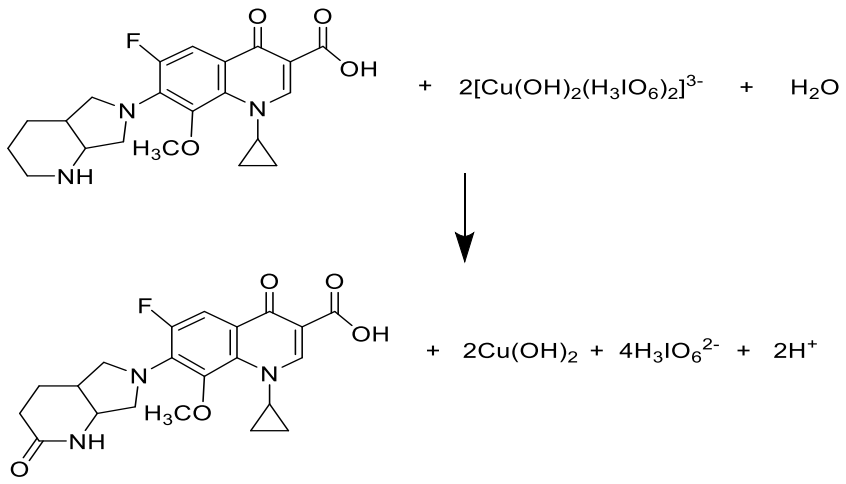

(7.1)

The product was detached by ether after the completion of the kinetic experiments. The main oxidative product 1-cyclopropyl-6-fluoro-1,4-dihydro-7-(octahydro-2-oxopyrolol[3,4-b]pyridine-6-yl)-8-methoxy-4-oxo-quinolone-3-carboxylic acid} was identified with the help of LC-MS and FT-IR analysis.

LC-MS data were obtained on a Q-TOF Micromass, spectrometer. The mass spectrum showed a molecular ion peak at m/z 416 amu which corresponds to oxidation of the piperazine ring [29] **(Figure 7.2)**. The presence of C=O bond was confirmed by FT-IR analysis which showed C=O stretching at 1693.98 cm^{-1} and –NH stretching of the –NH group at 3322.92 cm^{-1} **(Figure 7.3)**.

7.3. Results

7.3.1. Diperiodatocuprate(III) dependence

The concentration of the oxidant, DPC was varied from 1.0×10^{-5} to 1.0×10^{-4} mol dm^{-3} at constant concentration of [MF] $=1.0 \times 10^{-3}$ mol dm^{-3}, $[OH^-] =1.0 \times 10^{-2}$ mol dm^{-3}, $[IO_4^-] = 2.0 \times 10^{-4}$ mol dm^{-3} and ionic strength of 2.0×10^{-2} mol dm^{-3}, at 30°C temperature. The k_{obs} values are nearly constant indicating the order with respect to DPC concentration is unity. This was also confirmed from the linearity of plots of log (absorbance) versus time to about 80% completion of the reaction **(Figure 7.4)**. Results are given in **Table 7.1**.

7.3.2. Moxifloxacin dependence

The effect of MF on the rate of reaction was studied at constant concentration of [DPC] $= 5.0 \times 10^{-5}$ mol dm^{-3}, $[IO_4^-] = 2.0 \times 10^{-4}$ mol dm^{-3}, ionic strength $= 2.0 \times 10^{-2}$ mol dm^{-3} and two different concentration of alkali $= 1.0 \times 10^{-2}$ mol dm^{-3} and 30.0×10^{-2} mol dm^{-3} at three different temperature 25˚C, 30˚C and 35˚C. The substrate, MF was varied in the range of 5.0×10^{-4} to 5.0×10^{-3} mol dm^{-3}. The rate of reaction increases with increasing concentration of MF in the both alkali conditions and tends towards a limiting at higher concentration of MF **(Figure 7.5 and 7.6)**. The order with respect to MF concentration was obtained from the plot of log k_{obs} versus log [MF] and found to be less than unity (r = 0.63). Results are given in **Table 7.2, 7.3, 7.4, 7.5, 7.6 and 7.7.**

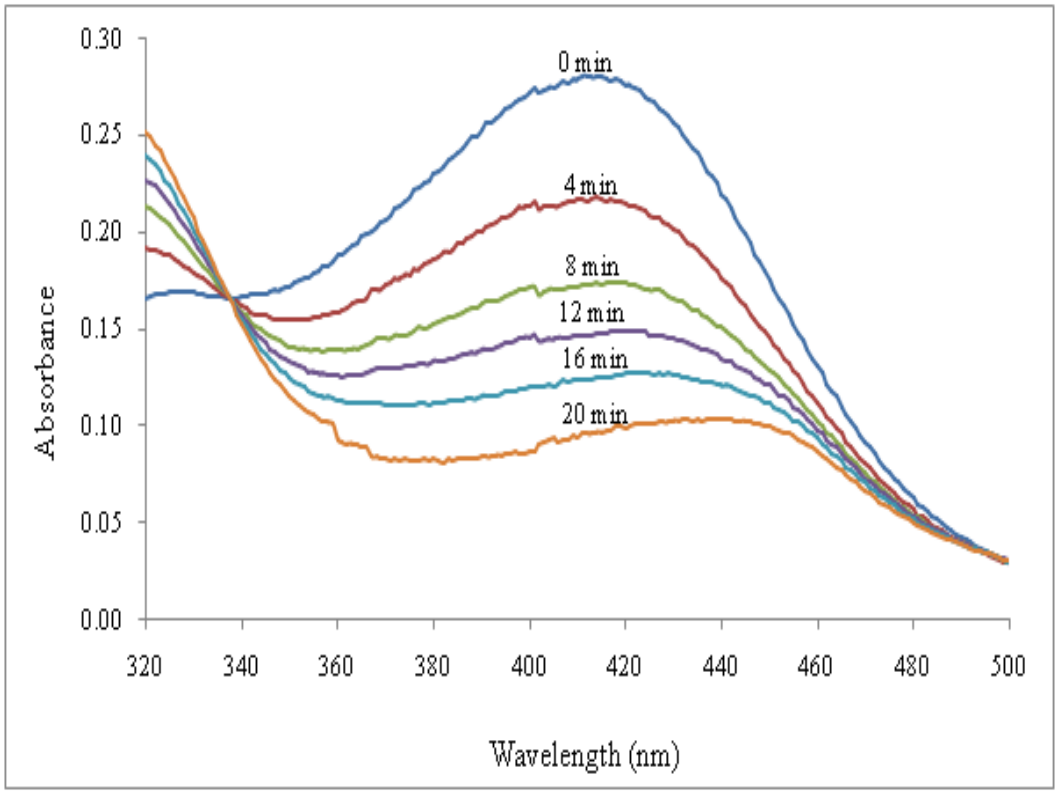

Figure 7.1: Spectral changes during oxidation of moxifloxacin (MF) by diperiodatocuprate(III) (DPC) in alkaline medium at 30ºC.

[DPC] = 5.0×10^{-5} mol dm^{-3}; [OH^-] = 1.0×10^{-2} mol dm^{-3};

[MF] = 1.0×10^{-3} mol dm^{-3}; I = 2.0×10^{-2} mol dm^{-3}.

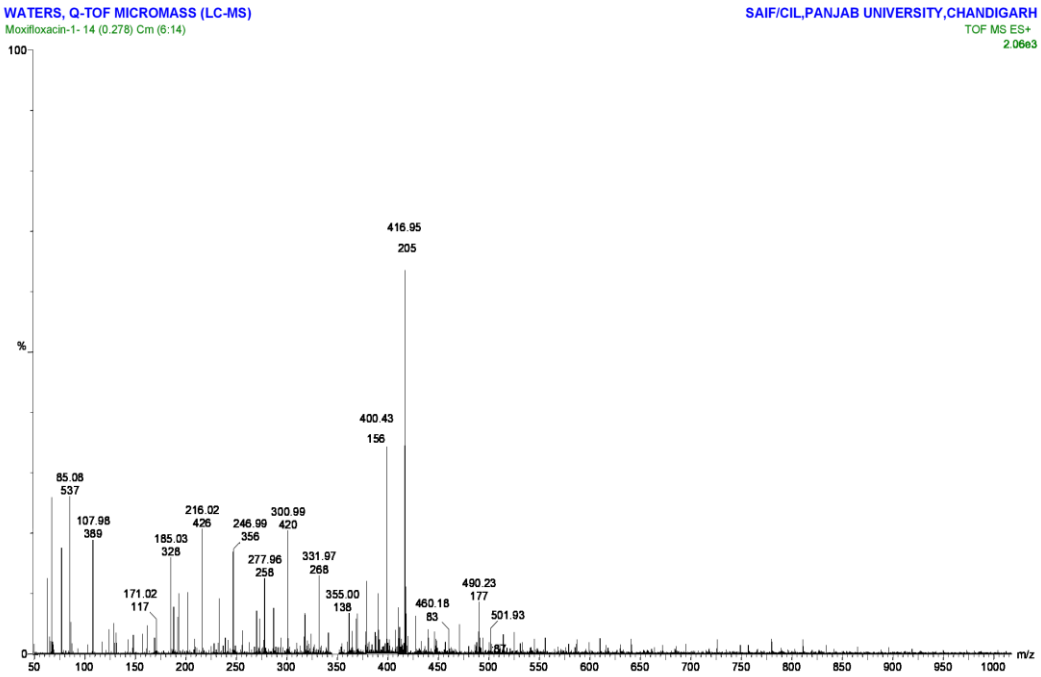

Figure 7.2: LC-ESI-MS spectra of oxidation product of moxifloxacin.

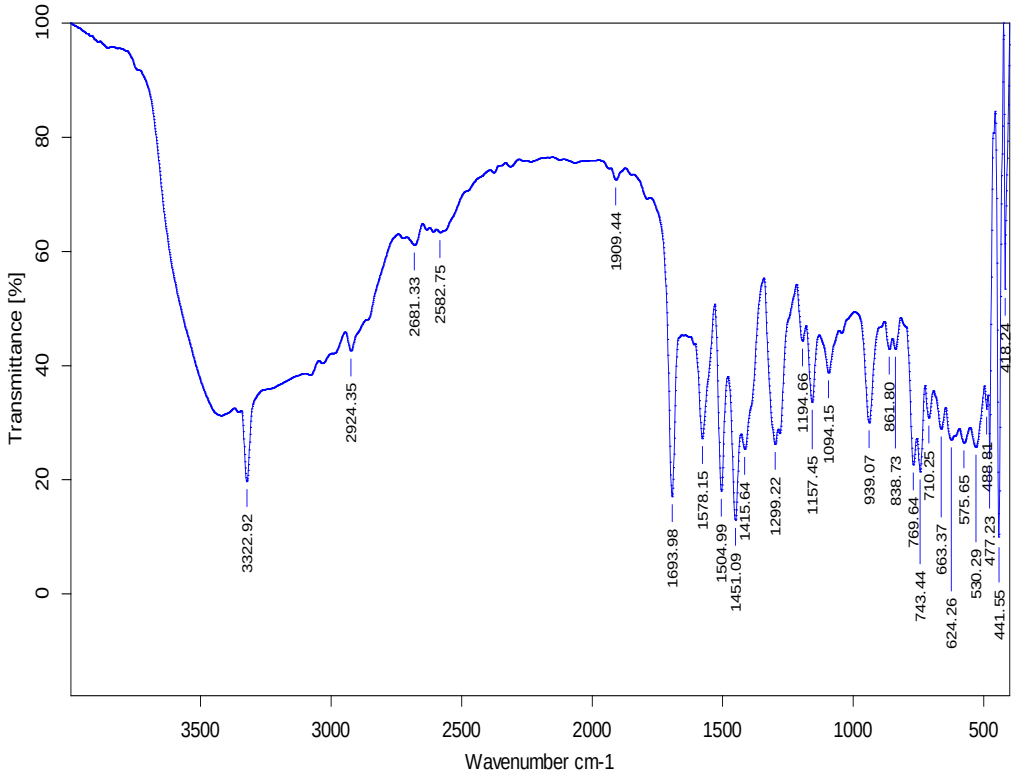

Figure 7.3: FTIR spectra of the oxidative product of moxifloxacin by diperiodatocuprate(III) in aqueous alkaline medium.

TABLE: 7.1
VARIATION OF DIPERIODATOCUPRATE(III)

[MF] = 1.0 x 10^{-3} mol dm^{-3} **Temp. = 30°C**

[OH^-] = 1.0 x 10^{-2} mol dm^{-3} **I = 2.0 x 10^{-2} mol dm^{-3}**

[IO_4^-] = 2.0 x 10^{-4} mol dm^{-3}

10^5 [DPC], mol dm^{-3}	**1.0**	**2.5**	**3.0**	**5.0**	**7.0**	**7.5**	**8.0**	**10.0**
Time in minutes				**Absorbance**				
0	0.062	0.156	0.187	0.311	0.437	0.468	0.499	0.622
5	0.045	0.113	0.136	0.225	0.317	0.339	0.362	0.451
10	0.033	0.082	0.098	0.163	0.230	0.245	0.262	0.327
15	0.024	0.059	0.071	0.118	0.167	0.178	0.190	0.237
20	0.017	0.043	0.052	0.086	0.121	0.129	0.138	0.172
25	0.012	0.031	0.038	0.062	0.088	0.093	0.100	0.125
10^4 (k_{obs}), sec^{-1}	**10.73**	**10.70**	**10.72**	**10.73**	**10.70**	**10.73**	**10.71**	**10.69**

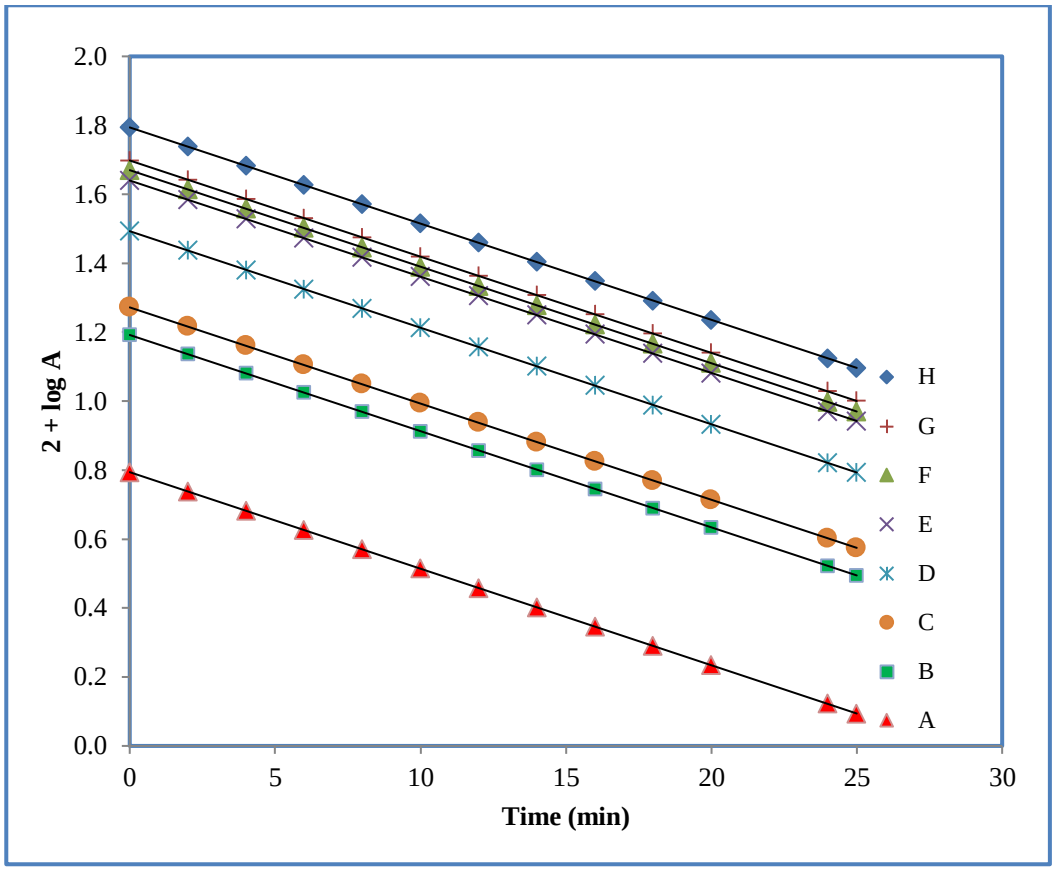

Figure 7.4: First order plots of the variation of diperiodatocuprate(III) concentration.

[MF] = 1.0 x 10^{-3} mol dm^{-3}; Temp. = 30 °C;

[OH^-] = 1.0 x 10^{-2} mol dm^{-3}; I = 2.0 x 10^{-2} mol dm^{-3};

[IO_4^-] = 2.0 x 10^{-4} mol dm^{-3};

[DPC] = (A) 1.0 × 10^{-5} mol dm^{-3}; (B) 2.5 × 10^{-5} mol dm^{-3};

(C) 3.0 × 10^{-5} mol dm^{-3}; (D) 5.0 × 10^{-5} mol dm^{-3};

(E) 7.0 × 10^{-5} mol dm^{-3}; (F) 7.5 × 10^{-5} mol dm^{-3};

(G) 8.0 × 10^{-5} mol dm^{-3}; (H) 10.0× 10^{-5} mol dm^{-3}.

(Ref. Table 7.1)

TABLE: 7.2
VARIATION OF MOXIFLOXACIN

[DPC] = 5.0 x 10^{-5} mol dm^{-3} **Temp. = 25°C**
[OH^-] = 1.0 x 10^{-2} mol dm^{-3} **I = 2.0 x10^{-2}mol dm^{-3}**
[IO_4^-] = 2.0 x 10^{-4} mol dm^{-3}

10^3 [MF], mol dm^{-3}	**0.5**	**0.75**	**1.0**	**2.0**	**3.0**	**4.0**	**5.0**
Time in minutes				**Absorbance**			
0	(0)0.312	(0)0.311	(0)0.310	0.311	0.313	0.310	0.312
4	(10)0.248	(7)0.250	(7)0.240	0.249	0.243	0.232	0.227
8	(20)0.197	(14)0.201	(14)0.185	0.200	0.189	0.173	0.165
12	(30)0.157	(21)0.162	(21)0.142	0.160	0.148	0.129	0.120
16	(40)0.125	(28)0.130	(28)0.109	0.129	0.115	0.096	0.088
20	(50)0.100	(35)0.105	(35)0.084	0.103	0.090	0.071	0.064
24	(60)0.079	(42)0.084	(42)0.065	0.083	0.070	0.053	0.046
28	(70)0.063	(49)0.068	(49)0.050	0.066	0.055	-	-
10^4 (k_{obs}), sec^{-1}	**3.8**	**5.2**	**6.2**	**9.2**	**11.0**	**12.3**	**13.2**

Figures in parentheses denote time in minutes.

TABLE: 7.3
VARIATION OF MOXIFLOXACIN

[DPC] = 5.0 x 10^{-5} mol dm^{-3} **Temp. = 30 °C**
[OH^-] = 1.0 x 10^{-2} mol dm^{-3} **I = 2.0 x 10^{-2} mol dm^{-3}**
[IO_4^-] = 2.0 x 10^{-4} mol dm^{-3}

10^3 [MF], mol dm^{-3}	**0.5**	**0.75**	**1.0**	**2.0**	**3.0**	**4.0**	**5.0**
Time in minutes				**Absorbance**			
0	(0)0.310	(0) 0.311	(0)0.312	(0)0.310	0.313	0.311	0.312
2	(7)0.228	(4)0.249	(4)0.240	(3)0.241	0.256	0.252	0.251
4	(14)0.167	(8)0.199	(8)0.186	(6)0.187	0.211	0.204	0.202
6	(21)0.122	(12)0.159	(12)0.144	(9)0.145	0.174	0.166	0.163
8	(28)0.090	(16)0.128	(16)0.111	(12)0.112	0.143	0.134	0.131
10	(35)0.066	(20)0.102	(20)0.086	(15)0.087	0.118	0.109	0.106
12	(42)0.048	(24)0.082	(24)0.066	(18)0.067	0.097	0.088	0.085
14	(49)0.035	(28)0.065	(28)0.051	(21)0.052	0.080	0.072	0.069
10^4 (k_{obs}), sec^{-1}	**7.4**	**9.3**	**10.7**	**14.2**	**16.2**	**17.5**	**18.0**

Figures in parentheses denote time in minutes.

TABLE: 7.4
VARIATION OF MOXIFLOXACIN

[DPC] = 5.0 x 10^{-5} mol dm^{-3} **Temp. = 35 °C**
[OH^-] = 1.0 x 10^{-2} mol dm^{-3} **I = 2.0 x 10^{-2} mol dm^{-3}**
[IO_4^-] = 2.0 x 10^{-4} mol dm^{-3}

10^3[MF], mol dm^{-3}	**0.5**	**0.75**	**1.0**	**2.0**	**3.0**	**4.0**	**5.0**
Time in minutes				**Absorbance**			
0	(0)0.311	(0)0.312	(0)0.312	0.311	0.310	0.313	0.312
4	(4)0.245	(3)0.248	(3)0.240	0.248	0.240	0.236	0.234
8	(8)0.192	(6)0.198	(6)0.185	0.198	0.186	0.179	0.176
12	(12)0.151	(9)0.158	(9)0.143	0.158	0.144	0.136	0.133
16	(16)0.119	(12)0.126	(12)0.110	0.126	0.111	0.103	0.100
20	(20)0.094	(15)0.100	(15)0.085	0.101	0.086	0.078	0.075
24	(24)0.074	(18)0.080	(18)0.066	0.080	0.066	0.059	0.057
28	(28)0.058	(21)0.064	(21)0.051	0.064	0.051	0.045	0.043
10^4 (k_{obs}), sec^{-1}	**10.0**	**12.6**	**14.4**	**18.8**	**21.5**	**23.0**	**23.7**

Figures in parentheses denote time in minutes.

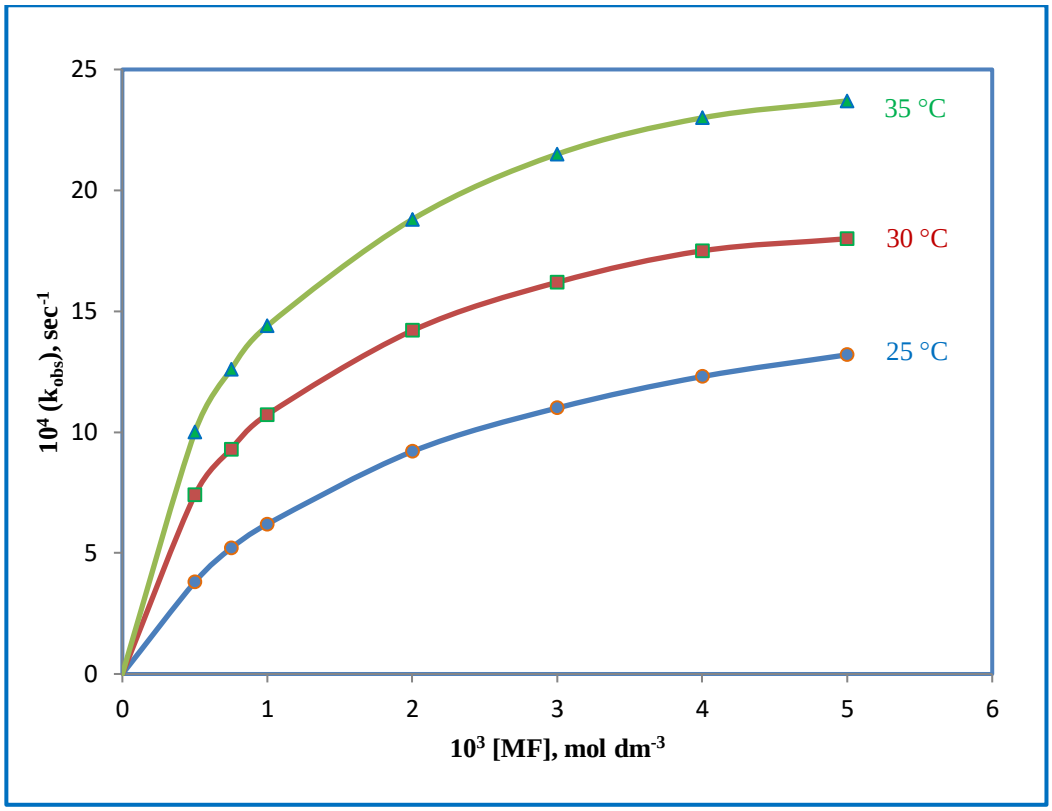

Figure 7.5: Variation of moxifloxacin at different temperature.

[DPC] = 5.0×10^{-5} mol dm^{-3}; [OH^-] = 1.0×10^{-2} mol dm^{-3};

[IO_4^-] = 2.0×10^{-4} mol dm^{-3}; I = 2.0×10^{-2} mol dm^{-3}.

(Ref. Table: 7.2, 7.3, 7.4)

TABLE: 7.5
VARIATION OF MOXIFLOXACIN

[DPC] = 5.0 x 10^{-5} mol dm^{-3} **Temp. = 25 °C**

[OH^-] = 30.0 x 10^{-2} mol dm^{-3} **I = 2.0 x 10^{-2} mol dm^{-3}**

[IO_4^-]= 2.0 x 10^{-4} mol dm^{-3}

10^3 [MF], mol dm^{-3}	**0.5**	**0.75**	**1.0**	**2.0**	**3.0**	**4.0**	**5.0**
Time in minutes				**Absorbance**			
0	(0)0.310	(0)0.312	(0)0.311	0.312	0.310	0.313	0.311
0.5	(1)0.248	(1)0.232	(1)0.220	0.242	0.229	0.224	0.220
1.0	(2)0.197	(2)0.173	(2)0.155	0.188	0.169	0.161	0.156
1.5	(3)0.157	(3)0.129	(3)0.110	0.146	0.124	0.116	0.111
2.0	(4)0.125	(4)0.096	(4)0.077	0.114	0.092	0.083	0.078
2.5	(5)0.100	(5)0.072	(5)0.055	0.088	0.067	0.060	0.055
3.0	(6)0.079	(6)0.053	(6)0.039	0.069	0.050	0.043	0.039
10^4 (k_{obs}), sec^{-1}	**38**	**49**	**58**	**84**	**102**	**110**	**115**

Figures in parentheses denote time in minutes.

TABLE: 7.6
VARIATION OF MOXIFLOXACIN

[DPC] = 5.0 x 10^{-5} mol dm^{-3} **Temp. = 30 °C**
[OH^-] = 30.0 x 10^{-2} mol dm^{-3} **I = 2.0 x 10^{-2} mol dm^{-3}**
[IO_4^-] = 2.0 x 10^{-4} mol dm^{-3}

10^3[MF], mol dm^{-3}	**0.5**	**0.75**	**1.0**	**2.0**	**3.0**	**4.0**	**5.0**
Time in minutes				**Absorbance**			
0	0.312	0.310	0.311	0.313	0.310	0.312	0.311
0.5	0.260	0.246	0.238	0.217	0.207	0.203	0.199
1.0	0.217	0.195	0.181	0.151	0.138	0.133	0.127
1.5	0.181	0.154	0.138	0.106	0.092	0.087	0.081
2.0	0.151	0.122	0.106	0.074	0.061	0.057	0.052
2.5	0.127	0.097	0.081	0.051	0.040	0.037	0.033
3.0	0.106	0.076	0.062	0.025	-	-	-
10^4 (k_{obs}), sec^{-1}	**60**	**78**	**90**	**120**	**136**	**145**	**150**

Figures in parentheses denote time in minutes.

TABLE: 7.7
VARIATION OF MOXIFLOXACIN

[DPC] = 5.0 x 10^{-5} mol dm^{-3} **Temp. = 35 °C**

[OH^-] = 30.0 x 10^{-2} mol dm^{-3} **I = 2.0 x 10^{-2} mol dm^{-3}**

[IO_4^-]= 2.0 x 10^{-4} mol dm^{-3}

10^3[MF], mol dm^{-3}	**0.5**	**0.75**	**1.0**	**2.0**	**3.0**	**4.0**	**5.0**
Time in minutes				**Absorbance**			
0	0.311	0.312	0.310	0.311	0.313	0.312	0.311
0.5	0.247	0.231	0.220	0.201	0.190	0.183	0.175
1.0	0.196	0.171	0.156	0.130	0.116	0.108	0.098
1.5	0.156	0.127	0.110	0.084	0.070	0.064	0.055
2.0	0.124	0.094	0.078	0.054	0.043	0.037	0.031
2.5	0.098	0.070	0.055	0.035	-	-	-
3.0	0.078	0.052	0.039	-	-	-	-
10^4 (k_{obs}), sec^{-1}	**76**	**98**	**112**	**146**	**165**	**176**	**182**

Figures in parentheses denote time in minutes.

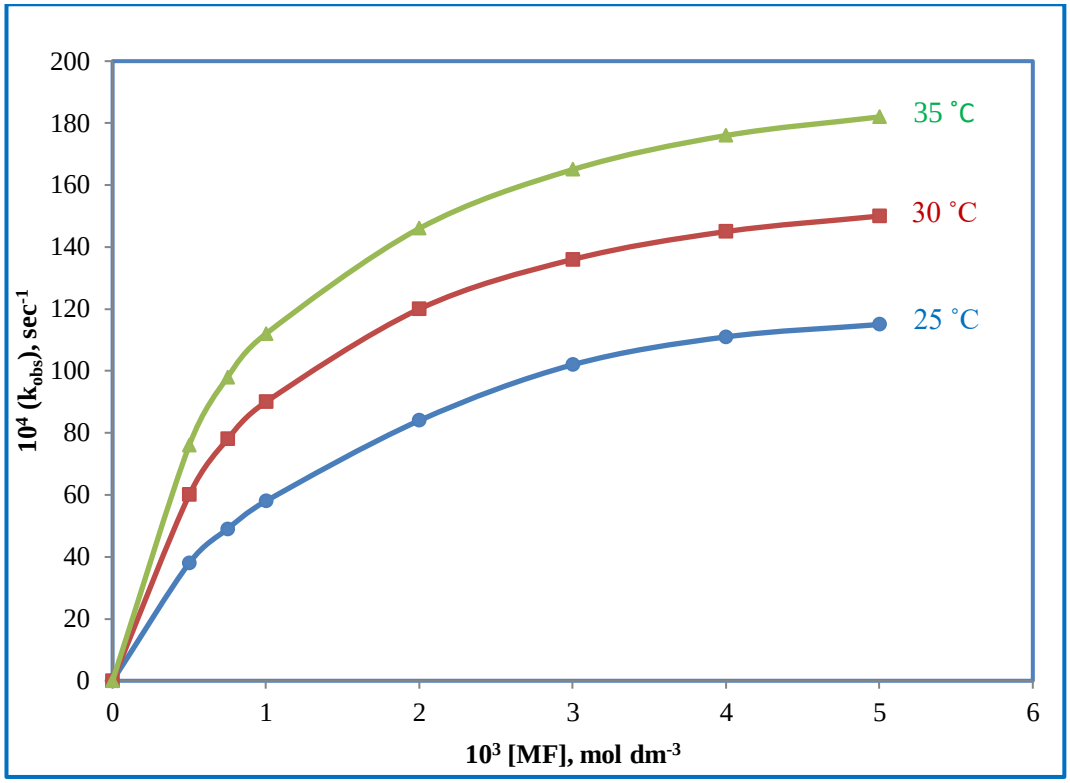

Figure 7.6: Variation of moxifloxacin at different temperature.

[DPC] = 5.0×10^{-5} mol dm^{-3}; [OH^-] = 30.0×10^{-2} mol dm^{-3};

[IO_4^-] = 2.0×10^{-4} mol dm^{-3}; I = 2.0×10^{-3} mol dm^{-3}.

(Ref. Table: 7.5, 7.6, 7.7)

7.3.3. Hydroxyl ion dependence

The effect of concentration variation of sodium hydroxide on the rate of reaction was studied in the concentration range 0.5×10^{-2} to 30.0×10^{-2} mol dm^{-3} at fixed concentration of [DPC] = 5.0×10^{-5} mol dm^{-3}, [MF] = 1.0×10^{-3} mol dm^{-3}, $[IO_4^-]$ = 2.0×10^{-4} mol dm^{-3}, ionic strength of 2.0×10^{-2} mol dm^{-3} at 30˚C temperature. The rate decreases quickly with increase in $[OH^-]$ till 2.0×10^{-2} mol dm^{-3}, and then increases with continuous increase in $[OH^-]$ **(Figure 7.7)**. The effect of hydroxyl ion on the rate of reaction indicate the reaction proceed by two different paths in the mechanism. Results are given in **Tables 7.8.**

7.3.4. Periodate ion dependence

The concentration of KIO_4 was varied from 2.0×10^{-4} to 3.5×10^{-4} mol dm^{-3} at constant concentration of [DPC] = 5.0×10^{-5} mol dm^{-3}, [MF] = 1.0×10^{-3} mol dm^{-3}, ionic strength = 2.0×10^{-2} mol dm^{-3} and two different concentration of alkali = 1.0×10^{-2} mol dm^{-3} and 30.0×10^{-2} mol dm^{-3} at 30°C. The effect of IO_4^- on the rate of reaction indicates the active form of Cu(III) periodate complex. At low $[OH^-]$ (1.0×10^{-2} mol dm^{-3}), the rate constant k_{obs} increased with increase in $[KIO_4]$. But at high $[OH^-]$ (30.0×10^{-2} mol dm^{-3}), k_{obs} decreased with increase in $[KIO_4]$. The effect of KIO_4on rate of reaction is suggested that the involvement of DPC in the multiple equilibria [33]. Results are given in **Tables 7.9 and 7.10**.

7.3.5. Effect of ionic strength and dielectric constant

At constant concentration of reactants, the ionic strength was varied by varying concentration of potassium nitrate from 0.5×10^{-2} to 3.0×10^{-2} mol dm^{-3} at constant concentration of [DPC] = 5.0×10^{-5} mol dm^{-3}, [MF] = 1.0×10^{-3} mol dm^{-3}, $[OH^-]$ =1.0×10^{-2} mol dm^{-3} and $[IO_4^-]$ = 2.0×10^{-4} mol dm^{-3}at 30°C temperature. The results indicate the ionic strength had negligible effect on the rate of reaction (**Table 7.11)**. The negligible effect of ionic strength on the rate of reaction suggests that the reaction is either between two neutral species or a neutral and a charged species.

At constant acidity and other constant conditions, as the t-butyl alcohol content increase from 0 to 50% (v/v) in the reaction, change in dielectric constant had negligible effect on the rate of reaction **Table 7.12**.

7.3.6. Effect of initially added product

The effect of initial added product, Cu(II) ($CuSO_4$) was studied by verifying concentration of $CuSO_4$ in the range of 1.0×10^{-4} to 10.0×10^{-4} mol dm^{-3} at constant concentration of [DPC] = 5.0×10^{-5} mol dm^{-3}, [MF] = 1.0×10^{-3} mol dm^{-3}, [OH^-] =1.0×10^{-2} mol dm^{-3}, [IO_4^-] = 2.0×10^{-4} mol $dm^{-3}$and ionic strength of 2.0×10^{-2} mol dm^{-3} at 30°C temperature, The added product did not have any significant effect on the rate of reaction. Results indicate no involvement of the product in the reaction. Results are given in **Table 7.13**.

7.3.7. Test for free radicals

To test the intervention of free radicals, in the reaction mixture, a known quantity of acrylonitrile had been added initially, was kept for two hours under nitrogen atmosphere. On dilution with methanol, white precipitate formed, indicating the presence of intervention of free radicals in the reaction.

TABLE: 7.8
VARIATION OF HYDROXYL ION

[DPC] = 5.0 x 10^{-5} mol dm^{-3} **Temp. = 30 °C**
[MF] = 1.0 x 10^{-3} mol dm^{-3} **I = 2.0 x 10^{-2} mol dm^{-3}**
[IO_4^-] = 2.0 x 10^{-4} mol dm^{-3}

10^2 [OH^-], mol dm^{-3}	0.5	0.75	1.0	2.0	3.0	4.0	5.0	7.5	10.0	20.0	30.0
Time in minutes	Absorbance										
0	(0)0.311	(0)0.311	(0)0.311	(0)0.310	(0)0.311	(0)0.311	(0)0.310	(0)0.311	(0)0.312	0.311	0.311
0.5	(1)0.217	(2)0.217	(4)0.240	(6)0.242	(5)0.238	(3)0.245	(3)0.225	(1)0.261	(1)0.245	0.252	0.238
1.0	(2)0.151	(4)0.151	(8)0.186	(12)0.188	(10)0.182	(6)0.193	(6)0.163	(2)0.218	(2)0.193	0.204	0.0.181
1.5	(3)0.106	(6)0.106	(12)0.144	(18)0.146	(15)0.139	(9)0.153	(9)0.118	(3)0.183	(3)0.151	0.166	0.138
2.0	(4)0.074	(8)0.074	(16)0.111	(24)0.114	(20)0.106	(12)0.120	(12)0.085	(4)0.153	(4)0.119	0.134	0.106
2.5	(5)0.051	(10)0.051	(20)0.086	(30)0.089	(25)0.081	(15)0.095	(15)0.062	(5)0.128	(5)0.094	0.109	0.081
3.0	(6)0.036	(12)0.036	(24)0.66	(36)0.069	(30)0.062	(18)0.075	(18)0.045	(6)0.107	(6)0.074	0.088	0.062
10^4 (k_{obs}), sec^{-1}	**60.00**	**30.01**	**10.73**	**7.02**	**9.10**	**13.20**	**18.00**	**29.60**	**40.00**	**70.01**	**90.02**

Figures in parentheses denote time in minutes.

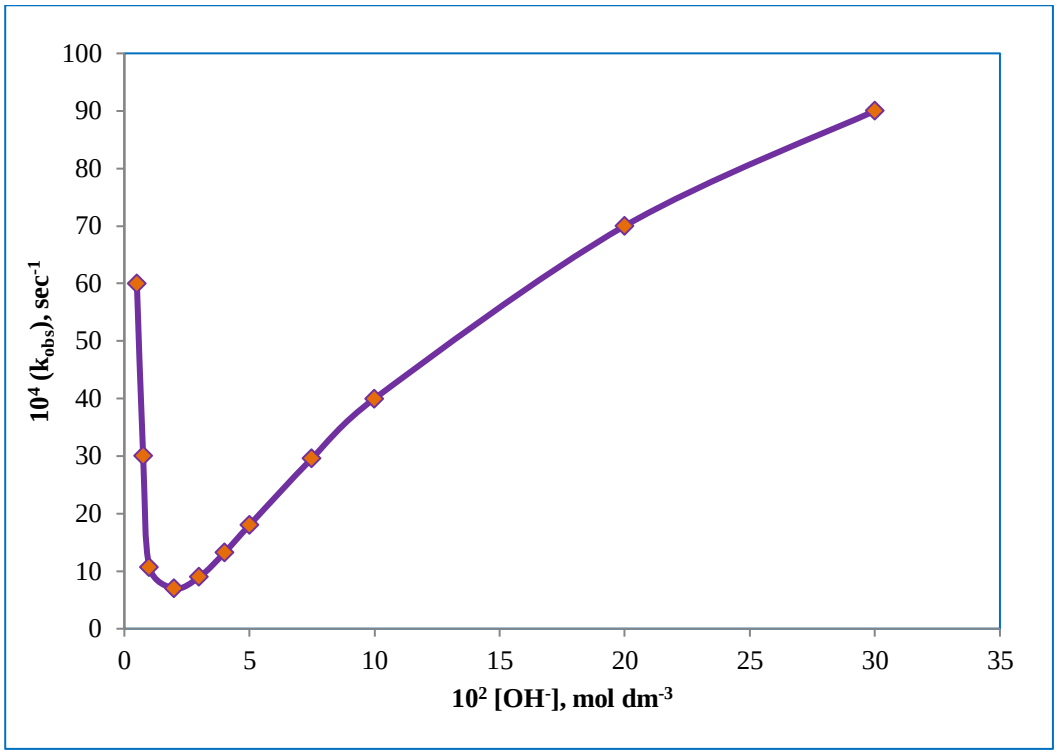

Figure 7.7: Variation of hydroxyl ion.

[MF] = 1.0 x 10^{-3} mol dm^{-3}; [DPC] = 5.0 × 10^{-5} mol dm^{-3};

[IO_4^-] = 2.0 × 10^{-4} mol dm^{-3}; I = 2.0× 10^{-2}mol dm^{-3};

Temp. = 30 ˚C

(Ref. Table: 7.8)

TABLE: 7.9

VARIATION OF POTTASIUM PERIODATE

[DPC] = 5.0 x 10^{-5} mol dm^{-3} **Temp. = 30 °C**
[MF] = 1.0 x 10^{-3} mol dm^{-3} **I = 2.0 x 10^{-2} mol dm^{-3}**
[OH^-] = 1.0 x 10^{-2} mol dm^{-3}

10^4 [IO_4^-], mol dm^{-3}	**2.0**	**2.5**	**3.0**	**3.5**
Time in minutes		**Absorbance**		
0	0.310	0.312	(0)0.311	(0)0.310
4	0.240	0.231	(3)0.242	(3)0.235
8	0.186	0.172	(6)0.189	(6)0.177
12	0.144	0.127	(9)0.147	(9)0.133
16	0.111	0.095	(12)0.114	(12)0.101
20	0.086	0.070	(15)0.089	(15)0.076
24	0.066	0.052	(18)0.069	(18)0.057
10^4 (k_{obs}), sec^{-1}	**10.73**	**12.40**	**13.90**	**15.70**

Figures in parentheses denote time in minutes.

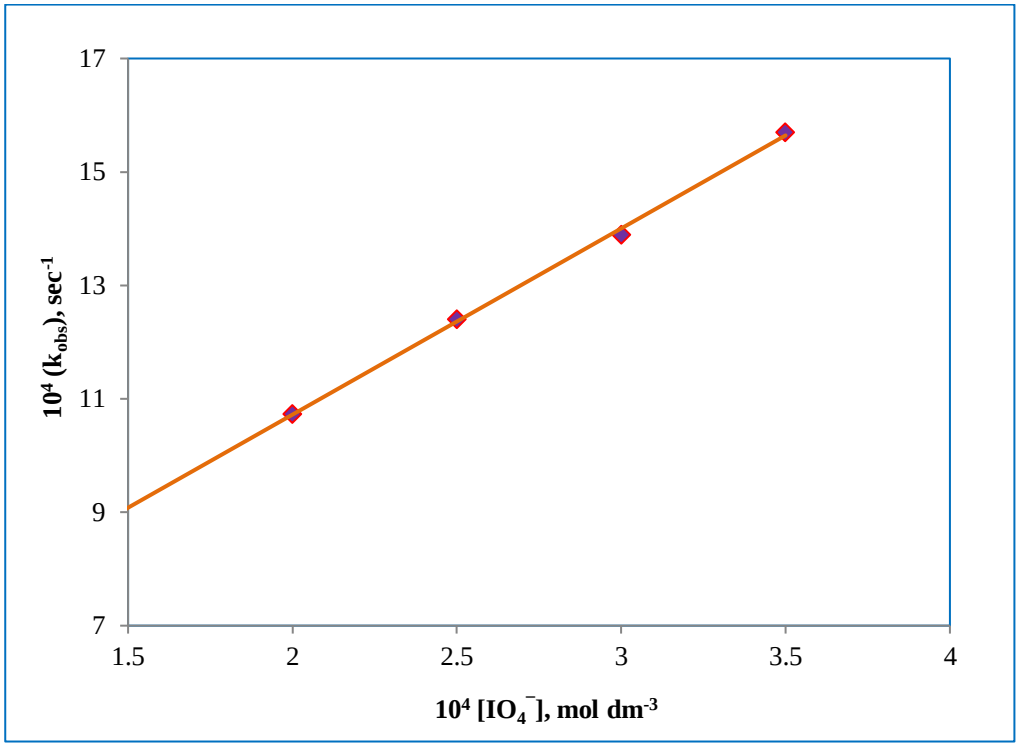

Figure 7.8: Variation of periodate ion.

[MF] = 1.0 x 10^{-3} mol dm^{-3}; [DPC] = 5.0 × 10^{-5} mol dm^{-3};

[OH^-] = 1.0 × 10^{-2} mol dm^{-3}; I = 2.0× 10^{-2}mol dm^{-3}:

Temp. = 30 ˚C.

(Ref. Table: 7.9)

TABLE: 7.10
VARIATION OF POTTASIUM PERIODATE

[DPC] = 5.0 x 10^{-5} mol dm^{-3} **Temp. = 30 °C**
[MF] = 1.0 x 10^{-3} mol dm^{-3} **I = 2.0 x 10^{-2} mol dm^{-3}**
[OH^-] = 30.0 x 10^{-2} mol dm^{-3}

10^4 [IO_4^-], mol dm^{-3}	**2.0**	**2.5**	**3.0**	**3.5**
Time in minutes		**Absorbance**		
0	0.310	0.311	0.312	0.311
0.5	0.238	0.244	0.251	0.257
1.0	0.181	0.191	0.202	0.212
1.5	0.138	0.150	0.163	0.175
2.0	0.106	0.118	0.131	0.144
2.5	0.081	0.092	0.106	0.119
3.0	0.062	0.072	0.085	0.098
10^4 (k_{obs}), sec^{-1}	**90**	**81**	**72**	**64**

Figures in parentheses denote time in minutes.

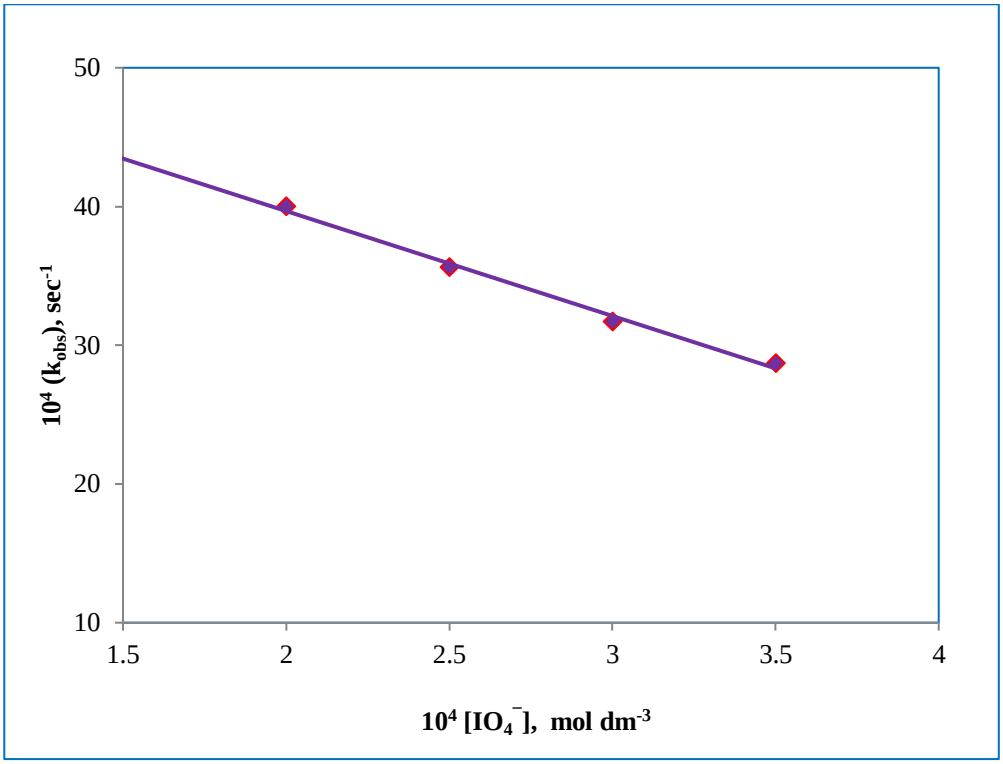

Figure 7.9: Variation of periodate ion

[MF] = 1.0 x 10^{-3} mol dm^{-3}; [DPC] = 5.0 × 10^{-5} mol dm^{-3};

[OH^-] = 30.0 × 10^{-2} mol dm^{-3}; I = 2.0 × 10^{-2} mol dm^{-3};

Temp. = 30 ˚C

(Ref. Table: 7.10)

TABLE: 7.11

VARIATION OF POTTASIUM NITRATE

[DPC] = 5.0 x 10^{-5} mol dm^{-3} **Temp. = 30 °C**

[MF] = 1.0 x 10^{-3} mol dm^{-3} **[OH^-] = 1.0 x 10^{-2} mol dm^{-3}**

10^2 [NO_3^-], mol dm^{-3}	**0.5**	**1.0**	**1.5**	**2.0**	**2.5**	**3.0**
Time in minutes			**Absorbance**			
0	0.311	0.310	0.312	0.311	0.310	0.311
4	0.232	0.230	0.228	0.231	0.228	0.227
8	0.169	0.170	0.163	0.167	0.169	0.170
12	0.123	0.121	0.119	0.120	0.121	0.119
16	0.100	0.098	0.095	0.092	0.088	0.090
20	0.070	0.069	0.064	0.067	0.065	0.071
10^4 (k_{obs}), sec^{-1}	**10.72**	**10.73**	**10.69**	**10.73**	**10.70**	**10.71**

TABLE: 7.12

EFFECT OF DIELECTRIC CONSTANT

[DPC] = 5.0 x 10^{-5} mol dm^{-3} **Temp. = 30 °C**

[MF] = 1.0 x 10^{-3} mol dm^{-3} **I = 2.0 x 10^{-2} mol dm^{-3}**

[OH^-] = 30.0 x 10^{-2} mol dm^{-3} **[IO_4^-] = 2.0 x 10^{-4} mol dm^{-3}**

[Acetic acid], %	**5**	**10**	**15**	**20**
Time in minutes		**Absorbance**		
0	0.313	0.312	0.313	0.311
4	0.237	0.240	0.245	0.243
8	0.181	0.186	0.190	0.184
12	0.139	0.144	0.141	0.142
16	0.107	0.111	0.116	0.113
20	0.089	0.086	0.090	0.088
24	0.068	0.066	0.069	0.067
10^4 (k_{obs}), sec^{-1}	**10.71**	**10.73**	**10.69**	**10.72**

TABLE: 7.13

EFFECT OF Cu(II) ION

[DPC] = 5.0 x 10^{-5} mol dm^{-3} **Temp. = 30 °C**

[MF] = 1.0 x 10^{-3} mol dm^{-3} **I = 2.0 x 10^{-2} mol dm^{-3}**

[OH^-] = 1.0 x 10^{-2} mol dm^{-3}

10^4 [Cu(II)]	**1.0**	**3.0**	**5.0**	**7.0**	**10.0**
Time in minutes			**Absorbance**		
0	0.313	0.310	0.312	0.311	0.312
4	0.242	0.239	0.240	0.241	0.241
8	0.188	0.185	0.186	0.187	0.186
12	0.146	0.143	0.144	0.146	0.145
16	0.113	0.110	0.111	0.112	0.112
20	0.089	0.085	0.086	0.087	0.086
24	0.068	0.065	0.066	0.067	0.065
10^4 (k_{obs}), sec^{-1}	**10.73**	**10.71**	**10.73**	**10.70**	**1.72**

7.4. Discussion

In aqueous alkaline medium $[Cu(IO_6)_2]^{7-}$or DPC gets hydrated which was expressed as $Cu(HL)_2$ [34] in which HL represents the $H_3IO_6^{2-}$. The three following equilibria were found in alkaline medium.

$$2IO_4^- + 2OH^- \overset{\beta_1}{\rightleftharpoons} H_2I_2O_{10}^{4-} \quad \text{(a)}$$

$$IO_4^- + 2OH^- + H_2O \overset{\beta_2}{\rightleftharpoons} H_3IO_6^{2-} \quad \text{(b)}$$

$$IO_4^- + 2OH^- \overset{\beta_3}{\rightleftharpoons} H_2IO_6^{3-} \quad \text{(c)}$$

Thus, under the present experimental conditions the main species are expected to be $H_2IO_6^{3-}$ and $H_3IO_6^{2-}$[34] and the dimer form $[H_2I_2O_{10}^{4-}]$ is negligible under these conditions. So the total concentration of $[IO_4^-]$ added in the reaction was as follows

$$[IO_4^-] = [H_3IO_6^{2-}] + [H_2IO_6^{3-}]_e$$

(e = equilibrium concentration of substrate)

Substitute equation (b) and (c) in the above equation, then

$$[H_3IO_6^{2-}] = [HL] = \frac{\beta_2}{\beta_2 + \beta_1[OH^-]}[IO_4^-]_T$$

$$\text{If } \frac{\beta_2}{\beta_2 + \beta_1} = \frac{1}{\phi}$$

$$\text{Then } [HL] = \phi[OH^-][IO_4^-]_T \quad \text{(d)}$$

Based on the experimental results and above discussion the possible mechanism could be as follows:

$$Cu(HL)_2 + 2OH^- \overset{K_1}{\rightleftharpoons} CuL(HL) + H_2O \quad (7.2)$$

$$Cu(HL) \overset{K_2}{\rightleftharpoons} CuL + HL \quad (7.3)$$

Where CuL and $Cu(HL)_2$ are two active species of DPC in the reaction.

(I) At higher concentration of [OH^-], the equilibria of equation (7.2) and (7.3) shift left to right and CuL form exist as active species of DPC, then mechanism are proposed as scheme 1

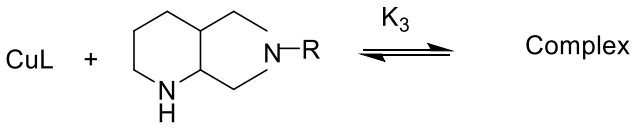

(7.4)

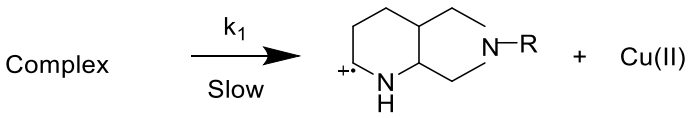

(7.5)

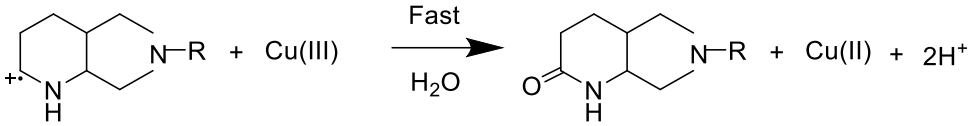

(7.6)

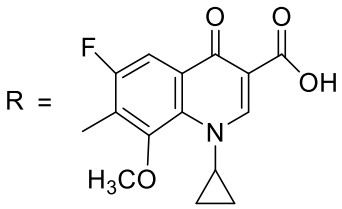

Scheme 7.1

The scheme 7.1 will lead to the following rate expression

$$\frac{-d[Cu(III)]_T}{dt} = 2k_1[C] = 2k_1K_3[CuL][MF] \tag{7.7}$$

Where [C] is the concentration of the intermediate adduct.

The total concentration of $[Cu(III)]_T$is given by equation (7.8)

$$[Cu(III)]_T = [Cu(HL)_2] + [CuL(HL)] + [CuL] + [C]$$

$$[Cu(III)]_T = \frac{[CuL][HL] + K_1[OH^-][CuL][HL] + K_1K_2[OH^-][CuL] + K_1K_2K_3[OH^-][MF][CuL]}{K_1K_2[OH^-]} \tag{7.8}$$

Substitute equation (7.8) in (7.7) then we get equation (7.9)

$$\frac{-d[Cu(III)]_T}{dt} = \frac{2k_1K_1K_2K_3[OH^-][Cu(III)]_T[MF]}{[HL]+K_1[OH^-][HL]+K_1K_2K_3[OH^-][MF]+K_1K_2[OH^-]} \quad (7.9)$$

Equation (7.9) conforms the reaction is first order with respect to DPC, under pseudo first order conditions [MF]>$[Cu(III)]_T$, the pseudo first order rate constant k_{obs} is as follows

$$k_{obs} = \frac{2k_1K_1K_2K_3[OH^-][MF]}{[HL]\{1+K_1[OH^-]\}+K_1K_2K_3[OH^-][MF]+K_1K_2[OH^-]} \quad (7.10)$$

Taking the reciprocal of equation (7.10) and after rearrangement obtained equation (7.11) is

$$\frac{1}{k_{obs}} = \frac{K_1K_2[OH^-]+[HL]+K_1[OH^-][HL]}{2k_1K_1K_2K_3[OH^-]} \bullet \frac{1}{[MF]} + \frac{1}{2k_1} \quad (7.11)$$

Equation (d) is substituted into equation (7.11), then

$$\frac{1}{k_{obs}} = \frac{K_1K_2+\phi[IO_4^-]+K_1\phi[OH^-][IO_4^-]}{2k_1K_1K_2K_3} \bullet \frac{1}{[MF]} + \frac{1}{2k_1} \quad (7.12)$$

From equation (7.12) k_{obs} decreases with increase in periodate (IO_4^-) concentration, which confirms to our results. The equation (7.11) is consistent with our experimental results and plot between $1/k_{obs}$ versus 1/[MF] **(Figure 7.10)** from the intercept of the plot the value of slow step rate constant k_1 were obtained at three different temperature [20] .The plot of log k_1 against 1/T was made and calculate the values of activation parameters **(Table 7.14)**.

(II) At low concentration of [OH^-], DPC complex exist mainly in $Cu(HL)_2$form, which means $Cu(HL)_2$ >>[CuL], so mechanism are as scheme 7.2

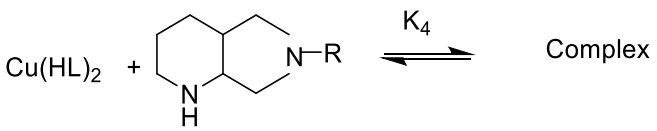

(7.13)

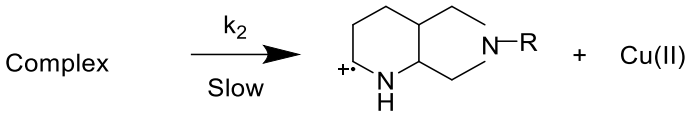

(7.14)

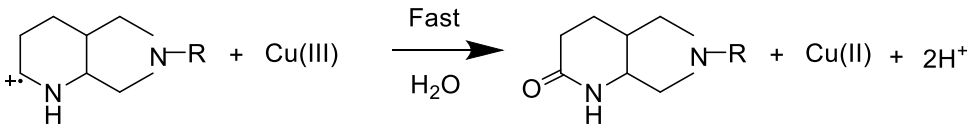

(7.15)

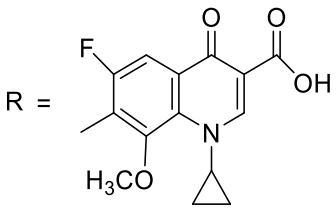

Scheme 7.2

The above scheme 7.2 leads to the following rate law

$$\frac{-d[Cu(III)_T}{dt} = 2K_1[C] = 2k_2K_4[Cu(HL)_2][MF] \tag{7.16}$$

The total concentration of Cu(III) are given as

$$[Cu(III)]_T = [Cu(HL)_2] + [CuL(HL)] + [CuL] + [C]$$

$$[Cu(III)]_T = [Cu(HL)_2]\left\{1 + K_1[OH^-] + \frac{K_1K_2[OH^-]}{[HL]} + K_4[MF]\right\} \tag{7.17}$$

$$\text{Thus } [Cu(HL)_2] = \frac{[Cu(III)]_T[HL]}{[HL] + K_1[OH^-][HL] + K_1K_2[OH^-] + K_4[MF][HL]} \tag{7.18}$$

Substituting equation (7.18) into (7.16) then resulting

$$\frac{-d[Cu(III)]_T}{dt} = \frac{2k_2K_4[Cu(III)]_T[MF][HL]}{[HL] + K_1[OH^-][HL] + K_1K_2[OH^-] + K_4[MF][HL]} \tag{7.19}$$

Hence the reaction is first order with respect to DPC so equation (7.19) becomes

$$k_{obs} = \frac{2k_2K_4[MF][HL]}{[HL]+K_1[OH^-][HL]+K_1K_2[OH^-]+K_4[MF][HL]} \quad (7.20)$$

The rearranging of equation (7.20)

$$\frac{1}{k_{obs}} = \frac{1}{2k_2K_4}\frac{(1+K_1[OH^-]+K_1K_2[OH^-][HL])}{[MF]}+\frac{1}{2k_2} \quad (7.21)$$

Equation (d) is substituted into equation (7.21), then

$$k_{obs} = \frac{2k_2K_4\phi[OH^-][IO_4^-]_T[MF]}{\phi[OH^-][IO_4^-]_T+K_1[OH^-]\phi[OH^-][IO_4^-]_T+K_1K_2[OH^-]+K_4[MF]\phi[OH^-][IO_4^-]_T} \quad (7.22)$$

$$k_{obs} = \frac{2k_2K_4[MF]}{1+K_1[OH^-]+K_4[MF]}+\frac{\phi[OH^-][IO_4^-]_T}{K_1K_2[OH^-]} \quad (7.23)$$

From equation (7.23) k_{obs} increases with increase in periodate (IO_4^-) concentration, which confirms to our results. A plot of graph between $1/k_{obs}$ versus 1/[MF] gives straight line at different three temperature and the intercept of the graph gives the value of slow step rate constant k_2 **(Figure 7.11)** [35] . A plot of log k_2 obtained at three different temperatures were made against 1/T, yielded a straight line and determine the activation parameters **(Table 7.14)**.

The entropy of activation ($\Delta S^{\neq}$) tends to be more negative for reaction of an inner-sphere nature, where as the reactions of positive $\Delta S^{\neq}$ values proceed via an outer-sphere mechanism. The obtained large negative values of $\Delta S^{\neq}$ express that the mechanism is one-electron transfer of inner-sphere nature which indicate that there is a decrease in the randomness during the reaction proceed by both two paths reaction process. This leads to the formation of intermediate complex and such activated complex is more ordered than the reactants due to loss of degree of freedom [36]. Whether, the positive value of $\Delta H^{\neq}$ indicates that the complex formation is endothermic and the value of $\Delta G^{\neq}$ suggests enhanced formation of the intermediate with raising temperature as well as to the non-spontaneity of the complex formation.

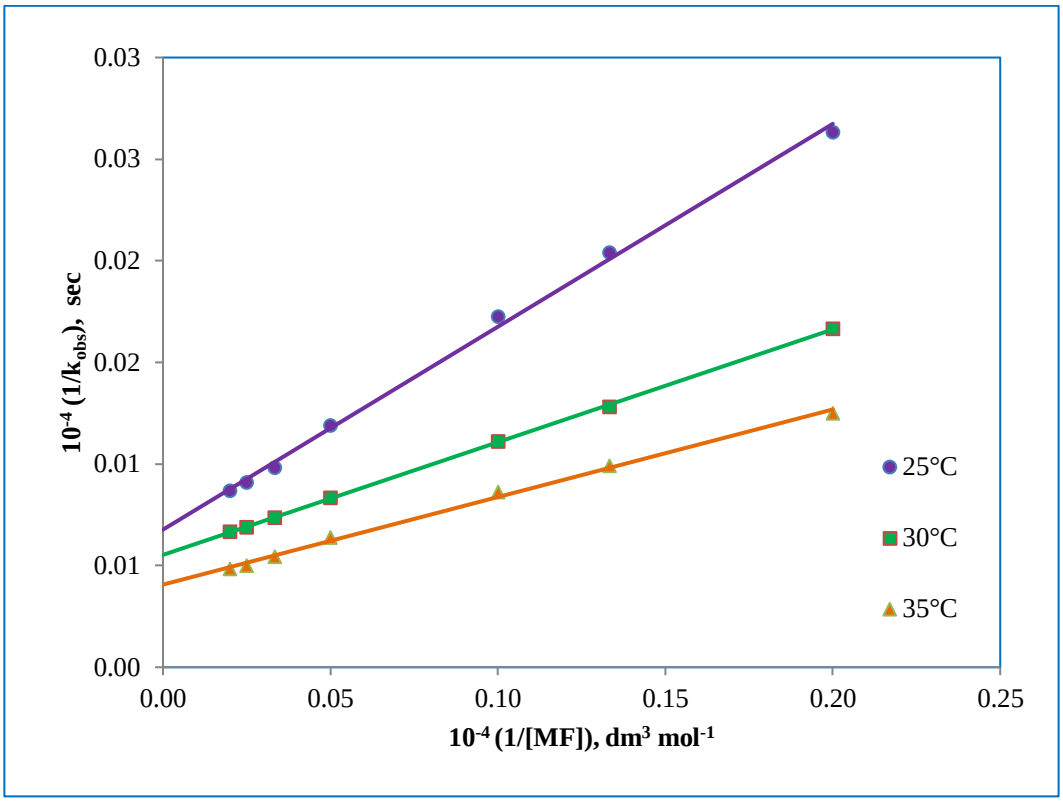

Figure 7.10: Plots of $1/k_{obs}$ versus 1/[MF] at different temperature.

[DPC] = 5.0×10^{-5} mol dm^{-3}; $[OH^-] = 30.0 \times 10^{-2}$ mol dm^{-3};

$[IO_4^-] = 2.0 \times 10^{-4}$ mol dm^{-3}; $I = 2.0 \times 10^{-2}$ mol dm^{-3}.

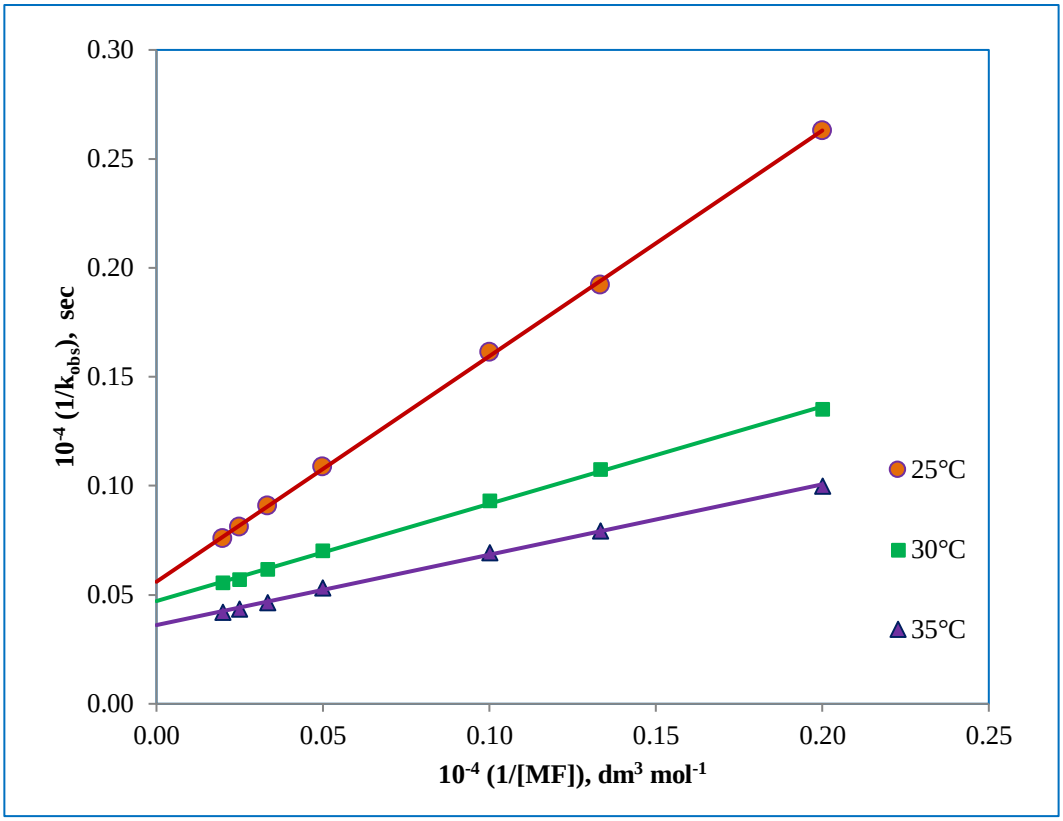

Figure 7.11: Plots of $1/k_{obs}$ versus 1/[MF] at different temperature.

[DPC] = 5.0×10^{-5} mol dm^{-3}; [OH^-] = 1.0×10^{-2} mol dm^{-3};

[IO_4^-] = 2.0×10^{-4} mol dm^{-3}; I = 2.0×10^{-2} mol dm^{-3}.

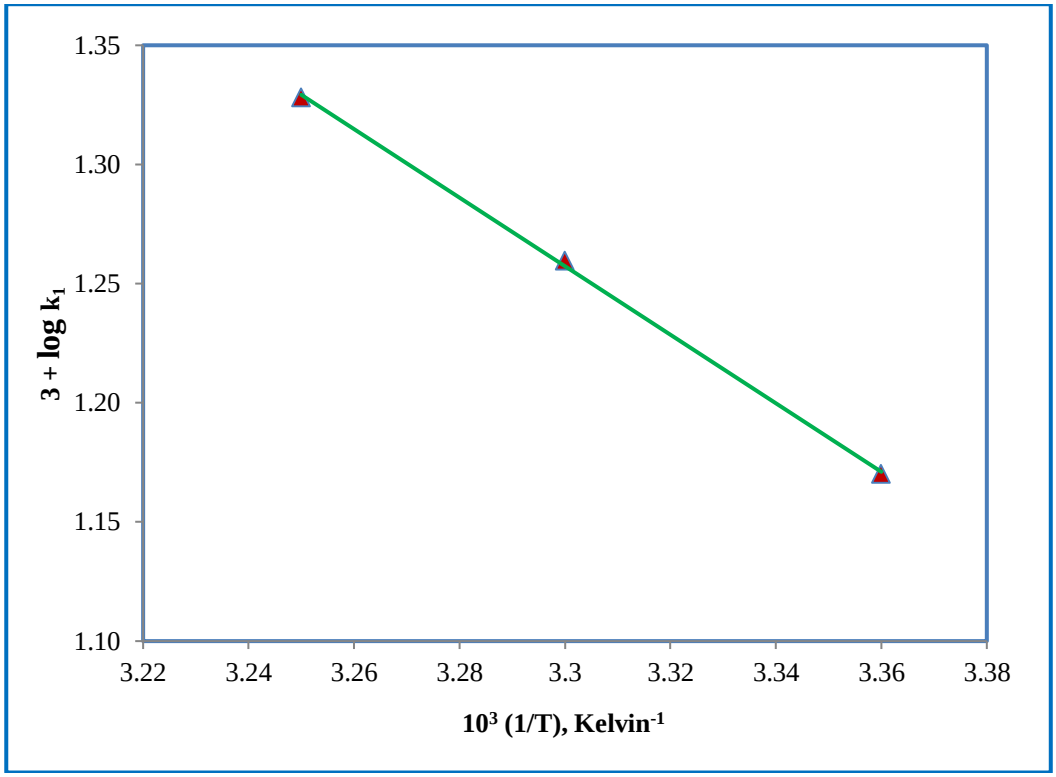

Figure 7.12: Plot of log k_1 versus 1/T.

(Ref. Table: 7.12)

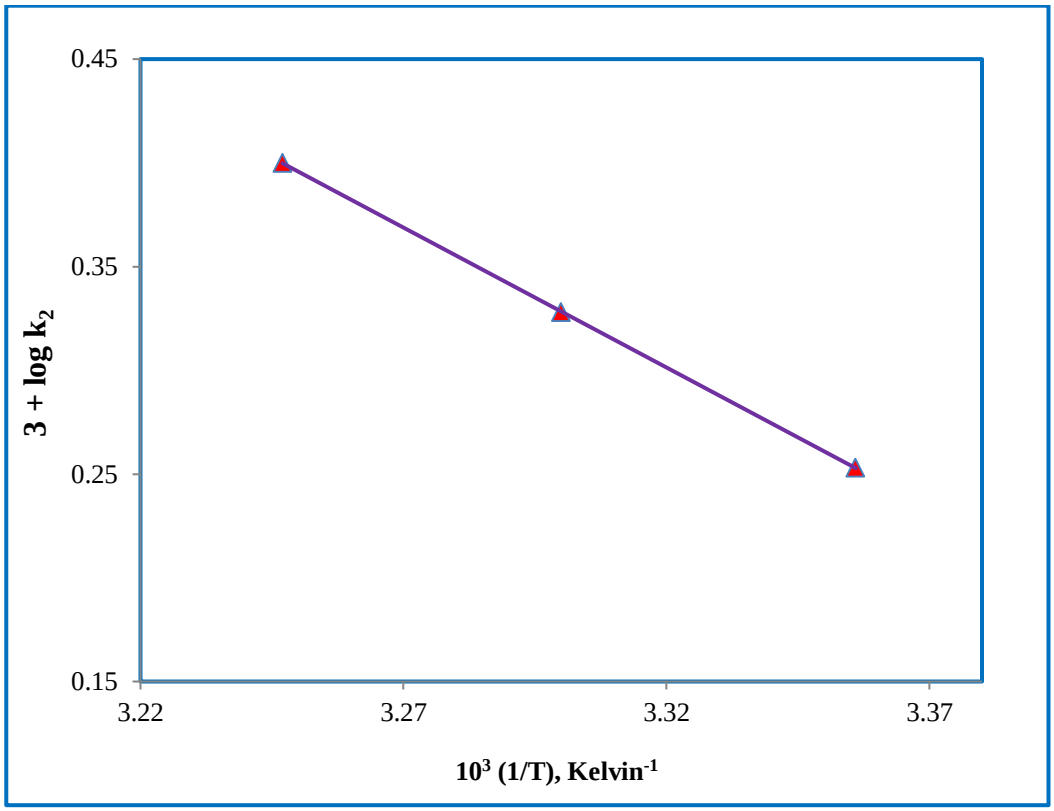

Figure 7.13: Plot of log k_2 versus 1/T.

(Ref. Table: 7.12)

TABLE: 7.14

ACTIVATION PARAMETERS EVALUATED FROM SCHEME 7.1 AND SCHEME 7.2.

Temperature (Kelvin)	**10^3 (k_1), sec^{-1} (At high $[OH^-]$)**	**Activation Parameters**	**10^3 (k_2), sec^{-1} (At low $[OH^-]$)**	**Activation Parameters**
298	14.71	E_a= 21.06 ($kJ\ mol^{-1}$)	1.79	E_a= 25.85 ($kJ\ mol^{-1}$)
303	18.18	$\Delta H^{\#}$= 18.54 ($kJ\ mol^{-1}$)	2.13	$\Delta H^{\#}$= 23.33 ($kJ\ mol^{-1}$)
308	21.28	$\Delta S^{\#}$ = – 217.13 ($JK^{-1}\ mol^{-1}$)	2.78	$\Delta S^{\#}$ = – 219.23 ($JK^{-1}\ mol^{-1}$)
		$\Delta G^{\#}$ = 84.35 ($kJ\ mol^{-1}$)		$\Delta G^{\#}$ = 89.75 ($kJ\ mol^{-1}$)

7.5. Conclusion

Oxidation of MF by DPC in aqueous alkaline medium was found to be first order with respect to diperiodatocuprate(III) and fractional order with respect to moxifloxacin. Among the various species of DPC, CuL and $Cu(HL)_2$ are two active species of DPC at different concentration of alkali. The reaction pathway involves complex formation and free radical mechanism. Rate constant of slow step and other equilibrium constants elaborate in the mechanism are calculated and activation parameters with respect to the slow step of the reaction were figure out. The overall sequence discussed here is dependable with all experimental results, including the product, mechanistic and kinetic studies. The results of the study are expected to useful for evaluating the potential risk of antibacterial agents.

7.6. References

[1] C. M. Oliphant, G. M. Green, ***Clin. Pharmacol.,*** *65* (2002) 455.

[2] R. C. Owens, P. G. Ambrose, ***Clin. Infect. Dis.,*** 41 (2005) 144.

[3] S. C. Sweetman, The complete drug reference. 36th ed. ***London: Pharmaceutical Press,*** (2009) 302.

[4] British Pharmacopoeia, Monograph on Moxifloxacin, ***London: Her Majesty's Stationary Office; Electronic version*** (2013).

[5] M. J. O'Neil, The Merck Index. 15th ed. Cambridge, ***The Royal Society of Chemistry***, (2013) 1171.

[6] M. Ferech, S. Coenen, S. M. Kumar, K.Dvorakova, E. Hendrickx, C. Seutens, H. Goossens, J. Antimicrob, ***Journal of Antimicrobial Chemotherapy***, 58(2006) 423.

[7] A. J. Watkinson, E. J. Murby, S. D. Costanzo, ***Water Res.,*** 41(2007) 4164.

[8] H. Stass, ***Drugs***, 58 (1999) 231.

[9] D. Calamari, E. Zuccato,S. Castiglioni, R. Bagnati, R. Fanelli, ***Environ. Sci. Technol.,*** 37 (2003) 1241.

[10] A. A. Robinson, J. B. Belden, M. J. Lydy, ***Environ. Toxicol. Chem.***, 24 (2005) 423.

[11] J. Fick, H. Soderstrom, R. H. Lindberg, C. Phan, M. Tysklind, D. G. J. Larsson, ***Environ. Toxicol. Chem.,*** *28* (2009) 2522.

[12] O. A. H. Jones, N. Voulvoulis, J. N. Lester, ***Crit. Rev. Toxicol.,*** 34 (2004)335.

[13] H. Yao, M. Zhang, W. Zeng, X. Zeng, Z. Zhang, ***Spectro. chim. Acta. Part A,*** 117 (2014)645.

[14] A. Kumar, P. Kumar, P. Ramamurthy, ***Polyhedron,*** 18 (1999) 773.

[15] R. S. Shettar, S. T. Nandibewoor,***J. Mol. Catal. A,*** 234 (2005)137.

[16] Y. Hu, G. Li, Z. Zhang, ***Luminescence***, 26 (2011) 313.

[17] J. E. Weder, C. T. Dillon, T. W. Hambley, B. J. Kennedy, P. A. Lay, J. R. Biffin, H. L. Regtop, N. M. Davies, ***Coord. Chem. Rev.***, 232 (2010) 95.

[18] A. M. Bagoji, P. A. Magdum, S. T. Nandibewoor, ***J. Solution Chem.,*** (2016).

[19] R. N. Hegde, N. P. Shetti, S. T. Nandibewoor, ***Polyhedron,*** 28 (2009) 3499.

[20] K. S. Byadagi, R. V. Hosahalli, S. T. Nandibewoor, S. A. Chimatadar, ***Z. Phys. Chem.***, 226 (2012) 233.

[21] K. Byadagi, M.Meti, S. T. Nandibewoor, S. Chimatadar, ***Ind. Eng. Chem. Res.,*** (2013).

[22] S. D. Lamani, P. N. Naik, S. T. Nandibewoor, ***Solution Chem.,*** 39 (2010)1291.

[23] U. R. Bagwan, A. L.Harihar, S. D. Lamani, I. N. Shaikh, A. B. Teradale, ***Research Journal of Pharmaceutical, Biological and Chemical Sciences***, 8 (2017) 1015.

[24] M. A. Angadi, S. T. Tuwar, ***J. Solution Chem.,*** 39 (2010) 165.

[25] S. A. Chimatadar, T. Basavaraj, A. Kiran, Thabaj, S. T. Nandibewoor. ***Journal of Molecular Catalysis A: Chemical,*** 267 (2007) 65.

[26] M. S. Yahya, N. Beqqal, A. Guessous, M. R. Arhoutane, K. R. K.Yahya, ***Cogent Chemistry,*** 3 (2017) 1290021.

[27] I. Ahmad, R. Bano, S. G. Musharraf, S. Ahmed, M. A. Sheraz, Q. Arfeen, M. S. Bhatti, Z. Shad, ***AAPS Pharm. Sci. Tech.,*** (2014).

[28] X. V. Doorslaer, P. M. Heynderickx, K. Demeestere, K.Debevere, H. V. Langenhove, J. Dewulf, ***Applied Catalysis B: Environmental,*** 111– 112, (2012) 150.

[29] S. S. Badi, S. M. Tuwar, ***Res. Chem. Intermed.,*** (2014).

[30] X. V. Doorslaer, K. Demeestere, P. M. Heynderickx, H. V. Langenhove, J. Dewulf, ***Applied Catalysis B: Environmental,*** 101 (2011) 540.

[31] G. H. Jeffery, J. Bassett, J. Mendham, R. C. Denney, Vogel's Textbook of Quantitative Chemical. Analysis, 5th edn. ELBS, ***Longman, Essex, UK*** 455 (1996).

[32] N. P. Shetti, S. T. Nandibewoor, ***Z. Phys. Chem.***, 223 (2009) 299.

[33] C. P. Murthy, B. Sethuram, N.Rao,***T. Z. Phys. Chem.***, 262 (1981) 252.

[34] N. Weiiun, Z. Yan, H. Kecheng, T. Changlun, Y. Hangshenc, ***Int. J.Chem. Kinet.,*** 28 (1996) 899.

[35] D. S. Munavalli, P. N. Naik, G. G. Ariga, S. T. Nandibewoor, C. Munavalli, ***Cogent Chemistry***, 1 (2015) 1068510.

[36] K. J. Laidler, 'Reaction Kinetics', ***pergamon press, oxford,*** pp. 86.

[37] A. Weissberger, E. S. Lewis, Investigation of rates and mechanism of reactions in techniques of chemistry, ***Wiley Interscience: New York,*** 4 (1974) 421.

CONCLUSION

Antibiotics are essential part of research due to their high detection frequency in the environment and the increasing bacterial resistance formation. Among various antibiotics, fluoroquinolones are of extreme interest, since they are broad spectrum antibacterials with a growing demand in hospitals, households and veterinary applications. There is major concern that antibiotics emitted into the aquatic environment can influence drinking water. Contamination with FQs has been widely disclosed all around the world in various aquatic forms including discharge or waste samples, surface water and ground water. For the degradation of FQs in aqueous solution, interesting remedy processes are desired because under oxidation–degradation process most of composed intermediates can be definitely mineralized into CO_2, water, and mineral species. Thus the present investigation is oxidative in nature, mostly drug transformations under the natural environment are most likely to follow oxidation path. Present study is based upon the kinetic and mechanistic study of oxidation-reduction reactions between useful oxidants with few of the most frequently used fluoroquinolone antibacterial agents. The proposed work will gives a novel application in the field of pharmaceuticals as well as kinetics. Nano sized colloidal manganese dioxide, hexacyanoferrate(III), diperiodatocuprate(III) used as an effective oxidants for oxidative degradation of different fluoroquinolone antibacterial agents in aqueous acidic/alkaline system. Rate constant of slow step and other equilibrium constants elaborate in the mechanism are calculated and activation parameters with respect to the slow step of the reaction were evaluated. The overall sequence discussed here is dependable with all experimental results, including the product, mechanistic and kinetic studies. The results of the study are expected to useful for evaluating the potential risk of antibacterial agents. So this study will be adequately used in waste-water treatment at the sites polluted by fluoroquinolone antibacterial agents.

SUMMARY

The fluoroquinolones have become an increasingly popular class of antibiotics for use in a variety of infections so they are extensively consumed annually in the world. Most of them are partially metabolized and excreted by humans and animals and spilled into waste water [1]. After the treatment procedure, several pharmaceuticals partially removed & remaining returned to the environment & could reach drinking water sources [2]. As a consequence of this problem, it is advisable to degrade the pharmaceuticals by different chemical procedure. In proposed research work degradation of fluoroquinolones was studied by spectrophotometric methods. These methods are of great importance in chemical & pharmaceutical analysis because of some specific advantages, such as selectively due to the measurement based on the absorbance with time of reaction, easily applicable, sensitive and processing cast is low as the reagents used are commonly available in laboratories. The importance of this study is developing a sensitive method by employing the kinetic degradation of fluoroquinolones antibacterial agents.

The present thesis describes the reaction kinetics and mechanism involved in oxidative degradation of environmentally significant few fluoroquinolones antibacterial agents by different oxidants in aqueous acidic/alkaline medium. The entire work is divided into seven chapters.

The **first chapter** deals with review on the kinetics of the oxidation of fluoroquinolone antibacterial agents in the presence of different oxidants such as manganese dioxide, hexocyanoferrate(III) and diperiodatocuperate(III). This chapter gives a brief idea about fluoroquinolones and different oxidants. The history, classification and structural developments of fluoroquinolones have also been discussed. The breakthrough for this class of antibacterial agents came when a fluorine atom and a piperazine ring were attached to the basic quinolone nucleus [3]. These substitutions increased absorption, increased antibacterial activity and reduced toxicities. The oxidation of fluoroquinolones is of interest as the oxidation products differ for different oxidants [4, 5]. The kinetics of the oxidation of various fluoroquinolones by a number of oxidants has been reported. Aqueous solutions of fluoroquinolones have been oxidized by various advanced oxidation processes [6-8], chloramine-B and N-chlorobenzotriazole [9], N-chlorosuccinimide [10], cerium(IV) [11], hexacyanoferrate(III) [12], chloramine-T [13, 14], N-bromosuccinimide [15], diperiodatoargentate(III) [16], Fe(VI) [17] etc. in both acidic and alkaline medium.

This chapter also sheds light on the oxidising properties of various oxidants. Among of these hexacyanoferrate(III) has some advantages that make it suitable for the oxidation of several organic substrates [18] and fluoroquinolone [19]. Permanganate ion oxidizes a greater variety of substrates and finds extensive application in organic synthesis [20-22]. Manganese dioxide has been most extensively studied due to good oxidizing property [23, 24]. Several forms of stable and perfectly transparent colloidal MnO_2 in aqueous [25] medium have been synthesized and kinetic study of its oxidizing behaviour in redox reactions were studied by UV-Visible spectrophotometric method. Diperiodatocuprate(III) (DPC) is one-electron transfer oxidant for the substrate [26] and kinetic study of DPC are scanty because of its low solubility and stability in aqueous medium [27, 28]. The current investigation was undertaken with the intent of computing reaction kinetics and clarifying the reaction pathways involved in oxidative degradation of the environmentally significant few fluoroquinolone antibacterial agents by various oxidants in aqueous acidic/alkaline medium.

The **second chapter** deals with the experimental part which divided into two sections. In the first section, we discuss about the numerous chemicals, reagents and their solutions prepared for the work like fluoroquinolone antibacterial agents, potassium permanganate, sodium thiosulphate, manganese sulphate, copper sulphate, potassiummetaperiodate, potassium persulphate, potassium hydroxide,sodium sulphate, sodium nitrate, sodium hydroxide, oxalic acid and sulphuric acid etc. In second section, we discuss the various analytical instruments used during the research work. The instruments such as Transmission electron microscopy (TEM),Energy dispersive X-ray (EDX) spectrometer, Zetasizer, Liquid chromatography–mass spectrophotometer (LC-MS), UV-Visible spectrophotometer, FTIR spectrophotometer, electronic balance, pH meter, are used throughout the study. TEM was used to study the morphology of synthesized MnO_2.The presence of metal in the sample was analysed by energy dispersive X-ray (EDX) spectrometer.Stability and average size have been investigated by zeta sizer. LC-MS is used for the characterization of the degradation products of the reaction. UV-Visible spectrophotometer and FTIR spectrophotometer were frequently employed to analyse the progress of reaction and identification of the reaction products of fluoroquinolones oxidation, respectively.

The **third chapter** deals with the formation and characterization of manganese dioxide and its application in oxidative kinetic study of ciprofloxacin. Soluble colloidal manganese dioxide was formed by reduction of potassium permanganate with sodium thiosulphate in neutral aqueous medium at 25 ºC. The obtained nanosized colloidal manganese dioxide was found to be dark reddish brown in color and stable for several months. The formation of manganese dioxidewas confirmed by UV-visible spectrophotometer and determination of oxidation state of Mn species in manganese dioxide. The effect of different concentration of sodium thiosulphate on formation of manganese dioxide was also studied. The nano sized colloid manganese dioxide was characterized by transmission electron microscopy and Fourier transform infrared spectrophotometer. The formed soluble colloidal manganese dioxidewas used as an oxidant in oxidation of ciprofloxacin in perchloric acid medium at 35ºC. The reaction was first order with respect to concentration of manganese dioxide and hydrogen ion but fractional order with ciprofloxacin. The results suggest formation of complex between ciprofloxacin and manganese dioxide. The oxidation products were also identified on the basis of stoichiometric and characterization results.

The **fourth chapter** illustrates the kinetics of oxidation of levofloxacin by water soluble manganese dioxide has been studied in aqueous acidic medium at 25 ºC temperature. The stoichiometry for the reaction was indicates that the oxidation of one mole of levofloxacin requires one mole of manganese dioxide. The reaction is second order that is first order with respect to manganese dioxide and levofloxacin. The rate of reaction is increases with the increasing of $[H^+]$ ion concentration. A probable reaction mechanism, in agreement with the observed kinetic results, has been proposed and discussed and activation parameters have also been calculated.

The **fifth chapter** consists the Cu(II) catalyzed oxidation of ciprofloxacin by hexacyanoferrate(III) has been investigated spectrophotometricallyin an aqueous alkaline medium at 40˚C. The stoichiometry for the reaction indicates that, the oxidation of one mole of ciprofloxacin requires two moles of hexacyanoferrate(III). The reaction exhibited first order kinetics with respect to [hexacyanoferrate(III)]and less than unit order with respect to [ciprofloxacin] and $[OH^-]$. The products were also identified on the basis of stoichiometric

results and confirm by the characterization results of LC-MS and FT-IR analysis. All the possible reactive species of the reactants have been discussed and a most probable kinetic model has been envisaged. Theactivation parameters with respect to the slow step of the mechanism were computed and thermodynamic quantities were also determined.

The **sixth chapter** deals with the uncatalyzed and Cu(II) catalyzed oxidative degradation of antibacterial drug ofloxacin by hexacyanoferrate(III) in aqueous alkaline medium at 40˚C temperature.The stoichiometry of the reaction indicates that the oxidation of one mole of ofloxacin requires two moles of hexacyanoferrate(III). The uncatalyzed reaction exhibited first order kinetics with respect to [hexacyanoferrate(III)] and [ofloxacin] and less than unit order with respect to [OH^-].The catalyzed reaction gives first order kinetics with respect to [hexacyanoferrate(III)] and [OH^-] and less than unit order with respect to [ofloxacin].The products were also identified on the basis of stoichiometric results and confirm by the characterization results of LC-MS and FT-IR analysis**.** The major product of the reaction obtained by the decarboxylation of the quinolones moiety and hence it may retain the antibacterial activity.

The **seven chapter** consists a kinetic study of oxidation of moxifloxacin by diperiodatocuprate(III) in aqueous alkaline medium. The stoichiometry of the reaction indicates one mole moxifloxacin oxidizes by two mole of diperiodatocuprate(III). The reaction was first order with respect to [diperiodatocuprate(III)] and less than unity order with [moxifloxacin]. The pseudo-first-order rate constant (k_{obs}) changes differently under different concentration of alkali. The results indicates at higher hydroxyl ion concentration diperiodatocuprate(III) complex exist in CuL whereas at lower hydroxyl ion concentration in form of $Cu(HL)_2$.The final product of oxidation was identified by instrumental techniques. Based on the experimental observations, a plausible mechanism and rate law is proposed at different concentration of alkali. The activation parameters were also determined and discussed.

REFERENCES

[1] R. M. Kulkarni,M. S. Hanagadakar, R. S. Malladi, M. S. Gudaganatti, H. S. Biswal, S. T. Nandibewoor, ***Indian J. Chem. Technol.,*** 21 (2014) 38.

[2] R. M. Kulkarni, R. S. Malladi, M. S. Hanagadakar, M. R. Doddamani, U. K. Bhat, ***Desalination and Water Treatment,*** 57 (2016) 16111.

[3] H. Salem, ***American Journal of Applied Sciences,*** 2 (2005) 719.

[4] M. S. Gudaganatti, M. S. Hanagadakar, R. M. Kulkarni, R. S. Malladi, R. K. Nagarale, ***Prog. React. Kinet. Mech.,*** 37 (2012) 366.

[5] M. B. Patgar, S. T. Nandibewoor, S. A. Chimatadar, ***Cogent Chemistry,*** 1 (2015) 1.

[6] P. Wang, H. Yi-Liang, C. H. Ching-Hua, ***Water Res.***44 (2010) 5989.

[7] M. C. Dodd, A. D. Shah, U.V. Gunten, C-H. Huang,***Environ. Sci. Technol.*****39 (**2005) 7065.

[8] B. De Witte, J. Dewulf, Demeestere, H. Langenhove, ***J. Hazard. Mater.,*** 161 (2009) 701.

[9] S. A. M. Ebraheem, A. A. Elbashir,N. Nanda, S. M. Mayanna, N. M. M. Gowda, ***Int. J. Chem. Kinet.***31 (1999) 153.

[10] N. Nanda, P. Kumar, Malini, ***Int. J. Pharm. Sci. Rev. Res.,*** 23(2013) 388.

[11] S. A. M. Ebraheem, A. A. Elbashir, ***American Academic & Scholarly Research Journal,*** 4 (2012) 89.

[12] N. Diab, I. Abu-Shqair, M. Al-Subu, R. Salim, ***International Journal of Chemistry,*** 34 (2013) 1388.

[13] A. A. P. Khan, A. M. Asiri,N. Azum,M. A. Rub,A. Khan,O. A. Al-Youbi, ***Ind. Eng. Chem. Res.,*** 51 (2012) 4819.

[14] A. Shrivastavaa, A. K. Singh, N. Sachdev, D. R. Shrivastava, Y. Katre, S. P. Singh, M. Singh, J. C. Mejuto, ***J. Mol. Catal. A: Chem.,*** 1 (2012) 361.

[15] A. A. P. Khan, A. Khan, A. M. Asiri, S. A. Khan, ***J. Mol. Liq.,*** 218 (2016) 604.

[16] H. T. Padavathil, S. Mavalangi, S. T. Nandibewoor, ***American International Journal of Research in Science, Technology, Engineering & Mathematics,*** 3 **(**2013) 63.

[17] B. Yang, R. S. Kookana, M. Williams, A. Kumar, ***J. Hazard. Mater.,*** (2016) 320.

[18] M. M. A. I. Suber, AnNajah, ***J. Res.,*** 7 (1992) 37.

[19] Ibrahim Diab Najeeb Aubu – Shquari, ***Ph.D. Thesis***, (2006).

[20] R. Stewart, ***Oxidation In Organic Chemistry Part (A), New York Academic Press,*** (1965).

[21] D. G. Lee, ***Oxidation In Organic Chemistry Part (D), New York Academic Press,*** (1982).

[22] A. J. Fatiadi, ***Synthesis,*** 106 (1987) 85.

[23] F. Kienzle, ***Tetrahedron Lett.,*** 24 (1983) 2213.

[24] S. Taniguchi, ***Bull. Chem. Soc. Jpn.,*** 57 (1984) 2683.

[25] J. F. Perez-Benito, E. Brillas, R. Pouplana, ***Inorg. Chem.,*** 28 (1989) 390.

[26] Y. Hu, G. Li, Z. Zhang, ***Luminescence,*** 26 (2011) 313.

[27] A. M. Bagoji, P. A. Magdum, S. T. Nandibewoor, ***J. Solution Chem.*** (2016) (doi 10.1007/s10953-016-0539-x)

[28] U. R. Bagwan, A. L. Harihar, S.D. Lamani, I. N. Shaikh, A. B. Teradale, ***Research Journal of Pharmaceutical, Biological and Chemical Sciences,*** 8 (2017) 1015.

Research Scholar **Supervisor**

Gajala Tazwar **Dr. (Mrs.) Vijay Devra**

(Associate Professor)

J.D.B. Govt. Girls College, Kota

BIBLIOGRAPHY

List of papers published and communicated: 12

1. "Uncatalyzed and Cu(II) Catalyzed Oxidation of Ofloxacin in Aqueous Alkaline Medium: A Kinetic and Mechanistic Study", **Gajala Tazwar**, Vijay Devra, **International Journal of Pharmaceutical Science and Research, (Communicated)**.

2. "Kinetics and Mechanism of Oxidation of Moxifloxacin – A Fluoroquinolone Drug by Diperiodatocuprate(III) in Aqueous Alkaline Medium," **Gajala Tazwar**, Vijay Devra, **, International Journal of Pharmaceutical Sciences and Drug Research (Communicated)**.

3. "Soluble Colloidal Manganese Dioxide: Formation, Characterization and Application in Oxidative Kinetic Study of Ciprofloxacin", **Gajala Tazwar**, Vijay Devra, **Journal of the Iranian Chemical Society, Springer, (Communicated)**.

4. "Kinetics and Mechanism of Electron-Transfer Reactions: Oxidation of Nalidixic Acid by Diperiodatocuprate (III) in Aqueous Alkaline Medium", **Gajala Tazwar,** Mahima Sharma, Vijay Devra, **International Journal of Pharmacy and Pharmaceutical Research**, 11 (2018) 231-247.

5. "Kinetic and Mechanistic Study of Ciprofloxacin in Aqueous Alkaline Medium", **Research Journal of Recent Sciences**, **Gajala Tazwar**, Naveen Mittal, Vijay Devra, 7 (2018) 6-12.

6. "Preparation of Colloidal Manganese Dioxide and their Application in Degradation of Antibacterial Drug", Mahima Sharma, **Gajala Tazwar**, Vijay Devra, **International Journal of Advance Research in Science and Engineering**, 7 (Special Issue No. 2) (2018) 416-421.

7. "Oxidative Degradation of Levofloxacin by Water-Soluble Manganese Dioxide in Aqueous Acidic Medium: A Kinetic Study", **Chemical Papers (Springer), Gajala Tazwar**, Ankita Jain, Vijay Devra, 71 (2017) 1749-1758, Doi: 10.1007/s11696-017-0167-y.

8. "Oxidation of Ciprofloxacin by Hexacyanoferrate(III) in the Presence of Cu(II) as a Catalyst: A Kinetic Study", **International Journal of Chemical Kinetics (John Wiley), Gajala Tazwar**, Ankita Jain, Naveen Mittal, Vijay Devra, (2017), Doi:10.1002/kin.21097.

9. "Catalytic Oxidation of Levofloxacin by Hexacyanoferrate (III) in Aqueous Alkaline Medium: A Kinetic Study", **Gajala Tazwar**, Ankita Jain, Vijay Devra, **International Journal of Advance Research in Science and Engineering**, 6 (2017) 654-665.

10. "Kinetics and Mechanism of Permanganate Oxidation of Nalidixic Acid in Aqueous Alkaline Medium", **Journal of Applied Pharmaceutical Science**, Ankita Jain, **Gajala Tazwar**, Vijay Devra, 7 (2017) 135-143.

11. "Oxidation of Levofloxacin by Acidic Permanganate: A Kinetic and Mechanistic Study", **International Journal of Research in Pharmacy and Science**, Ankita Jain, **Gajala Tazwar**, Vijay Devra, 5 (2015) 1-8.

12. "Synthesis, Characterization and Catalytic Application of Copper Nanoparticles on Oxidation of Alanine in Acid Aqueous Medium", Shikha Jain, **Niharika Nagar,** Vijay Devra, **International Journal of Current Engineering and Technology**, 5 (2015) 966-973.

Papers Presented and Participate in International and National Conferences/Seminars/ Workshops.

1. **Gajala Tazwar** participates in "Workshop on intellectual property right (IPR) and Indian patent system" organised by Rajasthan Technical University Kota and Department of Science & Technology (DST), Rajasthan Council of Science & Technology (RAJCOST) at Rajasthan Technical University Kota, during 28-29 September 2018.

2. "Environmental pollution" Vijay Devra, **Gajala Tazwar**, Niharika Nagar, Pranav Kachhawah, participate in "Rajasthan Hackathon 4.0" organised by Rajasthan State Pollution Control Board at Jaipur, during 19th-21th March 2018.

3. "Preparation of colloidal manganese dioxide and their application in degradation of antibacterial drug", **Gajala Tazwar**, Vijay Devra. Paper Presentation in **"13th International Conference on Recent trends in engineering Science and Management"** at Vedant College of Engineering & Technology, Bundi (Rajasthan), during 21th to 22nd January, 2018.

4. "A Kinetic Study of Oxidation of Fluoroquinolone Drug- An Environmental Pollutant", **Gajala Tazwar**, Vijay Devra, oral paper presentation in "Environmental Changes and their Impact on Plants and Human Health" at St. Wilfred's P.G. College, Jaipur during 15th to 17th January, 2018.

5. **Gajala Tazwar** participates in "Author Workshop jointly organized by Springer Nature and University of Kota" at University of Kota, Kota, during 2nd March 2017.

6. "Experimental investigation on green synthesis of metal nano particles and then catalytic application", Niharika Nagar, **Gajala Tazwar**, Vijay Devra,

research Project participation in "**Anveshan Students' Research Convention (West Zone)**" at Nims University (Jaipur), during 7th-8th March 2017.

7. "Experimental investigation on green synthesis of metal nanoparticles and then catalytic application", Niharika Nagar, **Gajala Tazwar**, Vijay Devra, research project presentation in "**University Student Research Convention**" at University of Kota, Kota, during 27th to 28th Feburary, 2017.

8. "Catalytic Oxidation of Levofloxacin by Hexacyanoferrate (III) in Aqueous Alkaline Medium: A Kinetic Study", **Gajala Tazwar**, Ankita Jain, Vijay Devra, Paper Presentation in **"International Conference on Innovative Research in Science, Technology and Management"** at Modi Institute of Management and Technology, Dadabari, Kota, Rajasthan during 22nd to 23rd January, 2017.

9. "**Synthesis and characterization of copper nanoparticles using ascorbic acid as reducing and capping agent", Gajala Tazwar**, Naveen Mittal, Vijay Devra, poster presentation in UGC-DAE Consortium for Scientific Research at University campus, Indore in Silver Jubilee Conference on Study of Matter Using Intense Radiation Sources and Under Extreme Conditions, during 6th – 7th November 2016.

10. **Gajala Tazwar** participates in "Workshop on patents, trade marks & copyrights" at Department of Science & Technology, Vigyan Kendra, Kota, during 19th March 2016.

11. "**Kinetic and Mechanistic Study of Ofloxacin in Aqueous Acidic Medium", Gajala Tazwar**, Naveen Mittal, Vijay Devra, oral paper presentation in Indian Chemical Society "**52nd Annual Convention of Chemists 2015**" at JECRC University, Jaipur (Rajasthan), during 28th – 30th December 2015.

12. "Synthesis of Copper Nanoparticles and their catalytic application in oxidation reaction", Shikha Jain, **Gajala Tazwar**, Niharika Nagar**,** Vijay Devra. Paper Presentation in 5th International Conference on **"Advance Trends in Engineering, Technology and Research" (ICATETR-2015),** at Bal Krishna Institute of Technology, Ranpur, Kota (Rajasthan), during 23rd to 24th December, 2015.

13. **Gajala Tazwar,** Vijay Devra. Oral Presentation of Research Work of Thesis in **Annual Research Seminar Organized by Centre For Excellence (Model College)** at J. D.B. Govt. Girls College, Kota on 30th January, 2015.

Oxidative degradation of levofloxacin by water-soluble manganese dioxide in aqueous acidic medium: a kinetic study

Gajala Tazwar, Ankita Jain & Vijay Devra

Chemical Papers

ISSN 0366-6352

Chem. Pap.
DOI 10.1007/s11696-017-0167-y

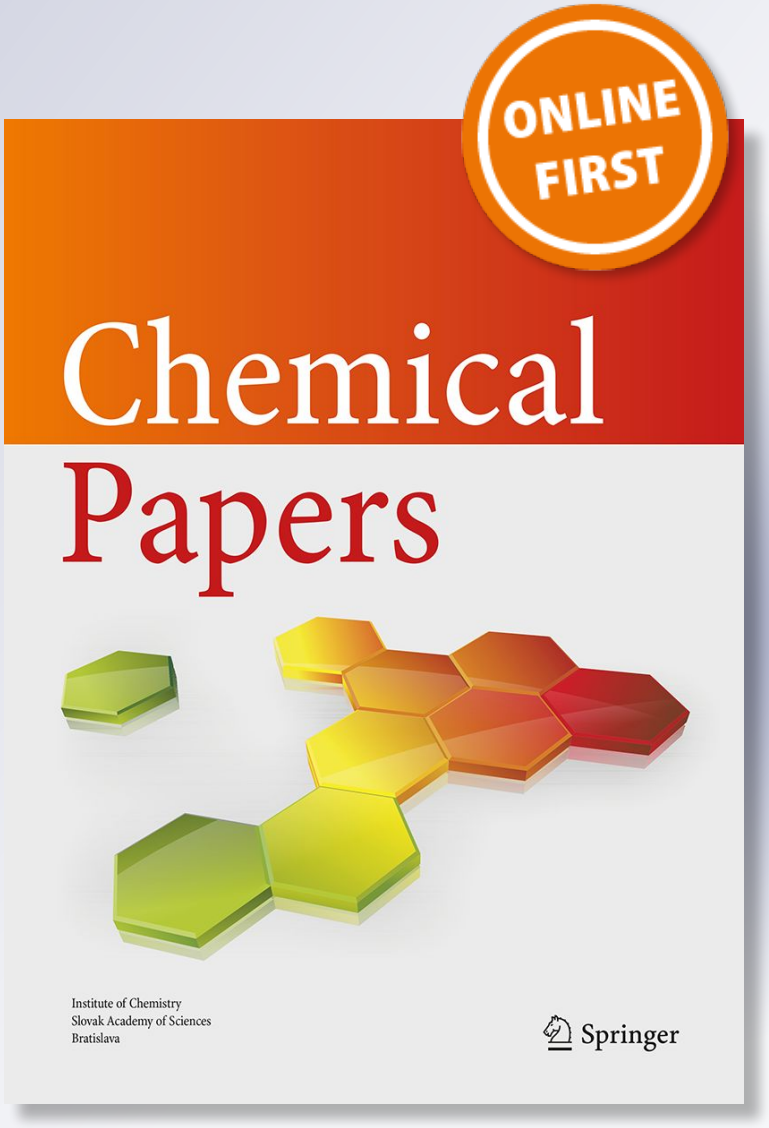

Springer

Chem. Pap.
DOI 10.1007/s11696-017-0167-y

ORIGINAL PAPER

Oxidative degradation of levofloxacin by water-soluble manganese dioxide in aqueous acidic medium: a kinetic study

Gajala Tazwar[1] · Ankita Jain[1] · Vijay Devra[1]

Received: 10 January 2017 / Accepted: 3 April 2017

Abstract Pharmaceuticals, especially fluoroquinolone antibiotics, have received increasing global concern, due to their intensive use in the environment and potential harm to ecological system as well as human health. Degradation of antibiotics, such as oxidative degradation by metal oxides, often plays an important role in the elimination of antibiotics from the environment. The kinetics of oxidation of levofloxacin by water-soluble manganese dioxide has been studied in aqueous acidic medium at 25 °C temperature. The stoichiometry for the reaction indicates that the oxidation of 1 mol of levofloxacin requires 1 mol of manganese dioxide. The reaction is second order, that is first order with respect to manganese dioxide and levofloxacin. The rate of reaction increases with the increasing $[H^+]$ ion concentration. A probable reaction mechanism, in agreement with the observed kinetic results, has been proposed and discussed. The energy and enthalpy of activation have been calculated to be 30.54 and 28.07 kJ mol^{-1}, respectively.

Keywords Levofloxacin · Manganese dioxide · Kinetics · Mechanism · Oxidation

✉ Vijay Devra
v_devra1@rediffmail.com

Gajala Tazwar
tazwar.gajala786@gmail.com

Ankita Jain
ankita.jainswm@gmail.com

[1] Department of Chemistry, J.D.B. Govt. Girls P.G. College, Kota, Rajasthan 324001, India

Introduction

In the past few decades, there has been great concern on pharmaceuticals waste which is a key source of impurities in the aquatic ecosystem, ground water and soil, and which leads to the bacterial resistance against antibiotics even at their low concentrations (Elmolla and Chaudhari 2010). Fluoroquinolones are anthropogenic contaminants which are comprehensively used as pharmaceuticals for both human and veterinary purposes (Kusari et al. 2009; Sturini et al. 2012). Levofloxacin (LEV), (-)-(*S*)-9-fluoro-2,3-dihydro-3-methyl-10-(4-methyl-1-piperazinyl)-7-oxo-7H pyrido [1,2,3-de]-1,4-benzoxazine-6-carboxylic acid hemihydrates, is one of the commonly used third-generation fluoroquinolone antimicrobials, being the active *S*-isomer isolated from racemic ofloxacin and is twice as active as the parent drug. LEV is a broad-spectrum drug of activity against various bacteria, including Gram-positive and Gram-negative microorganisms (Croisier et al. 2004; Roblin and Hammerschlag 2003). Because of its effective antibacterial activity and low frequency of adverse effects on oral administration, it has been widely used for the treatment of infectious diseases, such as community-acquired pneumonia and acute exacerbation of chronic bronchitis (Owens and Ambrose 2000). Waste water discharge from conventional waste water treatment plants is the main source of LEV in the aquatic environment (Kummerer 2009; Fatta-Kassinos et al. 2011). Removal of LEV residue from aquatic environment is, therefore, considered as a priority and serves as an important study. The oxidative study of LEV has been effectuated by various oxidants such as alkali permanganate (khan et al. 2010), acidic Chloramine-T (Khan et al. 2012), ozone and hydroxyl radicals (Najjar et al. 2013), aqueous chlorine (Kulkarni et al. 2013), acidic permanganate (Jain et al.

Published online: 12 April 2017

2015), hexacyanoferrate(III) (Patgar et al. 2015), etc. Many other degradation and transformation studies are also available in the literature (Gudaganatti et al. 2012; Gupta et al. 2017; Yahvya et al. 2016).

Manganese dioxide (MnO_2) is one of the most active and important oxidative components, showing high potency in degrading various organic pollutants such as antibacterial agents (Zhang and Haung 2005; Zhang et al. 2008). Perez-Benito et al. found first time that water-soluble manganese dioxide can be prepared from reduction of aqueous potassium permanganate by sodium thiosulfate under neutral condition (Perez-Benito et al. 1989) and the prepared MnO_2 was used in the oxidation of organic acids (Perez-Benito and Arias 1992; Perez-Benito et al. 1996; Perez-Benito 2002) by MnO_2. MnO_2 exhibits considerable activity in oxidation–reduction reactions due to the presence of different oxidation states of manganese ions (Stone and Morgan 1984). It has been reported in several studies that the intermediate (Mn(IV)) could be H_2MnO_4, H_2MnO_3, or a water-soluble colloidal MnO_2 (Mata-Perez and Perez-Benito 1985; Freeman et al. 1981). Water-soluble colloidal MnO_2 has the advantage over water-insoluble forms as conventional UV–visible spectrophotometer can be used to monitor their reactions with organic and inorganic subtracts.

A literature survey confessed that the kinetics and mechanism of degradation of some antibiotics by MnO_2 in aqueous acidic/alkaline medium have been studied earlier (Chen et al. 2011; Singh et al. 2016). But yet lack of literature on the oxidative degradation of LEV by MnO_2 in aqueous acidic medium has been reported, so the title reaction prompted us to understand the mechanism of the reaction.

Experimental

Chemicals

The solution of LEV (KORES India Limited) was prepared by dissolving known amounts of the samples in double distilled water. Solutions of LEV were always freshly prepared before experiment. Potassium permanganate (MERCK) and sodium thiosulfate (BDH) were used as received. Sulfuric acid (MERCK) and sodium sulfate (MERCK) were used to maintain the acidity and ionic strength, respectively. All other reagents were of AR or GR MERCK quality. Double distilled water was employed throughout the study.

Instrumentation

For kinetic measurements, a Peltier accessory (temperature-Controlled) attached to a double-beam UV 3000^+, UV–Visible spectrophotometer (LABINDIA) with UV path length 1.0 cm in the spectral range 200–800 nm, was used. Spectrum of sample was recorded from Fourier Transform Infrared (FT-IR) Spectrophotometer (ALPHA-T, Bruker) in the range of 400-4000 cm^{-1} by mixing the sample with dried KBr (in 1:20 weight ratio) with a resolution of 4 cm^{-1}. For product analysis, LC–ESI–MS (Q-TOF Micromass, WATERS Company, UK) was used.

Preparation of MnO_2

According to the Perez-Benito method, for the preparation of water-soluble MnO_2, the required volume of $Na_2S_2O_3$ solution (20 cm^3, 1.88 $\times$ 10^{-2} mol dm^{-3}) was added to a standard solution of $KMnO_4$ (10 cm^3, 0.1 mol dm^{-3}) and the reaction mixture was diluted by the required volume of water in 2 dm^{-3} standard flask (Perez-Benito et al. 1989). The stoichiometric equation is expressed as:

$$8MnO_4^- + 3S_2O_3^{2-} + 2H^+ \rightarrow 8MnO_2 + 6SO_4^{2-} + H_2O. \quad (1)$$

The resulting solution was dark brown and perfectly transparent and stable for several weeks. The absorption spectrum of the reaction mixture consists of one broad band covering the whole visible region of the spectrum with λ_{max} 390 nm. The application of Beer's law of MnO_2 at 390 nm had been verified giving $\varepsilon = 15{,}660$ dm^3 mol^{-1} cm^{-1} (Akram et al. 2011).

Kinetic measurements

The reaction was initiated by mixing the solutions of MnO_2 and LEV which also contained the required concentration of H_2SO_4 and Na_2SO_4 at 25 °C. The progress of the reaction was followed by spectrophotometrically at 390 nm (Fig. 1), that there was no interference from other species in the reaction mixture at this wave length. Initial rates were computed employing plane mirror method. The pseudo-first-order plots were also made wherever reaction conditions permitted. Results in triplicate were reproducible to within ±6%.

Stoichiometry and product analysis

The stoichiometry of the reaction was determined with various ratios of reactants and the constant concentration of H_2SO_4 and Na_2SO_4 was kept for 12 h at room temperature in a closed vessel. After completion of the reaction,

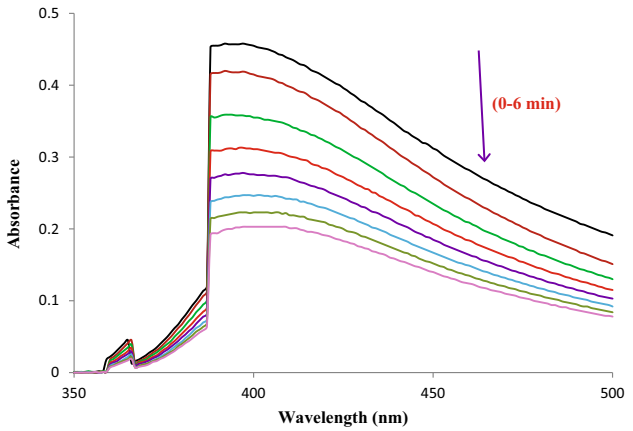

Fig. 1 Spectral changes during the oxidation of LEV by MnO_2 in acidic medium at 25 °C. $[MnO_2] = 3.0 \times 10^{-5}$ mol dm^{-3}, $[LEV] = 5.0 \times 10^{-5}$ mol dm^{-3}, $[H_2SO_4] = 2 \times 10^{-4}$ mol dm^{-3}, $I = 5 \times 10^{-4}$ mol dm^{-3}

unreacted MnO_2 indicates that one mole of LEV was oxidized by one mole of MnO_2, exhibiting 1:1 ratio for the consumption of reductant to oxidant (Table 1).

LC–MS analysis of LEV oxidation reaction indicates the formation of product with molecular ion of *m/z* 279 (Fig. 3). The *m/z* 279 corresponds to fully dealkylation of the piperazine ring (Li et al. 2015). It is worth noting that oxidation of piperazine moiety of LEV between oxidized centres and nitrogen atoms leads to distinctive mass loss $m/z = 83$. This was attributed to ring opening, dealkylation and deamination process, which finally yielded 7-amino fluoroquinolone product. The by-product formaldehyde was identified by spot test (Fiegl 1975). The other product ammonia was detected by Nesseler's reagent test (Vogel 1973).

Results and discussion

Effect of manganese dioxide concentration

The concentration of MnO_2 was varied in the range (0.75 to 7.5) $\times 10^{-5}$ mol dm^{-3} at two but fixed concentration of LEV to be 5×10^{-5} and 6×10^{-5} mol dm^{-3}, $[H_2$-

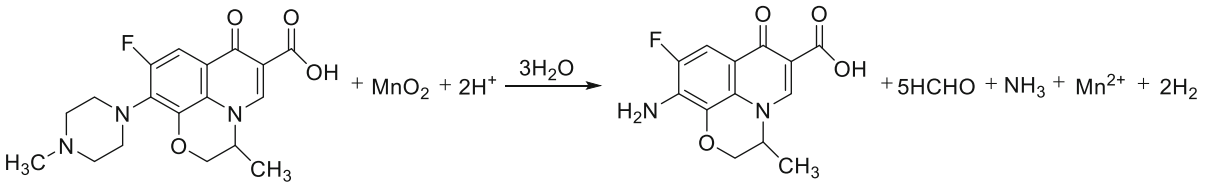

Levofloxacin

(2)

The product was extracted from the reaction mixture with ether. The product 10-amino-9-fluoro-2,3-dihydro-3-methyl-7-oxo-7H-pyrido [1,2,3-de]-1,4-benzoxazine-6-carboxylic acid was identified with the help of TLC and characterized by FT-IR and LC–MS analysis. FT-IR analysis confirmed the presence of $-NH_2$ group in the oxidation product (Fig. 2). The IR spectrum shows a peak at 3412.70 cm^{-1} which is due to –NH stretching of the $-NH_2$ group and the remaining peaks are of the parent compound.

Table 1 Stoichiometry of manganese dioxide and levofloxacin in aqueous acidic medium

$[MnO_2]$ mol dm^{-3}	[LEV] mol dm^{-3}	$\frac{\Delta[LEV]}{\Delta[MnO_2]}$
0.0005	0.0002	1:1
0.0005	0.0003	1:1
0.0005	0.0004	1:0.98
0.0006	0.0004	1:0.98

$SO_4] = 2 \times 10^{-4}$ mol dm^{-3} and $[Na_2SO_4] = 3 \times 10^{-4}$ mol dm^{-3} at 25 °C. Initial rates (k_i mol dm^{-3} s^{-1}) were calculated employing plane mirror method and a plot of initial rate (k_i) versus $[MnO_2]$ was made that yielded a straight line passing through the origin ascribing first-order dependence with respect to MnO_2 ($r^2 \geq 0.998$). Second-order plots were also made by making plots of log $([LEV]_t/[MnO_2]_t)$ against time ($r^2 \geq 0.985$) (Fig. 4). Second order rate constants constants have good agreement, calculated from initial rates as well as second order plots (Table 2).

Effect of levofloxacin concentration

The concentration of LEV was varied from (1.0–10.0) $\times 10^{-5}$ mol dm^{-3} at two but fixed concentration of MnO_2 viz. 2×10^{-5} and 3×10^{-5} mol dm^{-3}, $[H_2SO_4] = 2.0 \times 10^{-4}$ mol dm^{-3} and $[Na_2$-$SO_4] = 3.0 \times 10^{-4}$ mol dm^{-3} at 25 °C. Initial rates (k_i

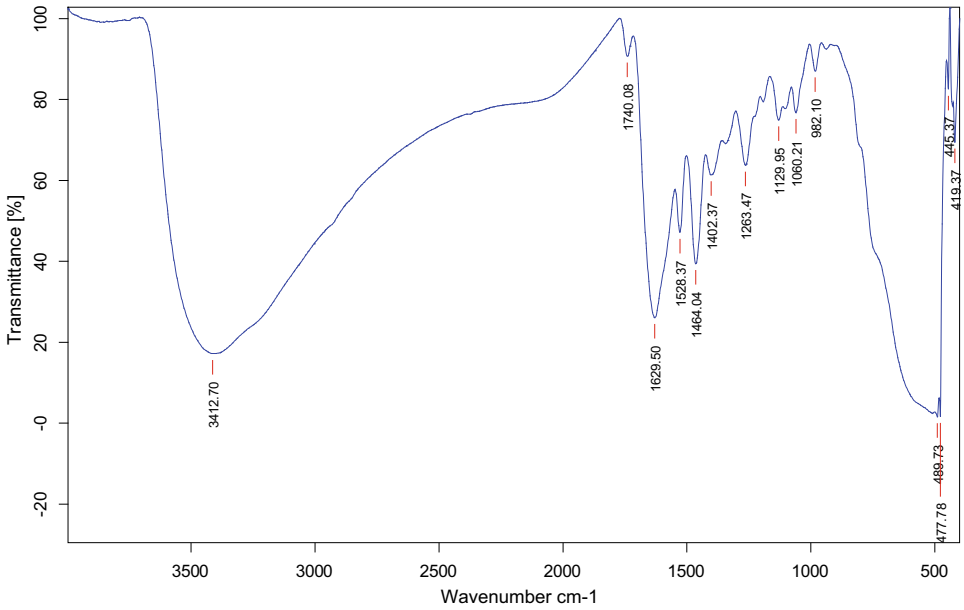

Fig. 2 FTIR spectra of the oxidative product of LEV by MnO_2 in aqueous acidic medium

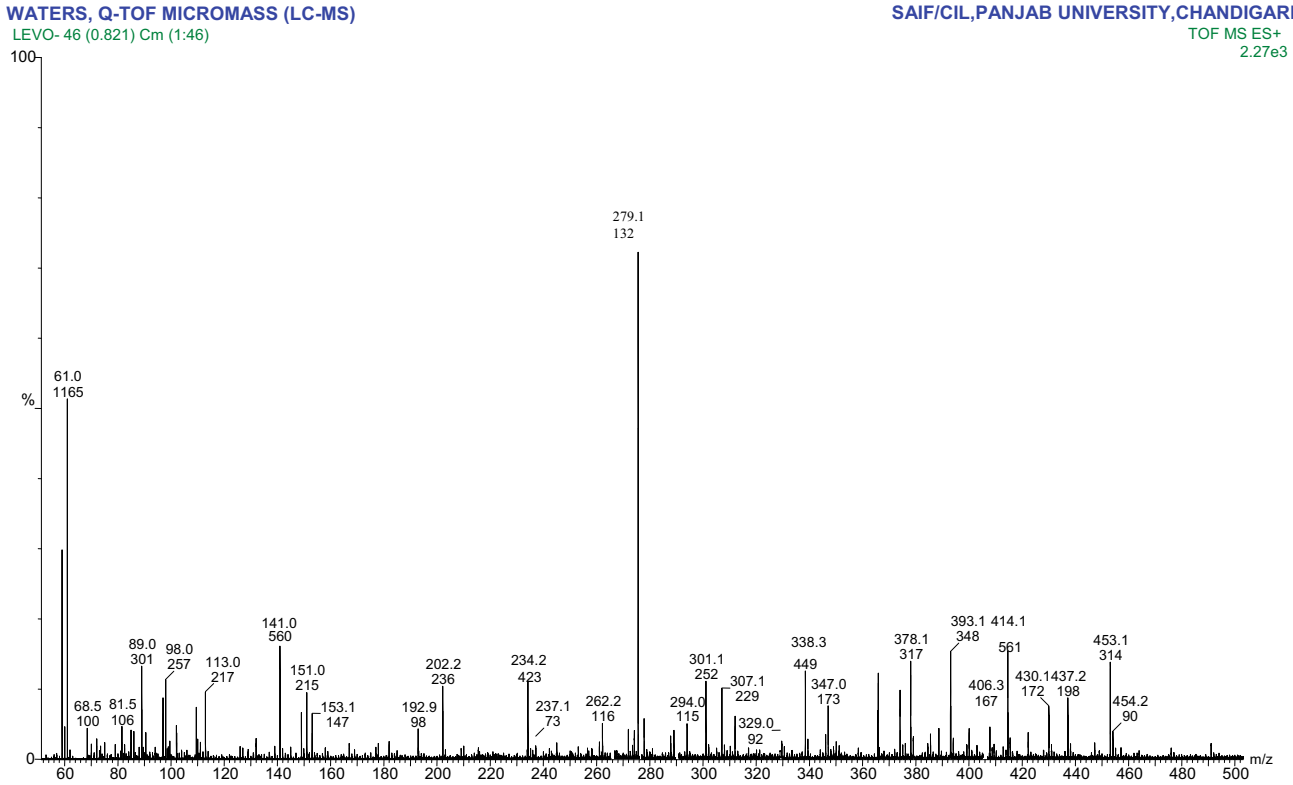

Fig. 3 LC–ESI–MS spectra of oxidation product of LEV

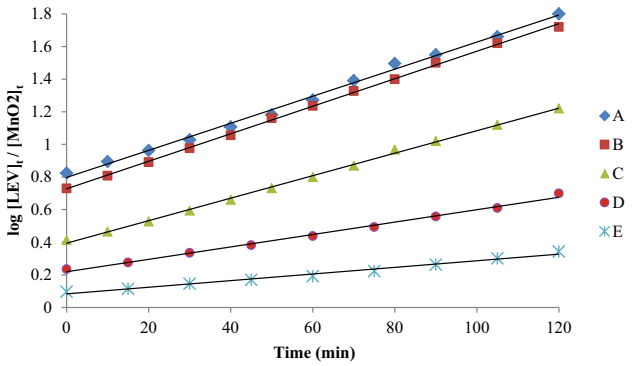

Fig. 4 Second-order plots for reaction between LEV and MnO_2 in aqueous acidic medium. [LEV] = 5.0 × 10^{-5} mol dm^{-3}, [H_2SO_4] = 2 × 10^{-4} mol dm^{-3}, I = 5 × 10^{-4} mol dm^{-3}, temperature = 25 °C, [MnO_2] × 10^{-5} mol dm^{-3} = *A* 0.75, *B* 1.0, *C* 2.0, *D* 3.0, *E* 4.0

mol dm^{-3} s^{-1}) were calculated and a plot of initial rate (k_i mol dm^{-3} s^{-1}) against [LEV] was made; a straight line passing through the origin was obtained confirming first-order dependence with respect to LEV ($r^2 \geq 0.998$). Certain reactions were also undertaken under pseudo-first-order conditions ([LEV] ≫ [MnO_2]) under identical experiment conditions varying from (1.0-10.0) × 10^{-4} mol dm^{-3}; pseudo-first-order plots were made and pseudo-first-order rate constants (k_{obs}, s^{-1}) evaluated from these plots were found to increase proportionately with the increasing concentration of LEV ($r^2 = 0.999$). Second order rate constants have good agreement, calculated from initial rates as well as second order plots (Table 2).

Effect of hydrogen ion and sulfate ion

The actual concentration of [H^+] and [SO_4^{2-}], i.e., [H^+]$_f$ and [SO_4^{2-}]$_f$ was calculated from acid-sulfate equilibrium constant (Tuwar et al. 1991) for the different concentration of sulfuric acid. The effect of concentration variation of [H^+] ion on the rate of reaction was studied in the concentration range (0.08–0.75) × 10^{-4} mol dm^{-3} at fixed concentration of LEV, MnO_2, ionic strength and [SO_4^{2-}] = 1.0 × 10^{-4} mol dm^{-3} at three temperatures viz. 20, 25, 30 °C, respectively. Pseudo-first-order rate constant (k_{obs}) was found to be increased with increase in [H^+] ($r^2 \geq 0.999$) (Table 2).

The effect of sulfate ion concentration on the reaction rate was studied by varying concentration range (0.5–1.5) × 10^{-4} mol dm^{-3}, all other reaction conditions being constant and concentration of H^+ ion (0.5 × 10^{-4} mol dm^{-3}) keep constant with the required concentration of H_2SO_4 calculated from acid and sulfate equilibrium constant for different added [$SO4^{2-}$]. The results indicate that [SO_4^{2-}] did not have significant effect on the rate of reaction (Table 2).

Effect of ionic strength and dielectric constant

At constant concentration of reactants, the ionic strength was varied by varying concentration of sodium sulfate (0.3–3.0) × 10^{-4} mol dm^{-3} at 25 °C. Ionic strength had negligible effect on the rate of reaction. At constant acidity and other constant conditions, as the t-butyl alcohol content increases from 0 to 50% (v/v) in the reaction, change in dielectric constant had negligible effect on the rate of reaction.

The negligible effect of ionic strength and dielectric constant on the rate of reaction suggests that the reaction is either between two neutral species or a neutral and a charged species (Laidler 2004).

Effect of temperature

The effect of temperature on the rate of the reaction was studied by studying the reaction at three temperature viz. 20, 25, 30 °C, respectively, at constant concentration of other reaction ingredients viz. [MnO_2] = 3.0 × 10^{-4} mol dm^{-3}, [LEV] = 5.0 × 10^{-4} mol dm^{-3}, [H_2SO_4] = 2.0 × 10^{-4} - mol dm^{-3} and [Na_2SO_4] = 3.0 × 10^{-4} mol dm^{-3}. The rate of reaction and observed rate constants increases with increasing temperature.

The energy of activation (E_a) of the reaction which is calculated by plotting the graph between log k_{obs} (s^{-1}) versus 1/T was found to be 30.54 kJ mol^{-1} and enthalpy of the reaction was 28.07 kJ mol^{-1}. The obtained parameters show good agreement with the oxidation of LEV by chlorine (Kulkarni et al. 2013).

Effect of added product

The effect of externally added Mn(II) on the rate of reaction was studied by varying concentration of $MnCl_2$ (1.0 × 10^{-5} to 10 × 10^{-5} mol dm^{-3}) keeping other experimental conditions constant. The results indicates that the rate of reaction is unaffected by the addition of Mn(II).

Table 2 Initial rate (k_i), pseudo first order rate constants (k_{obs}) and second order rate constant (k') in the reaction of LEV with MnO_2 in aqueous acidic medium at temperature = 25 °C and $I = 5.0 \times 10^{-4}$ mol dm^{-3} (here SD = Standard Deviation)

10^5 [MnO_2] (mol dm^{-3})	10^5 [LEV] (mol dm^{-3})	10^4 [H^+] (mol dm^{-3})	10^4 [SO_4^{2-}] (mol dm^{-3})	10^9 k_i (mol dm^{-3} s^{-1})	10^3 k_{obs} ± SD (s^{-1})	k' ± SD (dm^3 mol^{-1} s^{-1})
0.75	5.0	0.5	1.0	3.16	–	7.50 ± 0.21 (8.43)
1.0	5.0	0.5	1.0	4.16		8.10 ± 0.26 (8.33)
2.0	5.0	0.5	1.0	8.66	–	8.80 ± 0.53 (8.66)
3.0	5.0	0.5	1.0	12.0	–	7.29 ± 0.79 (8.00)
4.0	5.0	0.5	1.0	17.0	–	7.67 ± 1.0 (8.33)
5.0	5.0	0.5	1.0	20.5	–	– (8.33)
6.0	5.0	0.5	1.0	24.0		– (8.10)
7.5	5.0	0.5	1.0	30.8		– (8.20)
0.75	6.0	0.5	1.0	3.80		8.44 ± 0.32 (8.11)
1.0	6.0	0.5	1.0	5.00	–	8.06 ± 0.20 (8.33)
2.0	6.0	0.5	1.0	10.0	–	8.92 ± 0.60 (8.33)
3.0	6.0	0.5	1.0	14.4	–	7.29 ± 0.80 (8.02)
4.0	6.0	0.5	1.0	18.9	–	8.83 ± 0.53 (7.90)
5.0	6.0	0.5	1.0	24.5	–	8.06 ± 0.20 (8.10)
6.0	6.0	0.5	1.0	29.0		– (8.20)
7.5	6.0	0.5	1.0	36.0		– (8.30)
2.0	1.0	0.5	1.0	1.80	–	7.70 ± 1.0 (8.50)
2.0	2.5	0.5	1.0	4.00	–	8.11 ± 0.27 (8.70)
2.0	4.0	0.5	1.0	7.00	–	7.68 ± 0.90 (8.43)
2.0	7.0	0.5	1.0	11.7	–	7.67 ± 0.87 (8.33)
2.0	8.0	0.5	1.0	13.3	–	7.95 ± 1.1 (8.33)
2.0	9.0	0.5	1.0	15.2	–	8.33 ± 0.41 (8.40)
2.0	10.0	0.5	1.0	17.0	–	8.05 ± 0.20 (8.50)
3.0	1.0	0.5	1.0	2.50	–	8.33 ± 0.38 (8.00)
3.0	2.5	0.5	1.0	6.00	–	8.00 ± 0.10 (8.30)
3.0	4.0	0.5	1.0	9.70	–	8.10 ± 0.30 (8.00)
3.0	7.0	0.5	1.0	16.7	–	8.60 ± 0.70 (7.94)
3.0	8.0	0.5	1.0	19.2	–	8.00 ± 0.17 (7.99)
3.0	9.0	0.5	1.0	21.7	–	8.33 ± 0.40 (8.02)
3.0	10.0	0.5	1.0	23.8	–	8.06 ± 0.20 (7.90)
2.0	2.0	0.5	1.0	–	–	8.33 ± 0.40
3.0	3.0	0.5	1.0	–	–	8.33 ± 0.41
4.0	4.0	0.5	1.0	–	–	8.33 ± 0.40
2.0	20.0	0.5	1.0	–	1.58 ± 0.10	7.90 ± 0.10
2.0	30.0	0.5	1.0	–	243 ± 0.11	8.10 ± 0.11
2.0	40.0	0.5	1.0	–	3.12 ± 0.13	7.80 ± 0.13
2.0	50.0	0.5	1.0	–	4.00 ± 0.14	8.00 ± 0.14
2.0	60.0	0.5	1.0	–	4.77 ± 0.11	7.95 ± 0.11
2.0	80.0	0.5	1.0	–	6.39 ± 0.12	7.99 ± 0.12
2.0	100.0	0.5	1.0	–	7.90 ± 0.13	7.90 ± 0.13
3.0	20.0	0.5	1.0	–	1.57 ± 0.09	7.84 ± 0.09
3.0	30.0	0.5	1.0	–	2.39 ± 0.10	7.95 ± 0.10
3.0	40.0	0.5	1.0	–	3.12 ± 0.13	7.81 ± 0.13
3.0	50.0	0.5	1.0	–	4.05 ± 0.14	8.10 ± 0.14
3.0	60.0	0.5	1.0	–	4.78 ± 0.11	7.97 ± 0.11
3.0	80.0	0.5	1.0	–	6.40 ± 0.12	8.00 ± 0.12
3.0	100.0	0.5	1.0	–	7.88 ± 0.13	7.88 ± 0.13

Table 2 continued

10^5 [MnO_2] (mol dm^{-3})	10^5 [LEV] (mol dm^{-3})	10^4 [H^+] (mol dm^{-3})	10^4 [SO_4^{2-}] (mol dm^{-3})	10^9 k_i (mol dm^{-3} s^{-1})	10^3 k_{obs} ± SD (s^{-1})	k' ± SD (dm^3 mol^{-1} s^{-1})
2.0	5.0	0.08	1.0	–	0.06 ± 0.06	–
2.0	5.0	0.13	1.0	–	1.00 ± 0.08	–
2.0	5.0	0.25	1.0	–	2.00 ± 0.10	–
2.0	5.0	0.38	1.0	–	3.00 ± 0.15	–
2.0	5.0	0.44	1.0	–	3.50 ± 0.18	–
2.0	5.0	0.50	1.0	–	4.00 ± 0.20	–
2.0	5.0	0.56	1.0	–	4.50 ± 0.27	–
2.0	5.0	0.63	1.0	–	5.00 ± 0.30	–
2.0	5.0	0.75	1.0	–	6.00 ± 0.36	–
2.0	5.0	0.5	0.15	–	4.00 ± 0.20	–
2.0	5.0	0.5	0.25	–	4.10 ± 0.18	–
2.0	5.0	0.5	0.50	–	4.05 ± 0.20	–
2.0	5.0	0.5	0.75	–	4.11 ± 0.21	–
2.0	5.0	0.5	0.88	–	4.00 ± 0.20	–
2.0	5.0	0.5	1.00	–	4.10 ± 0.19	–
2.0	5.0	0.5	1.13	–	4.05 ± 0.22	–
2.0	5.0	0.5	1.25	–	4.10 ± 0.20	–
2.0	5.0	0.5	1.50	–	4.00 ± 0.21	–

Result in parenthesis shows the values of second order rate constants which derived from initial rates

Test for free radical

The formation of free radical was confirmed by the addition of acrylonitrile in the reaction mixture. After 5 h the reaction mixture was diluted with methanol then precipitate was formed which is indicating the presence of free radical during the progress of reaction.

On the basis of above results, the mechanism of oxidation of LEV by MnO_2 in acid aqueous media is given in Scheme 1.

Scheme 1 illustrates the mechanism of reaction between MnO_2 and LEV in acid aqueous medium. The reaction of MnO_2 and LEV occurs to form an intermediate complex (C_1) in the fast equilibrium step, and the complex (C_1) reacts with the H^+ ions to form another complex (C_2) in the second equilibrium step. The complex (C_2) is involved in the rate-determining step to form a free radical cation and $HMnO_2$. This free radical cation again reacts with $HMnO_2$ in the fast step and converts into dealkylated product of LEV and gives Mn^{2+}, HCHO, NH_3 as end products.

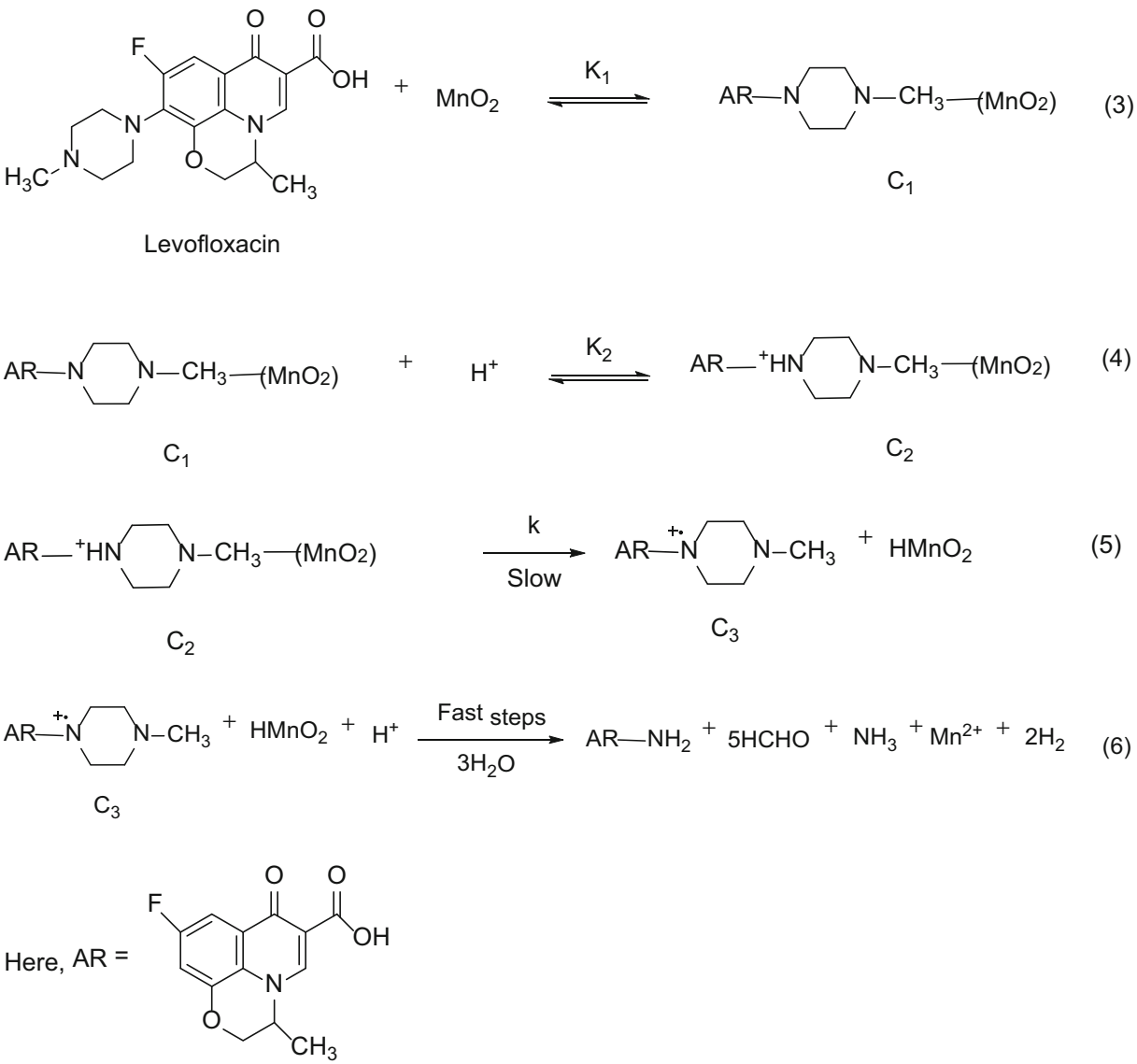

Scheme 1 Proposed mechanism for the oxidation of LEV by MnO_2

On the basis of above mechanism, the following rate equations can be proposed:

$$\text{Rate} = kK_1K_2[\text{MnO}_2][\text{LEV}][\text{H}^+], \tag{7}$$

$$\frac{\text{Rate}}{[\text{MnO}_2]} = k_{\text{obs}} = kK_1K_2[\text{LEV}][\text{H}^+], \tag{8}$$

$$\frac{k_{\text{obs}}}{[\text{LEV}]} = k' = kK_1K_2[\text{H}^+], \tag{9}$$

where k' is the second-order rate constant.

$$\frac{1}{k'} = \frac{1}{kK_1K_2[\text{H}^+]}, \tag{10}$$

Plot of $1/k'$ versus $1/[\text{H}^+]$ gives straight line passing through the origin (Fig. 5) to support the rate law.

It is further interesting to mention that the stoichiometry of the reaction was further justified kinetically when reactions were carried out in stoichiometric conditions. The plots of $[\text{MnO}_2]_t^{-1}$ versus time were made ($r^2 \geq 0.999$) (Fig. 6; Table 3) and the rate constants evaluated from these plots agree with the second-order plots.

Conclusion

A kinetic and mechanistic study of LEV oxidation by MnO_2 has been first time investigated in aqueous acidic medium. The reaction follows first-order kinetics with respect to MnO_2, LEV and H^+ ion under first-order reaction conditions. Results and mechanism indicate that H_2MnO_3 is reactive species of MnO_2. Since dealkylated

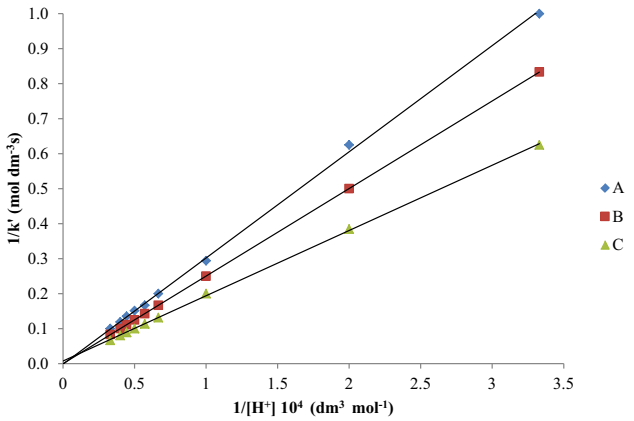

Fig. 5 Plot of $1/k'$ versus $1/[H^+]$ at three temperatures (A = 20 °C, B = 25 °C, C = 30 °C). $[MnO_2] = 3.0 \times 10^{-5}$ mol dm^{-3}, [LEV] = 5.0×10^{-4} mol dm^{-3}, $I = 5 \times 10^{-4}$ mol dm^{-3}

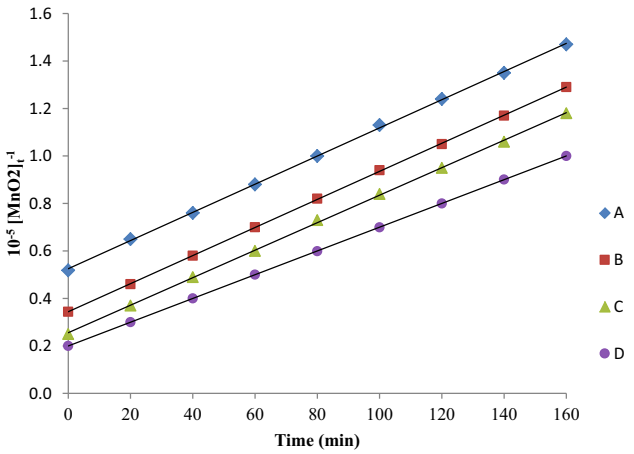

Fig. 6 A plot of $[MnO2]_t^{-1}$ versus time. $I = 5 \times 10^{-4}$ mol dm^{-3}, temperature = 25 °C, $[MnO_2] \times 10^{-5}$ mol dm^{-3} and [LEV] $\times 10^{-5}$ mol dm^{-3} = (A)2.0, (B) 3.0, (C) 4.0, (D) 5.0

Table 3 Second order rate constants from stoichiometric plots in MnO_2 and LEV reaction in aqueous acidic medium

10^5 [MnO_2], mol dm^{-3}	10^5 [LEV], mol dm^{-3}	k, mol^{-1} dm^3 s^{-1}
2.0	2.0	8.33
3.0	3.0	8.33
4.0	4.0	8.33
5.0	5.0	8.33

[H_2SO_4] = 2×10^{-4} mol dm^{-3}, $I = 5.0 \times 10^{-4}$ mol dm^{-3}, temperature = 25 °C

products are obtained in the present study, it is evident that the products of the title reaction have antimicrobial activity after oxidation. Thus, the degradation of fluoroquinolones plays an important role in the field of waste water treatment. The kinetic results have also been used to evaluate various activation parameters associated with the degradation of LEV by MnO_2 in aqueous acidic medium.

Acknowledgment We are grateful to the Department of Science and Technology sponsored FIST laboratory of our institution for experimental work and Sophisticated Analytical Instrumentation Facility, CIL, Punjab University, Chandigarh for LC–MS measurements.

Compliance with ethical standards

Conflict of interest The authors declare that they have no conflict of interest.

References

Akram M, Altaf M, Ud-Din K (2011) Oxidative degradation of dipeptide (glycyl-glycine) by water soluble colloidal manganese dioxide in the aqueous and micellar media. Colloids Surf B 82:217–223. doi:10.1016/j.colsurfb.2010.08.044

Chen G, Zhao L, Dong YH (2011) Oxidative degradation kinetics and products of chlortetracycline by manganese dioxide. J Hazard Mater 193:128–138. doi:10.1016/j.jhazmat.2011.07.039

Croisier D, Etienne M, Bergoin E et al (2004) Mutant selection window in levofloxacin and moxifloxacin treatments of experimental pneumo-coccal pneumonia in a rabbit model of human therapy. Antimicrob Agents Chemother 48:1699

Elmolla ES, Chaudhari M (2010) Photocatalytic degradation of amoxicillin, ampicillin and cloxacillin antibiotics in aqueous solution using UV/TiO_2 and UV/H_2O_2/TiO_2 photocatalysis. Desalination 252:46–52. doi:10.1016/j.desal.2009.11.003

Fatta-Kassinos D, Merics M, Nikolaou A (2011) Pharmaceutical residues in environmental waters and waste water: current state of knowledge and future research. Anal Bianal Chem 399:251–275. doi:10.1007/s00216-010-4300-9

Fiegl F (1975) Spot tests in organic analysis. Elsevier, New York, p 435

Freeman F, Fuselier CO, Armstead CR, Dalton CE, Davidson PA, Karchefski EM, Krochman DE, Johnson MN, Jones NK (1981) Permanganate ion oxidations. 13. Soluble manganese(IV) species in the oxidation of 2,4(1H,3H)-pyrimidinediones (uracils). J Am Chem Soc 103:1154–1159. doi:10.1021/ja00395a026

Gudaganatti MS, Hanagadakar MS, Kulkarni RM, Malladi S, Nagarale RK (2012) Transformatoion of levoflxacin during water chlorination process: kinetics and pathways. Prog React Kinet Mech 37:366–382. doi:10.3184/146867812X13440034591571

Gupta G, Kaur A, Sinha ASK, Kansal SK (2017) Photocatalytic degradation of levofloxacin in aqueous phase using Ag/AgBr/BiOBr microplates under visible light. Mater Res Bull 88:148–155. doi:10.1016/j.materresbull.2016.12.016

Jain A, Tazwar G, Devra V (2015) Oxidation of levofloxacin by acidic permanganate: a kinetic and mechanistic study. Int J Res Pharm Sci 5:1–8

Khan AAP, Mohd A, Bano S, Husain A, Siddiqi KS (2010) Kinetic and mechanistic investigation of the oxidation of the antibacterial agent levofloxacin by permanganate in alkaline medium. Trans Met Chem 35:117–123. doi:10.1007/s11243-009-9303-z

Khan AAP, Asiri AM, Azum N et al (2012) Kinetics and mechanistic investigation of decarboxylation for the oxidation of levofloxacin

by chloramine-T in acidic medium. Ind Eng Chem Res 51:4819–4824. doi:10.1021/ie202483c

Kulkarni RM, Hanagadakar MS, Malladi RS (2013) Silver (I) catalyzed and uncatalyzed oxidation of levofloxacin with aqueous chlorine: a comparative kinetic and mechanistic approach. Asian J Res Chem 6:1124–1132

Kummerer K (2009) The presence of pharmaceuticals in the environment due to human use- present knowledge and future challenges. J Environ Manag 90:2354–2366. doi:10.1016/j.jenvman.2009.01.023

Kusari S, Prabakaram D, Lamshoft M, Spiteller M (2009) In vitro residual anti-bacterial activity of difloxacin, sarafloxacin and their photoproducts after photolysis in water. Environ Pollut 157:2722–2730. doi:10.1016/j.envpol.2009.04.033

Laidler KJ (2004) Chemical kinetics, 3rd edn. Pearson Education (Singapore) Pte. Ltd, Indian Branch, Delhi, pp 183–198

Li Y, Wei D, Du Y (2015) Oxidative transformation of levofloxacin by δ-MnO_2: products, pathways and toxicity assessment. Chemosphere 119:282–288. doi:10.1016/j.chemosphere.2014.06.064

Mata-Perez F, Perez-Benito JF (1985) Identification of the product from the reduction of permanganate ion by trimethylamine in aqueous phosphate buffers. Can J Chem 63:988–992

Najjar NHE, Touffet E, Deborde M, Journel R, Leitner NKV (2013) Levofloxacin oxidation by ozone and hydroxyl radicals: kinetic study, transformation products and toxicity. Chemosphere 93:604–611. doi:10.1016/j.chemosphere.2013.05.086

Owens RCJ, Ambrose PG (2000) Clinical use of the fluoroquinolones. Med Clin North Am 84:1447–1469. doi:10.1016/S0025-7125(05)70297-2

Patgar MB, Nandibewoor ST, Chimatadar SA (2015) Spectroscopic investigations of the oxidation of levofloxacin by HCF(III) in aqueous alkaline medium-A kinetic & mechanistic approach. Cogent Chem 1:1–14. doi:10.1080/23312009.2015.1088788

Perez-Benito JF (2002) Reduction of colloidal manganese dioxide by manganese(II). J Colloid Interface Sci 284:130–135. doi:10.1006/jcis.2001.8145

Perez-Benito JF, Arias C (1992) A kinetic study of the reaction between soluble (colloidal) manganese dioxide and formic acid. J Colloid Interface Sci 149:92–97. doi:10.1016/0021-9797(92)90394-2

Perez-Benito JF, Brillas E, Pouplana R (1989) Identification of a soluble form of colloidal manganese (IV). Inorg Chem 28:390–392. doi:10.1021/ic00302a002

Perez-Benito JF, Arias C, Amat E (1996) A kinetic study of the reduction of colloidal manganese dioxide by oxalic acid. J Colloid Interface Sci 177:228–297. doi:10.1006/jcis1996.0034

Roblin PM, Hammerschlag MR (2003) In vitro activity of a new antibiotic VPPDF386(VRC4887) against chlamydia pneumoniae. Antimicrob Agents Chemother 47:1447

Singh AK, Sen N, Chatterjee SK (2016) Oxidative degradation of Norfloxacin by water soluble colloidal MnO_2 in the presence of cationic surfactant. Indian J Chem 55A:1059–1067

Stone AT, Morgan JJ (1984) Reduction and dissolution of manganese(III) and manganese(IV) oxides by organics: 2 survey of the reactivity of organics. Environ Sci Technol 18:617–624. doi:10.1021/es00126a010

Sturini M, Speltini A, Maraschi F et al (2012) Photodegradation of fluoroquinolones in surface water and antimicrobial activity of the photoproducts. Water Res 46:5575–5582. doi:10.1016/j.watres.2012.07.043

Tuwar SM, Morab VA, Nandibewoor ST (1991) Osmium (VIII)/palladium (II) catalysis of cerium (IV) oxidation of allyl alcohol in aqueous acid. Trans Met Chem 16:430–434. doi:10.1007/BF01129458

Vogel AI (1973) A Textbook of Practical Organic chemistry including Qualitative Organic Analysis. 3rd ed. Longman 332

Yahvya MS, Karbane ME, Oturan N, Kacemi KE, Outran MA (2016) Mineralization of the antibiotic levofloxacin in aqueous medium by electro-Fenton process: kinetics and intermediate products analysis. Environ Technol 37:1276–1287. doi:10.1080/09593330.2015.1111427

Zhang HC, Haung CH (2005) Oxidative transformation of fluoroquinolone antibacterial agents and structurally related amines by manganese oxide. Environ Sci Technol 39:4474–4483. doi:10.1021/es048166d

Zhang H, Chen WR, Haung CH (2008) Kinetic modeling of oxidation of antibacterial agents by manganese oxide. Environ Sci Technol 42:5548–5554. doi:10.1021/es703143g

Oxidation of Ciprofloxacin by Hexacyanoferrate(III) in the Presence of Cu(II) as a Catalyst: A Kinetic Study

GAJALA TAZWAR, ANKITA JAIN, NAVEEN MITTAL, VIJAY DEVRA

Department of Chemistry, J. D. B. Govt. Girls P. G. College, Kota, 324 001, India

Received 11 November 2016; revised 1 February 2017; accepted 28 March 2017

DOI 10.1002/kin.21097
Published online in Wiley Online Library (wileyonlinelibrary.com).

ABSTRACT: The Cu(II)-catalyzed oxidation of ciprofloxacin (CIP) by hexacyanoferrate(III) (HCF) has been investigated spectrophotometrically in an aqueous alkaline medium at 40°C. The stoichiometry for the reaction indicates that the oxidation of 1 mol of CIP requires 2 mol of HCF. The reaction exhibited first-order kinetics with respect to [HCF] and less than unit order with respect to [CIP] and [OH^-]. The products were also identified on the basis of stoichiometric results and confirmed by the characterization results of LC-MS and FT-IR analysis. All the possible reactive species of the reactants have been discussed, and a most probable kinetic model has been envisaged. The activation parameters with respect to the slow step of the mechanism were computed, and thermodynamic quantities were also determined. © 2017 Wiley Periodicals, Inc. Int J Chem Kinet 1–9, 2017

INTRODUCTION

A large number of the clinically prescribed antibacterial drugs are discharged into wastewater systems, which indicates the entry of useful antibacterial agents into aquatic environment [1]. Fluoroquinolones have been detected at various concentration ranges from dm^{-3} to ng dm^{-3} in wastewater [2]. Antibacterial resistant bacteria have been detected in wastewater effluents from sewage treatment plant and in drinking water. Recent research has verified the presence of numerous antibacterial compounds in the aquatic environment [3]. These antibacterial compounds have emerged as a new class of pollutants because of their adverse effects on human health [4]. The oxidative transformation of fluoroquinolone antibacterial agents in a water treatment process definitely plays a major role in this concern. Ciprofloxacin (CIP) {1-cyclopropyl-6-fluoro-1,4-dihydro-4-oxo-7-(piperazine-1-yl)-quinolone-3-carboxylic acid} is a second-generation fluoroquinolone antimicrobial agent with a wide spectrum of activity against many Gram-positive and Gram-negative aerobic and anaerobic bacteria. CIP is a member of the fluoroquinolone group and is used worldwide as a human and veterinary medicine [5]. There are studies on the modified pharmacological and toxicological properties of these drugs in the form of metallic complexes [6–8]. To properly assess the risk of CIP in aqueous solution and better understand its environmental fate and the transformation of fluoroquinolone pharmaceuticals in water systems, an oxidative kinetic study could be

Correspondence to: Vijay Devra; e-mail: v_devra1@rediffmail.com.

helpful in effective removal of CIP from environmental water.

In recent years, the use of transition metal ion such as Ru(II)/Ru(III), Os(IV)/Os(VIII), Pd(II)/Pd(IV), Mn(IV)/Mn(II), Cr(IV)/Cr(III), Ir(IV)/Ir(VI), and Cu(II)/Cu(I) as a catalyst in various redox processes has attracted considerable interest [9–11]. It has been shown [12] that a metal ion acts as a catalyst by one of several different paths, such as formation of complexes with reactants or oxidation of the substrate itself or through the formation of free radicals. The Cu(II) generally forms an activated complex with the substrate before converting into a final product [13]. The mechanism of the catalysis depends on the nature of substrate, oxidant, and experimental conditions.

Hexacyanoferrate(III) (HCF) has been widely used to oxidize various organic and inorganic compounds in basic, acidic, and neutral medium [14,15]. HCF is one electron oxidant with a redox potential of +0.45V for the $[Fe(CN)_6]^{-3}/[Fe(CN)_6]^{-4}$ couple in alkaline medium leading to its reduction to hexacyanoferrate(II), a stable product [16–18]. In most of the oxidations, HCF is mainly used as a hydrogen atom abstractor [19] and free radical generator [20]. HCF is a transition metal complex, consisting of a central iron ion, surrounded by six negative cyanide ions, or ligands, in an octahedral arrangement. A literature survey revealed that the kinetics and mechanism of oxidation of CIP by different oxidants such as ClO_2, ozone-free chlorine, and permanganate was carried out in both acidic and alkaline medium [21–24]. However, the reaction of CIP with HCF has not been investigated in detail and thus is the focus of this study, and title reaction is undertaken to understand the mechanism of the reaction and active species involved in the Cu(II)-catalyzed reaction.

MATERIALS AND METHODS

Chemicals

All chemicals used in this investigation were of analytical grade. Reaction solutions were prepared using double distilled water. Solution of CIP (Kores India Limited, Mumbai) was always freshly prepared before experiment. A stock solution of oxidant, HCF (MERCK, Mumbai) was prepared by dissolving $K_3[Fe(CN)_6]$ (BDH, Mumbai) in double distilled water and standardizing the solution iodometrically [25]. Copper sulfate (MERCK, Mumbai) was also prepared in double distilled water and standardized by the standard method. Corning glassware was employed both for storing the solutions and the kinetics of the reaction unless specified otherwise.

Instrumentation

For kinetic measurements, a Peltier accessory (temperature-controlled) attached to a double beam UV3000$^+$, UV–visible spectrophotometer (Labindia, Navi Mumbai) with UV path length 1.0 cm in the spectral range 200–800 nm, was used. Sample spectrum was recorded while recording the FT-IR spectra in the range of 400–4000 cm^{-1} by mixing the sample with dried KBr (in 1:20 weight ratio) with a resolution of 4 cm^{-1} by the Fourier Transform Infrared spectrophotometer (Bruker Optik GmbH, Germany). For product analysis, LC-ESI-MS (Q-TOF Micromass; Waters Company, UK) was used.

Kinetic Measurements

All kinetic measurements were conducted under pseudo–first-order conditions, where [CIP] was always in excess over [HCF], at a constant ionic strength in alkaline medium and temperature of 40 ± 1°C. The reaction was initiated by mixing the thermostatted solutions of HCF and CIP, which also contained the required concentration of Cu(II), NaOH, and $NaNO_3$. The progress of the reaction was studied by spectrophotometrically at 420 nm, that there was no interference from other species in the reaction mixture at this wavelength. The UV spectra indicate gradual disappearance of HCF(III) band with time as a result of its reduction with HCF(II) (Fig. 1). The application of Beer's law of HCF at 420 nm had been verified giving $\varepsilon = 1050$ dm^3 mol^{-1} cm^{-1} [26]; pseudo–first-order rate constant (k_{obs}) was calculated from the plot of the logarithm of absorbance versus time. The pseudo–first-order plot was linear up to 80% completion of the reaction, and the k_{obs} value was reproducible within ±6%.

RESULTS

Stoichiometry and Product Analysis

The stoichiometry of the reaction was determined with various ratios of reactants in the presence of Cu(II) as a catalyst, and constant concentration of NaOH and $NaNO_3$ was kept for 24 h at 40°C in a closed

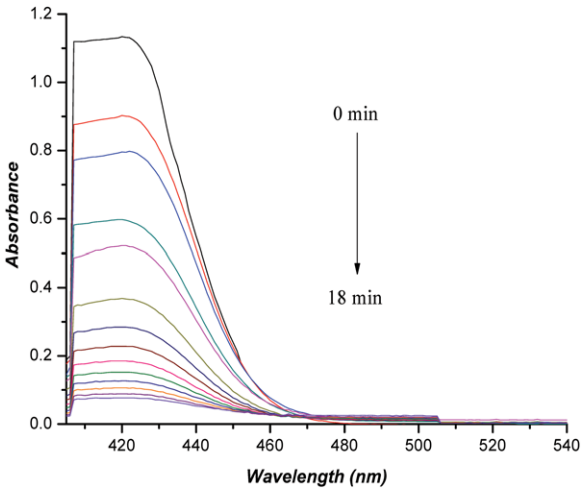

Figure 1 Spectral changes during the Cu(II)-catalyzed oxidation of CIP by HCF in alkaline medium at 40°C. [HCF] $= 1.0 \times 10^{-3}$ M, [CIP] $= 1.0 \times 10^{-2}$ M, [OH^-] = 1.0 M, [Cu(II)] $= 1.0 \times 10^{-3}$ M, and $I = 2.0$ M. [Color figure can be viewed at wileyonlinelibrary.com]

vessel. The results indicated that 1 mol of CIP reacts with 2 mol of HCF as given in the following equation (1):

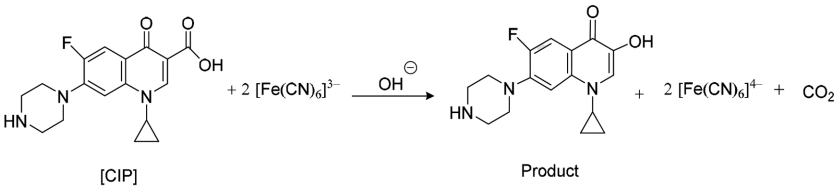

(1)

The remaining reaction mixture was acidified, concentrated, and extracted with ether. The main product {1-cyclopropyl-3-hydroxy-6-fluoro-1,4-dihydro-7-(piperazine-1-yl)-quinolin-4-one} was identified with the help of TLC and characterized by FT-IR and LC-MS analysis. FT-IR spectra of product show carbonyl stretching of the 7-oxo group at 1640.35 cm^{-1}; a broad peak at 3472.09 cm^{-1} is due to OH-stretching, and the carbonyl stretching of acid is disappeared (Fig. 2). LC-MS analysis of the CIP oxidation reaction indicates the formation of product with a molecular ion of *m/z* 304 amu (Fig. 3). The molecular ion of CIP is *m/z* 332; the *m/z* 304 corresponds to decarboxylation of the quinolones ring and yield {1-cyclopropyl-3-hydroxy-6-fluoro-1,4-dihydro-7-(piperazine-1-yl)-quinolin-4-one} as an oxidation product. The product was also in short written as (m-28), indicating the net mass loss of product from the parent CIP. The liberated CO_2 was identified by the limewater test.

Hexacyanoferrate(III) Dependence

The oxidant HCF concentration in the Cu(II)-catalyzed reaction was varied from 1.0×10^{-4} to 1.0×10^{-3} M, and all other reactant concentrations and conditions were constant. The plot of log absorbance versus time was linear (Fig. 4) indicating that the reaction is first order with respect to [HCF]. The observed pseudo–first-order rate constant (k_{obs}) was independent of the concentration of HCF.

Ciprofloxacin Dependence

The effect of different concentration variations of CIP in the Cu(II)-catalyzed reaction on the rate of reaction was studied in the range 0.5×10^{-2} M to 5×10^{-2} M at a constant concentration of HCF, Cu(II), alkali and ionic strength at 35°, 40°, 45°C temperatures, respectively. The rate of reaction increases with increasing concentration of CIP (Table I). A plot of log k_{obs} versus log [CIP] was linear with a slope of 0.73, thus indicating a fractional-order dependence on CIP concentration.

Hydroxyl Ion Dependence

The effect of concentration variation of sodium hydroxide on the Cu(II)-catalyzed reaction on the rate of reaction was studied in the concentration range 0.2–1.4 M at fixed concentration of HCF, CIP, Cu(II), and ionic strength at three temperatures, viz. 35°, 40°, 45°C, respectively. The pseudo–first-order rate constant (k_{obs}) was found to be increased with an increase in [OH^-] (Table I). A plot of log k_{obs} versus log [OH^-] was linear with a fractional slope of 0.64.

[Cu(II)] Ion Dependence

The concentration of Cu(II) catalyst was varied from 0.25×10^{-3} to 2.0×10^{-3} M at three different concentrations of CIP, viz. 0.5×10^{-2}, 1×10^{-2}, and 2×10^{-2} M, respectively, at constant [HCF], [OH^-],

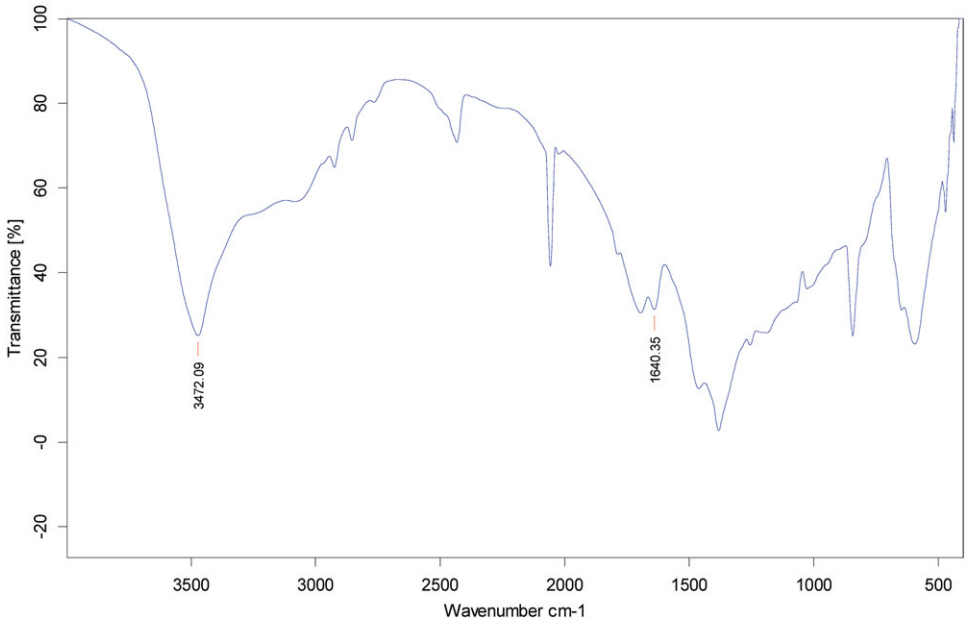

Figure 2 FT-IR spectra of the product of oxidation of CIP by HCF. [Color figure can be viewed at wileyonlinelibrary.com]

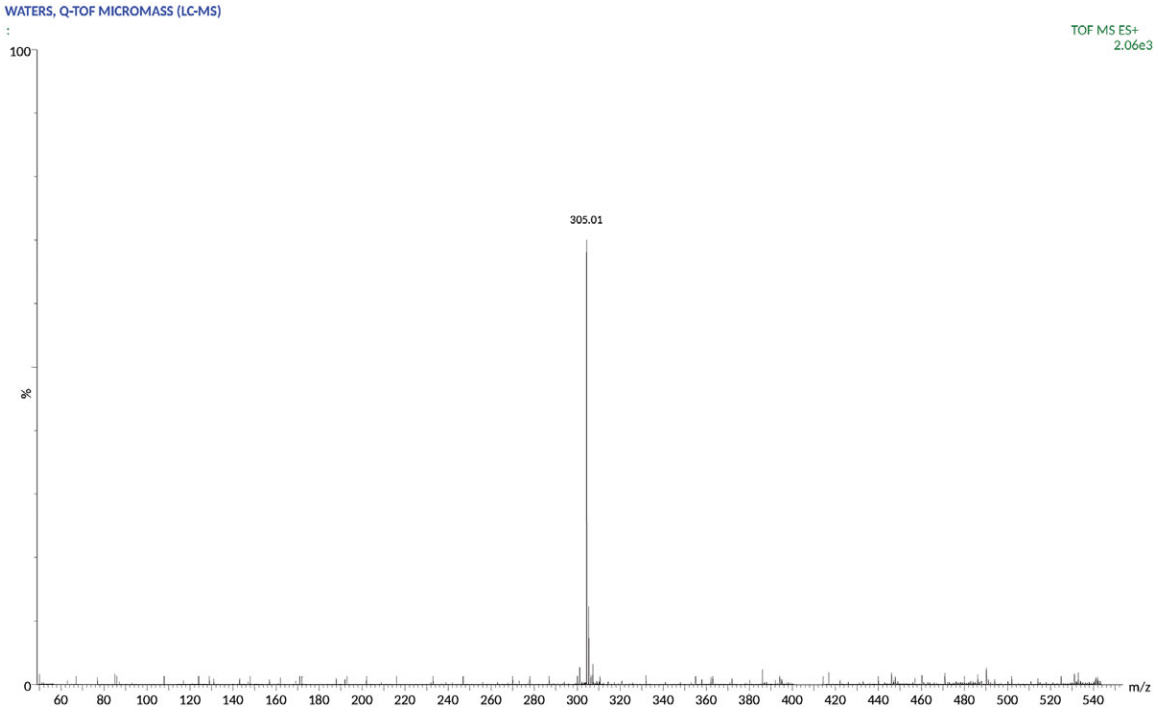

Figure 3 LC-ESI-MS spectra of oxidation product of CIP. [Color figure can be viewed at wileyonlinelibrary.com]

ionic strength, and temperature. The rate constant (k_{obs}) increases with increasing Cu(II) ion concentration (Table I). A plot of rate constant (k_{obs}) against [Cu(II)] yields a straight line with the zero intercept, indicating the unit order with respect to Cu(II).

Effect of Ionic Strength and Dielectric Constant

At constant concentration of reactants, the ionic strength was varied by varying concentration of sodium nitrate 1.0–2.0 M at 40°C. Ionic strength had

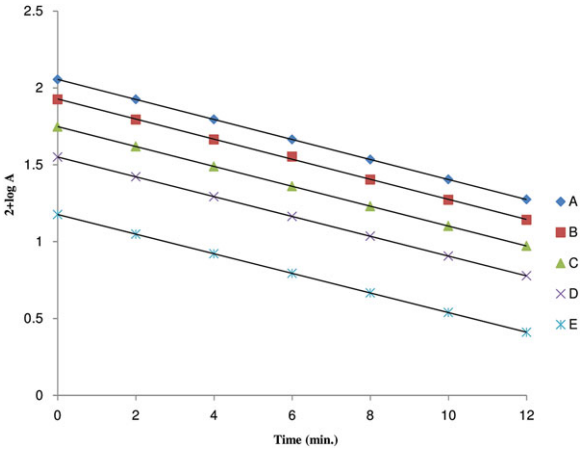

Figure 4 First-order plots of the variation of the HCF concentration at 40°C.[CIP] = 1.0×10^{-2} M, [OH^-] = 1.0 M, [Cu (II)] = 1.0×10^{-3} M, and I = 2.0 M. [HCF] × 10^{-4} M = (A) 1.0, (B) 2.5, (C) 5.0, (D) 7.5, (E) 10. [Color figure can be viewed at wileyonlinelibrary.com]

negligible effect on the rate of reaction. At constant acidity and other constant conditions, as the *t*-butyl alcohol content increases from 0 to 50% (v/v) in the reaction, change in dielectric constant had negligible effect on the rate of reaction.

Effect of Added Product

The initial added products, hexacyanoferrate(II), was studied in the range of 1×10^{-4} M to 10×10^{-4} M, the rate of reaction was unaffected, while keeping other reactants concentration and conditions constant.

Test for Free Radical

The formation of free radical was confirmed by the addition of acrylonitrile in the reaction mixture. After 5 h then diluted with methanol, white precipitate was formed, indicating the presence of free radical during the progress of reaction [27,28].

DISCUSSION

Cu(II) is known to be a catalyst in many redox reactions, particularly in alkaline medium [29], and catalysis has usually been explained by assuming the intermediate complex formed by an interaction of anionic form of CIP and Cu(II). This intermediate complex reacts with the oxidant in a rate-determining step, since order with respect to HCF and Cu(II) is one each and less than unit order with respect to [CIP]. Furthermore, the rate also increases with increasing of hydroxyl ion with fractional first-order dependence. Thus a mechanism consisting of scheme and also accounting for all experimental observations is proposed in Scheme 1.

In most of the oxidation reactions, HCF(III) resembles Cu(II) oxidation reactions [30–32], which involve free radical formation and rapidly oxidize it. However, our experimental results are contrary to that expectation. The HCF(III)–HCF(II) system has the redox potential +0.45 V, which has higher redox potential than a Cu(II)–Cu(I) couple (−0.34 V), proves a better possibility for the rapid oxidation of the free radical with HCF(III) in the alkaline medium.

The probable structure of the complex is given below:

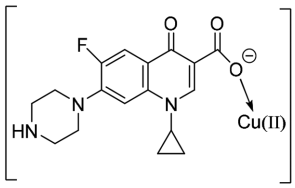

Complex

The formation of the complex is proven kinetically by the nonzero intercept of Cu(II)/k_{obs} verses 1/[CIP] (Fig. 5).

The following rate equation can be derived from Scheme 1:

$$\text{Rate} = \frac{-\text{d[HCF]}}{\text{d}t} = k[\text{C}][\text{HCF}] \tag{2}$$

$$K_1 = \frac{[\text{CIP}^-]}{[\text{CIP}]_\text{F}[\text{OH}^-]_\text{F}} \tag{3}$$

$$[\text{CIP}^-] = K_1[\text{CIP}]_\text{F}[\text{OH}^-]_\text{F}$$

$$K_2 = \frac{[\text{C}]}{[\text{CIP}^-][\text{Cu(II)}]_\text{F}}$$

$$[\text{C}] = K_2[\text{CIP}^-][\text{Cu(II)}]_\text{F}$$

$$[\text{C}] = K_1K_2[\text{CIP}]_\text{F}[\text{OH}^-]_\text{F}[\text{Cu(II)}]_\text{F} \tag{4}$$

Substituting Eq. (4) into Eq. (2) leads to

$$\text{Rate} = kK_1K_2[\text{CIP}]_\text{F}[\text{OH}^-]_\text{F}[\text{Cu(II)}]_\text{F}[\text{HCF}] \tag{5}$$

Table I Effect of Variation of [HCF], [CIP], [NaOH], and [Cu(II)] on the Oxidation of CIP by Alkaline HCF at 40°C and I = 2.0 M

10^4 [HCF] (mol dm^{-3})	10^2 [CIP] (mol dm^{-3})	[NaOH] (mol dm^{-3})	10^3 [Cu(II)] (mol dm^{-3})	10^4 k_{obs} (s^{-1})
1.0	1.0	1.0	1.0	24.50
2.5	1.0	1.0	1.0	24.70
5.0	1.0	1.0	1.0	24.85
7.5	1.0	1.0	1.0	25.05
10	1.0	1.0	1.0	25.00
10	0.5	1.0	1.0	11.50
10	0.75	1.0	1.0	16.08
10	1.0	1.0	1.0	25.00
10	2.0	1.0	1.0	34.40
10	3.0	1.0	1.0	48.75
10	4.0	1.0	1.0	57.22
10	5.0	1.0	1.0	61.50
10	1.0	0.2	1.0	07.84
10	1.0	0.4	1.0	14.36
10	1.0	0.6	1.0	18.37
10	1.0	0.8	1.0	22.05
10	1.0	1.0	1.0	25.00
10	1.0	1.2	1.0	26.80
10	1.0	1.4	1.0	27.00
10	1.0	1.0	0.25	06.05
10	1.0	1.0	0.5	12.50
10	1.0	1.0	0.75	19.22
10	1.0	1.0	1.0	25.00
10	1.0	1.0	1.25	30.82
10	1.0	1.0	1.5	37.50
10	1.0	1.0	1.75	44.00
10	1.0	1.0	2.0	50.02

The total concentration of CIP is given by

$$[\mathrm{CIP}]_T = [\mathrm{CIP}]_F + [\mathrm{CIP}^-] + [\mathrm{C}] \quad (6)$$

where "T" and "F" stand for total and free concentrations, respectively.

Substituting Eqs. (3) and (4) into Eq. (6) and rearrangement gives

$$[\mathrm{CIP}]_T = [\mathrm{CIP}]_F + K_1[\mathrm{CIP}]_F[\mathrm{OH}^-]_F + K_1K_2[\mathrm{CIP}]_F[\mathrm{OH}^-]_F[\mathrm{Cu(II)}]_F \quad (7)$$

$$[\mathrm{CIP}]_T = [\mathrm{CIP}]_F\{1 + K_1[\mathrm{OH}^-]_F + K_1K_2[\mathrm{OH}^-]_F[\mathrm{Cu(II)}]_F\} \quad (8)$$

Therefore,

$$[\mathrm{CIP}]_F = \frac{[\mathrm{CIP}]_T}{1 + K_1[\mathrm{OH}^-]_F + K_1K_2[\mathrm{OH}^-]_F[\mathrm{Cu(II)}]_F} \quad (9)$$

In view of low $[\mathrm{Cu(II)}]_F$, the third denominator term $K_1K_2[\mathrm{OH}^-]$ [Cu(II)] in the above equation can be neglected. Therefore, Eq. (9) can be simplified to the following equation:

$$[\mathrm{CIP}]_F = \frac{[\mathrm{CIP}]_T}{1 + K_1[\mathrm{OH}^-]_F} \quad (10)$$

The concentration of Cu(II) can be calculated as

$$[\mathrm{Cu(II)}]_T = [\mathrm{Cu(II)}]_F + [\mathrm{C}] \quad (11)$$

$$[\mathrm{Cu(II)}]_T = [\mathrm{Cu(II)}]_F\{1 + K_1K_2[\mathrm{CIP}]_F[\mathrm{OH}^-]_F\} \quad (12)$$

$$[\mathrm{Cu(II)}]_F = \frac{[\mathrm{Cu(II)}]_T}{1 + K_1K_2[\mathrm{CIP}]_F[\mathrm{OH}^-]_F} \quad (13)$$

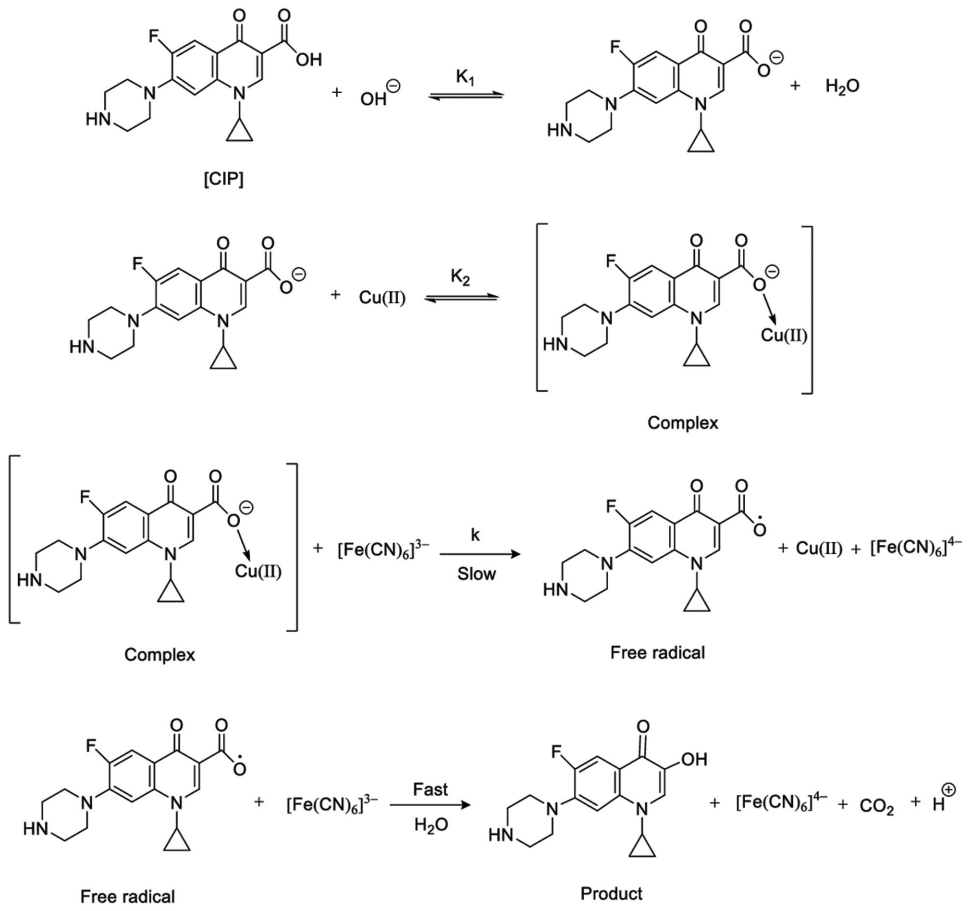

Scheme 1 Proposed mechanism for the Cu(II)-catalyzed oxidation of CIP by HCF in alkaline medium.

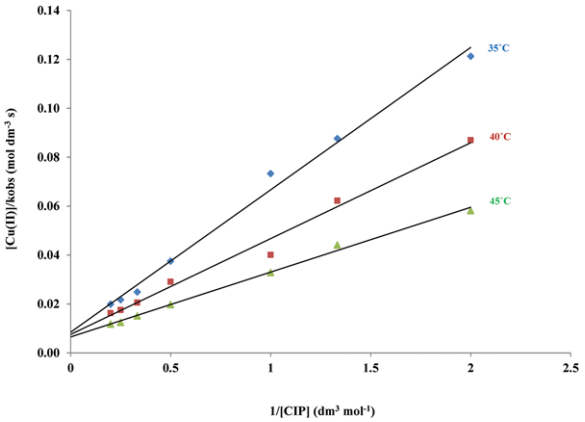

Figure 5 Plots of $[Cu(II)]/k_{obs}$ versus 1/[CIP] at three different temperatures. [Color figure can be viewed at wileyonlinelibrary.com]

Regarding to the concentration of OH^-,

$$[OH^-]_F = [OH^-]_T \tag{14}$$

Substituting Eqs. (10), (13) and (14) into Eq. (15) (and omitting T and F subscripts) leads to

$$\text{Rate} = \frac{kK_1K_2[\text{CIP}][OH^-][\text{Cu(II)}][\text{HCF}]}{\{1 + K_1[OH^-]\}\{1 + K_1K_2[\text{CIP}][OH^-]\}} \tag{15}$$

$$\text{Rate} = \frac{kK_1K_2[\text{CIP}][OH^-][\text{Cu(II)}][\text{HCF}]}{1 + K_1[OH^-] + K_1K_2[\text{CIP}][OH^-] + K_1^2K_2[\text{CIP}][OH^-]^2} \tag{16}$$

The term $K_1{}^2K_2$ $[\text{CIP}][OH^-]^2$ in the denominator of Eq. (16) is negligibly small compared to unity in view of the low concentration of CIP used.

Therefore, Eq. (16) can be written as

$$\text{Rate} = \frac{kK_1K_2[\text{CIP}][OH^-][\text{Cu(II)}][\text{HCF}]}{1 + K_1[OH^-] + K_1K_2[\text{CIP}][OH^-]} \tag{17}$$

Under the pseudo–first-order condition, the rate law can be expressed by Eq. (18):

$$\text{Rate} = \frac{-\text{d[HCF]}}{\text{d}t} = k_{\text{obs}}[\text{HCF}] \tag{18}$$

Therefore, comparing Eqs. (17) and (18), the following relationship is obtained:

$$k_{\text{obs}} = \frac{\text{Rate}}{[\text{HCF}]} = \frac{kK_1K_2[\text{CIP}][\text{OH}^-][\text{Cu(II)}]}{1 + K_1[\text{OH}^-] + K_1K_2[\text{CIP}][\text{OH}^-]} \tag{19}$$

Equation (17) can be rearranged to the following forms, which is suitable for verification:

$$\frac{[\text{Cu(II)}]}{k_{\text{obs}}} = \left[\frac{1}{kK_1K_2[\text{OH}^-]} + \frac{1}{kK_1}\right]\frac{1}{[\text{CIP}]} + \frac{1}{k} \tag{20}$$

$$\frac{[\text{Cu(II)}]}{k_{\text{obs}}} = \left[\frac{1}{kK_1K_2[\text{CIP}]}\right]\frac{1}{[\text{OH}^-]} + \frac{1}{kK_2[\text{CIP}]} + \frac{1}{k} \tag{21}$$

According to Eq. (20), the plot of $[\text{Cu(II)}]/k_{\text{obs}}$ versus $1/[\text{CIP}]$ (Fig. 5) is linear with the positive intercept and slope at three different temperatures. The rate constant k, of the slow step (Scheme 1) was obtained from the intercept of the plots $[\text{Cu(II)}]/k_{\text{obs}}$ versus $1/[\text{CIP}]$ (Table II). The energy of activation was determined by the plot of log k versus $1/T$ from which activation parameters were calculated (Table II). Also, the values of the equilibrium constants associated with the mechanistic Scheme 1 (K_1 and K_2) are evaluated from the intercept and slope of the plots of $[\text{Cu(II)}]/k_{\text{obs}}$ versus $1/[\text{CIP}]$ and $[\text{Cu(II)}]/k_{\text{obs}}$ versus $1/[\text{OH}^-]$ (Fig. 6), Table II. The value of equilibrium constant K_1 is in good agreement with earlier work [11] at 40°C. Thermodynamic quantities were calculated from the Van't Hoff plot (Table II).

The entropy of activation ($\Delta S^{\neq}$) tends to be more negative for reaction of an inner-sphere nature, where as the reactions of positive $\Delta S^{\neq}$ values proceed via an outer-sphere mechanism [33–35]. The obtained large negative values of $\Delta S^{\neq}$ (Table II) express that the mechanism is one-electron transfer of inner-sphere nature, which indicate that there is a decrease in the randomness during the reaction process. This leads to the formation of intermediate complex and such an activated complex is more ordered than the reactants due to loss of degree of freedom. Whether the positive value of $\Delta H^{\neq}$ indicates that the complex formation is endothermic and the value of $\Delta G^{\neq}$ suggests enhanced formation of the intermediate with raising temperature as well as to the nonspontaneity of the complex formation.

Table II Activation and Thermodynamic Quantities for the Oxidation of CIP by Alkaline HCF from Scheme 1

Temperature (K)	k (dm^3 mol^{-1}s^{-1})
308	12.5
313	14.3
318	16.7
Activation parameters	Value
E_a (kJ mol^{-1})	23.93
$\Delta H^{\#}$ (kJ mol^{-1})	21.33
$\Delta S^{\#} \pm$ (J K^{-1} mol^{-1})	–202
$\Delta G^{\#} \pm$ (kJ mol^{-1})	84.56

Equilibrium Constants at Different Temperatures

Temperature (K)	K_1 (dm^3 mol^{-1})	$\times 10\ K_2$ (dm^3 mol^{-1})
308	13.79	7.11
313	17.95	9.05
318	23.08	10
Thermodynamic Quantities	Using K_1 Values	Using K_2 Values
$\Delta H^{\#}$ (kJ mol^{-1})	40.19	25.74
$\Delta S^{\#} \pm$ (J K^{-1} mol^{-1})	–181.52	–220.57
$\Delta G^{\#} \pm$ (kJ mol^{-1})	97.11	94.78

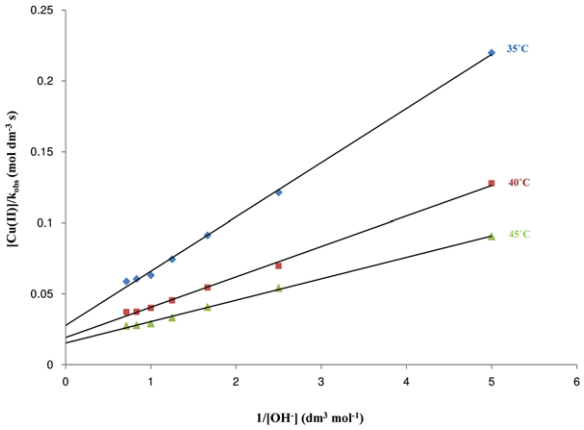

Figure 6 Plots of $[\text{Cu(II)}]/k_{\text{obs}}$ versus $1/[\text{OH}^-]$ at three different temperatures. [Color figure can be viewed at wileyonlinelibrary.com]

CONCLUSION

The Cu(II)-catalyzed oxidation of CIP by HCF in aqueous alkaline medium was found to be first order with respect to oxidant and fractional order with respect

to substrate and alkali. The reaction pathway involves complex formation and free radical mechanism. The observed stoichiometry indicates that the oxidation of 1 mol of CIP requires 2 mol of HCF. The major product of reaction obtained by the decarboxylation of quinolones moiety, and hence it may retain the antibacterial activity. The overall sequence described here is consistent with all experimental findings, including the product and mechanistic and kinetic studies.

We are grateful to Department of Science and Technology sponsored FIST laboratory of our institution for experimental work and Sophisticated Analytical Instrumentation Facility, CIL, Punjab University, Chandigarh, India, for LC-MS measurements.

BIBLIOGRAPHY

1. Kulkarni, R. M.; Hanagadakar, M. S.; Malladi, R. S.; Gudaganatti, M. S.; Biswal, H. S.; Nandibewoor, S. T. Indian J Chem Technol 2014, 21, 38–43.
2. Gudaganatti, M. S.; Hanagadakar, M. S.; Kulkarni, R. M.; Malladi, R. S.; Nagarale, R. K. Prog React Kinet 2012, 37, 366–382.
3. Kulkarni, R. M.; Malladi, R. S.; Hanagadakar, M. S.; Doddamani, M. R.; Bhat, U. K. Desalin Water Treat 2016, 57, 16111–16118.
4. Kulkarni, R. M.; Hanagadakar, M. S.; Malladi, R. S.; Biswal, H. S.; Cuerda-correa, E. M. Desalin Water Treat 2016, 57, 10826–10838.
5. Zhang, H.; Haung, C. H. Environ Sci Technol 2005, 39, 4474–4483.
6. Ruyz, M.; Perello, L.; Ortiz, R.; Castineiras, A.; Maichle-Mossmer, C.; Canton, E. J Inorg Biochem 1995, 59, 801–810.
7. Turel, I.; Leban, I.; Bukovec, N. J Inorg Biochem 1997, 66, 241.
8. Lopez-Gresa, M. P.; Oritz, R.; Parello, L.; Latorre, J.; Liu-Gonzalez, M.; Perez-Priede, S.; Canton, E. J Inorg Biochem 2002, 92, 65–74.
9. Das, A. K. Coord Chem Rev 2001, 213, 307.
10. Diab, N.; Abu-Shquair, I.; Al-Sunei, M.; Salim, R. Int J Chem 2013, 4, 1388–1394.
11. Meti, M. D.; Bayadgi, K. S.; Nandibewoor, S. T.; Chimatadar, S. A. Montash Chem 2014, 123, 1561–1573.
12. Singh, A. K.; Srivastava, S.; Srivastava, J.; Srivastava, R.; Singh, P. J Mol Catal A: Chem 2007, 278, 72–81.
13. Kulkarni, R. M.; Hanagadakar, M. S.; Malladi, R. S.; Santhakumari, B.; Nandibewoor, S. T. Prog React Kinet 2016, 41, 245–257.
14. Kelson, E. P.; Phengsy, P. P. Int J Chem Kinet 2000, 32, 760–770.
15. Vovk, A. I.; MuravevaI, V.; Kukhar, V. P. Russ J Gen Chem 2000, 70, 1108–1112.
16. Dasgupta, G.; Mahanti, K. Bull Soc Chim Fr 1986, 4, 492–496.
17. Farokhi, S. A.; Nandibewoor, S. T. Tetrahedron 2003, 59, 7595–7602.
18. Nowdari, A.; Adari, K. K.; Gollapalli, N. R.; Parvataneni, V. Eur J Chem 2009, 6, 93–98.
19. Martinez, M.; Pitarque, M.; Eldik, R. V. J Chem Soc, Dalton Trans 1966, 2665–2669.
20. Patgar, M. B.; Nandibewoor, S. T.; Chimatadar, S. A. Cogent Chem 2015, 1, 1–14.
21. Wang, P.; He, Y. L.; Huang, C. H. Water Res 2010, 44, 5989–5998.
22. Guinea, E.; Brillas, E.; Centellas, F.; Canizares, P.; Radrigo, M. A.; Saez, C. Water Res 2009, 43, 2131–2138.
23. Dodd, M. C.; Shah, A. D.; Vongunten, U.; Huang, C. H. Environ Sci Technol 2005, 39, 7065–7076.
24. Jain, A.; Jain, S.; Devra, V. Int J Pharm Sci Drug Res 2015, 7, 205–210.
25. Jeffery, G. H.; Bassett, J.; Mendham, J.; Denny, R. C. Vogel's Text Book of Quantitative Chemical Analysis, 5th edn.; ELBS, Longman: Essex, UK 1996; 339 p.
26. Nowduri, A.; Duggada, A. B.; Kurimella, V. R. Int J Sci Res 2014, 3, 131–133.
27. Khan, A. A. P.; Khan, A.; Asiri, A. M.; Azum, N.; Rub, M. A. J Taiwan Inst Chem Eng 2014, 45, 127–133.
28. Asiri, A. M.; Khan, A. A. P.; Khan, A. J Mol Liq 2015, 203, 1–6.
29. Sateesh, B. S.; Shastry, V.; Shashidhar, S. Int J Res Phys Chem 2013, 3, 18–23.
30. Singh, M. P.; Ghosh, S. Z Phys Chem 1955, 204, 1–5.
31. Kochi, J. K.; Graybill, B. M.; Kurtz, M. J Am Chem Soc 1964, 86, 5257–5264.
32. Wilberg, K. B.; Nigh, W. G. J Am Chem Soc 1965, 87, 3849–3855.
33. Khan, A. A. P.; Asiri, A. M.; Azum, N.; Rub, M. A.; Khan, A.; Al-Youbi, A. O. Ind Eng Chem Res 2012, 51, 4819–4824.
34. Khan, A. A. P.; Khan, A.; Asiri, A. M.; Rub, M. A. J Ind Eng Chem 2014, 20, 3590–3595.
35. Khan, A. A. P.; Khan, A.; Asiri, A. M.; Khan, S. A. J Mol Liq 2016, 218, 604–610.